Behaviour of milk protein–stabilized oil-in-water emulsions in simulated physiological fluids

A thesis presented in partial fulfilment

of the requirements for the degree of

Doctor of Philosophy in Food Technology

at Massey University, Palmerston North, New Zealand

Anwesha Sarkar

2010

Dedicated to

My Beloved Parents

Abstract

Emulsions form a major part of processed food formulations, either being the end products in themselves or as parts of a more complex food system. For the past few decades, colloid scientists have focussed mainly on the effects of processing conditions (*e.g.* heat, high pressure, and shear) on the physicochemical properties of emulsions (*e.g.* viscosity, droplet size distribution and phase stability). However, the information about the behaviour of food structures post consumption is very limited. Fundamental knowledge of how the food structures behave in the mouth is critical, as these oral interactions of food components influence the common sensorial perceptions (*e.g.* creaminess, smoothness) and the release of fat–soluble flavours. Initial studies also suggest that the breakdown of emulsions in the gastrointestinal tract and the generated interfacial structures impact lipid digestion, which can consequently influence post-prandial metabolic responses. This area of research needs to be intensively investigated before the knowledge can be applied to rational design of healthier food structures that could modulate the rate of lipid metabolism, bioavailability of nutrients, and also help in providing targeted delivery of flavour molecules and/or bioactive components.

Hence, the objective of this research was to gain understanding of how emulsions behave during their passage through the gastrointestinal tract. *In vitro* digestion models that mimic the physicochemical processes and biological conditions in the mouth and gastrointestinal tract were successfully employed. Behaviour of model protein–stabilized emulsions (both positively charged (lactoferrin) as well as negatively charged [β-lactoglobulin (β-lg)] oil-in-water emulsions) at each step of simulated physiological processing (using model oral, gastric and duodenal fluids individually) were investigated.

In simulated mouth conditions, oil-in-water emulsions stabilized by lactoferrin or β-lg at the interfacial layers were mixed with artificial saliva at neutral pH that contained a range of mucin concentrations and salts. The β-lg emulsions did not interact with the artificial saliva due to the dominant repulsion between mutually

opposite charges of anionic mucin and anionic β-lg interfacial layer at neutral pH. However, β-lg emulsions underwent some depletion flocculation on addition of higher concentrations of mucin due to the presence of unadsorbed mucin molecules in the continuous phase. In contrast, positively charged lactoferrin emulsions showed considerable salt–induced aggregation in the presence of salts (from the saliva) alone. Furthermore, lactoferrin emulsions underwent bridging flocculation because of electrostatic binding of anionic mucin to the positively charged lactoferrin–stabilized emulsion droplets.

In acidic pH conditions (pH 1.2) of the simulated gastric fluid (SGF), both protein–stabilized emulsions were positively charged. Addition of pepsin resulted in extensive droplet flocculation in both emulsions with a greater extent of droplet instability in lactoferrin emulsions. Coalescence of the droplets was observed as a result of peptic hydrolysis of the interfacial protein layers. Conditions such as ionic strength, pH and exposure to mucin were shown to significantly influence the rate of hydrolysis of β-lg–stabilized emulsion by pepsin.

Addition of simulated intestinal fluid (SIF) containing physiological concentrations of bile salts to the emulsions showed competitive interfacial displacement of β-lg by bile salts. In the case of lactoferrin–stabilized emulsion droplets, there was considerable aggregation in the presence of intestinal electrolytes alone (without added bile salts) at pH 7.5. Binding of anionic bile salts to cationic interfacial lactoferrin layer resulted in re-stabilization of salt–aggregated lactoferrin emulsions. On mixing with physiological concentrations of pancreatin (mixture of pancreatic lipase, amylase and protease), significant degree of coalescence and fatty acid release occurred for both the emulsions. This was attributed to the interfacial proteolysis by trypsin (proteolytic fractions of pancreatin) resulting in interfacial film rupturing. Exchange of initial interfacial materials by bile salts and trypsin–induced film breakage enhanced the potential for lipolytic fractions of pancreatin to act on the hydrophobic lipid core. The lipid digestion products (free fatty acids and mono-

and/or diglycerides) generated at the droplet surface further removed the residual intact protein layers from the interface by competitive displacement mechanisms.

The sequential treatment of the cationic and anionic emulsions with artificial saliva, SGF and SIF, respectively, was determined to understand the impact of initial protein type during complete physiological processing from mouth to intestine. Broadly, both the protein–stabilized emulsions underwent charge reversals, extensive droplet flocculation, and significant coalescence as they passed through various stages of the *in vitro* digestion conditions. Except in the simulated mouth environment, the initial charge of the emulsifiers had relatively limited influence on droplet behaviour during the simulated digestion.

The results contribute to the knowledge of how structure and charge of the emulsified lipid droplets impact digestion at various stages of physiology. This information might have important consequences for developing suitable microstructures that allow controlled breakdown of droplets in the mouth and predictable release of lipids in the gastrointestinal tract.

Acknowledgements

It is undeniably my proud privilege to express my deepest sense of gratitude to Professor Harjinder Singh, my chief supervisor for his conscientious guidance, continuous encouragement, generous help, and enormous freedom, which he gave me during my doctoral study. His continuous enthusiasm, immense patience, astute intellectual capabilities, deep scientific insights, dedication and his critical way of thinking in both academic areas and in providing commercial solutions have been a learning experience and I am grateful to him for his earnest interest in my overall wellbeing. It was a rewarding experience to work under his supervision and this thesis would not have appeared in its present form without his expert assistance, support, ideas and substantial corrective comments.

I am sincerely grateful to my co-supervisor Assoc. Professor Kelvin K. T. (Institute of Food Nutrition and Human Health). His untiring guidance, luminous concepts, excellent graphical ideas, continuous support, and encouragement at each step of practical work as well as writing of thesis have been the driving force of this work. I would like to thank my co-supervisor Professor R. Paul Singh (University of California, Davis, USA) for his valuable scientific inputs and advices throughout the entire period of my doctoral study. I am also grateful to his sincere interest in my welfare. It is my pleasure to express my heartfelt gratitude to Professor David S. Horne (ex Hannah Research Institute, UK) for his meticulous supervision, constant support, critical suggestions, constructive criticisms, advice on mathematical equations, guidance for experiments and his immense help in preparing publication materials based on findings of the interfacial displacement studies.

I am truly thankful to New Zealand International Doctoral Research Scholarship (Education New Zealand) and Massey University Doctoral Scholarship for providing me the financial assistance during the three years of my research. I wish to thank Riddet Institute for funding this project as well as providing travel grant to attend conferences. I would also like to thank Brian Scarlett Scholarship, Royal Society of Chemistry, UK for providing the travel bursary for attending overseas conference.

I am thankful to Professor Paul Moughan for his encouragements, support, guidance, stimulating discussions and motivations for successful journey of my PhD study. I am thankful to Professor Ravindran Ravindran (Institute of Food, Nutrition and Human Health) for being so kind and for timely approval of six monthly reports and priceless

suggestions for PhD study. I would also like to specially thank Professor Geoff Jameson (Institute of Fundamental sciences) for his helpful scientific advices and guidance to analyse the results of proteolysis experiments and biopolymer interaction studies. Professor Srikanta Chatterjee (Department of Economics and Finance) for his valuable advice, critical suggestions and inspirations, always helping me to keep thinking positive even in the discouraging phase of my doctoral studies. I wish to thank Dr. Shantanu Das for encouraging me to do a PhD in the first place at New Zealand and for his several valuable advices, support, ideas, thought provoking discussions, and motivations.

I am indeed thankful to Ms. Michelle Tamehana, Mr. Warwick Johnson and Mr. Steve Glasgow (Institute of Food Nutrition and Human Health), Ms. Janiene Gilliland and Mr. Chris Hall (Riddet Institute) for being excellent lab managers, providing trainings, ordering chemicals at right time, laboratory demonstrations, technical help, encouragements, scientific advices and for allowing me to use the facilities in the departments. I am sincerely grateful to Mr. Shane Rutherfurd and Ms. Maggie Zhou (Riddet Institute, New Zealand) for all of their assistance for HPLC experiments and for many helpful technical discussions. I would like to thank Ms. Fliss Jackson, Garry Radford (Institute of Food Nutrition and Human Health) for their assistance during laboratory work. I am thankful to Dr. Dmitry Sokolov (Manawatu Microscopy & Imaging Centre) for his scientific advices and demonstrations of confocal scanning laser microscopy. I am very grateful to Ms. Terri Palmer, Ms. Felicia Stibbards, Ms. Ansley Te Hiwi (Riddet institute) and Ms. Parkes Yvonne (Institute of Food Nutrition and Human Health) for their unforgettable cooperation, administrative help and invaluable assistance. I would like to express my sincere gratitude to Mr. Matt Levin and Mr. Peter Jeffrey for their timely help and excellent services in information systems (Institute of Food Nutrition and Human Health). I wish to sincerely thank Ms. Claire Woodhall for being proof-reader of my publications. I am also thankful to Dr. Mike Boland, Mr. Mark Ward, Ms. Paula McCool, Ms. Willi Twilight and Mr. John Henley-King for being so supportive and helpful.

I express my deep sense of gratitude to Dr. Derek Haisman, Dr. Simon Loveday and Dr. Aiqian Ye for valuable discussions, encouragements and providing me holistic learning by offering research assistantships for doing some scientific projects.

I am thankful to all the staff and research fellows in the Riddet Institute and Institute of Food, Nutrition and Human Health Department for their help during the course of this work. Thanks to my office mates Dr. Daniel Ries and Ms. Xuemei Tang for their

company and support. I thank all my lab mates specially Ms. Zeinab Dehghan-Shoar, Ms. Oni Yularti, Ms. Norfezah, Md, Ms. Binosha Fernando, Dr. Sina Hosseiniparvar, Ms Elham Khanipour,Mr. Abdollahi Reza, Dr. Jiahong Su, Dr. Sharon Henare, Dr. Lovedeep Kaur, Dr. Catootji Nalle, Ms. Teresa Wegrzyn, Ms. Lakshmi Chaitanya, Ms. Sawatdeenaruenat, Ms. Chanapha, Mr. Jian Cui, Dr. Xiang-Qian Zhu, Ms. Sandra Kim and many others making the lab atmosphere very conducive to carry out my experiments and have academic and non–academic discussions.

This endeavour would not have a success without the enduring support and encouragement by my friends, who have given me so much support and made my life so enjoyable. I would like to wish my heartfelt thanks to my dearest Ms. Namrata Taneja and Mr. Amit Taneja for always being there for me, being so kind, extremely helpful and supportive during the good and difficult stages of PhD. I am also thankful to Mr. Mallesh Peram, Mr. Preet Singh, Mr. Prabir Chowdhury, Ms. Jinita Das, Mr. Palash Biswas, Mr. Manas Chakraborty, Dr. Shrabani Saha, Mr. Saptarshi Mukherjee, Mr. Arup Nag, Ms. Ranjita Sengupta, Mr. Prabhu Balan and Mr. Valentine Borges for their invaluable support, genial succour, care, constant motivations, great cooperation, stimulating discussions and friendship. I still cherish all the enjoyable and funfilled moments shared with all of them and keeping my "Indian" connection alive at New Zealand. I am also sincerely thankful to Dr. Anil K. Anal (Asian Institute of Technology, Thailand), Dr. Hasmukh A. Patel (Fonterra, New Zealand), Dr. Mily Bhattacharya (IISER, Mohali, India), Dr. T. Laha (IIT, Kharagpur, India) and Professor Debasis Bhattacharya (IIT, Kharagpur, India) for their enormous support, critical suggestion and constructive help for thesis writing. Heartfelt thanks to Mr. Anant Dave for all technical suggestions and proof reading assistance. I would like to thank all my friends who, are, directly or indirectly, associated with the successful completion of this work.

Finally the blessings of my family and my near and dear ones have given me the strength to take up this work and complete it to the best of my ability. Words are not enough to describe the incredible sense of gratitude and love that I have for my family. I am extremely thankful to my elder sister Ms. Sayantani Dasgupta and brother-in-law Mr. Debraj Dasgupta for their constant encouragement, love, and guidance throughout my PhD studies. Last but not the least, I am extremely grateful to the pillar and angel of my life i.e. my father, Mr. Arun Kumar Sarkar and my mother, Mrs. Kaberi Sarkar, respectively, for their constant encouragement, motivations, endless guidance, enormous support and most importantly, for their unconditional love and continual blessings.

Table of Contents

List of Figures

List of Tables

List of Peer-Reviewed Publications

1. Goh, K. K. T., **Sarkar, A.**, & Singh, H. (2008). Milk protein–polysaccharide interactions. In: A. Thompson, M. Boland, & H. Singh, Milk Proteins: From Expression to Food (pp. 347–376). New York: Academic Press.

2. **Sarkar, A.**, Goh, K. K. T., & Singh, H. (2009). Colloidal stability and interactions of milk protein–stabilized emulsions in an artificial saliva. *Food Hydrocolloids*, *23*(5), 1270–1278.

3. **Sarkar, A**., Goh, K. K. T., Singh, R. P., & Singh, H. (2009). Behaviour of an oil-in-water emulsion stabilized by *β*-lactoglobulin in an *in vitro* gastric model. *Food Hydrocolloids*, *23*(6), 1563–1569.

4. **Sarkar, A**., Horne, D. S., & Singh, H. (2010). Interactions of milk protein–stabilized oil-in-water emulsions with bile salts in a simulated upper intestinal model. *Food Hydrocolloids*, *24*(1–2), 142–151.

5. **Sarkar, A**., Goh, K. K. T. & Singh, H. (2010). Properties of oil-in-water emulsions stabilized by *β*-lactoglobulin in simulated gastric fluid as influenced by ionic strength and presence of mucin. *Food Hydrocolloids*, *24*(5), 534–541.

6. **Sarkar, A**., Horne, D. S., & Singh, H. (In Press). Pancreatin–induced coalescence of oil-in-water emulsions in an *in vitro* duodenal model. *International Dairy Journal*, doi:10.1016/j.idairyj.2009.12.007.

Chapter One: Introduction

The significance of nutrient lipids in the human diet has led to major advances in understanding the mechanisms of lipid digestion and absorption. With these advances has come new realization that the matrix in which lipids are presented (*i.e*. food structure) in the diet could influence lipid digestion in the gastrointestinal tract and hence modulate the bioavailability of lipid nutrients and fatty acids. Moreover, due to the appreciable increase in obesity, atherosclerosis and other cardiovascular diseases, there has been a growing interest in understanding how food material properties can be manipulated under physiological conditions that may help to regulate calorie intake, provide increased satiety responses, control lipid digestion and/or deliver bioactive molecules (*e.g.* $\omega-3$ fatty acids, carotenoids) *(Golding & Wooster, 2010; McClements et al., 2009; Singh et al., 2009)*.

The lipids (extracted from plant and animal sources) in many, if not most, of the processed foods are present as emulsified oil droplets, dispersed in a structurally and compositionally composite matrix of proteins, carbohydrates and other minor food components. Examples of these foods include imitation creams, salad dressings, mayonnaise, spreads, soups, gravies *etc. (McClements, 2005; Singh et al., 2009)*. The creation of food emulsions generally requires the generation of kinetically stable oil–water interfaces. These interfaces are stabilized using biopolymers mainly proteins and/or polysaccharides or low molecular weight emulsifiers, such as monoacylglycerols, diglycerides *etc*. Extensive research has been performed in this area of emulsion science with particular focus on the stability of protein–stabilized emulsions during processing and interactions with biopolymers, mainly polysaccharides (xanthan gum, carrageenans, dextran, guar gums *etc.*) that are expected to affect the physical and sensory properties of foods, such as texture, shelf life and flavour release *(Dickinson & Stainsby, 1988; Dickinson, 1998; Benichou et al., 2002; Dalgleish et al., 2002; Dickinson, 2003; McClements, 2004; McClements, 2005; Singh, 2005)*.

In contrast, there is currently limited knowledge of the physicochemical and structural changes, which an emulsion may undergo upon consumption *i.e.*

during oral processing in the mouth as well as gastrointestinal processing during digestion *(Dickinson, 2008)*. In general, on ingestion, an emulsion is exposed to a range of physical (*e.g.* shear, temperature) and biochemical (*e.g.* dilution effect, pH, electrolytes, pepsin, pancreatin, mucins and bile salts) environments as it passes through the mouth into the stomach and then into the intestines *(McClements et al., 2008; McClements et al., 2009; Singh et al., 2009)*.

Recently, a few studies have been conducted to understand the microstructural, physicochemical and biological processing of emulsions using *in vitro* models by mimicking one part of the physiological environment at a time (*i.e.* conditions in the mouth, stomach and intestine, individually) *(Mun et al., 2007; Vingerhoeds et al., 2005)* or the whole gastrointestinal system *(Beysseriat et al., 2006; Hur et al., 2009; Macierzanka et al., 2009)*. Broadly, droplet coalescence, different types and degrees of flocculation, competitive exchange of interfacial materials and binding of metabolites have been shown to occur, depending on the ratio of physiological fluid to emulsion, residence time, emulsifier type, pH, ionic strength, presence of biopolymers, phospholipids and other surface active molecules *(McClements et al., 2009; Singh et al., 2009)*.

However, the existing attempts in the literature do not successfully evaluate the fundamental mechanisms of interfacial interactions and the role of individual components of the physiological media when simulating human oral−to−gastric−to−duodenal model systems. Clearly, further work is required to elucidate the science of physiological processing of emulsions by carrying out *in vitro* experiments before the knowledge can be utilized for developing specific approaches to designing novel food emulsions that provide controlled release of fatty acids and lipophilic bioactive compounds.

Hence, this thesis describes the work aimed at gaining fundamental insights in this new direction of understanding the behaviour of food structures (using protein−stabilized oil-in-water emulsion systems) in the presence of simulated physiological media in an *in vitro* model system. Among the different food structures, milk protein−stabilized emulsions have attracted much interest as they

represent a good model system for a wide range of foods. Milk proteins possess a wide range of functional properties such as emulsification, gelling, flavor binding and foaming that significantly contribute to the sensorial and textural attributes of processed food products, including dairy, bakery and confectionary products *(Mulvihill & Fox, 1989; Ennis & Mulvihill, 2000; Mulvihill & Ennis, 2003; Singh, 2005)*. Therefore, two milk proteins, *i.e.* lactoferrin and *β*-lactoglobulin, have been particularly selected in this doctoral research to stabilize the soy oil-in-water emulsions as they allow the formation of cationic and anionic droplets at neutral pH, respectively *(Ye & Singh, 2006a; Ye & Singh, 2007)*.

The main objectives of this research were:

1) To investigate the colloidal interactions of the milk protein−stabilized emulsions in an artificial saliva (*i.e.* in the presence of high molecular weight mucins and electrolytes).

2) To determine the behaviour of emulsion droplets passing through an *in vitro* gastric model containing pepsin under different physiological pH and ionic strength conditions.

3) To understand the interfacial characteristics of emulsion droplets on exposure to simulated intestinal fluid (*i.e.* in the presence of bile salts and pancreatin).

4) To explore the overall behaviour of the emulsion droplets on mixing with total simulated oral−to−gastrointestinal fluids (a situation, which a food matrix might be exposed to during its transit though the gastrointestinal tract).

Chapter Two: Literature Review

The aim of this review is to discuss the creation and stability of emulsions with a particular focus on milk protein–stabilized oil-in-water emulsions. The effects of various physicochemical factors such as pH, ionic strength and enzymes on the emulsion stability are summarized. Furthermore, the current understanding on behaviour of emulsions in simulated oral and gastrointestinal systems is covered. Implications of gastrointestinal behaviour of emulsions on the development of strategies to control lipid digestion are also considered.

2.1 Introduction

An emulsion may be defined as an intimate dispersion of at least one immiscible liquid in another in the form of discrete droplets (diameter in general ranges from 0.1—100 μm). There is an interfacial layer between the two phases, which is occupied by some surface active agents, such as proteins, polysaccharides, phospholipids, monoacyl glycerol esters *etc. (Singh et al., 2009)*. Basically, there are three types of emulsions *(McClements, 2005; Kim et al., 2006)*: oil-in-water (O/W), water-in-oil (W/O) and multiple emulsions *i.e.* oil-in-water-in-oil (O/W/O) emulsion or water-in-oil-in-water (W/O/W) as shown in Figure 2.1-1.

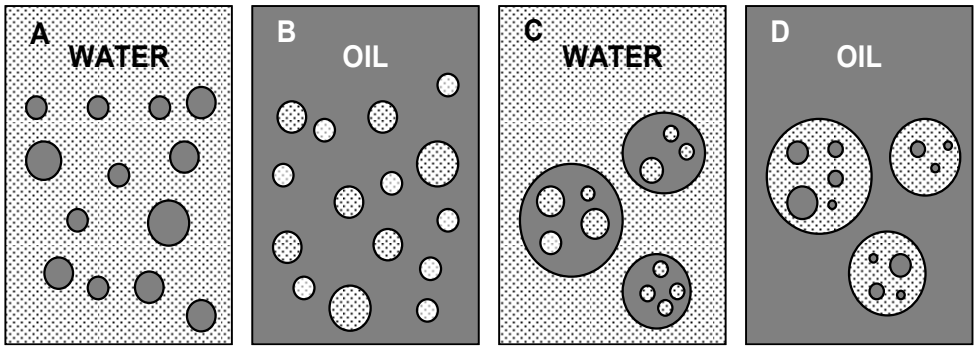

Figure 2.1-1: Schematic representation of emulsion systems: O/W Emulsion (A), W/O Emulsion (B), W/O/W Emulsion (C) and O/W/O Emulsion (D) (Gray and dotted white represent oil and water phases respectively).

Oil-in-water emulsion (O/W) refers to the type of dispersion in which oil is dispersed as droplets in the continuous aqueous phase (Figure 2.1-1 A). Milk and cream are best-known oil-in-water emulsions, in which the milk fat globules are

dispersed in aqueous phase containing milk proteins, lactose, salts and minerals. The fat globules are stabilized by natural surfactants *i.e.* lipoprotein membrane, phospholipids and adsorbed casein. On the other hand, in case of water-in-oil emulsion (W/O), oil forms the continuous phase and water exists as the dispersed phase (Figure 2.1-1 B). Butter is a common water-in-oil emulsion, in which aqueous phase, which comprised of milk proteins, phospholipids, sugar and salts, is dispersed in at least 80% fat cream.

Multiple emulsions refer to the systems, in which the dispersed phase is also an emulsion (Figure 2.1-1 C and D). In other words, the multiple emulsion droplets themselves contain a number of internal dispersed droplets in such a way that the final dispersed phase is actually the continuous phase for the internal dispersed droplets. These multiple emulsions can further be classified as either oil-in-water-in-oil (O/W/O) emulsion or water-in-oil-in-water (W/O/W) multiple emulsions *(Florence & Whitehill, 1981; Florence & Whitehill, 1982; Garti, 1997; Kim et al., 2006)*. In the case of an O/W/O multiple emulsion, the internal droplets and the external continuous phase matrix are composed of oil; the internal oil droplets are separated from the external oil phase by the aqueous phase. A W/O/W multiple emulsion consists of small aqueous droplets dispersed in oil and this water-in-oil (W/O) emulsion itself is dispersed as large droplets in the continuous aqueous phase *(Florence & Whitehill, 1981; Garti, 1997; Kim et al., 2006)*.

In this review, only oil-in-water emulsions have been considered. Detailed information about emulsions has been covered in a number of books *(Dickinson & Stainsby, 1982; Dickinson, 1992; Friberg et al., 2004; McClements, 2005)*.

2.2 Emulsion formation

Generally, food emulsions are prepared using high shear equipment items, such as colloid mills, high speed blenders, high pressure valve homogenizers that emulsify an oil phase and an aqueous phase together in the presence of a surface active agent *(McClements, 2005)*. The basic procedure is to force a coarse mixture of oil and aqueous phases though a narrow slit under the action of high pressure, resulting in cavitation, intense laminar shear flow and turbulence. At

the same time, the surface active agents, such as emulsifiers being structurally amphiphilic molecules (having both hydrophobic and hydrophilic moieties), are adsorbed at the oil–water interface *(Dickinson, 2003)*, creating a stabilizing interfacial layer at the oil droplet surface, finally leading to the generation of fine uniformly dispersed droplets. The physicochemical properties and stability of the emulsions formed are largely determined by the type and concentrations of the dispersed phase and continuous phase, the nature of the interfacial layer, temperature, pH, viscosity, as well as the homogenization conditions and other processing parameters employed, such as heat treatments and enzymatic hydrolysis *(Dickinson, 2003; Dickinson et al., 2003; McClements, 2005)*.

2.3 Emulsion stability

The term "emulsion stability" refers to the ability of an emulsion to resist any alteration in its properties over the time scale of observation (*McClements, 2005*). An emulsion is a thermodynamically unstable system, as the free energy of mixing is always positive due to the large interfacial area between the oil and the aqueous phase. The thermodynamic instability arising by comparing free energy of an oil–water system before and after emulsification has been illustrated by mathematical equations *(Hunter, 1989)*:

Initial free energy equation:

$$G^i = G^i{}_O + G^i{}_W + G^i{}_I - TS^i{}_{configuration} \qquad \textbf{(2.3-1)}$$

Final free energy equation after homogenization:

$$G^f = G^f{}_O + G^f{}_W + G^f{}_I - TS^f{}_{configuration} \qquad \textbf{(2.3-2)}$$

where, G_O, G_W, G_I are the free energies associated with oil phase, water phase and interfacial layer between oil and water phase respectively, T is the absolute temperature and $S_{configuration}$ is the configurational entropy of the system. The superscripts i and f represent the initial state (before emulsification) and final state (after emulsification) of the system, respectively. Since free energy of oil

and aqueous bulk phases remain constant after emulsification process, $G^i_O = G^f_O$ and $G^i_W = G^f_W$, the difference in free energy is basically the difference in free interfacial energy as given by the following mathematical expression *(Hunter, 1989)*:

$$\Delta G_{formation} = G^f - G^i$$
$$= (G^f{}_O + G^f{}_W + G^f{}_I - TS^f{}_{configuration}) - (G^i{}_O + G^i{}_W + G^i{}_I - TS^i{}_{configuration})$$
$$= (G^f{}_I - G^i{}_I) - (TS^f{}_{configuration} - TS^i{}_{configuration})$$

$$\Delta G_{formation} = \Delta G_I - T\Delta S_{configuration} \quad \textbf{(2.3-3)}$$

By definition $\Delta G_I = \gamma \Delta A$, where, A = change in interfacial energy, γ = interfacial tension, so the above expression becomes as follows:

$$\Delta G_{formation} = \gamma \Delta A - T\Delta S_{configuration} \quad \textbf{(2.3-4)}$$

The term $\gamma \Delta A$ is always a positive term, as the interfacial area always increases after homogenization *(McClements, 2005)*. The configurational entropy term *($-T\Delta S_{configuration}$)* is always negative, as the possible arrangements after emulsification are much greater than that of the initial state. As compared to the $\gamma \Delta A$ term, the entropy term is almost 10^7 times negligible and hence ($-T\Delta S_{configuration}$) can be neglected *(Hunter, 1989; McClements, 2005)*.

Therefore, the mathematical expression of free energy change of emulsification can be illustrated as:

$$\Delta G_{formation} = \gamma \Delta A \quad \textbf{(2.3-5)}$$

Thus, the free energy of emulsion formation is net positive, due to increase in interfacial area in emulsion formation process and the system is thermodynamically unstable. However, if the interfacial tension is significantly lower as compared to the configurational entropy, then there is a chance of thermodynamically stable system formation *(Hunter, 1989; McClements, 2005)*.

Almost all food emulsions are thermodynamically unstable and may breakdown into individual phases after certain time periods. Hence, the time period for which the emulsion is stable is more important, which is determined by its kinetic stability *(Damodaran, 1997; Dickinson, 2003; McClements, 2005)*. An emulsion may become unstable due to various types of physical and chemical processes. Physical instability refers to the modification in spatial arrangement or size distribution of emulsion droplets, such as creaming, flocculation and coalescence; whereas chemical instability includes change in the composition of the emulsion droplets itself, such as oxidation and hydrolysis *(McClements & Decker, 2000; McClements, 2005)*.

In case of an emulsion, Stokes' law can explain the physical instability particularly the creaming (*i.e.* the movement of oil droplets under gravity or applied centrifugal force to form a concentrated cream layer at the top of the emulsion without any change in the droplet size distribution) by the following mathematical expression *(Hunter, 1989; McClements, 2005; Singh et al., 2009)*:

$$v_{stokes} = \frac{2}{9}\frac{(\rho_1 - \rho_2)gr^2}{\eta} \qquad \textbf{(2.3-6)}$$

where, v_{stokes}= velocity of creaming, r = emulsion droplet radius, ρ_1 and ρ_2 = densities of continuous and dispersed phases respectively, η = shear viscosity of the continuous phase and g = acceleration due to gravity. Hence, kinetic stability of an emulsion can be increased or creaming rate can be decreased by lowering the radius of droplets, increasing the viscosity of the continuous phase or by decreasing the difference of density between the two phases.

However, this law often fails to define the rate of creaming due to flocculation or coalescence. Flocculation has been described as the reversible aggregation mechanism, which arises when droplets associate, due to unbalanced inter–atomic attractive and repulsive forces *(Dalgleish, 1997)*. On the other hand, coalescence refers to a completely irreversible increase in droplet size gradually leading to the separation of the oil and the aqueous phase.

Commonly, two types of droplet–droplet interactions are notable, *i.e.*, depletion and bridging flocculation *(Dickinson, 2003)*. The kind of mechanism of flocculation prevailing depends upon the interaction between the interfacial layer and the emulsion droplets.

2.3.1 Depletion flocculation

Generally, depletion flocculation occurs due to the presence of a non–adsorbing biopolymer in the continuous phase of the emulsion, which can promote association of emulsion droplets by inducing an osmotic pressure gradient within the continuous phase surrounding the droplets. The mechanism of depletion flocculation is illustrated in Figure 2.3-1.

Basically, when the biopolymer added into the continuous phase is either unadsorbed or poorly adsorbed, the biopolymer is squeezed out of the area between two approaching emulsion droplets. The local aqueous phase concentration immediately surrounding the emulsion droplets becomes significantly lower than the overall concentration of the bulk continuous phase, resulting in osmotic pressure imbalance. Hence, the droplets are attracted towards each other, causing flocculation and leading to loss of emulsion stability. This attraction energy can be calculated by measuring the concentration of the biopolymer and the radius of gyration of the biopolymer molecule as shown by the following interaction potential [$-\omega_{dep}(0)$] *(McClements, 2000)*:

$$\omega dep(0) = \frac{-3kT}{2}\frac{cRv}{\rho}\left(1+\frac{1}{2}\frac{cRv}{\rho}\right)\left(\frac{\gamma d}{\gamma g}+\frac{2}{3}\right) \qquad \textbf{(2.3-7)}$$

where, c is the biopolymer concentration (kg/m^3), γ_d *and* γ_g are the radius of the emulsion droplet and radius of gyration of the biopolymer, respectively, ρ is the density of biopolymer and Rv is given by the following expression:

$$Rv = \frac{4\pi\gamma_g{}^3\rho N_A}{3M} \qquad \textbf{(2.3-8)}$$

where, N_A is the Avogadro number and M is the molecular weight of the biopolymer molecule (kg/mol).

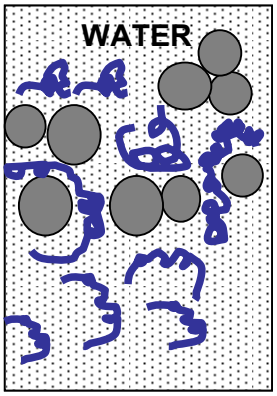

Figure 2.3-1: Depletion flocculation in an oil-in-water emulsion. Particles approach due to osmotic pressure gradient pushing out the unadsorbed biopolymer (Gray and dotted white represent oil and water phases respectively. Dark blue coil structure represents the biopolymer added for stabilizing the emulsion droplets).

It is suggested that most droplets are flocculated (at droplet–droplet separation distance $h = 0$) when the depletion potential [$-\omega_{dep}(0)$] exceeds 4 kT *(McClements, 2000)*. The reversible bonds formed during this depletion flocculation are generally weak and flexible *(Blijdenstein et al., 2003; Blijdenstein et al., 2004a)*. A wide variety of proteins (caseinates, whey proteins) and polysaccharides (xanthan gum, guar gum, gum arabic, dextran *etc.*) caused depletion flocculation when added in sufficiently large amounts into emulsion systems *(Dickinson & Golding, 1997; Tuinier et al., 1999; Tuinier et al., 2000; Chanamai & McClements, 2001; Blijdenstein et al., 2004a; Blijdenstein et al., 2004b; McClements, 2005)*.

The influence of sodium caseinate as the sole emulsifying agent in stabilizing an oil-in-water emulsion (35.0 or 45.0 vol% oil) was investigated *(Dickinson et al., 1997)*. It was shown that at protein content of nearly 2.0 wt%, the emulsion droplets were protected from flocculation by a thick steric stabilizing layer of sodium caseinate. The emulsion was stable against flocculation, coalescence and creaming for several weeks. However, when the protein content was increased to above 3.0 wt%, presence of unadsorbed caseinate in the continuous phase gave

rise to depletion flocculation resulting in serum separation. Hence, when the biopolymer present in the bulk phase exceeds a certain critical concentration, the emulsion droplets may become flocculated by depletion mechanism because of an osmotic pressure gradient associated with the exclusion of biopolymer molecules from a narrow region surrounding the droplets. Although if the same protein or polysaccharide is present in just sufficient quantity to completely saturate the droplet surface, the emulsion may remain kinetically stable for many weeks due to secondary steric stabilizing layer of biopolymer or by viscosity enhanced network formation *(Dickinson & Euston, 1991; Dickinson & Pawlowsky, 1997)*.

On the other hand, if the biopolymer is non–adsorbing type with respect to the droplet surface, then addition of even low levels of polysaccharides can result in depletion flocculation of a protein–stabilized emulsion. This was shown in an emulsion stability study with 30.0 wt% soy oil emulsions stabilized by 0.5 or 3.0 wt% whey protein isolate (WPI) and various concentrations of κ-carrageenan *(Singh et al., 2003)*. The authors clearly identified that addition of low concentration of κ-carrageenan (0.025 wt%) caused extensive droplet flocculation through depletion mechanism due to the thermodynamic incompatibility between WPI and κ-carrageenan at neutral pH.

2.3.2 Bridging flocculation

Bridging flocculation normally occurs when a high molecular weight biopolymer at a sufficiently low concentration adsorbs onto two or more emulsion droplets resulting in bridges *(Dickinson et al., 1989a; Dickinson & Eriksson, 1991; Dickinson & Pawlowsky, 1997; Dickinson & Pawlowsky, 1998; Dickinson, 2003; Dickinson et al., 2003; Blijdenstein et al., 2004a; McClements, 2005; Fellows & Doherty, 2006)*. In general, higher molecular weight biopolymers are expected to provide better protection against flocculation by formation of thick steric stabilizing layer around the emulsion droplets. However, if such biopolymer added at lower levels has more than one potential point of attachment to the droplet surface, there is a possibility that the various possible points of attachments may encounter two different droplets rather than attaching to the

surface of the same droplet. Thus droplets may be bridged together resulting in flocculation as shown in Figure 2.3-2.

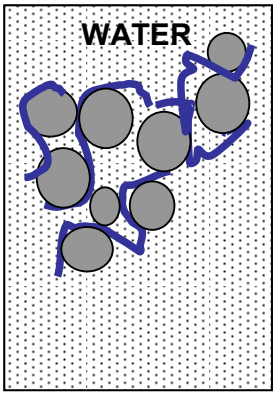

Figure 2.3-2: Bridging flocculation in an oil-in-water emulsion. Particles approach due to bridges formed by a biopolymer (Gray and dotted white represent oil and water phases respectively. Dark blue coil structure represents the biopolymer stabilizing the emulsion droplets).

The attractive forces of the biopolymer to the droplet surface may be of electrostatic origin and are rigid, generally irreversible and relatively stronger than that generated in depletion interactions *(Blijdenstein et al., 2004a)*. Generally, when protein–polysaccharide mixtures are present to stabilize an emulsion, low concentration of polysaccharide may cause polymeric linkages between protein–adsorbed emulsion droplets, thereby leading to bridging flocculation *(Dickinson & Galazka, 1991)*. However, if the same polysaccharide is present at higher concentration, which is sufficient to completely cover the emulsion droplet surface; the emulsion can be stabilized by steric and electrostatic effects *(Dickinson & Eriksson, 1991)*.

The influence of *ι*-carrageenan on the properties of bovine serum albumin (BSA)–stabilized emulsion droplets was investigated *(Dickinson & Pawlowsky, 1997)*. The emulsion (20.0 vol% oil, 1.7 wt% BSA, pH 6.0) without the addition of the polysaccharide was kinetically stable over a period of 10 days. Flocculation was observed by the addition of low levels of *ι*-carrageenan (~ 0.005 wt%), which was not reversible upon dilution but re-stabilization of the emulsion was observed at a higher polysaccharide concentration (~ 0.1 wt%).

The flocculation behaviour was explained in terms of bridging interaction, as addition of *ι*-carrageenan was not enough to completely saturate the total surface of emulsion droplets. However, bridging flocculation was replaced by re-stabilization when higher concentration of *ι*-carrageenan was added leading to increased emulsion stability.

In a recent study, the effect of pH and pectin type on the stability and properties of sodium caseinate stabilized oil-in-water emulsions was investigated *(Surh et al., 2006)*. At pH 3–4, below the isoelectric point of the adsorbed casein, negatively charged pectin molecules adsorbed to the surface of positively charged caseinate–coated droplets, inducing irreversible bridging flocculation, which resulted in the formation of strongly aggregated network of emulsion droplets showing shear thinning behaviour and serum separation. Hence, not only the concentration of the biopolymer, but also net associative interactions between the emulsion droplet surface and the added biopolymer might result in bridging flocculation.

2.3.3 Coalescence

Coalescence refers to the fusion of two or more emulsion droplets to form a single droplet of greater volume but lower interfacial area as shown in Figure 2.3-3. Coalescence generally occurs when the stabilizing film surrounding the emulsion droplets is thinned to a certain critical thickness resulting in film rupture of the interfacial layer separating the two adjoining emulsion droplets *(van Aken et al., 2003; van Aken, 2004)*. Generally, emulsions are stable to coalescence as the biopolymer molecules adsorb at the droplet surfaces, forming a dense viscoelastic interfacial layer *(Dickinson & Stainsby, 1988)*. However, any extreme processing conditions, like high shear or enzymatic hydrolysis resulting in significant attrition of the interfacial film, can give rise to gradual agglomeration of bare emulsion droplets resulting in coalescence and oiling off. Coalescence has been largely reported in emulsions stabilized by whey protein hydrolysates due to the thinner interfacial film formation and reduced surface viscosity of the predominantly shorter peptides *(Agboola et al., 1998a; Singh & Dalgleish, 1998)*.

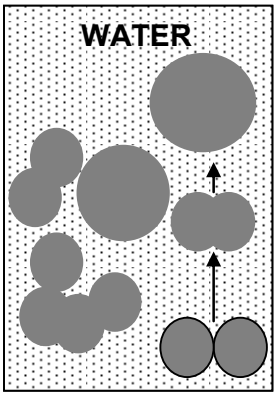

Figure 2.3-3: Coalescence in an oil-in-water emulsion. Particles approach due to rupture of interfacial layer leading to fusion to a single droplet (Gray and dotted white represent oil and water phases respectively).

In general, coalescence of emulsion droplets follows first-order kinetics *(Walstra, 1987)*, which can be expressed by the following equation:

$$\frac{N_t}{N_0} = e^{-K_c t} \qquad \textbf{(2.3-9)}$$

where, N_t is the number concentration of emulsion droplets at time t; N_0 is the initial number concentration of freshly homogenised emulsion droplets (time zero); K_c is the coalescence rate constant, which is related to the possibility of rupturing of the interdroplet film (interfacial protein layer in our study) in time t *(Darling, 1987)*. The degree of coalescence of emulsion droplets is also inversely related to the viscosity of the continuous phase. The slope of the logarithmic plot of (N_t/N_o) *versus* time t can give an indication of the rate of coalescence; this calculated value depends on the initial number concentration of the droplets, together with the effects of other destabilization mechanisms, *e.g.*, depletion flocculation and salt induced aggregation *(Walstra, 1987)*, where the interfacial film is relatively thin and might lead to coalescence on prolonged storage conditions.

2.4 Biopolymers as adsorbed layers

In most food emulsions, the droplets are stabilized by a layer of adsorbed materials such as proteins, phospholipids or low molecular weight commercial emulsifiers, such as monoacylglycerols. Generally, biopolymers (proteins and polysaccharides) are widely known being essential functional ingredients determining the texture and stability of most processed food. Biopolymers can be effective emulsifiers provided that they exhibit some surface activity *i.e.* they should have sufficient hydrophobic groups to strongly adsorb to the oil–surface and hydrophilic groups to spread out in the aqueous continuous phase, and thus reduce the interfacial tension *(Dickinson, 2003)*. The solubility of the biopolymer is also significant, as it affects the hydrophilic character. But once the emulsion is formed with sufficiently small droplets, then the surface activities are not relevant, rather the molecular abilities of the biopolymer to form thick steric stabilizing layer play a major role. The physical characteristics of the interfacial layer formed around the droplets depend on the types, structures, amounts, and interactions of the adsorbed biopolymer molecules. *Dickinson (2003)* has mentioned the characteristics of biopolymers necessary to be effective emulsifiers, which are as follows:

a) *Amphiphilic character:* The biopolymer should have enough hydrophobic groups to become strongly anchored at the oil–water interface. The biopolymer should have sufficient hydrophilic character. It should have good solubility in aqueous medium and preferably contribute to change the rheology of continuous aqueous phase.

b) *Sufficient biopolymer concentration:* The concentration of the biopolymer should be just sufficient to fully cover the oil–water interface providing stabilization, thereby avoiding any depletion or bridging interactions.

c) *Steric Stabilizing property:* The biopolymer should be of high molecular weight and provide thick steric stabilizing layer around the emulsion droplets.

Proteins being an indispensable component of all processed foods have proved to be effective functionally, providing desirable textural and other attributes to the final food products, because of their naturally amphiphilic nature.

Milk proteins such as caseins, caseinates, whey protein isolates, β-lactoglobulin and bovine serum albumins have been known for many decades as emulsifiers and a lot of work has been done on dairy based emulsion systems such as milk, cream, butter and ice–cream. In this review, we are concerned only with milk protein–stabilized emulsions.

2.5 Milk protein–stabilized emulsions

Milk proteins in both soluble as well as in dispersed form are known to be excellent emulsifiers because of their amphiphilic nature *(Morr, 1982; Mulvihill & Fox, 1989)*. They exhibit good surface active properties by reducing the tension at the oil–water interface and form interfacial films with different rheological properties. The sequence of surface activity reported for milk proteins is β-casein> monodispersed casein micelle> serum albumin> α-lactalbumin> α_s-casein = κ-casein> β-lactoglobulin> euglobulins *(Ennis & Mulvihill, 2000)*. The β-casein is the most important milk protein fraction because of its high surface activity and flexible nature, due to numerous proline residues, little ordered structure and negligible intermolecular cross–links *(Swaisgood, 1982; Dickinson, 1994)*. Caseins and whey proteins and their respective products are widely used in different processed foods because of their excellent surface activities, film forming, water binding and whipping abilities *(Singh, 2005)*. The roles of caseins and whey proteins in stabilizing oil–water emulsions have been thoroughly investigated and published [see reviews *(Kinsella, 1984; Morr & Ha, 1993; Dalgleish, 1995; Wong et al., 1996; Dickinson, 1999; Dickinson, 2001; Dalgleish, 2006)*]. Nevertheless, a brief synopsis of milk protein–stabilized oil-in-water emulsions has been included in the following section.

2.5.1 Caseins and/ or Caseinates

Caseins are known to adsorb strongly at the oil–water interface, thus stabilizing the emulsion droplets *(Dickinson, 1989; Dickinson et al., 1989b; Dickinson, 1999)*. Both electrostatic and steric stabilization effects contribute to the long–term stability of emulsions against coalescence as the surface active caseins, containing both hydrophilic and hydrophobic groups, adsorb rapidly at the oil–water interface during the emulsification process *(Dickinson, 2006)*. Caseins do not contain much rigid secondary structure (both α-helix and β-pleated sheet) *(Holt & Sawyer, 1988)* and have significant number of hydrophobic residues *(Swaisgood, 1992)*, and thus adsorb strongly *(Graham & Phillips, 1979)* at the droplet surface. However, because of lack of clarity of the native structure, the conformational changes occurring during casein adsorption process are not completely understood *(Dalgleish, 2004)*.

2.5.1.1 Pure caseins

Two major caseins α_{s1}-casein and β-casein contribute to almost 75% of the total milk casein as shown in milk. The α_{s1}-casein and β-casein are expected to provide similar emulsifying properties based on their amino-acid sequences *(Swaisgood, 1982)*. The surface and emulsifying properties of α_{s1}-casein and β-casein have been thoroughly studied [see reviews *(Dickinson et al., 1987; Dickinson, 1989; Dickinson et al., 1989b; Dickinson, 1997b; Dickinson, 1999)*]. Both α_{s1}-casein and β-casein, which carry a net negative charge at neutral pH, are distinctly amphiphilic, have some similarities in terms of linear disordered chains of around 200 residues with phosphoserine chains and have strong tendency to adsorb at oil–water interfaces. On the basis of experimental analysis, β-casein has been shown to adsorb to the droplet surface with its hydrophobic region strongly bound to the oil phase, while the hydrophilic region (4–50 residues at the *N*–terminal) protrudes into the continuous phase *(Dalgleish, 1996a; Dickinson, 1999)*. In contrast to the tail–like anchoring phenomenon of β-casein, α_{s1}-casein shows a loop–like conformation that binds to droplet surface *via* peptide towards the middle of the sequence (as compared to that of end of the sequence in case of former).

Both pure caseins can be used to prepare stable oil-in-water emulsions by lowering interfacial tensions with adsorbed layers of similar rheology *(Dickinson, 1989; Dickinson et al., 1989b; Swaisgood, 1992; Dickinson, 1999)*. However, the rate of lowering of interfacial tension is higher for β-casein as compared to α_{s1}-casein. Moreover, α_{s1}-casein–stabilized emulsion droplets have more electrostatic charge in general, as compared to that of β-casein–stabilized ones at neutral pH and are relatively more susceptible to flocculation, as compared to the latter at high ionic strengths *(Dickinson et al., 1998)*. Although few experimental details are available on the surface behavior of α_{s1}-casein, it has been reported that α_{s1}-casein accounts for less surface coverage resulting in thinner interfacial film than β-casein *(Brooksbank et al., 1993; Dalgleish, 1993; Dalgleish, 1996b)*. The β-casein, because of its relatively higher surface activity, has shown competitive adsorption at the oil–water interface as compared to α_{s1}-casein and has also appeared to displace α_{s1}-casein from the droplet surface *(Dickinson et al., 1988; Dickinson & Stainsby, 1988)*.

2.5.1.2 Caseinates

Caseinates are produced from skim milk by lowering the pH to 4.6, either by addition of lactic or hydrochloric acid or by addition of microbial cultures to precipitate the casein and then by resolubilizing the casein with alkali or alkaline salts of sodium, potassium or calcium at neutral pH, and then spray dried *(Mulvihill, 1989)*.

The stability of oil-in-water emulsions made with sodium caseinate largely depends on the composition of the adsorbed layer, quantities of proteins and the conformation of the casein in the continuous phase. Sodium caseinate not only consists of α_{s1}- and β-caseins but also κ-, α_{s2}-caseins and small quantities of lipids and inorganic calcium salts that also influence the emulsifying abilities of sodium caseinate *(Dickinson, 1999)*. However, it has been indicated that the salt stability properties of sodium caseinate–stabilized emulsions lie close to that of β-casein–stabilized emulsions *(Dickinson et al., 1998)*.

In case of sodium caseinate–stabilized oil-in-water emulsion, all kinds of caseins (α_{s1}-, α_{s2}-, β- and κ-caseins) are adsorbed at the emulsion droplet surface *(Robson & Dalgleish, 1987; Hunt & Dalgleish, 1994; Srinivasan et al., 1996)* providing stability against coalescence and flocculation. In contrast to pure caseins, the competitive adsorption phenomena in caseinate–stabilized emulsions is reported to be largely driven by the total protein content in the caseinates or the ratio of caseinate to oil. Several researchers have shown that the preferential adsorption of β-casein at the interface consists only at lower casein concentrations and/or when the ratio of caseinate to oil is low (1:60), where caseins are predicted to exist as monomers *(Srinivasan et al., 1996; Srinivasan et al., 1999)*. However, at higher total caseinate concentrations, α_{s1}-casein is preferentially adsorbed as compared to other casein fractions and β-casein loses its competitive adsorption ability; this has been attributed to the self aggregating tendency of β-casein to form micelles or complexation with other casein fractions, such as α_{s1}-casein *via* hydrophobic interactions *(Lucey et al., 2000)*. Furthermore, these aggregated complexes appear to have less emulsifying capability, as the hydrophobic areas are mutually blocked in the complex formation process *(Lorient et al., 1989)*. Irrespective of all caseinate concentrations, κ-casein from sodium caseinate has been found to be least adsorbed at the droplet surface.

2.5.2 Whey proteins

Whey proteins (β-lactoglobulin, α-lactalbumin, serum albumin and immunoglobulins) are characterized by three–dimensional arrangements held together by disulphide bridges *(Kinsella, 1984)*. Whey proteins are extremely important nutritionally as well as possessing excellent emulsifying capabilities. The main whey protein constituents are β-lactoglobulin and α-lactalbumin, two smaller globular proteins that account for ~ 70–80% of total whey protein. It is well known that both of the major whey proteins, β-lactoglobulin and α-lactalbumin, adsorb onto oil–water interfaces to form stable emulsions, although less stable than casein–stabilized emulsions under same conditions *(Hunt & Dalgleish, 1994; Dalgleish, 1995)*.

Whey proteins are soluble over wide pH range; but because of their globular nature, they are susceptible to thermal denaturation above 70 °C *(Kinsella & Whitehead, 1989; Hunt & Dalgleish, 1995; Singh, 2005)*. The available forms of emulsifiers in relation to whey proteins are isolates and concentrates. Whey protein concentrates (WPC) and whey protein isolates (WPI) are concentrated forms of whey proteins, which are produced by ultra–filtration, ion–exchange and dialysis followed by drying steps to obtain protein levels of ~ 80–95% *(Mulvihill & Ennis, 2003)*. Both WPC and WPI are widely used in processed food applications because of their water–binding, gelling, foaming and surface active properties *(Mulvihill & Ennis, 2003; Singh, 2005)*. Processing treatments during manufacturing of WPC and WPI tend to denature some of the whey proteins that generally affect their functionality.

The β-lactoglobulin (β-lg) and α-lactalbumin (α-la) are the main fractions, which contribute to emulsifying properties of whey proteins.

2.5.2.1 Beta-lactoglobulin (β-lg)

Structurally, bovine β-lg is a compact globular protein, containing 162 amino acids along with two disulphide bonds and one thiol group *(Swaisgood, 1982)*. The three dimensional structure of β-lg is composed of nine–stranded anti–parallel β-sheet converging at one end into a conical β-hydrophobic barrel unit, and a flanking three–turn α-helix *(Sawyer et al., 1985; Papiz et al., 1986; Oliveira et al., 2001)*. Under ambient conditions, β-lg mostly exists as non–covalently linked dimer with a molecular weight of ~ 36 kDa at pH 7 *(McKenzie & Sawyer, 1967; Ziegler & Foegeding, 1990)*.

Being the main constituent of whey protein, β-lg dominates the surface active properties. Native β-lg has excellent gelling and foaming properties *(Korhonen et al., 1998)*. Because of its amphiphilic nature, β-lg shows good emulsifying properties by saturating at the interfacial layer, where it partially unfolds and forms continuous and homogeneous membranes through intermolecular β-pleated sheets interactions, exposing reactive sulfydryl groups leading to self–aggregation, and slow polymerization of the adsorbed protein *via*

sulfydryl–disulphide interchange mechanisms *(Dickinson & Matsumura, 1991; Mcclements et al., 1993; Lefèvre & Subirade, 2003)*. Of different whey proteins, β-lg has been most extensively used for stabilizing oil-in-water emulsions, because of its well defined structure and properties *(McKenzie, 1971; Kinsella & Whitehead, 1989)*.

2.5.2.2 Alpha-lactalbumin (α-la)

Another major protein α-la, is a globular calcium metallo–protein, which is stabilized by four intra–chain disulphide bonds and does not contain a free thiol group *(Swaisgood, 1982; Brew & Grobler, 1992)*. It denatures at a relatively lower temperature but does not aggregate because of absence of free thiol groups *(Dalgleish et al., 1997)*. Native α-lactalbumin has good emulsifying capabilities, but has poor gelation properties. Studies of the behaviour of whey proteins have shown that although α-la has poor gelation properties but it synergistically promotes the gelation behaviour of β-lg induced gels by protein cross–linking to form a cohesive film or hydrophobically bonded co-aggregates *(Fang et al., 2002)*.

It has been reported that the sulfydryl–disulphide interchange reaction occurs in β-lg or mixture of β-lg with α-la–stabilized emulsions, but not in pure α-la–stabilized emulsions *(Dickinson & Matsumura, 1991; Monahan et al., 1995; Damodaran & Anand, 1997)*. It has been clearly elucidated that once adsorbed, β-lg and α-la are capable of forming intermolecular *S–S* bridges in the interfacial layer of the emulsion droplets, which are not observed in solutions *(Dalgleish, 2004)*. However, it is interesting to note here, that when WPC or WPI is used to stabilize emulsions, there is no competitive adsorption between β-lg and α-la at the droplet surface regardless of the protein–to–oil proportions, unlike caseins *(Euston et al., 1996; Ye & Singh, 2000; Ye & Singh, 2006b)*.

2.5.2.3 Lactoferrin

Whey proteins also contain low levels of lactoferrin, a glycoprotein of molecular weight ~ 80 kDa, which has about 700 amino acid residues and well known for its iron binding capacities *(Baker & Baker, 2005)*. Lactoferrin has a unique

property of possessing high positive surface charge at neutral pH [isoelectric point (p*I*) ~ 8.0] unlike other milk protein fractions, which have p*I* ranging from 4.5 to 5.5, and consequently latter being negatively charged under the same conditions. This high positive charge density of lactoferrin has been predicted to allow the formation of cationic emulsion droplets over wide pH ranges *(Ye & Singh, 2006a)*. Recently, the adsorption behaviour of lactoferrin in oil-in-water emulsions at pH 7.0 to 3.0 was explored *(Ye & Singh, 2006a)*. Similar to other milk proteins such as caseinates and β-lg, lactoferrin adsorbed to the oil–water interface producing stable emulsion droplets with a net positive charge. In contrast to caseinates and β-lg, the lactoferrin–stabilized emulsions were stable over a wide range of pH from 7.0 to 3.0. The droplet sizes of lactoferrin emulsions were reported to be very similar to that of β-lg emulsions prepared under the same conditions of pH, oil–protein concentrations, and homogenization pressures. However, lactoferrin–stabilized emulsions had a comparatively higher surface coverage due to its relatively higher molecular weight.

Aqueous solutions of lactoferrin being highly positively charged has been shown to exhibit electrostatic complexation with anionic β-lg at neutral pH *(Wahlgren et al., 1993)*. Using the same theory, multilayered oil-in-water emulsions were produced by the electrostatic interactions of mutually oppositely charged milk proteins *i.e.* lactoferrin and β-lg complex at neutral pH at the droplet surface, resulting in stable emulsion droplets *via* thick interfacial layers, with greater amount of protein adsorption at the oil–water interface *(Ye & Singh, 2007)*. Initially the primary emulsion, containing either cationic (lactoferrin–coated) or anionic (β-lg–coated) droplets, was produced. The secondary emulsion was then made by adding either lactoferrin or β-lg solution to the primary emulsion based on mutually opposite charges. Interestingly, the overall charge of the emulsion droplets stabilized with the binary protein mixtures was close to zero at some concentrations. However, steric repulsion played a dominant role in such multilayered milk protein–stabilized emulsions, due to the dense interfacial films at the droplet surface, and thus protected the emulsion from flocculation and coalescence.

2.6 Influence of processing conditions on emulsions

During processing of formulated foods, the emulsions are generally subjected to a wide range of chemical (pH, ionic strengths, and interactions with other metabolites), physical (heat treatments, high pressure treatments) and biochemical (enzymes) challenges, which would largely influence their final emulsion stability.

The principal factors (pH, ionic strength and enzymatic treatments) influencing the physicochemical properties and stability of emulsion are discussed below:

2.6.1 pH

The pH of the continuous phase plays an important role, by affecting the ionization and surface charges of the emulsion droplets, and therefore significantly influences the droplet stability. Generally, most of the milk proteins have their p*I*, in the range of $4 < pH < 6$ (exception to lactoferrin, lysozyme *etc.*) at which, magnitude of positively charged groups becomes equal to the magnitude of negatively charged groups in the protein, and eventually the ζ-potential value of such protein coated droplet surface at p*I* becomes zero *(McClements, 2004; McClements, 2005)*. Hence, at pH ranges near p*I*, the emulsions are susceptible to extensive flocculation because the electrostatic repulsion between the droplets are not strong enough to overcome the predominant attractive interactions, such as van der Waals, hydrophobic or depletion forces *(McClements, 2004; McClements, 2005)*.

At pH values away from the p*I* of the protein, the droplet surfaces are highly electrically charged, which accounts for their emulsion stability and resistance to flocculation or coalescence *(Hunt & Dalgleish, 1994; Demetriades & McClements, 1998)*. Basically, at lower pH values ($pH < 4.0$) *i.e.* pH below the p*I*, most of the proteins have high positive ζ-potential magnitude as the amino groups (NH_3^+) are positively charged and carboxylic group (–COOH) are neutral. Similarly, when the pH is above p*I*, the magnitude of the positive charge on the droplets decreases, partly because carboxyl groups become negatively charged ($–COO^-$) and some of the amino groups become neutral ($–NH_2$). Hence the pH of

the continuous phase should be far away from the p*I* of the protein adsorbed to the droplets, in order to attain kinetic stability against aggregation and droplet creaming.

This characteristic of protein to acquire high charge potential below or above their p*I* has been largely utilized to prepare multilayered emulsions using protein as the primary stabilizing layer with another oppositely charged biopolymer (*e.g.* protein or polysaccharide) to form the secondary layer *via* successful manipulation of pH of the continuous phase of the primary emulsion droplets *(Gu et al., 2005; Güzey & McClements, 2006; Harnsilawat et al., 2006; Hong & McClements, 2007)*.

2.6.2 Ionic strength

Ionic strength may significantly influence the stability of emulsions in various ways primarily depending upon the valency, charge, concentration, and nature of ions available in the continuous phase *(McClements, 2005)*. Presence of salts either screens the charge of the protein–stabilized emulsions or the added ions may bind to oppositely charged groups on the droplet surface, reducing the ζ-potential magnitude and thus significantly decreasing the electrostatic repulsion between emulsion droplets, finally resulting in salt–induced aggregation effects.

This mechanism of salt–induced aggregation influencing the overall ζ-potential either by charge screening of the electrostatic repulsion between the protein–stabilized emulsion droplets by Ca^{2+}, Na^{+} and K^{+} salts or by ion binding to the droplet surfaces *(Agboola & Dalgleish, 1995; Kulmyrzaev et al., 2000; Güzey et al., 2004)* can be predicted by classical colloid science theory *(Hunter, 1986)*, which basically correlates the zeta potential (ζ) with the surface charge density (σ) as follows:

$$\sigma = -\mathrm{sgn}(\zeta)\sqrt{[2\varepsilon_o\varepsilon_R kT\sum n_i^{0}\{\exp(-z_i e\zeta / kT)-1\}]} \qquad \textbf{(2.6-1)}$$

where, ε_O is the dielectric constant of the vacuum, ε_R is the relative dielectric constant of the continuous medium, k is the Boltzmann's constant, T is the

absolute temperature, n_i^0 and z_i are the number per unit volume and valency of ions "*i*" respectively, *e* is the magnitude of electrical charge for a single electron and sgn describes the sign function i.e. sgn(x) = 0, if $x > 0$, and −1 if $x < 0$.

A number of studies have been performed to understand the effects of addition of different concentration and types of salts on emulsion characteristics, which are briefly summarized in the following subsections.

2.6.2.1 Monovalent cations

Addition of Na^+ *(Demetriades et al., 1997; Srinivasan et al., 2000)* and K^+ *(Hunt & Dalgleish, 1996; Kulmyrzaev & Schubert, 2004)* ions on the physicochemical characteristics of whey protein–stabilized emulsions have been explored. Authors have reported that presence of ≥ 150 mM NaCl can result in creaming and droplet flocculation in WPI–stabilized emulsions (28.0 wt% corn oil, 2.8 wt% WPI) by electrostatic charge screening effects *(Djordjevic et al., 2004)*. In presence of K^+ ions, whey protein–stabilized emulsions are stable to aggregation upto ~ 100 mM KCl, provided the pH is adjusted to < 4 or > 6 *(Kulmyrzaev & Schubert, 2004)*.

In case of sodium caseinate–stabilized emulsions, presence of K^+ or Na^+ ions not only influences the emulsion stability but also affects the surface composition and relative surface coverage of the individual casein fraction (α_{s1}-casein and/or β-casein). It has been observed that emulsions made with α_{s1}-casein are generally more susceptible to salt–induced flocculation by NaCl, showing extensive flocculation above 100 mM NaCl than that stabilized by β-casein, latter showing no aggregation under the same conditions *(Murray & Stainsby, 1987; Dickinson, 1997a)*. *Hunt and Dalgleish (1996)* reported that the addition of KCl > 25 mM concentration significantly influenced the adsorption behaviour of sodium caseinate to the droplet surface with relative increase in levels of adsorbed α_{s1}-casein at the expense of β-casein. Similar observations were also reported in the presence of NaCl *(Srinivasan et al., 2000)*. However, referring to relative surface concentration analysis, it appears that β-casein concentration at the interface remains largely unaffected by NaCl addition, whereas the surface concentration

of α_{s1}-casein increases substantially, indicating that the influence of ionic strength on emulsion stability also depends on the concentration and kind of the protein saturated at the droplet surface.

2.6.2.2 Divalent cations

A significant number of publications on the effects of Ca^{2+} ions *(Agboola & Dalgleish, 1995; Kulmyrzaev et al., 2000; Ye & Singh, 2000; Dickinson et al., 2003)* and to a lesser extent on Cu^{2+} ions *(Silvestre et al., 1999)* on flocculation of milk protein–stabilized emulsions have revealed important insights about the interactions of divalent cations with protein coated droplet surface. It was reported that the binding of Ca^{2+} ions to whey proteins reduces electrostatic repulsions and induces hydrophobic interactions *(Baumy & Brulé, 1988)*, which may unavoidably affect the adsorption behaviour of whey proteins to the droplet surface. The aggregation of β-lg–stabilized emulsion by added Ca^{2+} ions has also been reported due to the possible salting out of globular proteins *(Agboola & Dalgleish, 1995)*.

The effects of divalent cations on emulsion stability of WPC–stabilized emulsion droplets (30.0 wt% soy oil, 0.5 or 3.0 wt% WPC) have been studied *(Ye & Singh, 2000)*. In emulsions made with 3.0 wt% WPC, the emulsion stability decreased slightly at low $CaCl_2$ concentrations (< 15 mM), but markedly at higher Ca^{2+} concentrations (20 mM). This decrease in emulsion stability was explained by divalent cations inducing charge screening effects, resulting in flocculation and coalescence. Interestingly, in another study, the influence of both $CaCl_2$ (0 to 10 mM) and KCl (0 to 600 mM) in WPI–stabilized emulsions (7.0 wt% soy oil, 0.35 wt% WPI) at neutral pH was investigated *(Keowmaneechai & McClements, 2002)*. These authors reported extensive droplet flocculation and creaming instability of emulsions above critical $CaCl_2$ (3 mM) and KCl (200 mM) concentrations and also suggested that divalent Ca^{2+} ions are more effective than K^+ ions in causing droplet flocculation and creaming *via* charge screening effects.

In case of emulsions containing caseins as the adsorbed layer, calcium–induced flocculation has been demonstrated *(Dickinson et al., 1987; Agboola & Dalgleish, 1995; Dalgleish, 1997)*. Emulsions containing κ-casein were generally observed to be resistant to Ca^{2+}–induced aggregation. However, emulsions stabilized by either α_{s1}-casein or β-casein were generally flocculated by 15 mM $CaCl_2$ *(Dickinson et al., 1987)*, which can be explained by the specific binding of the Ca^{2+} ions to the negatively charged phosphoserine residues *(Swaisgood, 1982)* available on the α_{s1}-casein or β-caseins (not available in case of κ-casein), thus altering the molecular charge distribution, self–assembly behaviour and finally conformation of the adsorbed casein molecule. This conformational change possibly reduced the thickness of the interfacial layer, thereby decreasing the steric repulsion *(Horne, 1998)*. Hence, the calcium–induced flocculation in sodium caseinate emulsions is not only related to the screening of electrostatic droplet charges by divalent cations unlike whey protein, but also associated with the bound Ca^{2+} ions reducing the efficacy of steric stabilization and binding of Ca^{2+} ions between phosphoserine residues on casein–coated droplets causing bridging flocculation *(Horne & Leaver, 1995)*. It is worth noting that addition of a moderate concentration of $CaCl_2$ (5–8 mM Ca^{2+} ions) prior to homogenization can significantly enhance emulsion stability particularly in concentrated caseinate emulsion systems by inhibiting depletion flocculation *(Dickinson & Golding, 1998)*, which is an interesting observation as compared to well known destabilizing role of calcium salts.

2.6.3 Enzymatic hydrolysis

Enzymatic hydrolysis of milk proteins has received primary importance due to their extensive use in infant nutrition formulations and to encounter with allergenic proteins in specialized processed foods. Use of such enzymatic treatment before or after emulsification, particularly for the surfactant proteins (proteins used for stabilizing emulsions) can significantly affect the stability and properties of the emulsions *(Singh & Dalgleish, 1998)*. Hydrolysis of milk proteins generally influences the number of charged groups and average molecular weight due to the generation of low molecular weight peptides. These factors generally affect emulsion–forming and emulsion–stabilizing abilities of

milk protein hydrolysates *(Chobert et al., 1988; Agboola & Dalgleish, 1996; Caessens et al., 1999)*. It has been demonstrated that extensive hydrolysis (above 20% degree of hydrolysis) impairs the emulsion formation and stabilizing properties of whey proteins due to the poor emulsifying capacities of the shorter peptides resulting in weak interfacial layer, and thus providing little protection against coalescence *(Singh & Dalgleish, 1998)*. A study comparing the emulsion forming and stabilizing properties of casein and whey protein after being individually hydrolysed using 11 different commercially available enzymes also confirmed that the emulsion destabilization in both casein– or whey protein hydrolysate–stabilized emulsions was caused mainly due to coalescence *(van der Ven et al., 2001)*.

On the other hand, several authors have reported that the emulsifying capacities of whey proteins *(Chobert et al., 1988)* and caseins *(Haque & Mozaffar, 1992)* can be significantly improved by carrying out limited degree of hydrolysis of the parent proteins before emulsion formation. This low extent of hydrolysis allows better exposure of the hydrophobic groups for adsorption to the droplet surface and retains higher molecular weight peptides to form stable films at the interface, thus improving the emulsifying properties *(Panyam & Kilara, 1996; Sanchez et al., 1997; Foegeding et al., 2002)*. Even, fairly stable emulsions can be formed with highly hydrolysed whey proteins (27% degree of hydrolysis) as the sole emulsifier, by careful manipulation of peptide concentrations (1:1 w/w peptide–to–oil ratio) and lowering the homogenizing pressures during emulsion formation *(Agboola et al., 1998a)*. Under these conditons, sufficient quantities of high molecular weight peptides (> 5 kDa) are present at the interface to protect the emulsion droplets against coalescence. Although, the relatively high molecular weight peptides remaining in whey protein hydrolysate either by limited proteolysis or by increasing the peptide concentrations might be sufficiently surface active to protect emulsions against creaming over storage, they are generally incapable of preventing destabilization of emulsions during processing conditions, such as retort treatments *(Agboola et al., 1998b; Singh & Dalgleish, 1998)*.

2.7 Behaviour of emulsions under physiological conditions

A great deal of information is now available on the adsorption phenomena, conformation of proteins at the oil–water interface, competitive exchange reactions between adsorbed and unadsorbed proteins and factors controlling rheology and stability of emulsions *(Dickinson & Stainsby, 1988; McClements, 2004; McClements, 2005; Singh, 2005)*, as discussed in the previous sections of this review.

In contrast, understanding of the behaviour of emulsions during their passage through the physiological conditions is currently limited *(Dickinson, 2008)*. In general, on ingestion, an emulsion is exposed to a range of physical and biochemical environments, as it passes through the human body; some factors are illustrated in Figure 2.7-1.

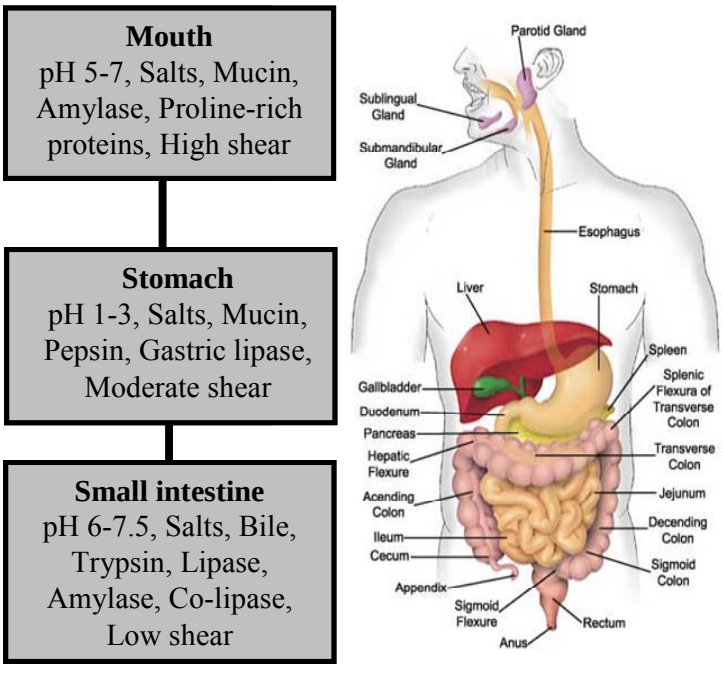

Figure 2.7-1: Schematic representation of the critical physiological factors that might influence emulsion behaviour as they pass through the gastrointestinal tract [adapted from *(Singh et al., 2009)*].

It is critical to gain insights about the oral behaviour of emulsions, to predict the sensorial attributes, such as creaminess, smoothness and flavour release in food matrices. Similarly, understanding the structural changes of the emulsions during their gastrointestinal passage could allow control of lipid digestion, increase the bioavailability of lipid soluble bioactives, such as carotenoids, phytosterols, fat soluble vitamins and/or reduce the absorption of unhealthy fats, such as saturated fats, *trans* fats and cholesterol *(McClements et al., 2008; Singh et al., 2009)*. Hence, this research area of physiological processing of emulsions needs to be intensively unravelled.

2.7.1 Oral processing

On ingestion, the properties and structure of a food matrix undergo significant changes due to the complex physical and biochemical events that occur in the human oral regime *(Malone et al., 2003a; Malone et al., 2003b; Chen, 2009)*. When a liquid food emulsion is consumed, it resides for a few seconds in the mouth. During this short residence time, the emulsion is generally subjected to a range of processing conditions, including mixing with saliva and air, heating or cooling to body temperature and shear between the epithelial surfaces of the tongue and the oral palate. In addition, the emulsion is exposed to salivary enzymes, various biopolymers such as mucins, changes in the ionic environment because of different electrolytes in the saliva and a moderate change in pH *(Glantz, 1997; Bardow et al., 2000; Malone et al., 2003a; Malone et al., 2003b; de Wijk et al., 2004; de Wijk & Prinz, 2005)*. The perceived taste, texture and flavour release of an emulsion largely depend on the initial composition of the emulsion and also on the way it behaves in the mouth *(Singh et al., 2009)*. Hence, it can be interpreted that emulsions interact with the complex salivary components and also experience a shear effect in the mouth.

2.7.1.1 Salivary components

Human saliva is a highly complex biological fluid, consisting mainly of water (~ 99.5%), various proteins (~ 0.3%), small organic compounds and inorganic compounds (strong and weak ions) (Table 2.7-1) contributing to its buffering

capacity and has a pH of around 6.8 *(Zalewska et al., 2000; Gal et al., 2001; Humphrey & Williamson, 2001; Schipper et al., 2007)*.

The proteins in saliva mainly include salivary enzymes, immunoglobulins, antibacterial proteins, proline–rich proteins, lysozyme, lactoferrin, peptides such as histatins and cystatins and highly glycosylated mucin *(Humphrey & Williamson, 2001; Amado et al., 2005; Hu et al., 2007)*. Detailed physiological analysis of human saliva can be found in a number of reviews *(Aps & Martens, 2005; Dodds et al., 2005; Chiappin et al., 2007; Schipper et al., 2007)*.

Table 2.7-1: Composition of whole human saliva [adapted from *(Aps & Martens, 2005)*].

Salivary components	Concentration in whole human saliva (mmol/L)	
	Stimulated	*Unstimulated*
Inorganic		
Na^+	5	20–80
K^+	22	20
Cl^-	15	30–100
Ca^{2+}	1–4	1–4
HCO_3^-	5	15–80
PO_4^{3-}	6	4
Mg^{2+}	0.2	0.2
SCN^-	2.5	2.0
NH_3	6	3
Organic		
$(NH_2)_2CO$	3.3	2–4
Protein (g/L)	3	3

Intuitively, one might expect that the pH, ionic composition and the organic compounds present in the saliva could significantly influence the emulsion behaviour. One of the most important organic constituents of saliva is mucin, which is expected to directly interact with protein–stabilized emulsions. This has been described in the following subsection.

2.7.1.1.1 Salivary Mucins

Salivary mucins are generally highly glycosylated extracellular proteins containing ~ 50–80% oligosaccharides mainly *N*–acetylgalactosamine, *N*–acetyl glucosamine, fucose, galactose, and sialic acid (*N*–acetylneuraminic acid) and traces of mannose and sulphate attached by *O*–glycosidic bonds to the hydroxyl groups of serine and threonine residues of the protein backbone, finally clustered in a "bottle brush" arrangement *(Thomsson et al., 2002; Bansil & Turner, 2006)*. Mucins generally account for ~ 10–25% of total salivary protein with high molecular weights ranging from 0.5 to 20 × 10^3 kDa, providing the typical viscoelastic behaviour to the saliva *(Rayment et al., 2000; Bansil & Turner, 2006; Schipper et al., 2007)*. The concentration of high molecular weight mucin (MUC 5B) in whole saliva varies approximately from 30 to 500 μg/mL depending on the stimulus.

Recently, a few studies on the effects of mixing unstimulated human saliva with emulsions stabilized by various proteins and surfactants, such as Tween, WPI, sodium caseinate and lysozyme, have been conducted *(van Aken et al., 2005; Vingerhoeds et al., 2005; Silletti et al., 2007a; Silletti et al., 2007b)*. The emulsion flocculation in presence of saliva was estimated to be regulated by depletion, van der Waals forces and/or electrostatic interactions between emulsion droplets and salivary proteins, and was largely dependent on the initial charge of the emulsion droplets *(Vingerhoeds et al., 2005; Silletti et al., 2007a; Silletti et al., 2007b)*. Mucins have been shown to play an important role in the flocculation of emulsions because of their negative charge at neutral pH. Although, mucin was mainly responsible for inducing flocculation, some irreversible aggregation occurred in emulsions even when mixed with parotid saliva *(Vingerhoeds et al., 2005)*, in which mucin concentration was almost negligible. Therefore, it appears salivary components other than mucin (salivary salts, proline–rich proteins *etc.*) might also contribute to flocculation phenomena in protein–stabilized emulsions in the oral environment by some unknown mechanisms.

2.7.1.2 Tribology

Apart from the role of saliva, the function of tribology, (*i.e.* study of friction and lubrication) in the field of oral processing of food *(Dresselhuis et al., 2007)* is gradually gaining importance. Upon swallowing a liquid food, the tongue is pressed against the oral palate giving a frictional effect *(Malone et al., 2003a)* and the saliva providing the lubrication *(Vingerhoeds et al., 2009)*. Despite, a number of attempts to mimic the oral surfaces and shear patterns in the mouth to understand the oral behaviour of emulsions, successful simulations have not yet been achieved. *In vitro* friction testers using tetrafluoroethylene (PTFE) and zirconium, respectively, as pin–on–disk *(Lee et al., 2004)* or a steel ball and silicon rubber as ball–on–disk *(Malone et al., 2003a)* set ups have been built to understand the adhesion, friction, and lubrication. Several authors have tried to modify the artificial surfaces by fabricating the roughness *(Cassin et al., 2001)*. Due to the large dissimilarities between artificial surfaces and human oral mucosa, pig's tongue has also been used to elucidate the effect of surface characteristics on the emulsion behaviour *(Dresselhuis et al., 2007; Dresselhuis et al., 2008)*. However, the use of animal tissues for tribological studies might not be practical due to individual variations in tissue structure, limited availability and fast tissue degradation.

Clearly, there is little knowledge about the influence of each salivary component and physicochemical factors such as pH, ionic strength and shear on emulsion droplet behaviour during consumption. Moreover, large variations exist in the quantity, composition and biochemical properties of saliva for a given individual at different times, as well as between different individuals *(Vingerhoeds et al., 2005)*. Therefore, the human saliva–emulsified lipid interactions are also expected to show intra– and inter–individual variations. Hence, to unravel the fundamental mechanisms of emulsion interactions during oral processing, artificial saliva formulations under more controlled systems need to be designed.

2.7.2 Gastric processing

After residing for a few seconds in the mouth, the emulsions are swallowed, which involves exposure to intense shear effects in pharynx, oesophagus and

finally stomach *(Weisbrodt, 2001b)*, and the behaviour of emulsion droplets during this integrated movement is largely unknown. The emulsion would remain in the stomach for a short period (from a few minutes to a few hours) depending on the nature of the food (*e.g.* chemical composition, droplet size, microstructure, pH, ionic conditions and rheological properties) *(Malagelada & Azpiroz, 1989)*. In the gastric tract, the emulsion is mixed with the digestive juices at a highly acidic pH containing various minerals, enzymes (both proteolytic and lipolytic) and also subjected to mechanical agitation due to peristalsis in the stomach *(Weisbrodt, 2001a; Ekmekcioglu, 2002; Kalantzi et al., 2006; Pal et al., 2007)*. Some of the important factors, possibly affecting emulsion stability during gastric processing, are discussed below:

2.7.2.1 Acidic pH and ionic strength

The pH of fasted human stomach ranges from 1–3 *(Ekmekcioglu, 2002; Kalantzi et al., 2006)*. However, the pH varies significantly depending on the composition and quantity of ingested food and also differs among individuals *(McClements et al., 2009; Singh et al., 2009)*. Generally, the pH of the stomach first increases from ~ 1.7 to ~ 6.0 immediately after consuming a neutral liquid meal, before returning back to the highly acidic fasting value of the stomach *(Kalantzi et al., 2006)*, owing to the meal–stimulated secretion of gastric acid *(Gardner et al., 2002)*. During this gradual decrease in pH from neutral to acidic, most of the milk protein–stabilized emulsions are expected to undergo substantial changes in droplet characteristics in terms of incomplete to full charge reversal as well as some possible aggregation effects around the p*I*, as p*I* ranges from ~ 4.5–5.2 for most of the milk proteins *(Singh et al., 2009)*.

Generally, the osmolality and ionic strength of fasted state (empty stomach condition) are ~ 190 mOsm/kg and ~ 100 mM respectively with concentration of important ions being: Na^+: 70 ± 30 mM, K^+: 13 ± 3 mM, Ca^{2+}: 0.6 ± 0.2 mM, and Cl^-: 100 ± 30 mM. *(Lindahl et al., 1997)*. When the meal enters into the stomach, there is a significant change in the osmolality and ionic strength of the stomach contents due to addition of more ions and solutes from the meal as compared to that of the fasted state. Authors have reported that the osmolality of stomach

increases from ~ 140 mOsm/kg in an empty stomach to ~ 560 mOsm/kg in fed state (after consuming a liquid meal). Osmolality gradually decreases as a function of gastric emptying time *(Kalantzi et al., 2006)*. High ionic strengths might contribute to electrostatic changes in the protein–stabilized emulsions, which might result in salt–induced aggregation of emulsion droplets, especially with reference to protein–stabilized droplets.

Clearly, the drastic change in pH and ionic strength in the stomach could result in changes in emulsion droplets *via* flocculation or change in the interfacial layers.

2.7.2.2 Biochemical factors

Apart from the variable pH and ionic strengths, the protein–stabilized oil-in-water emulsions are also exposed to various biochemical agents, mainly enzymes (pepsin, and gastric lipases), gastric mucin, other partly digested food or residual food components of the previous meal (*e.g.* proteins, polysaccharides, phospholipids *etc.*), which might result in modification of the adsorbed protein layers and droplet characteristics, finally affecting the emulsion stability.

2.7.2.2.1 Pepsin

Pepsin is a protease, which preferentially cleaves the peptide bonds involving aromatic amino acids (phenylalanine, tyrosine and tryptophan), and other hydrophobic residues (such as leucine) and to a lesser extent bonds involving acidic amino acids (such as glutamic acid) *(Tang, 1963; Weintraub et al., 1971; Lehninger et al., 1993; Sweeney & Walker, 1993; Blackman, 1994)*. However, pepsin does not cleave bonds containing valine, alanine or glycine.

Caseins, owing to their flexible random coil structure, are highly susceptible to hydrolysis by pepsin in their native state *(Modler, 1985; Guo et al., 1995)*. However, whey proteins particularly β-lg, because of its highly folded globular conformation, is largely resistant to gastric digestion as well as *in vitro* peptic hydrolysis in its native state *(Reddy et al., 1988; Schmidt & Poll, 1991; Schmidt & van Markwijk, 1993)*. Modifications of the native structure, using thermal and chemical treatments of β-lg solutions to render them accessible to physiological

enzymes, have been extensively studied *(Reddy et al., 1988; Guo et al., 1995; Kananen et al., 2000; Chevalier et al., 2002)*. However, little information on the conformational changes of *β*-lg in the adsorbed state with respect to its proteolytic digestion, especially at pH 1–2 by pepsin, is available in the literatures. Milk protein–stabilized emulsions would supposedly undergo major physicochemical changes in the stomach in terms of droplet aggregation or coalescence due to the possible action of pepsin on the interfacial layer.

2.7.2.2.2 Gastric lipase

Limited degree of lipolysis (~ 10–30%) of the ingested triacylglycerols occurs in the stomach, which can be mainly attributed to the gastric lipase activity *(Armand, 2007; Armand et al., 1994; Armand et al., 1999; Bauer et al., 2005; Carrière et al., 1993; Layer & Keller, 2005; Pafumi et al., 2002)*. Human gastric lipase, secreted by the chief cells located in the fundic mucosa of the stomach *(Moreau et al., 1988; Moreau et al., 1989)* is a globular glycoprotein of molecular weight ~ 50 kDa and is generally stable over a broad range of pH values (pH 2–7) *(Mukherjee, 2003; Bauer et al., 2005; Carrière et al., 2005; Armand, 2007)*.

Generally, gastric lipases are known to hydrolyse emulsified triglycerides containing medium chain fatty acids better than that of the ones with long chain fatty acids *(Mu & Hoy, 2004)*. They preferentially cleave at sn–3 ester bonds of triacylglycerols resulting in sn–1, 2 diacylglycerols and free fatty acids *(Moreau et al., 1988; Armand et al., 1996a; Carrière et al., 2005)*. Some of these lipid digestion products could competitively displace the initial emulsifier materials from the emulsion interface either fully or partially *(Armand et al., 1994; Pafumi et al., 2002)*. Moreover, the initial extent of lipolysis by gastric lipases in the stomach has also been proposed to facilitate subsequent hydrolysis by pancreatic lipase in the intestines *via* promoting droplet break–up, stimulating hormonal release, increasing binding of colipase and solubilizing the lipid digestion products *(Mu & Hoy, 2004; Bauer et al., 2005)*.

However, gastric lipases, normally present at 0.5–1 μM levels in human stomach *(Mcclements et al., 2009)* are assumed to play an insignificant role quantitatively, where lipid digestion in healthy human adults is concerned *(Fave et al., 2004; Bauer et al., 2005; Layer & Keller, 2005)*. They are reported to be substantially functional for individuals suffering from pancreatic lipase insufficiency. Moreover, these acid-stable lipases are positively charged in the harsh acidic pH of the gastric conditions, as their p*I* varies from 6.6 to 7.9 depending on their isoforms *(Miled et al., 2005)*. The quantitative importance of gastric lipase in lipolysis of ingested milk protein–stabilized emulsions in healthy human adults remains to be elucidated.

2.7.2.2.3 Gastric mucin

The presence of highly glycosylated mucin (molecular weight > 10^6 kDa), which forms a self–associated gel–like structure at gastric conditions (pH 1–3 and at high mucin concentrations of ≥ 20 mg/ml) has an important physiological role of protecting the stomach from digesting itself *(Nordman et al., 2002; Lee et al., 2005; Bansil & Turner, 2006)*. Importantly, mucin is the first barrier, with which any nutrient molecule must interact *(Bansil & Turner, 2006)*. Mucins are largely charged species, due mainly to the glutamic acid and aspartic acid residues in the polypeptide backbone ($pK_a \approx 4$) *(Cao et al., 1999)* as well as the sialic acid residues ($pK_a \approx 2.6$) and sulphate groups ($pK_a \approx 1$) present in the oligosaccharide side chains *(Waigh et al., 2002)*.

Recently, *Lee et al. (2005)* investigated the role of ionic strength and pH on the conformation of pig gastric mucin and its binding properties to polydimethylsiloxane (PDMS) surfaces. Authors predicted that the p*I* of mucin roughly lies between 2 and 3, indicating that the net charge on the mucin molecule significantly varies as the pH is altered. *Lee and others (2005)* explained the adsorption mechanism of mucin to PDMS on the basis of hydrophobic binding sites of polypeptide backbone of mucin which becomes anchored to the PDMS surface. It was reported that at pH 2, the tertiary structure of protein part of the mucin was altered (as pH was around p*I*), which exposed the hydrophobic groups, thus allowing stronger binding of mucin to the PDMS

surfaces. Therefore, it might be expected that mucin can act as a potential surface active agent, competitively displacing or binding to the protein interfaces in emulsified lipid during gastric digestion, thus altering the droplet behaviour.

Although a great deal of work on molecular approaches to enhance mucoadhesion, including, polyelectrolytic interactions (chitosans, poly–acrylic acid, *etc.*) or hydrogen bonds (hydrogels) *(Harding et al., 1999)*, and disulphide binding (thiolated polymers) *(Bernkop-Schnürch et al., 1999; Leitner et al., 2003)* has been carried out in pharmaceutical sciences; the interactions (if any) between gastric mucin and emulsified food lipids are still largely unknown.

In general, several systematic studies have been carried out on the behaviour of drug based micro–emulsions in gastrointestinal tract *(Calvo et al., 1997; MacGregor et al., 1997; Anal et al., 2003; AnnMarie et al., 2004)*. In contrast, the behaviour of food based emulsion droplets in gastric lumen remains largely unexplored. Although *in vitro* enzymatic digestion studies have been reported in food systems *(Gauthier et al., 1986; Picot & Lacroix, 2004)*, but no systematic studies on the flocculation or disruption behaviour of milk protein–stabilized emulsion droplets in the complex gastric environments (effects of variable pH, ionic strengths, pepsin and mucin) together with the role of peristaltic shear effects have been reported to date. Intuitively, some of the simulation approaches used in pharmaceutical research might be intelligently applied in food emulsion science to gain insights about the behaviour of the food colloids, when interacting with the gastric secretions.

2.7.3 Duodenal processing & lipid digestion

Once the emulsion passes from the stomach into the small intestine, the partially digested emulsified lipids are subjected to various salts, pancreatic enzymes, coenzymes and surface active agents (bile salts, phospholipids) secreted by the liver, gall bladder and pancreas in an alkaline condition *(Tso, 2000; McClements et al., 2009; Singh et al., 2009)*.

2.7.3.1 Alkaline pH and ionic strength

Generally, sodium bicarbonate is secreted in the small intestine to cause the pH to increase from highly acidic conditions (pH 1–3) in the stomach to nearly alkaline conditions (pH 6–7.5) in the duodenum, where the pancreatic enzymes can act effectively *(Bauer et al., 2005)*. During this drastic increase in pH, most of the protein–stabilized emulsions would be expected to be reverted back to their anionic form, with some possible aggregation while passing through their p*I* zone.

The osmolality and ionic strength of fasted duodenum is 180 mOsm/kg and 140 mM, respectively *(Lindahl et al., 1997)*. The osmolality of duodenum increases from ~ 180 mOsm/kg in fasted state to ~ 290 mOsm/kg in fed state (after ingestion of a nutrient drink), with the osmolality gradually decreasing over time *(Kalantzi et al., 2006)*. Both pH and ionic strengths are particularly important parameters as they might affect the electrostatic interactions of charged emulsified lipid droplets.

2.7.3.2 Biochemical factors

The possible interactions between emulsion droplets and intestinal components can be highly complicated as the intestine is the house to many enzymes, such as proteases and peptidases (trypsin, chymotrypsin, carboxypeptidases, *etc.*), lipases and esterases (pancreatic lipase, cholesterol esterase, phopholipase A_2, *etc.*) and pancreatic amylases *(Singh et al., 2009)*. Furthermore, the adsorbed layer surrounding the lipid droplets may change significantly, on entering the small intestine due to the secretion of not only surface active bile salts, but also the generation of various hydrolytic products of acidic nature, such as surface active monoacylglycerols and fatty acids (generated by lipolysis of triglycerides), peptides and oligosaccharides *(Bauer et al., 2005; Kalantzi et al., 2006)*.

2.7.3.2.1 Intestinal proteases

Protein–stabilized emulsions may undergo substantial alteration due to proteolysis of the interfacial layer by trypsin and/or chymotrypsin. Serine proteases, particularly trypsin predominantly catalyses the peptide chains at *C*–terminal of aliphatic amino acids mainly lysine and arginine, whereas

chymotrypsin favours large aromatic residues, such as phenylalanine, tyrosine, and tryptophan *(Vajda & Szabó, 1976; Honey et al., 1984; Olsen et al., 2004; Ma et al., 2005)*. Over the last few decades, several studies have reported the effects of hydrolysis of protein–stabilized oil-in-water emulsions by trypsin *(Shimizu et al., 1986; Kaminogawa et al., 1987; Leaver & Dalgleish, 1990)*, detailing on peptides generated and their respective functionalities *(Turgeon et al., 1992)*. The inability of the peptide films to provide effective surface coverage, resulting in coalescence of droplets, has also been explored *(Agboola & Dalgleish, 1996)*.

However, the complex interactions of these proteases with the adsorbed proteins in presence of pancreatic lipases and bile salts have not been unravelled as yet.

2.7.3.2.2 Bile salts

Bile salts originate from the liver *via* gall bladder, which basically facilitate emulsification by adsorbing to the droplet surface *(Tso, 2000)*. They are synthesized from cholesterol and contain cholic acid as the "backbone" conjugated with amino acids taurine or glycine to form taurocholates and glycocholates respectively *(Bauer et al., 2005)*. In humans, bile salts are the surface active mixtures of mainly sodium salts of taurocholic, taurodeoxycholic, taurochenodeoxycholic, glycocholic and glycodeoxycholic acids respectively, and these can possibly displace the adsorbed materials from the surface of emulsion droplets, thus promoting the accessibility of active site of lipase to the hydrophobic lipid core *(Wickham et al., 1998; Fave et al., 2004; Mun et al., 2006)*. Broadly, the surface activities of interfacial material adsorbed on the emulsion droplets and the thickness of the adsorbed layer dictate the displacement mechanism of bile salts *(Singh et al., 2009)*.

Recently, *Mun et al. (2006)* reported that bile salts displace whey proteins more readily than caseinates from the interface of emulsion droplets during storage. Dependence of bile salt–induced displacement mechanisms on the nature of adsorbed layer was further supported by another study, where the digestibility of adsorbed milk proteins in simulated gastrointestinal conditions was investigated *(Macierzanka et al., 2009)*. The *in vitro* digestibility of *β*-lg– and *β*-

casein–adsorbed surfaces was compared with or without the addition of surfactants (bile salts and phosphatidyl choline). *Macierzanka and others (2009)* reported that the final structure of the *β*-lg–stabilized interface was largely driven by competitive displacement by bile salts and/or phosphatidyl choline in contrast to adsorbed *β*-casein, where the gastric hydrolysis by pepsin was the major cause of destabilization for *β*-casein–stabilized interface. In another study, the competitive displacement of *β*-lg by bile salts from air–water and oil–water interfaces was investigated in an *in vitro* duodenal model *(Maldonado-Valderrama et al., 2008)*. These authors suggested that bile salts might completely displace the *β*-lg from the interface, when passing through the duodenum *in vivo*, which in turn would affect the rate of lipid digestion in case of *β*-lg–stabilized emulsified droplets.

A typical range of bile salt concentrations found in the healthy human small intestine varies from 4 to 6 mM and from 10 to 20 mM in the fasted and fed states respectively *(Porter & Charman, 2001; Rich et al., 2003; Wright et al., 2008)*. At low concentrations, bile salts promote lipase activity mainly by allowing the adsorption of lipase to the oil–water interface *(Gargouri et al., 1983; Mun et al., 2007)*. Moreover, bile salts also solubilize the lipid hydrolytic products (fatty acids, monoacylglycerols, *etc.*) and remove these inhibitory reaction products from the oil–water interface, thus allowing the lipase to have access to the triacylglycerols within the emulsion droplets *(McClements et al., 2009)*. However, at higher concentrations, the bile salts generally compete with lipases for the oil–water interfaces, inhibiting the point of contact between the non–polar lipid core and lipase *(Gargouri et al., 1983)*, thus retarding lipase activity. Hence, the presence of bile salts may either facilitate or inhibit the activity of pancreatic lipase depending on their concentration *(Lowe, 2002; Bauer et al., 2005)*. Monoacylglycerols, diacylglycerols and fatty acids generated from the hydrophobic core of the emulsion droplets by the action of pancreatic lipase also play an important role in the interfacial displacement mechanisms *(Mun et al., 2007; McClements et al., 2009; Singh et al., 2009)*.

2.7.3.2.3 Pancreatic lipase

The majority of lipid digestion (~ 70–90%) occurs in the upper part of the intestine *(Fave et al., 2004; Bauer et al., 2005; Mun et al., 2006)*. Partially hydrolysed lipids enter the small intestine as fine droplets less than 0.5 μm, largely due to the peristaltic shear–induced disruption in the stomach *(Carey et al., 1983)*. However, it has been suggested that the lipid droplet size in the duodenum typically varies from 1–50 μm *(Armand et al., 1996a)*. Once the lipid droplets enter the intestine, pancreatic lipase adsorbs to the droplet interface usually by a complexation with colipase and/or bile salts *(Bauer et al., 2005)*. Colipase is a short polypeptide of molecular weight ~ 10 kDa, which forms a stoichiometric complex with lipase in the ratio of 1:1 w/w, allowing the pancreatic lipase to anchor firmly to the substrate (hydrophobic lipid core) at the oil–water interface *(Patton et al., 1978; Erlanson-Albertsson, 1992)*. Colipase is a coenzyme, which is an amphiphilic molecule; its hydrophobic residues are assumed to be bound to the oil phase of the emulsified droplets and hydrophilic side is bound to the lipase *(Bläckberg et al., 1979)*. This orientation facilitates anchoring of the lipase's active site to its substrate. Presence of this coenzyme has been also assumed to remove the inhibitory effects of bile salts and phospholipids *(Crandall & Lowe, 2001)*.

As compared to gastric lipase in the stomach, pancreatic lipase has a pH optimum of ~ 8–9 *(Patton & Carey, 1981)*, but acts even at pH 6.5 and has little specificity for fatty acid chain length *(McClements et al., 2009)*. Pancreatic lipase cleaves triacylglycerols to form 2–monoacylglycerols and fatty acids. The diacylglycerols, monoacylglycerols, free fatty acids, thus released as digestion products, might be adsorbed at the droplet surface displacing the initial adsorbed moieties from the interface *(McClements et al., 2008; McClements et al., 2009; Singh et al., 2009)*. This competitive exchange of interfacial layer by the lipid digestion products, which in turn depends on the relative concentrations and surface activities of the adsorbed layer, makes the composition of the adsorbed layers even more complicated to understand. In general, the compounds with higher surface activities would be expected to dominate the interface.

Currently, there is very limited understanding about the fundamental mechanisms of interactions of different intestinal surface active agents, which might influence the kinetics of interfacial exchange of emulsified lipids, and thereby affect lipid digestion. Hence, further research is clearly required.

2.8 Controlling lipid digestion

The interactions between the adsorbed layers and the lipase and/or bile salts are critical in controlling the rate of lipid hydrolysis. These interactions would largely depend on the emulsion droplet size, initial interfacial layer composition, physical state of the lipid core, presence of dietary fibres and/or other lipid–binding materials *(McClements et al., 2009; Singh et al., 2009)*.

2.8.1 Droplet size

The droplet size of the emulsion determines the specific surface area of lipids exposed to the aqueous phase, which could impact the rate of lipid digestion by the gastrointestinal enzymes. Therefore, one would expect that by lowering the emulsion droplet size, there would be a proportionately larger surface area of exposed lipids available for lipases to bind, and, thus higher will be the overall rate of lipolysis *(McClements et al., 2009; Singh et al., 2009)*. The droplet size in the intestine will further depend on the initial droplet size as well as the disruption, flocculation and/or coalescence experienced by the emulsified lipids during their passage through the oral– to–gastrointestinal environments.

In an *in vitro* study, it has been shown that the rate of lipid hydrolysis was an inverse function of the average emulsion droplet size *(Armand et al., 1992)*. An emulsion with a smaller droplet size was more rapidly hydrolysed than the emulsion with a larger droplet size, which was largely explained to be a surface area phenomenon *(Borel et al., 1994)*. However, the droplet size did not affect the affinities of pancreatic lipase. This *in vitro* study was further confirmed by *in vivo* trials, injecting emulsions directly into the stomach *(Borel et al., 1994; Armand et al., 1999)*, which also suggested that the rate and extent of lipid digestion in the duodenum was principally controlled by the initial size of emulsion droplets. Depending upon the droplets size, the degree of triglyceride

hydrolysis varied from ~ 5 to 37% and ~ 30 to 75% in the stomach and duodenum, respectively. The increase in lipolysis in case of smaller sized droplets was assumed to be due to larger lipid–water interfacial area available for the lipase molecules to bind to the emulsified lipid droplets.

Typically, the mean droplet diameter of food emulsions varies from 0.1 to 100 μm *(McClements, 2005)*. However, as seen in the previous sections, the droplets size may either increase or decrease during its transit through the gastrointestinal tract, depending upon the relative importance of physical, enzymatic and chemical processing resulting in flocculation, coalescence, droplet disruption, dissolution, breakdown and enzymatic digestion *(Armand et al., 1999; Fave et al., 2004; Bauer et al., 2005)*. Interestingly, it has been shown that the destabilized emulsions, which tend to aggregate and/or coalesce leading in the stomach, give rise to a feeling of satiety *(Norton et al., 2007)*. The mechanism of feeling of fullness in case of unstable emulsion might be instinctively explained in terms of reduction of the overall surface area of the emulsions during aggregation or coalescence, thus potentially influencing the accessibility of gastric lipase and reducing the rate of lipid digestion and assuming a state of fullness *(Armand et al., 1999)*. Nevertheless, it has been predicted by a different mechanism which states that the coalesced droplets would interact with the stomach receptors and send signals to the brain, giving a feeling of satiety *(Norton et al., 2007)*.

However, it has also been reported that the lipid droplets in human milk (average droplet size 4.0 μm) were more readily digested by gastric lipase, as compared to that in infant formula (average droplet size 0.6 μm) in premature infants *(Armand et al., 1996b)*, which indicates that there are some other factors influencing lipid hydrolysis.

2.8.2 Interfacial layer

The initial interfacial layer influences lipid digestion essentially by altering the stability of the emulsified lipid droplets in the mouth, stomach and intestines. The interfacial layer also affects the ability of gastric and/or pancreatic lipases to

adsorb to the lipid droplet surface *(McClements et al., 2009)*. Interestingly, the final droplet size, which an emulsion acquires in the small intestines, is also shown to be largely affected by the kind of emulsifier initially present at the oil–water interface. For example, phospholipid–stabilized emulsion droplets showed a mean droplet diameter of ~ 10–20 μm in the duodenum due to coalescence or droplet disruption phenomena, irrespective of their initial droplet size *(Armand et al., 1999; Fave et al., 2004; Bauer et al., 2005)*. However, milk protein–stabilized emulsions showed that emulsion droplets remained small during the entire digestion process, because the milk protein molecules were strongly adsorbed at the interface, providing significant emulsion stability during physiological processing *(Armand et al., 1996b; Michalski et al., 2005)*.

A number of studies have been attempted to gain insights into the mechanisms, by which initial emulsifier type affects the ability of lipases to hydrolyse emulsified lipids. Several surface active agents, such as small molecular detergents *(Gargouri et al., 1983)*, phospholipids *(Wickham et al., 1998)* and proteins *(Ivanova et al., 1990)* have been shown to inhibit the activity of lipase by fully or partially displacing the lipase molecules at the oil–water interface, thus reducing the possible point of contact between the lipase and the hydrophobic lipid core. Recently *Mun and others (2007)* showed that the emulsion droplet characteristics during *in vitro* pancreatic hydrolysis was strongly dependent upon the initial emulsifier type (WPI, caseinates, lecithin or Tween 20) stabilizing the droplets, with the WPI–stabilized emulsions being the least stable and Tween-20 emulsions being the most stable to droplet flocculation and coalescence. The droplet coalescence in WPI–stabilized emulsions was mainly explained on the basis of competitive adsorption by lipase, bile extract and/ or fatty acids and monoglycerides (digestion products generated by lipase catalysed hydrolysis of the lipid core), which possibly displaced the whey protein from the oil–water interface and thus, the emulsions had little protection against coalescence *(Mun et al., 2007)*. Moreover, the presence of possible trypsin and other proteolytic fractions in the commercial lipase used in this investigation might have caused proteolysis of the adsorbed protein *(Singh et al., 2009)*. Since, interfacial Tween 20 was expected to be more surface active than bile and/or

lipase digestion products *(Mun et al., 2007)* and was also not catalysed by proteases, Tween 20–stabilized emulsion droplets were more stable against lipase–induced coalescence.

However, in another recent *in vitro* trial, *Hur et al. (2009)* studied the interactions between emulsions stabilized by different emulsifiers (*i.e.* lecithin, Tween 20, WPI isolate and sodium caseinate) and total oral–to–gastrointestinal simulation model (a fairly complex system mimicking the pH, electrolytes, surface active components, biopolymers and enzymes of the mouth, stomach and intestines respectively) and inferred that the initial emulsifier used to stabilize the oil–water interface only had a limited effect on the physicochemical and structural changes that occurred during passage of lipid droplets though the artificial digestion model. This was explained on the basis of the competitive displacement of the adsorbed initial emulsifiers by the phospholipids/bile salts and/or surface active lipid digestion products as well as the enzymatic hydrolysis of proteins and lipids, regardless of the initial emulsifier type at the droplet surface *(Hur et al., 2009)*.

Modulation of the interfacial layer by thermal denaturation or by using a mixture of caseinate and resistant starch may also influence the degree of triglyceride hydrolysis as compared to emulsions stabilized by caseinates alone *(Chung et al., 2008)*. Heat treatment of caseinates before emulsion formation increased the lipolysis of the caseinate stabilized emulsions. However, thermal treatment of mixture of caseinate and modified starch reduced the lipolysis of emulsions.

There is a clear need of further research in this area to have a better understanding of the role of initial emulsifier in determining the droplet stability throughout the oral–to–gastrointestinal transit and influencing the competitive displacement mechanisms occurring in the intestine. Using this knowledge, interfacial layers could be carefully designed, which might be used as an effective strategy to control lipid digestion.

2.8.3 Physical state of lipid

Lipids, in most of the processed foods, vary significantly in their physical state namely liquid or solid (*i.e.* crystalline lipid) phases depending upon the sources (*e.g.* plants, animal, synthetic) from which they are extracted and also on the temperature of the food matrix *(Singh et al., 2009)*. The physical state *(Boulby et al., 1999)* of the non–polar lipid core in the emulsified structure might influence the rate of lipid digestion during its passage through the gastrointestinal tract, with solid fats digesting more slowly than liquid fats. It has been shown that long chain fatty acids form insoluble soaps in the presence of divalent cations (*e.g.* Ca^{2+}, Mg^{2+}), thus impairing lipid hydrolysis *(Vaskonen, 2003)*. Interestingly, using the same emulsified lipid (tripalmitin), it was reported that the emulsion containing liquid–lipid droplets were more susceptible to pancreatic lipase attack as compared to that containing solid–lipid particles in an *in vitro* digestion model *(Bonnaire et al., 2008)*. This increased rate and extent of lipid hydrolysis in case of emulsions containing liquid–lipid droplets was attributed to the greater adsorption and solubilization of pancreatic lipase into the liquid particle surface than that of the solid one.

In general, the crystallinity and the structural assembly of the lipid phase have been shown to affect the release of lipophilic components from the emulsified lipid droplets during digestion, with the rate of release increasing as a function of decreasing crystallinity *(Reid, 2004; Olbrich et al., 2002)*. Emulsions containing solid–lipid droplets are very common in drug delivery techniques, formed by homogenizing a lipid phase (of usually high melting point) and an aqueous phase in the presence of an emulsifier at a temperature above the melting point of the lipid phase *(Wissing & Müller, 2002; Souto et al., 2004; Üner et al., 2004; Wissing et al., 2004; Saupe et al., 2005)*, followed by cooling so that the lipid droplets may partially or fully crystallize within the emulsified droplets. Different types of solid–lipid particles can be formed by manipulating the crystallization of lipids within the emulsified droplets resulting in different kinds of structures (*e.g.* core–shell, crystal dispersion, homogeneous) and the location of the different phases can also be altered (*e.g.* shell is liquid and core is solid or *vice versa*) *(Müller et al., 2000; Muller & Keck, 2004)*. These solid–lipid particle emulsions

can be excellent carriers to deliver lipophilic functional components *(Müller et al., 2000; Wissing et al., 2004; McClements et al., 2007)*.

However, the use of higher temperature (at least 10 °C higher than the melting point of the lipid phase) during the formation of these solid–lipid particles might degrade the heat sensitive lipophilic bioactives *(Ribeiro et al., 2003)*. Moreover, the lipid phase needs to be highly saturated so that it has sufficiently high melting points to form the solid–lipid emulsions, which largely limits the application of this technology in food delivery systems, as they may have adverse health issues *(McClements et al., 2007)*. Hence, proper processing conditions for appropriate solid–lipid delivery technique need to be explored for their potential use in foods.

2.8.4 Dietary fibres

Use of dietary fibres in the food matrix might significantly affect lipid digestion process by directly interacting with the lipase and/or colipase, thereby reducing the overall hydrolysis by lipase *(Han et al., 1999; O'Connor et al., 2003)*. Dietary fibres may also get adsorbed to the emulsion droplet interface providing a protective multi–layer coating around the lipid droplets, thus possibly inhibiting lipase–colipase from coming to close proximity with the lipid core *(Fäldt et al., 1993; Ogawa et al., 2003; Peniche et al., 2003; Mun et al., 2006)*. Some dietary fibres may bind with the bile salts and phospholipids in the small intestine, thereby preventing emulsification and solubilization of lipid droplets *(Kern et al., 1978; Lairon et al., 1985; Dongowski, 1997; Thongngam & McClements, 2005)*. Most importantly, dietary fibres are well known for their viscosity enhancement abilities. This may increase the emulsion droplet stability against coalescence in the stomach or intestine. Dietary fibres are known for their delayed gastric emptying effects due to the gel formation in the gastric environment, causing slower transport of molecules (lipase, bile salts, phospholipids) from/ to the lipid droplet surfaces *(Norton et al., 2006; Ebihara & Schneeman, 1989; Armand et al., 1996a; Pasquier et al., 1996)*.

A study to understand the role of dietary fibres (pectin or chitosan) on the interfacial characteristics of Tween 80–stabilized emulsions droplets during its

passage through an *in vitro* digestion model showed that pectin can promote depletion flocculation whereas chitosan can lead to bridging flocculation depending upon the pH of the aqueous phase *(Beysseriat et al., 2006)*. These kinds of aggregation processes are claimed to be helpful in reducing the overall surface area of lipids, thus decreasing the rate and extent of lipid hydrolysis by pancreatic lipase in the gastrointestinal tract. Another *in vitro* study involving lecithin–stabilized emulsions coated with chitosan as a secondary layer showed that the ability of chitosan to form a protective secondary coating as well as promoting droplet flocculation, both of which retarded the ability of pancreatic lipase to interact with the lipid core *(Mun et al., 2006)*. However, *in vivo* studies suggested that lipid digestibility is not reduced by encapsulation of fat droplets with chitosan *(Park et al., 2007)*, which clearly suggests the discrepancies between *in vitro* and *in vivo* trials.

2.9 Experimental physiological trials

To achieve desirable outcomes related to the utilization of food structures and their physiochemical properties for controlling lipid bioavailability, an increased understanding of the physiological interactions of the emulsions is definitely required. Insights about the gastrointestinal processing of emulsions can be carefully gained using a variety of approaches ranging from *in vitro* to *in vivo* studies (involving animals) to clinical trials with human subjects *(McClements et al., 2009)*.

2.9.1 *In vitro* studies

In vitro studies basically involve 3 stages: processing in the oral, gastric and duodenal conditions respectively *(Wickham et al., 2009)*, either studied separately or in combination depending upon the specific purpose of the investigation. Broadly, attempts have been made to simulate the temperature, pH, ionic strengths, enzymes, coenzymes, bile salts, biopolymers *etc.* of the physiological fluids by either mimicking one part or more parts of the human digestive tract, *e.g.* mouth, stomach and small intestines. And, then the composition, microstructures, lipid droplet size distribution, droplet charge, rheology, interfacial compositions, binding interactions with the physiological

biopolymers, competitive interfacial exchange reactions are determined upon treating the emulsions with these simulated physiological fluids in appropriate mixing conditions *(Versantvoort et al., 2005; Beysseriat et al., 2006; Mun et al., 2007; Maldonado-Valderrama et al., 2008; Wright et al., 2008; Hur et al., 2009; Macierzanka et al., 2009)*.

Artificial saliva *(Shellis, 1978; Leung & Darvell, 1997; Gal et al., 2001)*, simulated gastric *(Pharmacopeia, 2000)* and simulated duodenal *(Pharmacopeia, 1995)* fluids have been largely utilized in pharmaceutical research to carry out *in vitro* drug delivery studies *(Porter & Charman, 2001; Anal et al., 2003; AnnMarie et al., 2004)*. However, the use of such artificial compositions has only just begun to be explored in food emulsion systems *(Beysseriat et al., 2006; Mun et al., 2007; Macierzanka et al., 2009)*. Recently, a complete *in vitro* digestion model has been proposed by some researchers for toxicological studies to simulate various physiological processing occurring in mouth, stomach and small intestine respectively, at temperature of 37 °C *(de Zwart et al., 2004; Versantvoort et al., 2005)*. Such *in vitro* digestion model can be applicable as a protocol for studying digestion of emulsified lipids in fed state conditions *(Hur et al., 2009; McClements et al., 2009)* as shown in Figure 2.8-1. The emulsion–biological fluid mixtures also need to be carefully agitated depending upon the shear and motilities in the mouth and human stomach, respectively.

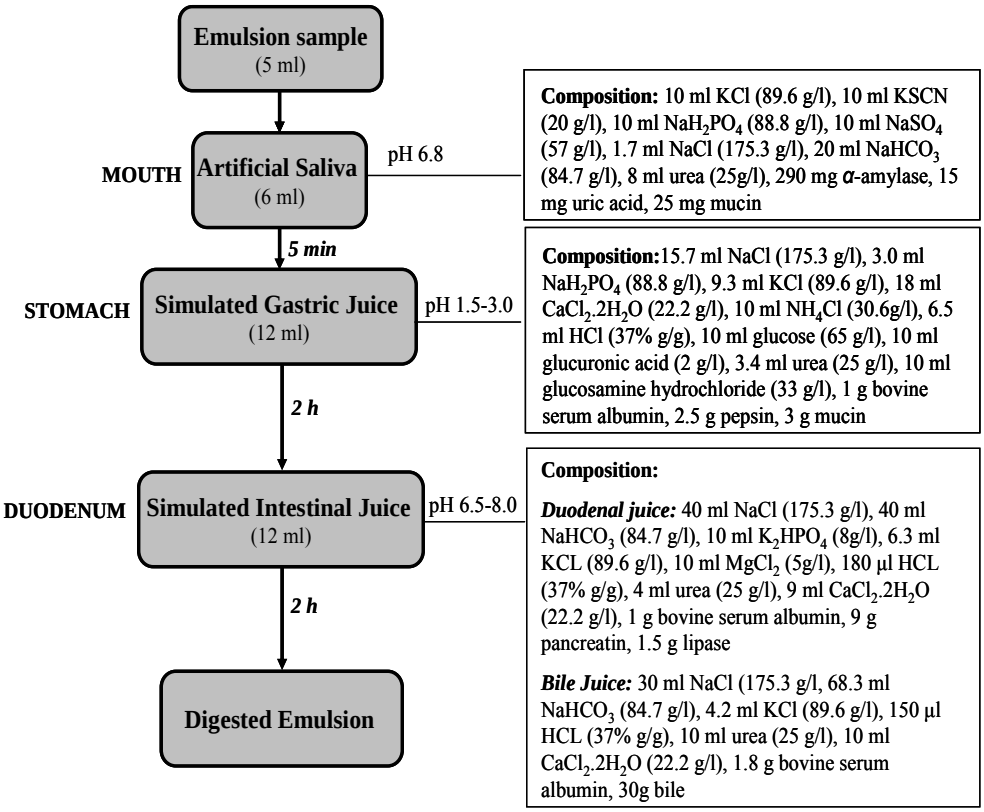

Figure 2.8-1: *In vitro* static digestion model to mimic oral, gastric and intestinal processing of an emulsion [adapted from (*Hur et al., 2009; McClements et al., 2009; Versantvoort et al., 2005*)]

However, most of these *in vitro* biochemical models are static, and thus, the gradual changes and physical processes that occur *in vivo* (*e.g.* gastric emptying, peristalsis, hydration *etc.*) are not generally mimicked *(Wickham et al., 2009)*. To obtain an overall understanding of total digestion and gastric transit, dynamic models are more relevant. The TNO *in vitro* gastrointestinal model (TIM), a patented technology *(Minekus & Havenaar, 1996; Minekus & Havenaar, 1998)* developed at TNO Nutrition and Food Research (The Netherlands), represents a computerized dynamic digestion process which together with gastrointestinal processing involves the simulation of absorption mechanism in the intestine by incorporating a dialysis membrane. Moreover, this dynamic digestion model provides valuable information about real time digestion and also avoids build up of the digestion products in the lumen by employing dialysis. TIM–1 represents the gastrointestinal tract from the stomach to small intestine and TIM–2 simulates the large intestine. TIM-1 contains four glass compartments

(interconnected by computer-controlled valves) jacketed with flexible walls inside to simulate the conditions (mainly pH, body temperature, shearing, gastric emptying, salivary, gastric, biliary and pancreatic secretions and the absorption of water and small molecules like nutrients and drugs) in the stomach, duodenum, jejunum, and ileum, respectively *(Minekus et al., 1995; Blanquet et al., 2004)*. Gastric peristalsis is achieved by pumping water (of physiological temperature *i.e.* 37 °C) into the space between the glass tubing and the flexible wall at regular intervals. The computerized valves allow the sequential squeezing of the walls, causing the food to mix efficiently with the simulated physiological fluids and pass on from one step of digestion to the next step, mimicking the physical processing during gastrointestinal transit.

TIM-2, simulating the colon, also consists of a series of interlinked glass units with flexible wall inside. The anaerobic environment in TIM-2 is obtained by flushing the glass units with nitrogen gas to provide suitable conditions for the growth of colonic microflora (of human or animal origin). The model is provided with hollow fibre membranes and also equipped with a dialysis system that maintains physiological concentrations of small molecules (such as electrolytes) and prevents accumulation of microbial fermentation products (such as short chain fatty acids) *(Minekus et al., 1999; van der Werf & Venema, 2000)*. A number of sampling points at the beginning and the end of this simulated colon model provides the opportunities for studying differences in the microflora at different stages of colonic fermentation.

Another recent advancement in the area of dynamic *in vitro* digestion is the computer-controlled 'model gut' or dynamic gastric model (DGM) developed at Institute of Food Research (United Kingdom) *(Wickham et al., 2009)*. It consists mainly of two stages to simulate the physical and biochemical digestion process of the gastrointestinal tract. The first stage mimics the peristalsis, flow profiles of acids and enzymes, and gastric emptying of the human stomach (fundus). This is followed by the second module simulating the lower part of the stomach (antrum), where high shear and mixing dynamics result in progressive breakdown of food structure. The digesta from DGM can further be processed using simulated small intestine, in which the intestinal mixing profiles is integrated

with the gradual diffusion of complex biochemical constituents such as bicarbonates, pancreatic enzymes, bile salts and other surface active agents.

Clearly, *in vitro* studies offer several advantages over *in vivo* studies being usually less time consuming, less expensive, more reproducible (no biological variations), require less manpower, have no ethical constraints, are easy to perform and allow the collection of samples at any level of the gastrointestinal tract at any time of digestion. Both static and dynamic *in vitro* models help to provide an improved understanding about the fundamental physicochemical mechanisms by unravelling the interactions between food structures (emulsions) and individual or total physiological variants (including real time measurements as in case of dynamic digestion models).

However, in reality, the dilution with the saliva and the salivary flow, the amount of gastric juice released, quantities of surface active agents and enzymes present in the gastrointestinal tract may largely vary according to the type of food (chemical composition, constituents, quantity, physical state, *etc.*), individual's physiology (age, gender, appetite, blood group, *etc.*) and also within the same human subject at different time of the day. Thus, one of the major drawbacks of using *in vitro* models is that the composition and quantity of physiological fluids, surfactants, enzymes, *etc.* involved, is not always comparable to real physiological conditions. For example, it is frequently debated that the pepsin:substrate ratios in most of the *in vitro* studies vary from 1:3 to 1:10 w/w, which greatly in excess of those likely to be found in the stomach, even in fed state conditions *(Wickham et al., 2009)*. It should be worth noting here, that it is extremely difficult to select an optimal protein:pepsin ratio in an *in vitro* digestion model that exactly mimics the secretion found physiologically in humans because a wide variation (up to about 10,000 fold) in gastric and pancreatic secretions has been suggested depending on the individual's health and the type of food intake *(da Silva Gomes et al., 2003)*. Interestingly, gastric lipases are not used in most of the preliminary *in vitro* lipolysis studies *(Mun et al., 2006; Mun et al., 2007; Hur et al., 2009)* due to unavailability of commercial gastric lipases.

This is indubitably a crucial challenge to simulate the exact complexities of physiological processes occurring in human digestive system using more realistic *in vitro* models, which might be potentially rewarding in understanding the complex physiological interactions. Nevertheless, it is recommended to complement these well–defined *in vitro* investigations by *in vivo* trials involving animals as well as clinical trials with human subjects.

2.9.2 *In vivo* studies and clinical trials

Clinical trials with human subjects are necessary to better understand the complex lipid digestion process in real physiological situation. However, they have the limitations of being extremely expensive, have strict regulations, show significant variations among individuals and involve difficulties in controlling diets and lifestyles of human beings. Hence, *in vivo* trials with animals mainly rodents *(Gallaher, 1992; Qi et al., 2006) i.e.* rats or mice and some larger animals *e.g.* pigs *(Miller & Ullrey, 1987)*, cows *(Allen et al., 2005)* can be considered to study the factors affecting lipid digestion.

However, *in vivo* animal studies are not only expensive and have serious ethical considerations; concerns are frequently raised regarding their reproducibility (due to variations between animals) and relevance to human systems. For example, lipid digestion starts from mouth itself in rats, due to the presence of lingual lipases. However, these salivary lipases are not quantitatively significant in human adults *(Mu & Hoy, 2004)* and thus the results from rat trials might not be applicable for human subjects, especially in the case of lipid digestion studies. In case of larger animals, such as cows and sheep being herbivores, their dietary pattern (high fibre–low lipid diets) is significantly different from that of human beings *(Allen et al., 2005)*, and consequently, less suitable for understanding human lipid metabolism. However, the anatomy and physiology of digestive systems of pigs together with their dietary patterns (being omnivores) have been shown to be similar to those in human beings *(Pond & Houpt, 1978)*, and hence *in vivo* trials with pigs can be an efficient approach to study lipid metabolism.

With *in vivo* studies, it is possible to sacrifice and characterize a particular tissue (liver, pancreas *etc.*) of interest, of the animals after feeding trials *(Avula & Fernandes, 1999; Yeom et al., 2003; Navarro et al., 2007)*. Apart from that, influence of specific food components can be analysed using bodyweights *(Engstrom et al., 2006)*, collection of samples from different regions of the stomach using invasive tubing *(Armand et al., 1994; Lairon et al., 2007)* and/or examination of blood *(Mukuddem-Petersen et al., 2005)* and faecal samples *(Park et al., 2007)*. To understand the digestion and absorption of bioactive nutrients, stable isotope (^{13}C or ^{3}H) can also be used, in which these markers are administered with the known targeted bioactive compound in dietary components and the gradual disappearance of these isotopes from the faeces, breathe, blood *etc.* can be detected using analytical techniques such as mass spectrometry to indirectly trace the fate of the biological compound of interest *(Michalski et al., 2005; Stellaard, 2005; Ton et al., 2005)*.

Recently, a few non–invasive techniques have also been applied to monitor the fate of food behaviour in physiology *e.g.* ultrasound, X–rays, magnetic resonance imaging (MRI) *(Schwizer et al., 2003; Schulze, 2006)*. The MRI has been found to be extremely useful to understand gastric emptying *(Kunz et al., 1998; Feinle et al., 1999; Szarka & Camilleri, 2009)*, dynamics of food flow in the physiological tract *(Boulby et al., 1999)* as well as to follow the distribution of lipids and other ingredients of food structures during the complex digestive action *(Faas et al., 2002)*. An interesting clinical trial involving nine healthy human subjects, showed that acid unstable food emulsions may be broken down during complex processing in the stomach and MRI studies revealed that the oily phase released due to phase separation of the emulsion resulted in accelerated gastric emptying *(Marciani et al., 2007)*. However, acid–stable emulsions delayed gastric emptying and increased postprandial cholecystokinin levels. Hence these non–invasive imaging tools might be useful in providing novel insights about lipid digestion in animals and humans in real time.

2.10 Concluding remarks

In most of the modern processed foods, lipids from animals and plants are present in the form of emulsions, which are either end food products in themselves (*e.g.* butter, margarine, spreads, mayonnaise and ice cream) or ingredients (soups, confectionery, chocolates) of a more complex food matrix. The creation of stable emulsion droplets is extremely critical in determining their interactions with other food components. Although the composition, physicochemical properties and stability of emulsions with respect to physical (thermal treatments, high pressure effects, and shear) and chemical (pH, ionic strengths) processing conditions together with biopolymer interactions (protein–polysaccharide) in the adsorbed layers have been largely understood due to the conscientious research in the past few decades, the behaviour of emulsions after consumption *i.e.* during physiological processing is largely unknown. It is critical to understand the oral behaviour of the emulsions to deliver better sensorial attributes, texture perceptions and control the release of flavour and/or aroma molecules. Recently, researchers have found evidence that the behaviour of emulsions in the gastrointestinal tract is largely affected by their physicochemical properties and that the interfacial properties of the emulsions can be intelligently altered to modulate lipid digestion, and thereby control the bioavailability of lipid soluble bioactive nutrients and/or reduce the absorption of saturated fats, cholesterol and *trans* fats.

In recent years, although few preliminary studies have been conducted on the physiological processing of emulsions, there are many apparent contradictions and disagreements among various studies. This area of gastrointestinal processing in emulsion science needs to be further developed before the insights can be used to design specific approaches for formulating food structures that control flavour release and/or modulate lipid digestion, absorption and bioavailability.

Several areas need to be investigated, including understanding the influence of different physical (peristaltic shear, body temperature) and biochemical (pH, ionic strengths, pepsin and mucin) variants on changing the microstructure and

stability of the emulsions during their passage through the stomach; whether or not the action of lipase can be modified by the microstructure and composition of the adsorbed layer; influence of bile salts, surface active agents and lipid digestion products on competitive exchange phenomena.

Bridging these fundamental gaps primarily requires focussing on independent systematic *in vitro* trials as they are less time consuming, less expensive and more reproducible than *in vivo* ones and would give fundamental insights based on interactions with each individual physiological variant. Food systems are highly complex consisting of various food components. Therefore, first and foremost, consistent results using simple model emulsion systems should be obtained before investigating more difficult problems. Studies focussing on the behaviour of emulsion systems at either mouth or stomach or intestines individually as well as interfacial interactions with the whole oral–to–gastrointestinal fluids need to be carefully investigated. Despite the complexities in physiological situations and food matrices, the fundamental principles of interactions established in model emulsion studies *in vitro* will have potential applicability under physiological conditions when real food colloids are consumed and digested. Hence, consolidations of such insights obtained from *in vitro* studies of model colloidal systems, together with further research involving *in vivo* trials and intensive clinical studies in human will be required to test the efficacy of these functional colloidal structures, which will have tremendous potential in healthier food applications.

Chapter Three: Materials & Methods

3.1 Materials

The common materials used in most of the experiments are included in this chapter. Materials specific to any particular study have been included in specific chapters.

3.1.1 Beta-lactoglobulin (β-lg)

The β-lg (containing both β-lg A and B) from bovine milk was purchased from Sigma Aldrich Chemical Co., St. Louis, MO, USA. It was a lyophilized powder of approximately 90.0% purity.

3.1.2 Lactoferrin

Lactoferrin was a gift from Tatua Co-operative Dairy Company Limited, Morrinsville, New Zealand. The powder contained 99.7% protein, of which 95.8% was lactoferrin. Lactoferrin consisted of 0.3% moisture, 0.8% ash and the iron content was 130 ppm.

3.1.3 Soy Oil

Refined bleached deodorized soy oil was obtained from Davis Trading Company, Palmerston North, New Zealand. It contained tertiary butylhydroquinone as an antioxidant and polydimethylsiloxane as antifoaming agent. The soy oil was used without any further purification.

3.1.4 Chemicals

Milli-Q water (water purified by treatment with a Milli-Q apparatus; Millipore Corp., Bedford, MA, USA) was used as the solvent throughout the experiments. Sodium azide was purchased from Sigma Aldrich Chemical Co. (St. Louis, MO, USA). The electrophoresis reagents were of analytical grade and obtained from BDH Chemicals (BDH Ltd, Poole, UK) unless otherwise specified. Precision Plus protein standards (*i.e.* molecular weight markers) of molecular weight range of 10-250 kDa was purchased from Biorad Laboratories (Hercules, CA, USA).

Ammonium persulphate of ≥ 98% purity (used for acrylamide polymerization) and *N*,*N*′-methylene-bis-acrylamide (used for making polyacrylamide gels) were purchased from Sigma Aldrich Chemical Co., St. Louis, MO, USA.

All other chemicals used in different experiments, mentioned in specific chapters were of analytical grade and purchased from BDH Chemicals (BDH Ltd, Poole, England) unless otherwise specified.

3.2 Methods

The common methods and analytical techniques applicable to most of the experiments are presented in this chapter. Experimental methodologies and characterization techniques specific to any particular study have been included in specific chapters.

3.2.1 Emulsion Preparation

Protein solutions (1.0 wt%) were prepared by dispersing appropriate quantities of lactoferrin or *β*-lg in milli-Q water and stirring for 2 h at 20 °C to allow complete dissolution. Sodium azide (0.02 wt%) was added to avoid microbial growth. The pH was adjusted to 6.8 using 1 M NaOH or 1 M HCl. Soy oil was then added to the protein solutions to form final emulsions containing 20.0 wt% soy oil and 80.0 wt% aqueous phases. The mixture of soy oil and protein solution was heated to nearly 50 °C and mixed using a rotor–stator type mixer at 20,500 min^{-1} (Heidolph DIAX 600, Germany). These pre-emulsions were then homogenized by two passes through a two–stage valve homogenizer (APV 2000, Silkeborg, Denmark) operating at 250 bar for the first-stage and 50 bar for the second-stage. A photograph of the homogenizer used in this study is shown in Figure 3.2-1. Emulsions were prepared at least in duplicate.

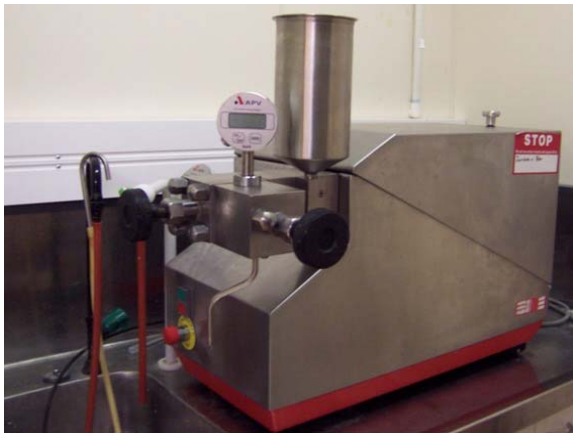

Figure 3.2-1: Lab scale two–stage valve homogenizer (APV 2000, Silkeborg, Denmark).

3.2.2 Characterization techniques

The analytical techniques used to characterize the physicochemical properties and microstructures of fresh emulsions (as well as the emulsions after various treatments mentioned in subsequent chapters) are discussed in this chapter.

3.2.2.1 Particle size

One of the most important and widely used characterization techniques in emulsion science is the determination of particle size using light scattering (also called laser diffraction) techniques *(McClements, 2005)*. The two main instruments generally used to measure emulsion droplet size are Mastersizer and Zetasizer. Mastersizer uses static light scattering, whereas Zetasizer uses dynamic light scattering (DLS). The Mastersizer measures the angular dependence of the scattered light from the emulsion droplets and fits the scattering intensity data to well known theoretical models. In Mastersizer, the droplet sizes are mostly weighted towards the bulk of droplets having the highest refractive index. The sample to be analyzed is generally diluted to an appropriate concentration with the continuous phase. A monochromatic light beam, generated by a laser (helium/neon, λ = 632.8 nm), is passed through the measurement cell where it is scattered by the emulsion droplets. The intensity of the scattered light is measured as a function of scattering angle, using an array of photosensitive detectors. Generally, the scattering angle is an inverse function of the droplet size, so that the scattering pattern contains information about the droplet size

distribution of the emulsion. Thus, low-angle scattering are more sensitive to larger droplets, and wide-angle measurements are generally more responsive to smaller droplets. The droplet size distribution, which gives the best statistical fit between the measurements of intensity *versus* scattering angles and those predicted by the Mie theory, is then calculated.

Malvern MasterSizer MSE (Malvern Instruments Ltd, Malvern, Worcestershire, UK) was used to determine the average droplet size (μm) and the overall size distribution of the emulsions using the presentation code 2NAD. The relative refractive index (N) of the emulsion was 1.095, *i.e.* the ratio of the refractive index of soy oil (1.456) to that of the dispersion medium (1.33). The absorbance value of the emulsion particles was 0.001. The Sauter-average diameter, d_{32} (μm) was given by the following expression:

$$d_{32} = \sum \frac{n_i d_i^3}{n_i d_i^2} \qquad \textbf{(3.2-1)}$$

And, the volume-mean diameter, d_{43} (μm) was calculated as follows:

$$d_{43} = \sum \frac{n_i d_i^4}{n_i d_i^3} \qquad \textbf{(3.2-2)}$$

where, n_i is the number of particles with diameter d_i of the emulsion droplets.

The average droplet size and the droplet size distribution were measured under two conditions: (a) samples dispersed in continuous phase *i.e.* water and (b) samples dispersed gently in 2% sodium dodecyl sulphate (SDS) solution. Mean particle diameters were calculated as the average of triplicate measurements. In Chapter 9, static light scattering technique was performed using the latest version of MasterSizer *i.e.* Malvern MasterSizer 2000 Hydro MU (Malvern Instruments Ltd, Malvern, Worcestershire, UK) as shown in Figure 3.2-2, equipped with a broad measurement range of 0.02–2000 μm using general purpose analysis model. The droplet size distribution was measured using a designated pump speed of 2500 rpm.

Figure 3.2-2: MasterSizer 2000 Hydro MU, supplied by Malvern Instruments Ltd, Malvern, Worcestershire, UK.

The mean hydrodynamic diameter (*Z*-average diameter) (μm) of emulsion samples was measured by a DLS technique using a Zetasizer Nano ZS, Model ZEN 3600 (Malvern Instruments Ltd, Malvern, Worcestershire, UK) (photograph shown in Figure 3.2-3) equipped with a 4 mW helium/neon laser at a wavelength output of 633 nm. Droplet sizing was performed at 10 s intervals in a particle-sizing cell using backscattering technology at a detection angle of 173°.

Figure 3.2-3: Zetasizer Nano ZS, Model ZEN 3600, supplied by Malvern Instruments Ltd, Malvern, Worcestershire, UK.

Basically, DLS measures the velocity of light scattered from the emulsion droplets in the dispersion. The autocorrelation function is transformed into the size distribution using cumulant analysis *(Koppel, 1972)* by the Zetasizer Nano ZS software package (Malvern Instruments Ltd, Malvern, Worcestershire, UK)

and the intensity of scattered light from the dispersed droplets in Brownian motion is converted to the mean hydrodynamic diameter (*Z*-average diameter, or also called scattering intensity-weighted mean diameter), *via* the Stokes–Einstein equation, assuming the emulsion droplets to be spherical.

Although, Mastersizer works best on larger sizes (~ 0.1–2000 μm), Zetasizer is most suitable for the measurement of sizes up to a few microns (≤ 10 μm).

For each sample, the mean and the standard deviations were calculated from a series of ten measurements. All measurements were carried out on two freshly prepared emulsions.

3.2.2.2 Zeta potential

The zeta potential (ζ-potential) (mV) values of the emulsions were measured by laser doppler velocimetry and phase analysis light scattering (M3-PALS) technique using a Malvern Zetasizer Nano ZS (ZEN 3600) instrument (Malvern Instruments Ltd, Malvern, Worcestershire, UK) (photograph shown in Figure 3.2-3). This micro-electrophoresis system is a capillary cell with electrodes at either end, to which a potential is applied. Droplets within the dispersion move towards the oppositely charged electrode at a certain velocity, which is determined by measuring the frequency shift of the incident laser beam. This velocity (electrophoretic mobility *i.e.* U_E) at which the droplets move in the applied electric field is converted to a zeta-potential (ζ) by substituting the known variables, such as the dielectric constant of the medium (ε) and viscosity (η) in Henry's equation as follows:

$$U_E = \frac{2\varepsilon\zeta f(ka)}{3\eta} \qquad \textbf{(3.2-3)}$$

where, *f(ka)* is the Henry's function taken as 1.5, referred to as Smoluchowski approximation, which is generally used for emulsions having aqueous phase as the dispersant.

One millilitre of sample (diluted with continuous phase or appropriate background buffer to approximately 0.005 wt% droplet concentration) was placed in a universal folded capillary cell (Model DTS 1060C, Malvern Instruments Ltd, Malvern, Worcestershire, UK) equipped with platinum electrodes. The temperature of the electrophoresis cell was maintained at 25 °C using a water jacket that was temperature controlled by the Peltier system. The ζ-potential measurements were reported as the mean and standard deviation of at least ten readings. All measurements were carried out on at least two freshly prepared emulsions.

3.2.2.3 SDS-PAGE

The emulsions were analysed using a sodium dodecyl sulphate polyacrylamide gel electrophoresis (SDS-PAGE) technique *(Laemmli, 1970)*. The SDS-PAGE gels were prepared using a resolving gel and a stacking gel mounted on a vertical Mini-Protean II dual cell unit (Bio-Rad Laboratories, Richmond, CA, USA), which is described in details as follows:

3.2.2.3.1 Resolving gel

The resolving gel mixture (16%) contained 3.75 mL of SDS resolving gel buffer [stock solution prepared containing 2.5 mL Tris (by dissolving 4.5375 g of Tris (hydroxy methyl) aminomethane base in about 10 mL of milli-Q water, adjusted to pH 8.8 and finally volume made up to 25 mL *i.e.* 1.5 M Tris-HCl at pH 8.8), 2.02 mL water, 5.3 mL acrylamide solution (30% stock solution of a 37:5:1 (2.6% C) mixture of acrylamide and *N*,*N*′-methylene-bis-acrylamide) and 100 µl of 10% SDS solution]. The mixture was mixed well, degassed under vacuum for 20 min. Meanwhile, the vertical dual gel casting apparatus was assembled using 0.75 mm spacers, followed by standard description in Biorad manual. After degassing the gel mixture solution and just prior to the gels being poured, 50 µl of 10% ammonium persulphate solution (freshly prepared) and 5 µl of TEMED (*N*,*N*,*N*′-tetramethylethylenediamine) were added and the final mixture was transferred between the pair of glass plates. About 0.5–1.0 mL of water was then added above the resolving gel to prevent drying out of the gel and to give the resolving gel a smooth surface after gel setting. The gel mixture solution was left

undisturbed for about 30–45 min at room temperature (25 °C) to allow for setting of the gel. The water from the top layer was removed completely with a blotting paper wick before the addition of stacking gel (discussed in the section below).

3.2.2.3.2 Stacking gel

The stacking gel (4%) was made up of 1.5 mL of stacking gel buffer [stock solution prepared containing 1.25 mL Tris base (by dissolving 1.5 g of Tris base in about 10 mL of milli-Q water, adjusted to pH 6.8 and finally volume made up to 25 mL *i.e.* 0.5 M Tris-HCl at pH 6.8), 3.05 mL water, 650 µl acrylamide solution (as described above) and 50 µl of 10% SDS solution]. The mixture was then mixed well, degassed and just prior to the gels being poured, 25 µl of 10% ammonium per sulphate solution and 5 µl of TEMED was added (to give 3.9% T and 2.67% C gels). Consequently, the final mixture was added into the gap between the pair of glass plates, on top of the preset resolving gel, and a 0.75 mm plastic comb with 10 slots was inserted to form loading well, taking care to remove any air bubbles. The gel was allowed to set for 45–60 min for complete polymerization. The entire gel assembly was then transferred to an airtight container.

3.2.2.3.3 Sample Buffer

SDS-PAGE sample buffer (pH 6.8) was prepared by mixing 3.125 mL of 0.5 M Tris adjusted to pH 6.8, 5 mL of 10% SDS, 2.5 mL glycerol and 625 µl of 0.4% Bromophenol blue solution, finally made upto 25 mL of total volume. The use of SDS was to provide a net negative charge to the protein so that the proteins were separated based on their molecular weights rather than their initial charges. Small aliquots (200 µL) of emulsions were periodically sampled after various treatments and were immediately treated with 800 µl of SDS buffer. Now the emulsion–sample buffer mixtures were heated to 95–100 °C for 5 min with the addition of 0.05% *β*-mercaptoethanol *(Srinivasan et al., 1996)*. Addition of *β*-mercaptoethanol was to reduce the disulphide linkages resulting in unfolded protein bands. The samples were cooled to room temperature.

3.2.2.3.4 Electrode buffer

The stock SDS electrode buffer (5*X*) was prepared by dissolving 7.5g Tris, 36g glycine and 2.5g SDS powder in milli-Q water, finally made upto 1 L. The pH of the stock solution was about 8.6. The stock solution was then diluted with milli-Q water in the ratio of 1:4 for using in the electrophoresis chamber (also called tank).

3.2.2.3.5 Running of gels

The electrode buffer after the dilution was added to the chamber containing the gel system. The samples (10 μL) were then loaded on to SDS gels previously prepared on the dual cell system. Molecular weight markers (of range 10-250 kDa) were also loaded on some of the SDS-PAGE gels. And then, the electrophoresis was carried out at a constant voltage of 200 mV, starting with a current of 70 mA for a period of 1 h on the power unit (EC 135, E-C Apparatus Corporation, Sr. Petersons, FL, USA). After the bromophenol blue dye had reached the bottom of the gel, the power was turned off; gels were carefully removed and transferred into transparent plastic containers and were subsequently stained and destained.

3.2.2.3.6 Staining and destaining the gels

The gels were stained by dispensing sufficient quantities of staining solution *i.e.* Coomassie Blue R-250 [0.05% (w/v) in 25.0% (v/v) iso-propanol, 10.0% (v/v) acetic acid] into the container to cover the entire gel. The container was set on a platform rocker and allowed to stain for 30-45 min. After the gels were adequately stained, the staining solution was drained and nearly 100 mL of destaining solution [10.0% (v/v) iso-propanol, 10.0% (v/v) acetic acid] was added and the container was again kept on the rocker for 1 h. After 1 h, the destaining solution was drained off and replenished with 100 mL of fresh destaining solution. The container was again allowed to destain on the rocker for 6 h and the procedure was repeated twice at further 6 h intervals.

3.2.2.3.7 Scanning and quantification of the protein bands

The gels were then scanned using a dual media flat-bed scanner (Scanmaker *i*900, Microtek, Carson, CA, USA) and the intensities of the protein bands were quantified using GelQuant (version 2.7) software. The total absorbance or integrated intensity of each protein band of the emulsion samples was determined and compared with the relative intensity of the protein bands in untreated samples (*e.g.* freshly prepared *β*-lg or lactoferrin emulsion or solution respectively) run on each gel as a control.

3.2.2.3.8 SDS-PAGE of unadsorbed and adsorbed protein

To determine the behaviour of the unadsorbed protein (present in the continuous phase), the emulsion samples after various treatments were centrifuged for 40 min at 45,000*g* and 20 °C (Sorvall RC5C, DuPont Co., Wilmington, DE, USA), and the subnatant was carefully removed using a syringe, filtered sequentially through 0.45 and 0.22 μm filters (Millipore Corp., Bedford, MA, USA), and examined using SDS-PAGE (sample:sample buffer = 400 μl:800 μl, with 10 μl of sample being loaded).

The protein composition at the interface of the emulsion droplets (adsorbed protein) was also determined by analysing the cream phase using SDS-PAGE *(Srinivasan et al., 2000)*. The cream layer obtained by the centrifugation of the emulsions (as mentioned above) was carefully removed, dispersed in milli-Q water and again centrifuged at 45,000*g* for 40 min at 20 °C. The cream layer was collected carefully and a certain amount of cream was spread on to a filter paper (Whatman No. 42, Whatman International Ltd, Maidstone, Kent, UK) and air-dried. The dried cream was then mixed with SDS buffer in glass vials and heated in a boiling water bath for 5 min with the addition of 0.05% *β*-mercaptoethanol (sample:sample buffer = 100 μg:1000 μL, with 10 μL of sample being loaded). SDS-PAGE and quantification by gel scanning was carried out as described previously.

3.2.2.4 Determination of nitrogen content

The emulsion samples after various treatments were analysed for nitrogen content (*N*) using the Kjeldahl method (1026 Distilling Unit and 1007 Digestor Block, Tecator AB, Hoganas, Sweden) and converted to total protein content using the requisite factor ($N \times 6.38$) to quantitatively estimate the amount of protein.

3.2.2.5 Confocal laser scanning microscopy

Confocal scanning laser microscopy was used to provide high resolution images of microstructures of emulsions. Confocal scanning laser microscope (CSLM) (Leica SP5 DM6000B, Leica Microsystems, Heidelberg, Germany) had a motorized z-focus and a 7*x* nose piece along with a 100 mm oil immersion objective lens (photograph shown in Figure 3.2-4).

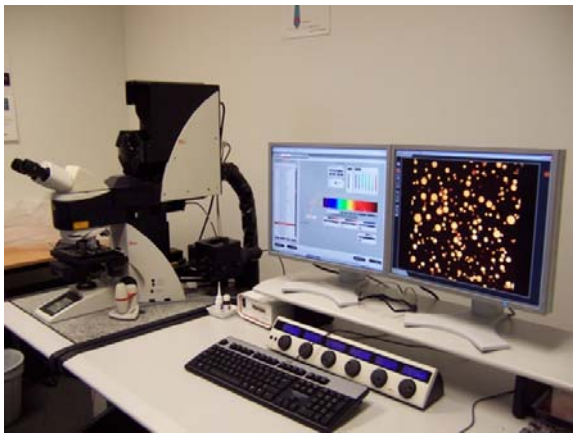

Figure 3.2-4: Confocal scanning laser microscope, Model Leica SP5 DM6000B, supplied by Leica Microsystems, Heidelberg, Germany.

Nile blue was used to selectively stain the oil in the emulsion. A sample (about 3 mL) of the emulsion was taken in a test tube and mixed with 0.3 mL of 1.0 wt% Nile blue (fluorescent dye). An aliquot of the stained emulsion was placed on a concave confocal microscope slide (Sail, Sailing Medical-Lab Industries Co. Ltd, China). The slide was then covered with a cover slip (0.17 mm thick) and it was ensured that there was no air gap (or bubbles) trapped between the sample and cover slip. The emulsion sample was then immediately examined with a 100× magnification lens using an argon/krypton laser with an excitation line of 488 nm

and observed under the microscope to determine the microstructures of the emulsions. The position of the confocal plane was held constant throughout the whole sequence of imaging. Micrographs of emulsions after various treatments are presented in specific chapters.

3.2.2.6 Statistical analyses

Data were statistically analyzed by analysis of variance using Minitab 15 English software (Minitab Inc., State College, PA, USA). Differences were considered to be significant at $p \leq 0.05$. Mean ($\overline{X}$) and standard deviation (σ_X) from at least ten measurements carried out on two freshly prepared emulsions were calculated as follows:

$$\overline{X} = \frac{1}{n}\sum_{i=1}^{n} X_i \qquad \textbf{(3.2-4)}$$

$$\sigma_X = \frac{1}{n-1}\sqrt{\sum_{i=1}^{n}(X_i - \overline{X})^2} \qquad \textbf{(3.2-5)}$$

where, X_i = individual sample value

n = number of samples.

Chapter Four: Colloidal Interactions of Milk Protein–Stabilized Emulsions in Artificial Saliva [1]

4.1 Abstract

Lactoferrin produces a stable cationic oil-in-water emulsion whereas β-lg forms an anionic emulsion at neutral pH. Oil-in-water emulsions (20 wt% soy oil) stabilized by lactoferrin or β-lactoglobulin (β-lg) as the interfacial layers were mixed with artificial saliva that contained a range of mucin concentrations and salts. Negatively charged mucin was shown to interact readily with the positively charged lactoferrin–stabilized emulsion droplets to provide a mucin coverage of approximately 1 mg/m^2. As expected, the negatively charged β-lg–stabilized emulsion droplets had lower mucin coverage (0.6 mg/m^2 surface load) under the same conditions. The β-lg–stabilized emulsions were stable but showed depletion flocculation at higher mucin levels (≥ 1.0 wt%). In contrast, lactoferrin–stabilized emulsion droplets showed considerable aggregation in the presence of salts but in the absence of mucin. This salt–induced aggregation was reduced in the presence of mucin, possibly because of its binding to the positively charged lactoferrin–stabilized emulsion droplets and thus a reduction in the positive charge at the lactoferrin–coated droplet surface. However, at higher mucin concentration (≥ 2.0 wt%), lactoferrin–stabilized emulsions also showed droplet aggregation.

4.2 Introduction

Food emulsions are generally exposed to a range of processing conditions during consumption such as dilution effects due to mixing with saliva, access to salivary enzymes such as amylases, various biopolymers such as mucins, different electrolytes in the saliva together with a moderate change in pH, temperature (around 37 °C) and friction between the tongue and the oral mucosa *(Malone et*

[1] Part of the contents presented in this chapter has been published previously as a peer-reviewed paper: Sarkar, A., Goh, K. K. T., and Singh, H. (2009), Colloidal stability and interactions of milk-protein–stabilized emulsions in an artificial saliva. *Food Hydrocolloids*, *23*(5), 1270–1278.

al., 2003a; Malone et al., 2003b; de Wijk et al., 2004; de Wijk & Prinz, 2005; Vingerhoeds et al., 2005). Although, effects of processing conditions on the stability of emulsions (prior to consumption) have been largely investigated in the past few decades, there is very little understanding of the behaviour of emulsions after consumption *(Singh et al., 2009)*. It is critical to understand the oral processing of emulsion to successfully manipulate the physical and sensorial attributes of colloidal food systems, such as emulsion stability, creaminess, smoothness and rate of flavour release.

Literature dealing with oral processing of emulsions has been largely directed towards sensory analysis using food emulsions *(Kilcast & Clegg, 2002; Metcalf & Vickers, 2002; de Wijk et al., 2003; Engelen et al., 2003)* and flavour release *(de Roos, 2003)* using in mouth models *(van Ruth & Roozen, 2000b; van Ruth & Roozen, 2000a; Doyen et al., 2001; van Ruth et al., 2002)* and *in vivo* experiments using electronic nose *(Miettinen et al., 2002)*. However, physiochemical changes of emulsions on mixing with saliva are not that well-understood.

Recently, some authors have reported coalescence of emulsion droplets after consumption, which has been related to shear, surface, saliva or air–induced interactions in the oral cavity *(van Aken, 2004; Dresselhuis et al., 2008)*. Interestingly, there has been some evidence to show that the behaviour of emulsions during oral processing is largely driven by emulsion–saliva interactions *(van Aken et al., 2005; Vingerhoeds et al., 2009)*. Studies involving mixing of different protein– and surfactant–stabilized emulsions with unstimulated human saliva have reported saliva–induced emulsion flocculation, which was predominantly stated to be of non-covalent origin and claimed to driven by highly glycosylated negatively charged mucin present in human saliva *(Vingerhoeds et al., 2005; Silletti et al., 2007a; Silletti et al., 2007b)*. However, the minimum mucin concentration required to induce flocculation in emulsion (0.4 wt%) was found to be much higher than mucin content in human saliva (generally 0.02 wt%). Hence, it is not only the mucin, but also other salivary components that may possibly drive the emulsion flocculation by unknown

mechanism. However, the role of such salivary components other than mucins in flocculation is still not understood.

Human saliva is a highly complex biological fluid. Many parameters (*e.g.* diet, sex, duration, drug, age, stimulus, size of salivary gland and other physiological factors) affect the composition, ionic strength and pH of human saliva *(Neyraud et al., 2003; Schipper et al., 2007)*. Because of the variability and the complexity of the composition of human saliva, it is difficult to understand fully the effects of various components of saliva on the properties of emulsions. To overcome this problem, an artificial saliva formulation with a known composition needs to be used for understanding the salivary interactions of emulsions.

Hence, this chapter describes the use of artificial saliva to investigate the physicochemical effects of the salts and highly glycosylated mucins present in saliva on the behaviour of both positively charged lactoferrin–stabilized and negatively charged β-lactoglobulin (β-lg)–stabilized emulsions. The adsorption behaviour of lactoferrin in oil-in-water emulsions at neutral pH to produce a stable cationic emulsion has recently been studied *(Ye & Singh, 2006a)*. The lactoferrin–stabilized emulsion and the β-lg–stabilized emulsion were mixed with the artificial saliva of a known composition to provide an *in vitro* model for studying the behaviour of both cationic and anionic emulsion droplets in the mouth.

4.3 Materials and Methods

4.3.1 Materials

Porcine gastric mucin Type II (Sigma Chemical Co., St. Louis, MO, USA) contained 5.8% moisture, 61.4% protein, 3.6% fat, 25.3% carbohydrate and 1% bound sialic acids. The reagents used for making the artificial saliva and all other chemicals were purchased from BDH Chemicals (BDH Ltd, Poole, England) unless otherwise specified. All the chemicals used were of analytical grade.

4.3.2 Artificial saliva

The artificial saliva was prepared according to the composition used in dental studies *(Leung & Darvell, 1991; Leung & Darvell, 1997; Gal et al., 2001)*, as shown in Table 4.3-1. The mucin used in this study was porcine gastric mucin, which comprises of both MUC5AC and MUC6 *(Nordman et al., 2002)* and is said to simulate human salivary mucins (MUC5B) *(Offner et al., 1998; van Klinken et al., 1998)*.

Table 4.3-1: Chemical composition of artificial saliva [adapted from *(West et al., 2002)*].

Chemical name	Chemical formula	Concentration (g/L)
Sodium chloride	NaCl	1.594
Ammonium nitrate	NH_4NO_3	0.328
Potassium phosphate	KH_2PO_4	0.636
Potassium chloride	KCl	0.202
Potassium citrate	$K_3C_6H_5O_7.H_2O$	0.308
Uric acid sodium salt	$C_5H_3N_4O_3Na$	0.021
Urea	H_2NCONH_2	0.198
Lactic acid sodium salt	$C_3H_5O_3Na$	0.146
Porcine gastric Mucin Type II		Varying concentrations (0–30 g/L)
Water	H_2O	

The mucin concentration in the saliva varies considerably, generally in the range 0.02–0.1 wt%. Also, it has been reported that porcine or bovine mucin at a concentration of 3.0 wt% has been reported to simulate the viscosity of human saliva *(Shellis, 1978; Gal et al., 2001; West et al., 2002)*. Hence, a wide range of mucin concentrations was used to better understand the mechanism of interactions of mucin with the protein–stabilized emulsion droplets. However, it should be noted that commercially available porcine gastric mucin, which is widely used as a standard for artificial saliva preparations, might contain impurities, such as salts, immunoglobulins and other proteins *(Lee et al., 2005)*. In the present study, the concentration of mucin was varied from 0 to 3.0 wt% and the pH of the artificial saliva was adjusted to pH 6.8 using 0.1 M NaOH. In some experiments, the concentration of salivary salts was varied from 0 to 0.5

wt% (0.5 wt% implies concentration of salts in artificial saliva formulation mentioned in Table 4.3-1) without the addition of mucin, to understand the role of salivary salt–emulsion interactions. As starch has not been used in any of our emulsion preparations, salivary amylases were deliberately excluded from our artificial saliva preparation.

4.3.3 Size–Exclusion Chromatography combined with Multi–Angle laser Light Scattering (SEC–MALLS)

Porcine gastric mucin Type II (0.2 wt%) was dispersed in 0.1 M NaCl with 0.02 wt% sodium azide at ambient temperature (20 °C). The pH was adjusted to 6.8 with 0.1 M NaOH. The sample (50 μL), sequentially filtered through 0.45 and 0.22 μm filters (Millipore Corp., Bedford, MA, USA), was injected into a high performance liquid chromatography (HPLC) system (GBC Scientific Equipment Ltd, Victoria, Australia) at a flow rate of 0.5 mL/min. Separation of mucins was achieved using a size exclusion column (Shodex SB–806M; Pharmacia, Uppsala, Sweden). The Shodex SB–806M column separates proteins in a range from 2.0×10^4 to 2.0×10^7 Da. The size exclusion column (8.0 × 300mm) was densely packed with polyhydroxymethacrylate gel, which is suited for separation of water soluble biopolymers. The particle size of the gel was 13 μm with pore size of 1.0×10^3 Angstrom. The maximum pressure and flow rate of the column was 30 kgf/cm^2 and 1.2 mL/min respectively. The eluted molecular fractions were detected by ultraviolet (UV, 280 nm absorbance, GBC Scientific Equipment Ltd, Victoria, Australia), multi–angle laser light scattering (MALLS) [DAWN DSP laser photometer (Wyatt Technology, Santa Barbara, CA, USA), consisting of a linearly polarized helium/neon laser (λ = 632.8 nm; 5 mW), a K5 flow cell and 18 detectors at various angles] and differential refractive index (DRI) detection (R401; Millipore-Waters, Milford, MA, USA). Upon completion of each run, the chromatograms were aligned to correct for the time delay of the samples reaching the detectors *i.e.* UV, MALLS and DRI detectors.

A solution containing 0.1 M NaCl at pH 6.8 and filtered through 0.22 and 0.025 μm filters (Millipore Corp., Bedford, MA, USA) was used as the eluent. Astra

(version 4.50) (Wyatt Technology, Santa Barbara, CA, USA) software was used to analyse the light scattering data, with Debye plots to obtain the weight-average molecular weight (M_w) and the root-mean square radius (R_z). The MALLS detectors indicated the intensity of light scattered by the mucin molecules, while the DRI detector determined the polymer concentration. The UV signal provided an indication of the presence of the polypeptide backbone of the mucin.

4.3.4 Mixing emulsions with saliva

Protein stabilized emulsions containing 20% soy oil were prepared using lactoferrin or β-lg as the interfacial layer respectively (as described in Chapter 3, Section 3.2.1). Stock emulsions were mixed gently with artificial saliva containing different concentrations of mucin for 30 min; the final mixture contained 10.0 wt% oil.

4.3.5 Physicochemical and microstructural characterization

The average droplet size and the droplet size distribution of the emulsion–saliva mixtures were measured using Malvern MasterSizer MSE. Emulsion–saliva mixture samples were diluted to approximately 0.005 wt% droplet concentration using appropriate background buffer solution (pH and ionic strength of artificial saliva mixed in 1:1 w/w ratio with milli-Q water) and analyzed for ζ-potential measurements using a Malvern Zetasizer Nano ZS (ZEN 3600) instrument (Malvern Instruments Ltd, Malvern, Worcestershire, UK).The microstructures of the emulsion–saliva mixtures containing varying concentrations of mucin were obtained using a confocal scanning laser microscope (Leica DM6000 B, Heidelberg, Germany), with a 100 mm oil immersion objective lens by staining the samples with Nile blue. Details of the physicochemical and microstructural characterization techniques have been described in Chapter 3 (Section 3.2.2).

4.3.6 Determination of creaming stability

The emulsion–saliva mixtures were transferred (in triplicates) into graduated glass tubes (1 cm diameter and 15 cm high). The tubes were graduated with each

division equal to 0.1 mL. The cream layer heights were recorded as a function of time for a period of 30 days at 20 °C *(Agboola et al., 1998a)*. Creaming stability was measured as:

$$Cream\ layer\ (\%) = \frac{Volume\ of\ cream\ layer}{Volume\ of\ total\ emulsion} \times 100\% \qquad \textbf{(4.3-1)}$$

4.3.7 Rheological measurements

The viscosities of lactoferrin–stabilized and *β*-lg–stabilized emulsions on addition of artificial saliva were determined using a controlled-stress rheometer Paar Physica rheometer MCR 301 (Anton-Paar, GmbH Graz, Austria) equipped with double gap geometry [DG 26.7-SIN5514, Measuring bob (diameter $_{internal}$: 24.680 mm, diameter $_{external}$: 26.679 mm, concentricity ±9 μm), Measuring cup (diameter $_{internal}$: 23.822 mm, diameter $_{external}$: 27.594 mm]. The flow curves were recorded at 20 °C, using 25 measuring data points from shear rates ranging from 10 to 1000 s^{-1} as reliable responses were not obtained at lower shear ranges. The shear rate and shear stress data were obtained from the RheoSOLVE software (version 2.1). Triplicate measurements were carried out for each of the duplicate samples.

4.3.8 Determination of mucin coverage

To determine the amount of mucin at the fat globule interface, the emulsion–saliva mixture was centrifuged for 50 min at 45,000*g* and 20 °C (Sorvall RC5C, DuPont Co., Wilmington, DE, USA). The subnatants were carefully removed using a syringe and then filtered sequentially through 0.45 and 0.22 μm filters (Millipore Corp., Bedford, MA, USA). The filtrates were separated using the size exclusion column (Shodex SB–806M) connected to a GBC HPLC system. The eluted fractions were detected by a UV detector at an absorption wavelength of 280 nm. The area under the UV peak was used to calculate the mucin concentration, based on a standard curve obtained using different concentrations of mucin. The mucin surface coverage (mg/m^2) of the protein–stabilized emulsion droplets was calculated from the specific surface

area of the oil droplets, determined by the Malvern Mastersizer, and the difference between the amount of mucin added to the emulsion and that measured in the subnatant. The emulsion mixed with saliva containing more than 0.75 wt% mucin could not be filtered properly possibly due to the large aggregates of mucin molecules blocking the filter pore.

4.4 Results and Discussion

4.4.1 Porcine gastric mucin characterization

The separation of the porcine gastric mucin was successfully achieved using the Shodex SB−806 M column. The overlayed signals (UV, DRI and light scattering at 90°) of the mucin are shown in Figure 4.4-1. The light scattering signal and the first DRI peak (from left) of the chromatogram indicated the large molecular weight materials of interest. The other fractions eluted subsequently contained smaller molecular species (approximately < 10^3 Da), and thus poor light scattering to noise ratio was observed. Different fractions of the molecular species separated by column were detected by the DRI and/ or UV detectors, indicating signals proportional to the concentration of the mucin molecules. By dividing the light scattering signals with the concentration signals obtained from the UV detectors, which used a calculated specific incremental refractive index (*dn/dc*) value of 0.11 and assuming second virial coefficient (A_2) to be zero, the molecular weight (M_w) and radius of gyration R_g of biopolymer eluting within the selected elution volume (Figure 4.4-1) were calculated using a first-order Debye fit (higher order polynomials were also attempted but gave a poorer fit to the data). The molecular parameters derived from Debye plot are shown in Table 4.4-1.

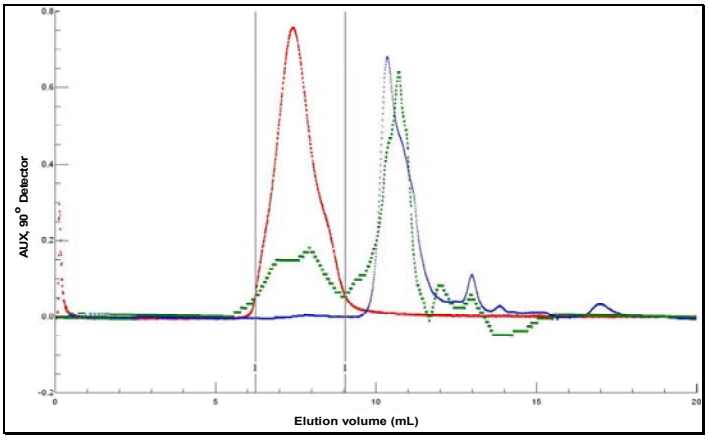

Figure 4.4-1: Light scattering (red), DRI (green), and UV (blue) signals from porcine gastric mucin sample separated using Shodex SB–806 M column. The light scattering was traced by the detector at an angle of 90°. Auxiliary scaling factor for DRI and UV signals was 0.90. The two vertical lines represent the peak boundary and indicate the area of the chromatogram selected for calculation of molecular weight by the ASTRA software.

Table 4.4-1: Molecular parameters of porcine gastric mucin by SEC–MALLS.

Molecular weight (Da)	
M_n	$2.519 \pm 0.044 \times 10^6$
M_w	$3.639 \pm 0.099 \times 10^6$
M_z	$5.060 \pm 0.374 \times 10^6$
Root mean square radius (nm)	
$(R_g^2)^{1/2}_n$	50.1 ± 0.7
$(R_g^2)^{1/2}_w$	60.2 ± 0.9
$(R_g^2)^{1/2}_z$	71.6 ± 1.2
Polydispersity	
M_w/M_n	1.445 ± 0.047
M_z/M_n	2.009 ± 0.152

Results indicated that mucin is a relatively large biopolymer with M_w of ~ 3.6×10^6 Da and R_g of ~ 72 nm. The results were in good agreement with previous studies on porcine gastric mucin *(Wu et al., 1994; Vingerhoeds et al., 2005)*. The molecular mass distribution and the light scattering intensity of the first eluted fraction of mucin molecules from the column are shown in Figure 4.4-2. The

linear decrease in molecular weight with elution volume implies a good separation of the mucin moieties from the size exclusion column.

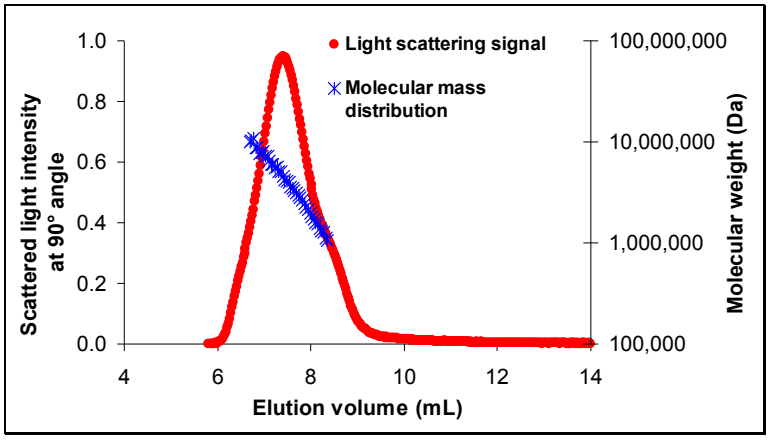

Figure 4.4-2: Scattering intensity and molecular weight distribution of porcine gastric mucin.

The molecular weight of porcine gastric mucin ranged from ~ 1.0×10^6 Da to ~ 8.8×10^6 Da. The shape of the mucin molecule was predicted using the slope obtained from linear regression of a log–log plot of the $(R_g^2)_z^{1/2}$ versus M_w as shown in Figure 4.4-3.

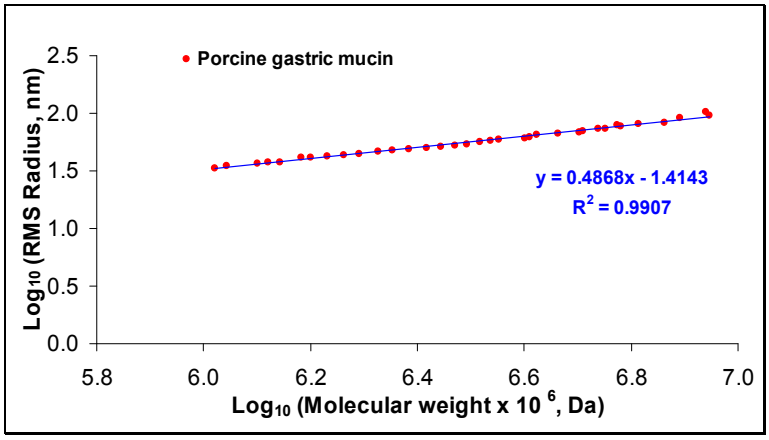

Figure 4.4-3: Logarithmic plot of RMS radius (R_z) as a function of weight-average molar mass for porcine gastric mucin.

The gradient obtained for porcine gastric mucin was ~ 0.49, which suggested that mucin had a flexible random coil conformation in dilute aqueous solution at neutral pH. Mucin of different concentrations were used to prepare the artificial saliva as described in Section 4.3.2 and added to the emulsions.

4.4.2 Droplet size distribution

Both lactoferrin and *β*-lg (*i.e.* before mixing with artificial saliva) formed stable emulsions and showed monomodal distributions (Figure 4.4-4).

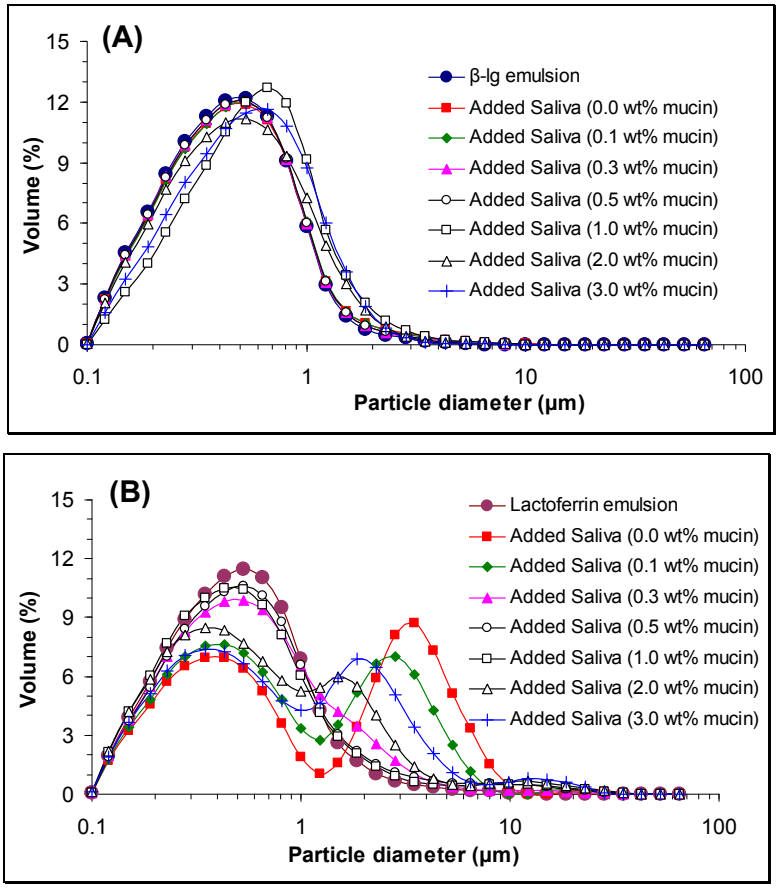

Figure 4.4-4: Droplet size distribution of *β*-lg– (A) or lactoferrin– (B) stabilized emulsions upon mixing with artificial saliva containing various concentrations of mucin. (Sample containing 0.0 wt% mucin implies emulsion–saliva mixture contained 0.5 wt% artificial saliva salts only with no added mucin unless otherwise specified). Each data point is the average of measurements on triplicate samples.

Both the milk protein–stabilized emulsions showed average droplet size (d_{43}) of ~ 0.60 µm (Figure 4.4-5). Addition of saliva without mucin or containing different mucin levels to *β*-lg–stabilized emulsions had no significant effect on the droplet size distribution (Figure 4.4-4 A). The d_{43} values also remained rather constant on addition of artificial saliva (Figure 4.4-5) ($p > 0.05$). In contrast, when lactoferrin–stabilized emulsions were mixed with artificial saliva containing different levels of mucin (0.0–3.0 wt%), the emulsion droplets showed both mono- and bimodal size distributions (Figure 4.4-4 B). Interestingly, the addition of artificial saliva without mucin (*i.e.* containing 0.5 wt% salts only) resulted in a bimodal size distribution (Figure 4.4-4 B), with a considerable proportion of the droplets in the size range 1–10 µm and d_{43} being ~ 2.30 µm (Figure 4.4-5), as compared to *β*-lg–stabilized emulsions (no change with addition of salivary salts). Even on addition of saliva containing lower concentration of salivary salts (0.16–0.33 wt%), the droplet size distribution of lactoferrin emulsions still retained a tendency towards bimodality (Figure 4.4-6 A).

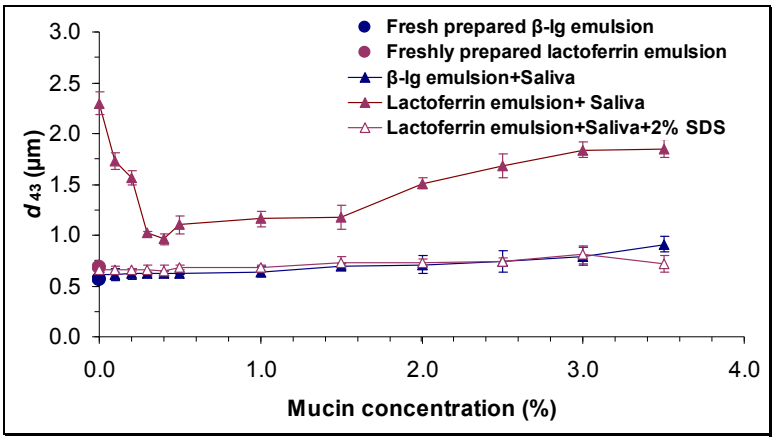

Figure 4.4-5: Change in droplet size *i.e.* d_{43} (µm) of the milk protein–stabilized emulsion droplets after mixing with artificial saliva as a function of different concentrations of added mucin and d_{43} (µm) values of lactoferrin emulsion–saliva mixtures upon dispersion in 2.0% SDS solution. Errors bar indicate standard deviations.

However, when these lactoferrin–stabilized emulsion–saliva mixtures containing different concentrations of salts were gently dispersed in 2.0% SDS, all the distributions became monomodal distributions, similar to that of the untreated

emulsions (Figure 4.4-6 B), which indicates that the larger particles were aggregates, which were redispersed by SDS.

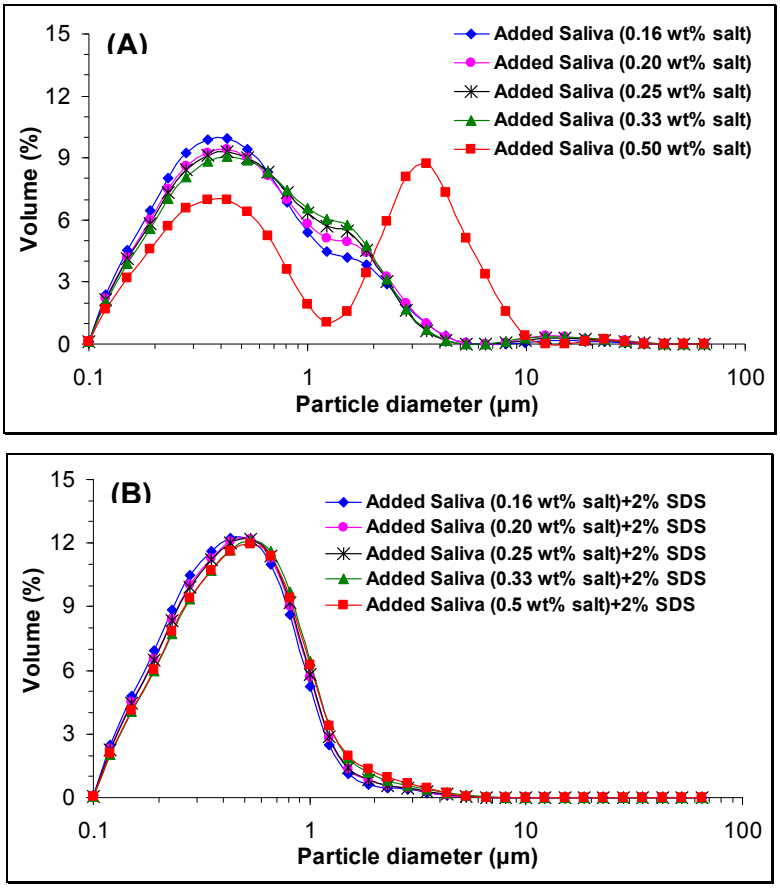

Figure 4.4-6: Droplet size distribution of emulsions made with lactoferrin upon mixing with artificial saliva containing different concentrations of salivary salts (without any added mucin) (A) and with addition of 2.0% SDS solution to the above emulsion–saliva mixtures (B) mentioned in A. Each data point is the average of measurements on triplicate samples.

On mixing with saliva containing lower mucin concentrations (0.01–0.2 wt%), the lactoferrin emulsion continued to show bimodal distributions, but the d_{43} values showed a gradual reduction. A further increase in the mucin levels (0.3–1.0 wt%) caused the emulsions to revert to monomodal distributions (Figure 4.4-4 B) and a further decrease in d_{43} (Figure 4.4-5). At higher mucin concentrations (≥ 2.0 wt%), the size distribution again showed a slightly bimodal pattern (Figure 4.4-4 B) and a significant increase in d_{43} ($p < 0.05$). When the lactoferrin emulsion–saliva mixtures containing various concentrations of mucin

were mixed gently with 2.0% SDS, all the bimodal distributions reverted to monomodal, similar to that of the untreated emulsion (Figure 4.4-7), with d_{43} of ~ 0.66 μm (Figure 4.4-5).

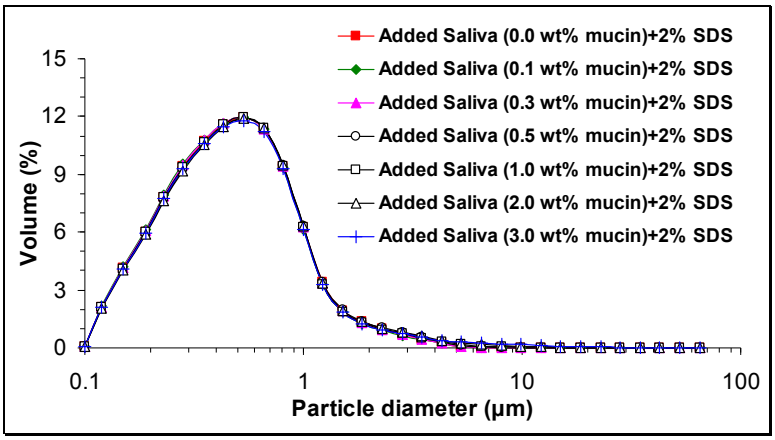

Figure 4.4-7: Droplet size distribution of lactoferrin emulsions–artificial saliva mixtures (containing various concentrations of mucin as shown in Figure 4.4-4 B) after mixing with 2.0% SDS solution. Each data point is the average of measurements on triplicate samples.

4.4.3 Stability and microstructure of emulsions

The creaming stability of emulsions mixed with artificial saliva containing different amounts of mucin is shown in Figure 4.4-8. The lactoferrin– and *β*-lg–stabilized emulsions (before mixing with saliva) did not show any creaming even after storage for 30 days storage at 20 °C (data shown for 7 days, Figure 4.4-8 A). Lactoferrin–stabilized emulsions, mixed with saliva containing 0.0–0.2 wt% mucin, showed extensive creaming, but emulsions containing 0.3 wt% mucin were stable to creaming (Figure 4.4-8). The extent of creaming increased gradually as a function of mucin concentration above 0.3%. The *β*-lg–stabilized emulsion showed an increasing cream separation above a mucin concentration of approximately 1.0%. However, there was no cream separation in *β*-lg–stabilized emulsion on addition of artificial saliva containing below 0.5 wt% of added mucin.

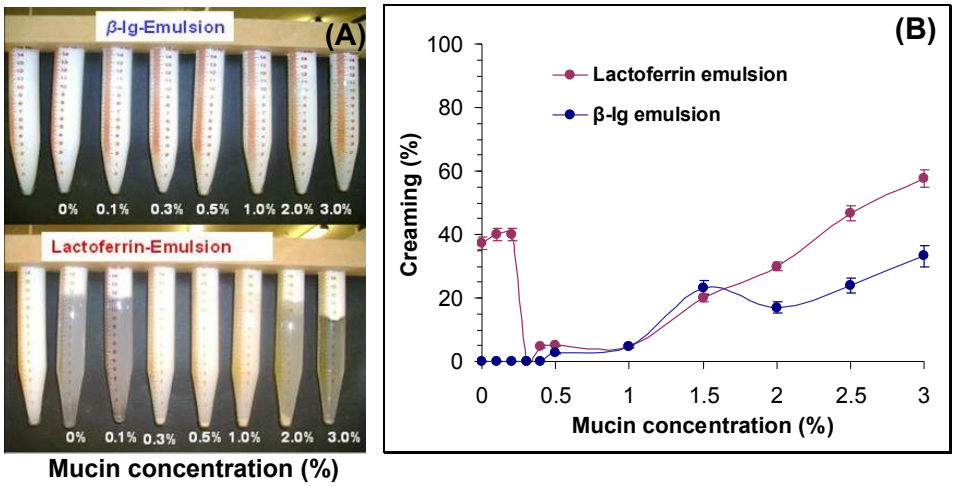

Figure 4.4-8: Creaming stability of emulsion–artificial saliva mixtures after 7 days (A), calculated as a function of mucin concentration (B). Errors bars indicate standard deviations. The first graduated creaming tube in (A) represents the emulsions without addition of artificial saliva (control).

Figure 4.4-9 and Figure 4.4-10 show confocal microscopy images of emulsions after mixing with artificial saliva. Both lactoferrin–stabilized and *β*-lg–stabilized emulsions were rather monodisperse originally *i.e.* after homogenization showing an array of uniformly distributed droplets (Figure 4.4-9 A and Figure 4.4-10 B).

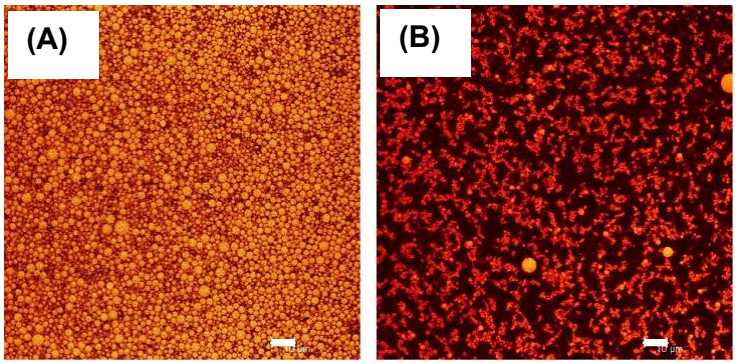

Figure 4.4-9: Confocal micrographs of *β*-lg–stabilized emulsions mixed with milli-Q water (A) or with artificial saliva containing 1.0 wt% added mucin (B). Scale bar corresponds to 10 µm.

The *β*-lg–stabilized emulsions showed no droplet aggregation when they were mixed with saliva containing only salts and the emulsions remained homogeneous in the presence of low mucin concentrations (data not shown). However, the emulsions showed network–like flocculation at 1.0 wt% added

mucin (Figure 4.4-9 B). These emulsion–saliva mixtures (containing added 1.0 wt% mucin) reverted back to homogenous dispersions after dilution with water, which indicated that the flocculation was reversible. In contrast to the *β*-lg–stabilized emulsions, pronounced droplet aggregation was observed in the lactoferrin–stabilized emulsions in the presence of salts (without mucin) (Figure 4.4-10 B).

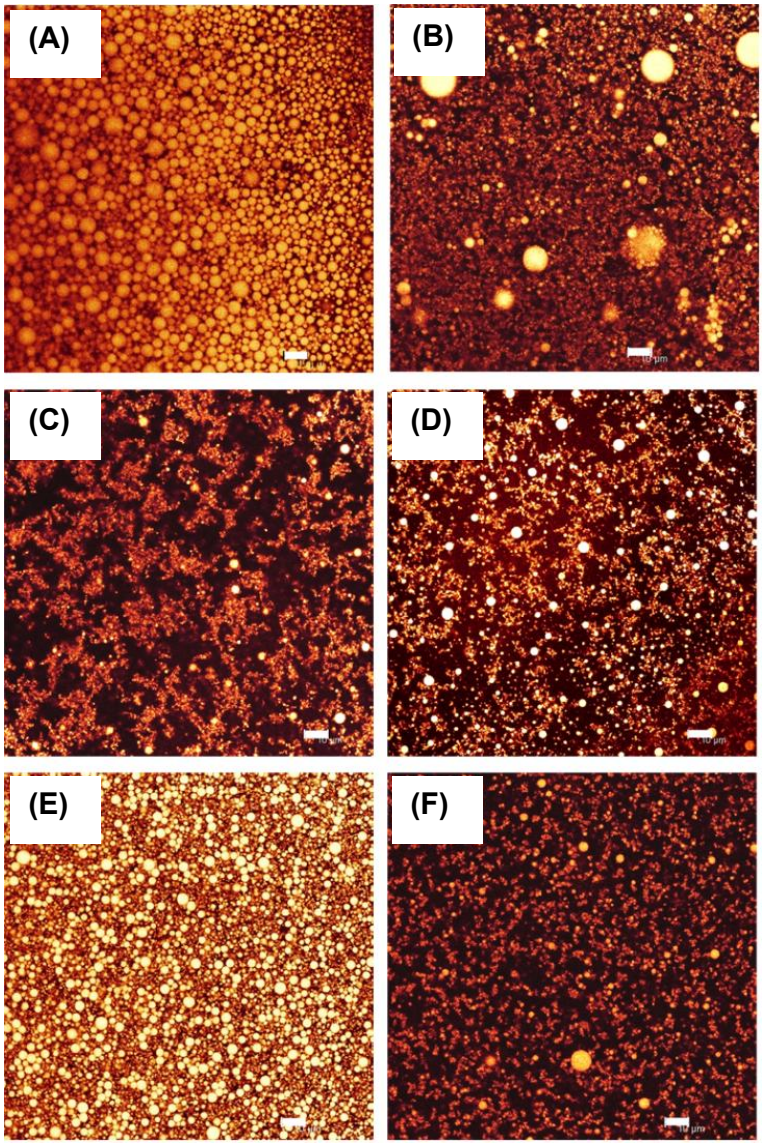

Figure 4.4-10: Confocal micrographs of lactoferrin–stabilized emulsion mixed with milli-Q water (A) or with artificial saliva containing 0.0 (B), 0.02 (C), 0.2 (D), 0.5 (E), and 2.0 wt% (F) of added mucin, respectively. Scale bar corresponds to 10 µm.

At mucin level similar to that found generally in real human saliva (0.02 wt%), lactoferrin–stabilized emulsions appeared to be densely aggregated (Figure 4.4-10 C), with the size of the droplet aggregates appearing to decrease at 0.2 wt% added mucin concentration (Figure 4.4-10 D). Interestingly, the emulsions appeared to be rather monodisperse at intermediate mucin concentrations (0.5 wt%) (Figure 4.4-10 E). However, at higher mucin concentrations (2.0 wt%), the lactoferrin–stabilized emulsions again showed aggregation of the oil droplets (Figure 4.4-10 F). Both the particle size results and confocal microscopy results clearly show that the negatively charged *β*-lg–stabilized emulsion droplets were stable in the presence of saliva with mucin levels below 1.0 wt%, as the repulsive forces between the two negatively charged biopolymers dominated successfully over the weak van der Waals' attractive forces. However, at higher mucin concentrations (≥ 1.0 wt%), these emulsions showed extensive flocculation and phase separation without a significant change in droplet size. This behaviour is typical of an emulsion system displaying depletion flocculation *(Singh et al., 2003)*. The effects of mucin on the positively charged lactoferrin–stabilized emulsion droplets were more complicated and are discussed later.

4.4.4 Apparent viscosity

Viscosity curves for the different emulsion–saliva mixtures at 20 °C were obtained. Both *β*-lg–stabilized and lactoferrin–stabilized emulsions showed Newtonian behaviour in the absence of saliva, with a relatively low apparent viscosity of ~ 1.4 mPa-s (Figure 4.4-11 A and B). Shear thinning behaviour seemed to appear for *β*-lg–stabilized emulsion at added mucin concentration of 1.0 wt% (Figure 4.4-11 A), which was probably due to gradual break up of the network–like aggregates due to depletion flocculation (as observed in confocal micrographs in Figure 4.4-9 B). In addition, the presence of unadsorbed mucin molecules could also contribute to the shear thinning behaviour due to the stretching of the random coil polymer in the direction of the flow.

Interestingly, in case of lactoferrin–stabilized emulsions, pseudoplastic flow behaviour was observed when mixed with salivary salts alone (without mucin)

(Figure 4.4-11 B). This could suggest the presence of aggregates (based on a bimodal distribution) which were disrupted by shear during the viscosity measurement. The flow properties of the lactoferrin emulsion samples containing intermediate added mucin concentrations (0.3–1.0 wt%) appeared to be Newtonian. This was expected because the emulsions had monomodal size distributions (Figure 4.4-4 B) and uniformly dispersed droplets in confocal micrographs (Figure 4.4-10 E), as described earlier.

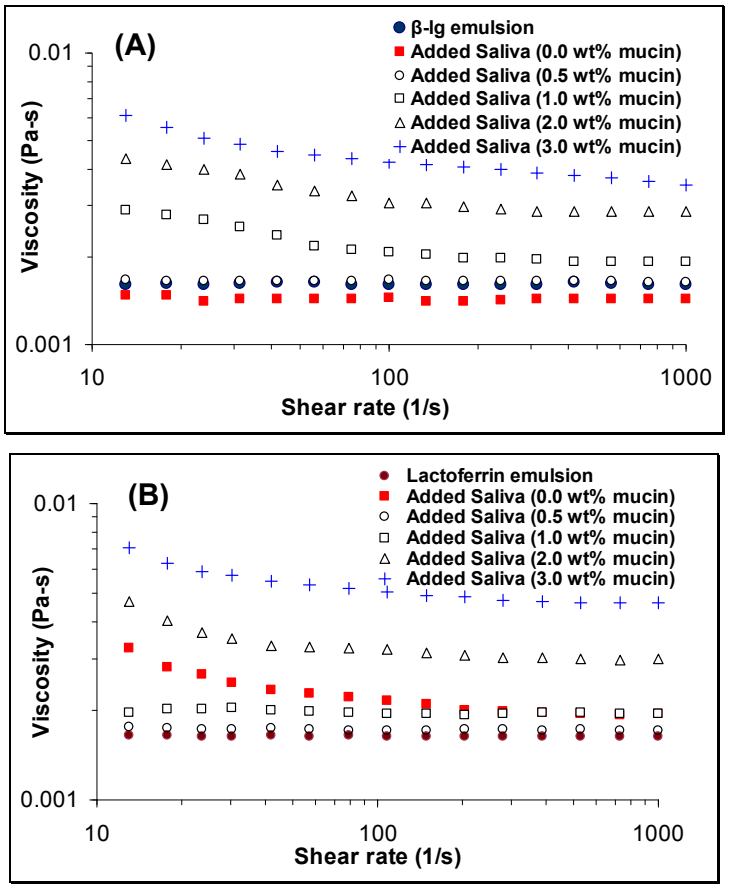

Figure 4.4-11: Apparent viscosity curves of emulsions stabilized by *β*-lg (A) or lactoferrin (B) upon mixing with artificial saliva. Each data point is the average of measurements on triplicate samples.

At sufficiently higher mucin concentration (≥ 2.0 wt%), lactoferrin–stabilized emulsions showed substantially pseudoplastic behaviour (Figure 4.4-11). This could possibly be attributed to the presence of unadsorbed mucin as well as the disruption of large aggregates (as indicated by bimodal size distribution (Figure 4.4-4 B) and confocal micrographs (Figure 4.4-10 F). The viscosities of the

emulsion–saliva mixtures (at shear rates ranging from 10 to 1000s^{-1}) were compared with calculated corresponding viscosities (Figure 4.4-12) based on the Maron-Pierce empirical equation for concentrated monodispersed emulsions *(Carreau et al., 1997; Singh et al., 2003)* as shown below:

$$\eta = \eta_s /(1-\phi/\phi_c)^2 \qquad \textbf{(4.4-1)}$$

where, η is the emulsion viscosity, η_s the viscosity of the continuous phase, ϕ the dispersed phase volume and ϕ_c was chosen as 0.64 for random close packing of monodispersed droplets. These shear rates (10, 100 and 1000s^{-1}) have been arbitrarily used to give an insight to the whole range of shear experienced in the mouth when a liquid food, such as protein–stabilized emulsion is consumed *(van Aken, 2007)*. As expected, at higher shear rates, the apparent viscosities of the *β*-lg–stabilized emulsion were close to those of the theoretical values (Figure 4.4-12 A). At low shear rates, the large increase in viscosities in *β*-lg–stabilized emulsions was clearly seen at higher mucin concentration (≥ 1.0%), which was mainly due to the depletion flocculation as proposed before. As mucin is a negatively charged polymer, it was not expected to interact with the net negative charge of the *β*-lg–stabilized emulsion droplet.

In contrast, lactoferrin emulsion showed significant difference in viscosities from the calculated values (Figure 4.4-12 B) particularly at lower (0–0.2%) and higher (≥ 2.0%) mucin levels. When mucin was added at lower concentration (0.0–0.2 wt%), the viscosity increased because of an increase in the average particle size, caused by aggregates. At intermediate mucin concentrations (particularly 0.3–0.5 wt%), where the lactoferrin–stabilized emulsions showed monomodal size distributions and Newtonian flow curves, the viscosities were only slightly higher than that of the calculated value.

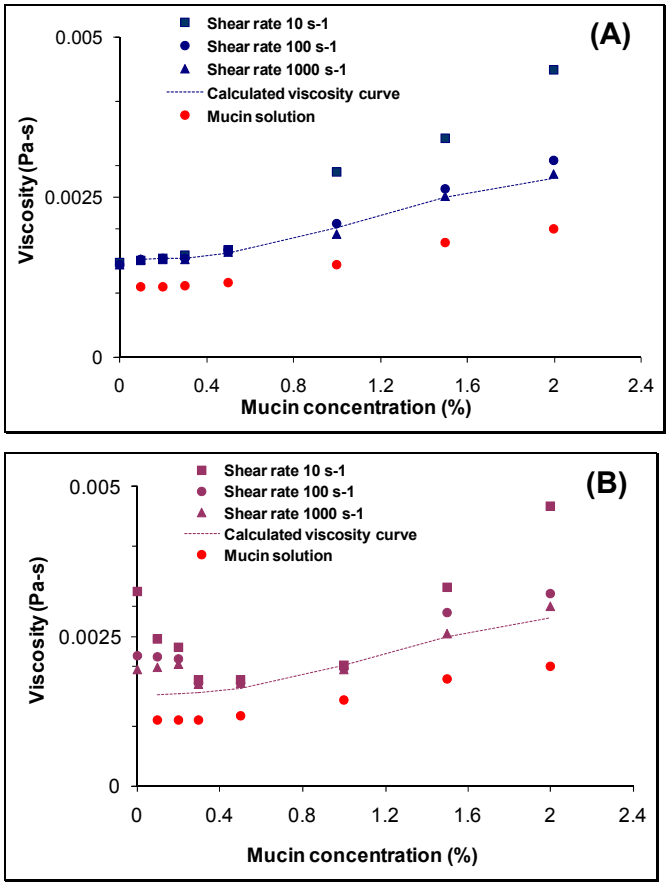

Figure 4.4-12: Dependence of apparent viscosity (mPa-s) of *β*-lg– (A) and lactoferrin– (B) stabilized emulsions on increasing concentrations of added mucin at ionic strength of artificial saliva.

The slightly higher viscosities could imply a slightly larger hydrodynamic volume because of a secondary mucin layer present at the interface of the lactoferrin–stabilized emulsion droplet. The secondary mucin layer on the lactoferrin–stabilized emulsion droplets was a result of electrostatic interaction between oppositely charged groups in the two species. At higher mucin concentrations (≥ 2.0%), the viscosity of the lactoferrin–stabilized emulsion appeared to be slightly higher than that of calculated values at high shear rate (1000 s^{-1}). This indicated the presence of some aggregates in these emulsions (as observed by the bimodal size distribution) which were resistant to high shear.

4.4.5 Zeta-potential

The ζ-potential data of the mixtures of emulsion and saliva at pH 6.8 are shown in Figure 4.4-13. Lactoferrin formed a strongly cationic emulsion (~ +53 mV) and *β*-lg formed an anionic emulsion (~ –62 mV) at neutral pH, in agreement with previous reports *(Ye & Singh, 2006a)*.

For the *β*-lg–stabilized emulsions, there was no change in the ζ-potential in the presence of saliva containing salts alone, probably because the low ionic strength (27 mM NaCl) of the artificial saliva composition used. However, the ζ-potential became less negative with increasing mucin concentration, as mucin has less overall negative charge (nearly –20 mV) than *β*-lg–stabilized emulsion droplets (nearly –60 mV) at neutral pH, which could also imply some coverage of mucin on weakly anionic emulsion droplets.

For the lactoferrin–stabilized emulsions mixed with saliva containing salts (without mucin), the ζ-potential was sharply reduced from ~ +50 to ~ +27 mV, suggesting an electrostatic screening effect by the salts.

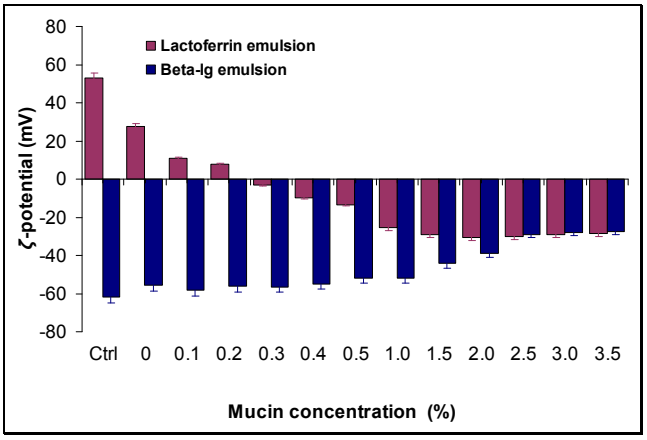

Figure 4.4-13: The ζ-potential of emulsion droplets at pH 6.8 after mixing with artificial saliva as a function of different concentrations of added mucin. Standard deviation is indicated by error bars. (Ctrl represents freshly prepared emulsions (control) without any treatment with saliva).

To investigate further the role of salts, lactoferrin–stabilized emulsions were mixed with saliva containing different concentration of salts (upto 0.5 wt% *i.e.*

original salt concentration of artificial saliva) and examined for ζ-potential values as shown in Figure 4.4-14. The ζ-potential magnitudes decreased significantly as a function of increased salivary salt concentration ($p < 0.05$), which together with the observed bimodal distribution (Figure 4.4-7 B), gravity creaming (Figure 4.4-8), aggregated confocal micrographs (Figure 4.4-10 B) and shear thinning behaviour (Figure 4.4-11 B) indicated salt–induced aggregation effects in lactoferrin emulsions. With the addition of mucin, the ζ-potential of the lactoferrin–stabilized emulsion gradually decreased from ~ +27 to ~ –27 mV at added mucin concentrations varying from 0.1 to 1.5 wt% (Figure 4.4-13). This was possibly a result of gradual electrostatic binding of negatively charged mucin to the positively charged lactoferrin–stabilized emulsion droplets.

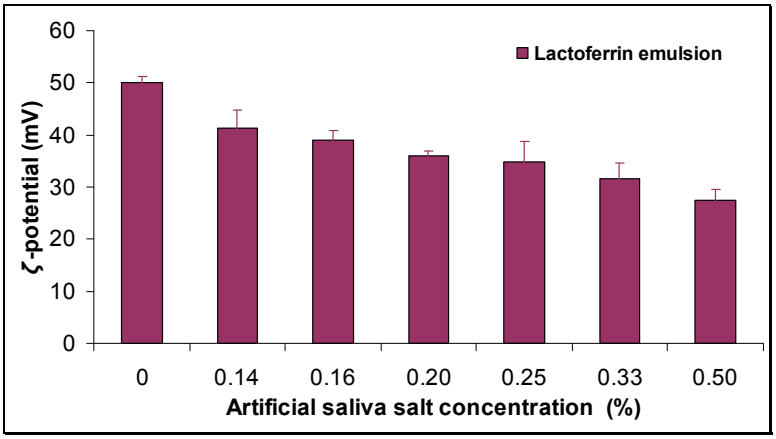

Figure 4.4-14: The ζ-potential of emulsion droplets at pH 6.8 after mixing with artificial saliva as a function of different concentrations of salt concentrations (without addition of mucin). Standard deviation is indicated by error bars.

4.4.6 Mucin coverage as a secondary layer

The β-lg–stabilized emulsion droplets showed a relatively small increase in mucin surface coverage, with a maximum of ~ 0.6 mg/m^2 at a concentration of 0.75% mucin (Figure 4.4-15). In contrast, there were considerably higher amounts of mucin binding at the lactoferrin–stabilized emulsion droplet interface than at the β-lg–stabilized emulsion droplet interface at a given mucin concentration. The amount of mucin surface coverage (mg/m^2) of the

lactoferrin–stabilized emulsion increased almost linearly to approximately 1 mg/m^2 with an increase in the added mucin concentration from 0.1 to 0.75 wt%. The higher mucin coverage in the lactoferrin–stabilized emulsion was attributed to the electrostatic attraction between mutually oppositely charged mucin molecules (negative) and lactoferrin molecules (positive) adsorbed at the droplet surface. However, for the *β*-lg–coated droplets, the presence of some positive patches along the adsorbed *β*-lg molecules probably resulted in some electrostatic interactions with the negatively charged mucin molecules *(Dickinson & Galazka, 1991; Tolstoguzov, 1991; Gu et al., 2005)*. Moreover, there is also possibility of hydrophobic interactions between unfolded *β*-lg at the adsorbed layer and mucin at low ionic strengths of artificial saliva *(Lee et al., 2005)*.

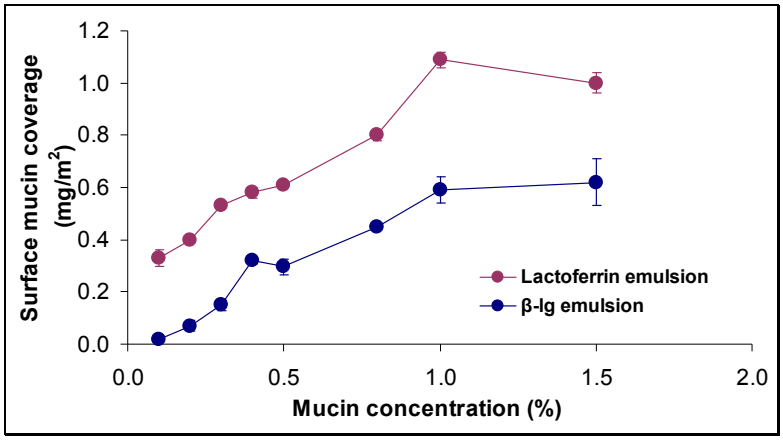

Figure 4.4-15: Surface mucin coverage (mg/m^2) of milk protein–stabilized emulsion droplets mixed with artificial saliva containing different concentrations of added mucin. Standard deviation is indicated by error bars.

The critical concentration of biopolymer where the lactoferrin–coated droplets are fully saturated with mucin can be theoretically calculated using the empirical model *(Gu et al., 2007)*:

$$\frac{\zeta(c)-\zeta_{sat}}{\zeta_0-\zeta_{sat}} \approx \exp\left(-\frac{3c}{c_{sat}}\right) \qquad \textbf{(4.4-2)}$$

In this study, $\zeta(c)$ is the ζ-potential of emulsion at mucin concentration c, ζ_0 is the ζ-potential without the addition of mucin, ζ_{sat} is the ζ-potential where the emulsion is saturated with mucin and c_{sat} is the critical concentration at which 95% of the lactoferrin emulsion droplet surface is covered with mucin. The critical concentration of mucin to cover lactoferrin–coated droplets fully was predicted to be ~ 0.15% using ζ-potential curve (Figure 4.4-13) and $\Delta\zeta$ = –80.6 mV (ζ_{sat} - ζ_0), which corresponds to ~ 0.3 wt% of added mucin. As expected at this concentration of mucin, the lactoferrin emulsions were stable with monomodal size distribution (Figure 4.4-4). The surface mucin coverage Γ_{sat} (mg/m^2) at the saturation can be theoretically predicted using the following expression *(McClements, 2005)*:

$$\Gamma_{sat} = \frac{c_{sat} d_{32}}{6\phi} \qquad \textbf{(4.4-3)}$$

Here, c_{sat} is the mass of mucin adsorbed to the droplet surface per unit volume (= 1.5 kg/m^3 as calculated above), d_{32} is the volume-surface mean droplet diameter (= 0.35 μm) and ϕ is the droplet volume fraction = 0.1 (10.0 wt% soy oil in the emulsion–saliva mixture). Putting the respective values in the above equation, the surface mucin concentration (Γ_{sat}) is 0.875 mg/m^2, which is higher than the observed value of ~ 0.7 mg/m^2 (Figure 4.4-15). This difference in surface load ($\Delta\Gamma_{sat}$=0.175 mg/m^2) in experimental and calculated values can be attributed to the amount of mucin loss in the filtration process.

4.4.7 Interactions of mucin with emulsion droplets

The mechanisms of interaction for both β-lg–stabilized and lactoferrin–stabilized emulsions in the presence of artificial saliva containing different levels of mucin can be explained from the particle size analysis, viscosity profiles, confocal microscopy, surface coverage and ζ-potential results. Schematic representations of the interactions are given in Figure 4.4-16.

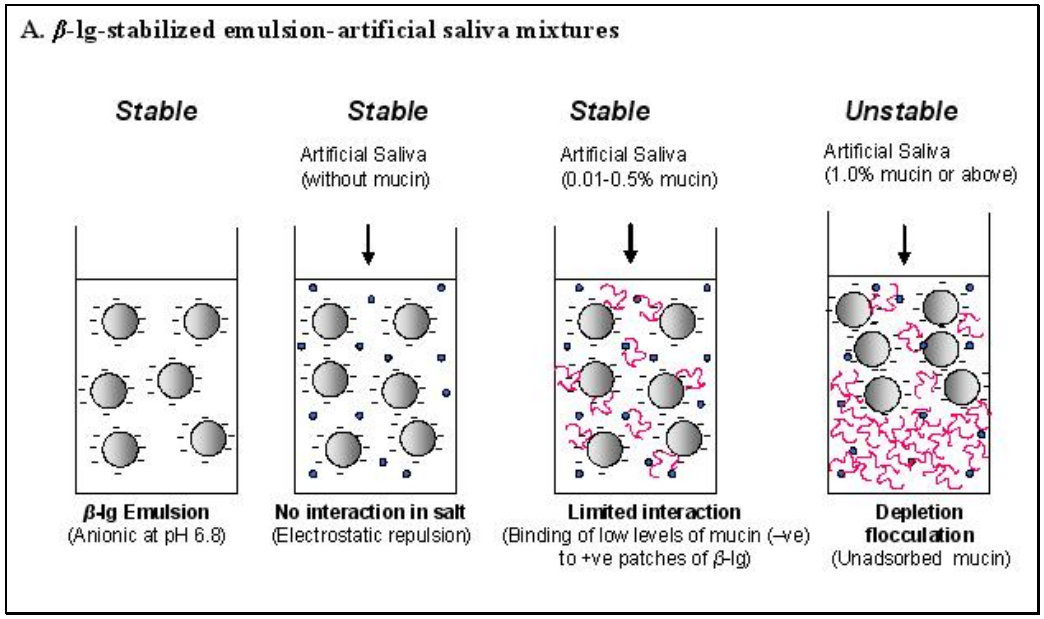

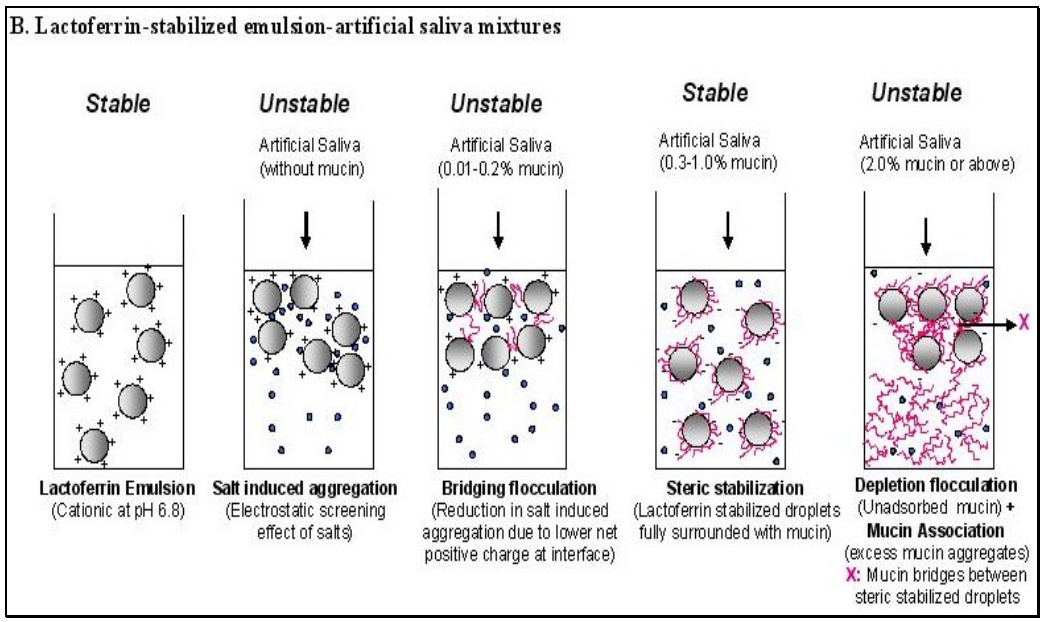

Figure 4.4-16: Mechanisms of interactions of *β*-lg–stabilized emulsion (A) and lactoferrin–stabilized emulsion (B) with artificial saliva, respectively. Big shaded circle represents emulsion droplets; small solid dot represents salivary salts and pink coil structure represents mucin molecules.

The *β*-lg–stabilized emulsion droplet binds very small amounts of mucin from the artificial saliva, and this binding does not cause any flocculation or phase separation of the droplets. Adding saliva containing only salts (without mucin) to *β*-lg–stabilized emulsion did not show any significant change. Electrostatic screening by salt was not observed probably because the ionic strength of

artificial saliva composition was appreciably lower (27 mM NaCl) as compared to 150 mM NaCl required to cause salt induced aggregation in β-lg–stabilized emulsion *(Djordjevic et al., 2004)*. When the concentration of unadsorbed mucin exceeded a concentration of 0.5 wt% (*i.e.* 1.0 wt% of added mucin), depletion flocculation has been proposed (Figure 4.4-16 A). Theoretically, considering depletion to be the main interaction force for droplets coming in contact, the droplet interaction potential [$-\omega_{dep}(0)$] was calculated using the following equation *(McClements, 2000)*.

$$\omega dep(0) = \frac{-3kT}{2}\frac{cRv}{\rho}\left(1+\frac{1}{2}\frac{cRv}{\rho}\right)\left(\frac{\gamma d}{\gamma g}+\frac{2}{3}\right) \qquad \textbf{(4.4-4)}$$

where, in c is the biopolymer concentration (kg/m^3), γ_d *and* γ_g are the radius of the emulsion droplet and radius of gyration of the biopolymer respectively, ρ is the density of biopolymer and Rv is given by the following expression:

$$Rv = \frac{4\pi\gamma_g{}^3\rho N_A}{3M} \qquad \textbf{(4.4-5)}$$

where, N_A is the Avogadro number and M is the molecular weight of the biopolymer molecule (kg/mol).

Using the above theoretical equations, the droplet interaction potential [$-\omega_{dep}(0)$] at γ_d 0.21 μm (calculated from d_{32} value of 0.42 μm, obtained from MasterSizer experiments), γ_g 0.072 μm and 1.0 wt% added mucin was found to be ~ 11.5 kT. Since the magnitude of interaction potential exceeded 4 kT, depletion flocculation of emulsion droplets was predicted *(McClements, 2000)*. Thus, the theoretical calculation is consistent with the observed experimental confirmation for depletion flocculation, which is also indicated by the non-Newtonian rheological behaviour of emulsions (Figure 4.4-11 A) and confocal micrographs showing aggregated network at 1.0 wt% added mucin (Figure 4.4-17) as well as reversibility of flocculation upon dilution of flocculated emulsions.

Mixing lactoferrin–stabilized emulsion with saliva containing only salts (without mucin) promotes the aggregation of oil droplets, which can be attributed to the screening of the positive charges of the lactoferrin molecules on the droplet surface by the negatively charged electrolytes such as chlorides, citrates and phosphates in the saliva *(Dickinson, 1998; Schmitt et al., 1998)*. This type of "salt–induced" aggregation of oil droplets stabilized by lactoferrin has not been reported previously. Mucin appears to bind strongly to the lactoferrin–stabilized emulsion droplets, involving electrostatic interactions. Consequently, there is a reduction in the positive charge on the droplet surface, which gradually diminishes the extent of salt–induced aggregation. This protective effect of mucin against the salt–induced aggregation is directly proportional to the surface coverage of mucin on the lactoferrin–stabilized emulsion droplets.

At low mucin concentrations (< 0.3%), there is an insufficient amount of mucin to form a complete secondary layer around the lactoferrin–stabilized emulsion. In these systems, salt–induced aggregates still persist. In addition, the droplets may aggregate by a bridging mechanism *(Dickinson & Eriksson, 1991; Dickinson, 1998; Dickinson, 2003)*, as shown in Figure 4.4-16 B. At intermediate mucin concentrations (0.3–1.0 wt%), there is sufficient binding of mucin to cover the lactoferrin–stabilized emulsion droplets completely, giving rise to stable emulsions.

At mucin concentrations above ~ 2.0 wt%, droplets appear to aggregate, probably as a result of excessive mucin in the continuous phase *(Dickinson & Golding, 1997; Dickinson et al., 1997; Reiffers-Magnani et al., 2000)*. It would be tempting to attribute this effect to depletion flocculation (as in the case of *β*-lg emulsion), but confocal micrographs (Figure 4.4-17) showed the presence of some large aggregates of droplets even after dilution with milli-Q water and the droplet size distribution remained bimodal.

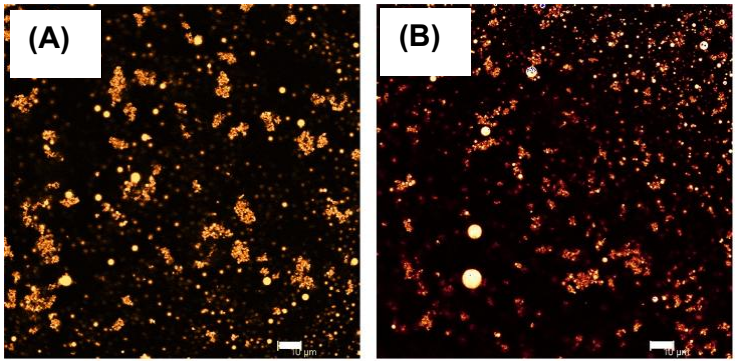

Figure 4.4-17: Confocal micrographs of lactoferrin–stabilized emulsion upon mixing with artificial saliva containing 2.0 wt% (A) and (B) 3.0 wt% of added mucin, respectively, after ten times dilution (w/w) in milli-Q water. Scale bar corresponds to 10 µm.

This indicates that at high levels of mucin in lactoferrin–stabilized emulsions in addition to the expected depletion flocculation, droplets were aggregated *via* some other mechanism. The mechanisms involved in the formation of these aggregates are still not entirely clear. As mucin molecules are known to associate with each other at sufficiently high concentrations *(Vingerhoeds et al., 2005)*, it is possible that this association also involves mucin molecules bound at the droplet surface. The association of mucin molecules bound to two different droplets could lead to some kind of aggregation.

4.5 Conclusions

This study provided a better understanding of the mechanisms of flocculation in protein–stabilized emulsion systems in the presence of artificial saliva containing mucin and salts. Model oil-in-water emulsion system stabilized by positively–(lactoferrin) and negatively–charged (*β*-lg) milk proteins at pH 6.8 were treated with an artificially buffered salivary system. The study elucidated the important roles of both the electrolytes and the highly glycosylated mucins present in saliva. A wide range of mucin concentrations was used in the artificial saliva composition to deal with wide variability and rheological implications of human saliva *in vivo*.

The colloidal stability and the interactions of the emulsion were determined by the initial surface charge on the emulsion droplet, interactions of mucins with the

droplet surface and the presence of salts using different characterization techniques. The observations of emulsion flocculation were largely strengthened by theoretical calculations based on interaction forces. Using the size of emulsion droplets, the amount of protein bound and the radius of gyration of the mucin molecule, the main driving force for flocculation was demonstrated. The mechanism of emulsion flocculation in presence of saliva was largely driven by electrostatic interactions in protein stabilized emulsions, which is in good agreement with the hypothesis of other authors.

This study particularly showed that negatively charged protein–stabilized emulsions *i.e.* β-lg emulsions did not interact with saliva significantly due to mutually opposite charges of anionic mucin and anionic β-lg interfacial layer at neutral pH, but underwent depletion flocculation on addition of higher concentrations of mucin ($\geq$ 1.0 wt%) due to presence of unadsorbed mucin molecules in the continuous phase. In contrast, positively charged protein–stabilized emulsions, *i.e.* lactoferrin emulsions showed salt–induced aggregation on addition of saliva containing only salts (even without addition of mucin), which has never been reported before. Additionally, lactoferrin–stabilized emulsions showed typical biopolymer–biopolymer kind of colloidal interactions *i.e.* bridging–to–stable–to–depletion type of flocculation behaviour on addition of low–to–sufficient–to–high concentrations of negatively charged mucin, respectively. These kinds of emulsion–saliva electrostatic interactions might occur upon consumption of emulsion in real situations and could result in different sensorial and textural perception *in vivo*.

Food emulsions, after residing for a relatively shorter period (few seconds to few minutes) in the mouth, are generally subjected to harsh physical and biochemical processing conditions, *i.e.* acidic pH, high ionic strength, proteolytic enzyme, biopolymer and peristaltic shear as they enter the stomach. Hence, the physicochemical changes, structure, stability and interfacial characteristics of emulsions during the passage of milk protein–stabilized emulsions through the stomach were investigated in the next chapter using an *in vitro* gastric model system.

Chapter Five: Behaviour of Milk Protein–Stabilized Emulsions in Simulated Gastric Fluid [2]

5.1 Abstract

The behaviour of lactoferrin– and β-lactoglobulin (β-lg)–stabilized emulsions (1.0 wt% protein and 20.0 wt% soy oil) using pepsin digestion under simulated gastric conditions (37 °C, pH 1.2 and 34 mM NaCl ionic strength, with continuous shaking at approximately 95 rev/min for 2 h) was investigated. Changes in particle size, ζ-potential and microstructure were monitored as a function of incubation time in the gastric fluid. Both the emulsions underwent extensive droplet flocculation with some degree of coalescence, on mixing with the simulated gastric fluid (SGF). For lactoferrin–stabilized droplets, the ζ-potential decreased gradually from +52.9 ± 0.3 mV to +9.8 ±1.2 mV as a result of pH change and peptic hydrolysis of the interfacial lactoferrin layer. For β-lg–stabilized droplets, the ζ-potential changed from -57.1 ± 0.5 mV to +17.6 ± 1.2 mV under the same conditions. Native β-lg was largely resistant to pepsin attack but, when β-lg was present at the interfacial layer of the oil-in-water emulsion, it was rapidly hydrolysed by pepsin, as shown by sodium dodecyl sulphate polyacrylamide gel electrophoresis (SDS-PAGE). The droplet flocculation and the coalescence observed during hydrolysis were markedly dependent on the digestion time.

5.2 Introduction

There is little understanding of the physico-chemical changes in a food product as it passes through the gastrointestinal tract. Simulations of the physiological conditions have been attempted but have not yet been very successful *(van Ruth & Roozen, 2000b; Beysseriat et al., 2006)*. To date, in an attempt to understand the changes that occur in food materials, most studies, using simple model food

[2] Part of the contents presented in this chapter has been published previously as a peer-reviewed paper: Sarkar, A., Goh, K. K. T., Singh, R. P., and Singh, H. (2009), Behaviour of an oil-in-water emulsion stabilized by β-lactoglobulin in an *in vitro* gastric model. *Food Hydrocolloids*, *23*(6), 1563–1569.

systems, have focused on simulating the conditions of only a portion of the physiological processes at one time (*i.e.* conditions in the mouth, stomach and intestine) *(Wickham et al., 1998; Beysseriat et al., 2006; Mun et al., 2007; Silletti et al., 2007b)*.

Once the food product after oral processing passes from the mouth through to the oesophagus and then into the stomach, it may remain in the stomach for a short period (from a few minutes to a few hours) depending on the nature of the food *e.g.* chemical composition, shape, size, microstructure, pH and ionic conditions, rheological properties *etc. (Malagelada & Azpiroz, 1989)*. In the case of an emulsion entering in the stomach, it will be mixed with the gastric fluid, which contains different enzymes (pepsin, gastric lipase) and electrolytes (Na^+, Cl^-, Ca^{2+} etc.). The emulsion will undergo a drastic change in pH (acidic environment: pH 1–3) while being exposed to shear because of the peristaltic movement in the stomach *(Lindahl et al., 1997; Weisbrodt, 2001a; Ekmekcioglu, 2002; Kalantzi et al., 2006; Pal et al., 2007)*.

A number of recent studies have reported the effect of lipases and bile salts on emulsion droplets stabilized by different surfactants at the oil interface *(Beysseriat et al., 2006; Mun et al., 2007)*. However, there is limited understanding of the effect of an acidic environment and the presence of proteolytic enzymes on emulsions. For example, protein–stabilized emulsions would be expected to undergo major changes in the stomach because of the possible action of pepsin on the interfacial layer.

In this study, lactoferrin– and *β*-lactoglobulin (*β*-lg)–stabilized emulsions were subjected to biochemical conditions using an *in vitro* gastric model at pH 1.5 for up to 2 h. The aim of this study was to unravel the physico-chemical characteristics of lactoferrin– and *β*-lg-stabilized emulsions as influenced by gastric proteolysis and low pH.

5.3 Materials and Methods

5.3.1 Materials

Pepsin from porcine gastric mucosa (EC 3.4.23.1; catalogue no. P7000, Sigma Chemical Co., St. Louis, MO, USA) had an enzymatic activity of 800–2500 units/mg protein, as stated by the manufacturer. The reagents used for making the simulated gastric fluid (SGF) and all other chemicals were purchased from BDH Chemicals (BDH Ltd, Poole, England) unless otherwise specified. All the chemicals used were of analytical grade.

5.3.2 *In vitro* gastric model

Simulated gastric fluid (SGF) containing 2 g of NaCl and 7 mL of HCl, with or without the addition of 3.2 g of pepsin, and diluted to 1 L and pH adjusted to 1.2 using 1.0 M HCl was prepared *(Pharmacopeia, 2000)*. The *in vitro* gastric model consisted of a conical flask (250 mL) containing SGF maintained at 37 °C with continuous shaking at 95 rpm in a temperature-controlled water bath (Lab-Line shaker bath, Model LZ33070, Barnstead International, Dubuque, IA, USA) to mimic the conditions in the stomach *(Beysseriat et al., 2006)*. The pH and the temperature were continuously monitored and controlled. Gastric lipase, which is normally present at a level of 0.5–1.0 μM in the human stomach *(McClements et al., 2009)* was not used in this model.

5.3.3 Mixing emulsions with simulated gastric fluid (SGF)

Protein–stabilized emulsions containing 20.0 wt% soy oil was prepared using 1.0 wt% lactoferrin or *β*-lg as the interfacial layer respectively (as described in Chapter 3, Section 3.2.1). Each stock emulsion was mixed with SGF (protein:enzyme ratio = 3:1 w/w). The final mixture, which contained 10.0 wt% oil, was incubated at 37 °C for up to 2 h in the *in vitro* gastric model and samples were periodically taken for characterization. The pH of the mixture was maintained at 1.5 using 1 M HCl.

5.3.4 Characterization of emulsion–SGF mixtures

The mean hydrodynamic diameter of emulsion samples of various degrees of hydrolysis was measured by a dynamic light scattering technique using a Zetasizer Nano ZS (Malvern Instruments Ltd, Malvern, Worcestershire, UK) and the droplet size distribution of the emulsion–SGF mixtures was measured using Malvern MasterSizer MSE. Emulsion–SGF mixture samples were diluted to approximately 0.005 wt% droplet concentration using appropriate background buffer solution (pH and ionic strength of SGF mixed in 1:1 ratio with milli-Q water) and analyzed for ζ-potential measurements using a Malvern Zetasizer Nano ZS (ZEN 3600) instrument (Malvern Instruments Ltd, Malvern, Worcestershire, UK). The microstructures of the emulsion–SGF mixtures after various degree of hydrolysis were obtained using a confocal scanning laser microscope (Leica DM6000 B, Heidelberg, Germany), with a 100 mm oil immersion objective lens by staining the samples with Nile blue. The time–dependent proteolysis of the protein–stabilized emulsions and subnatants obtained after centrifugation was examined using sodium dodecyl sulphate polyacrylamide gel electrophoresis (SDS-PAGE) technique. Native β-lg or lactoferrin solution (of the same protein percentage as that of the filtered subnatant respectively) were treated with SGF for different times and SDS-PAGE was carried out to compare the proteolysis patterns of unadsorbed proteins (β-lg or lactoferrin in the continuous phases respectively) in the emulsion and native proteins in the solutions (β-lg or lactoferrin solutions respectively). Details of the physicochemical, microstructural characterization and SDS-PAGE techniques are described in Chapter 3 (Section 3.2.2).

5.4 Results and Discussion

5.4.1 Droplet size distribution and microstructure

Figure 5.4-1 illustrates the mean hydrodynamic diameter (μm) of the emulsion–SGF mixtures, determined using dynamic light scattering. Both β-lg and lactoferrin formed a stable emulsion with a *Z*-average diameter of approximately 0.35 μm at pH 7.0. However, on mixing with SGF, both the emulsions showed an almost linear increase in hydrodynamic diameter with

incubation time up to 2 h ($p < 0.05$). The *Z*-average diameters of the lactoferrin–stabilized emulsion droplets were significantly higher than that of the *β*-lg–stabilized emulsions after treatment with SGF ($p < 0.05$). The lactoferrin emulsion–SGF mixture showed roughly a linear increase in hydrodynamic diameter to ~ 5.0 μm as a function of time. In contrast, *β*-lg emulsion droplets showed a comparatively smaller increase in diameter with a maximum of ~ 2.5 μm under the same conditions.

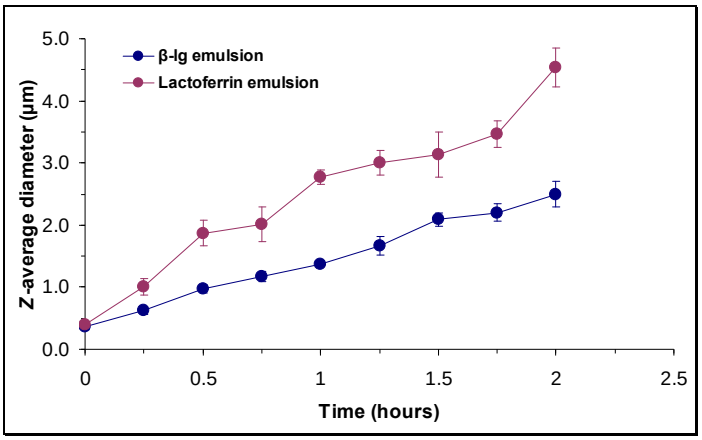

Figure 5.4-1: Change in *Z*-average diameter (μm) of emulsion droplets [20.0 wt% soy oil, 1.0 wt% *β*-lg or lactoferrin respectively] after mixing with SGF as a function of time. The error bars represent standard deviations.

The droplet size distributions of the emulsions studied using static light scattering (Malvern Mastersizer) showed that uniformly dispersed emulsions (with monomodal size distributions) were formed (Figure 5.4-2) immediately after homogenization in case of both lactoferrin and *β*-lg interfacial layers. However, after treatment with SGF for 1 h, *β*-lg–stabilized emulsions showed bimodal distributions, with a second peak in the region 2–10 μm and a corresponding decrease in the area of the first peak (Figure 5.4-2 A). After 2 h of incubation, the size distribution of the *β*-lg emulsion–SGF mixture droplets became multimodal with a third peak appearing in the range 9–50 μm. Lactoferrin–stabilized emulsions showed a higher proportion of larger sized droplets than those stabilized by *β*-lg after SGF treatment (Figure 5.4-2 B), which is in agreement with the dynamic light scattering results. When the emulsion–SGF mixtures (showing multiple peaks) were dispersed in 2.0% SDS buffer, the proportions of

larger droplets in both the emulsions were reduced, although the size distribution remained bimodal (Figure 5.4-2 A and B). This indicates that, in addition to droplet flocculation, some coalescence of the emulsion droplets in these systems had occurred. Similar effects have been seen in oil-in-water emulsions formed with extensively hydrolysed whey proteins (*Ye & Singh, 2006b)*.

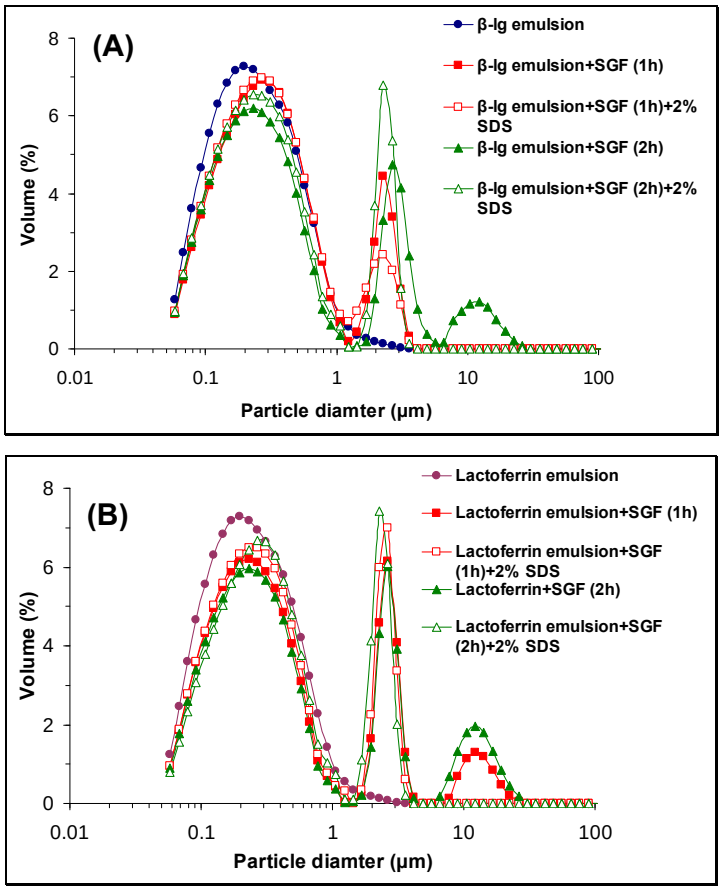

Figure 5.4-2: Droplet size distribution of emulsions after mixing with SGF at various incubation periods, without or with the addition of 2.0% SDS solution. Each data point is the average of measurements on duplicate samples.

Confocal laser scanning microscopy (CLSM) showed that the freshly prepared *β*-lg– (Figure 5.4-3 A) and lactoferrin–stabilized emulsions (Figure 5.4-4 A) before mixing with SGF had fine and uniform droplet distributions, confirming the light scattering results. However, the *β*-lg–stabilized droplets appeared to flocculate when the emulsions were treated with SGF (Figure 5.4-3 B–F). Some distinct large droplets (> 10 μm) were observed after 1 h of incubation (Figure 5.4-3

D–F), in agreement with the bimodal droplet size distribution. This confirms that some coalescence had occurred in these flocculated *β*-lg–stabilized emulsions.

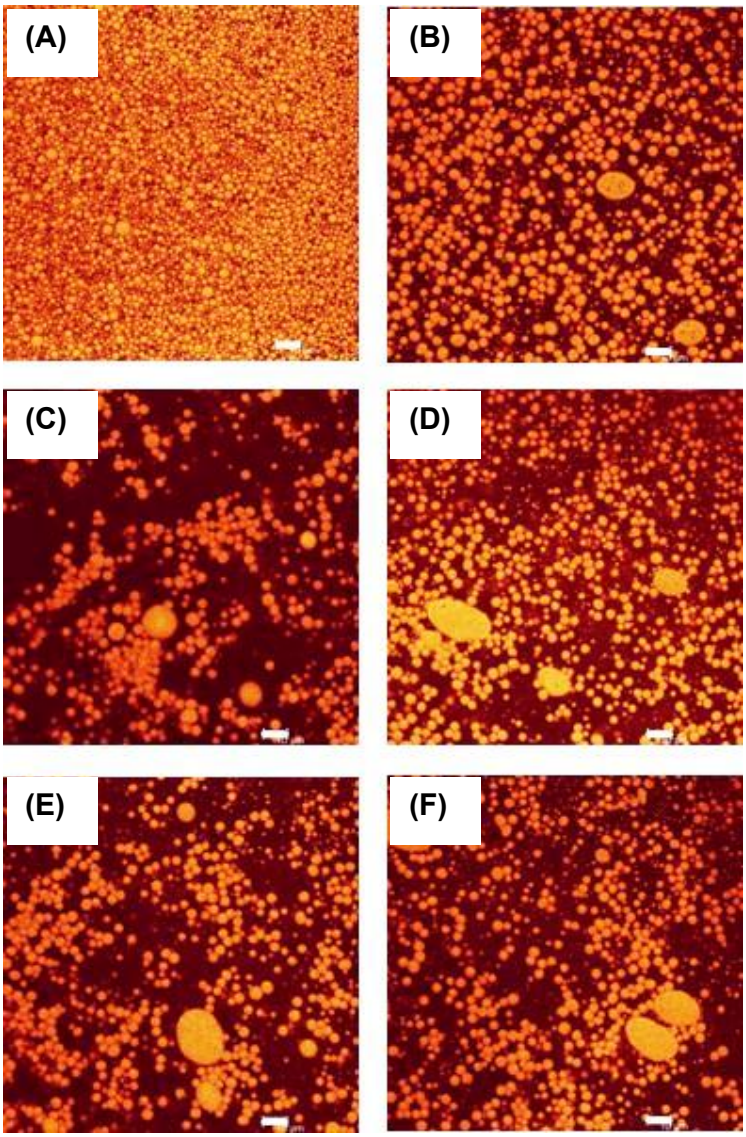

Figure 5.4-3: Changes in the microstructure of *β*-lg–stabilized emulsions (A) after mixing with SGF (mixture pH 1.5) as a function of incubation time: 30 min (B), 45 min (C), 1 h (D), 1h 30 min (E), and 2 h (F). Scale bar corresponds to 10 µm.

On the other hand, the emulsions stabilized by lactoferrin appeared to be more densely flocculated on addition of SGF (Figure 5.4-4 B–F). This can be viewed from larger emulsion droplets (~ 10 µm) and irregular flocs in the confocal micrographs immediately after 30 min of digestion with SGF. There was almost

complete absence of discrete lactoferrin emulsion droplets after addition of SGF as compared to some degree of uniformly dispersed droplets in β-lg emulsions–SGF mixtures.

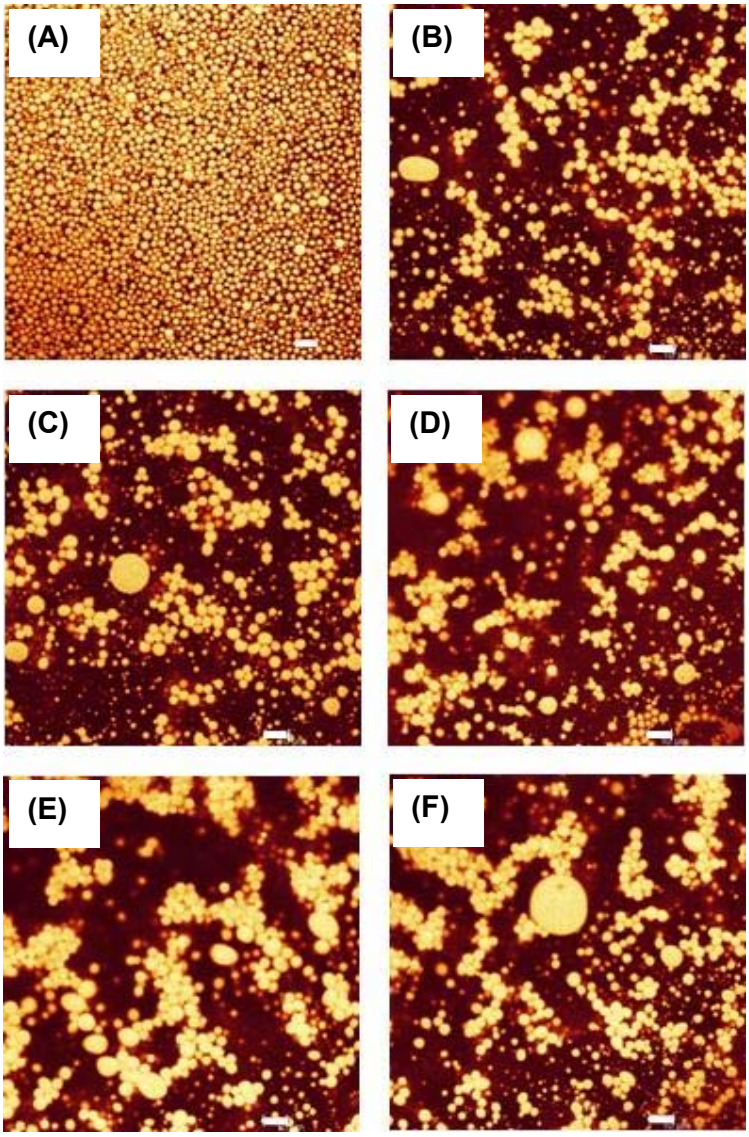

Figure 5.4-4: Changes in the microstructure of lactoferrin–stabilized emulsions (A) after mixing with SGF (mixture pH 1.5) as a function of incubation time: 30 min (B), 45 min (C), 1 h (D), 1h 30 min (E), and 2 h (F). Scale bar corresponds to 10 µm.

Clusters of many small droplets were also observed surrounding larger lactoferrin–stabilized emulsion–SGF droplets, which appeared to have flocculated (Figure 5.4-4 D–F). Onset of coalescence appeared to occur between

these large droplets (> 10 μm) and the adjacent droplets due to the probable rupture of the adsorbed lactoferrin film at the oil–water interface. The stronger and higher rate of flocculation observed in lactoferrin–stabilized emulsions could be attributed to the higher susceptibility of lactoferrin molecules to hydrolysis by pepsin.

Although, there was an obvious increase in droplet diameter, the light scattering studies did not show a dramatic rise in average size (> 10 μm) as expected due to the coalescence of droplets. It could be possible that the coalesced droplets were so large (considerable 'oiling-off' clearly visible by eye) that they immediately creamed to the top of the cuvette and thus were not detected by the laser *(Mun et al., 2007)*.

5.4.2 ζ-potential of emulsion droplets

Freshly prepared *β*-lg emulsion at pH 7.0 had a ζ-potential of −57 mV (Figure 5.4-5 A). Addition of SGF (without pepsin), and consequently the drastic shift in pH, changed the ζ-potential from a negative value to a positive value (from −57 mV to +63 mV) as the pH of the mixture was markedly lower than the isoelectric point (p*I* approximately 5.2) of *β*-lg *(Hong & McClements, 2007)*. There were no further significant changes in the ζ-potential of the emulsion droplets up to 2 h of incubation ($p > 0.05$) (Figure 5.4-5 A). However, the addition of pepsin to the emulsion significantly affected the ζ-potential values ($p < 0.05$), which reduced sharply from +49.4 ± 0.9 mV to +17.6 ± 1.2 mV over an incubation period of approximately 2 h (Figure 5.4-5 A).

On the other hand, initially lactoferrin formed a stable cationic emulsion (+53 mV) (Figure 5.4-5 B). The addition of SGF without pepsin gradually increased the ζ-potential from ~ +53 to ~ +68 mV over the digestion time. However, the addition of pepsin to the emulsion significantly affected the electrophoretic mobilities as shown in Figure 5.4-5 B. The ζ-potential sharply reduced from +59.8 ± 0.5 mV to +9.8 ± 1.2 mV for lactoferrin–stabilized emulsions.

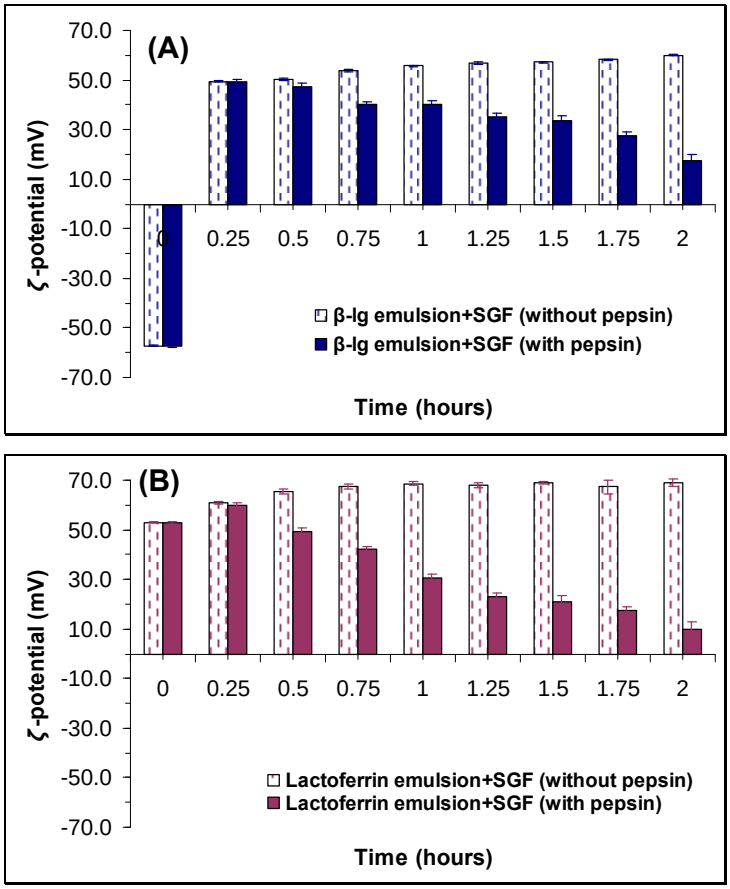

Figure 5.4-5: *ζ*-Potential of *β*-lg– (A) and lactoferrin– (B) stabilized emulsion–SGF mixtures with or without the addition of pepsin. 0.0 h represents the *ζ*-potential of emulsion droplets at pH 7.0. The error bars represent standard deviations.

The steady loss of the net positive surface charge in case of both the emulsion droplets can be related to the loss of some positively charged residues from the protein adsorbed at the emulsion droplet surface as a result of the action of pepsin. This surface hydrolysis diminishes the protective effect of protein, and possibly predisposes the droplets towards flocculation. The presence of a relatively high concentration of NaCl in the SGF could also promote further flocculation of the droplets. The size distribution and confocal microscopy results showed a number of large particles (above 10 μm) at longer hydrolysis times. This suggests that continued surface hydrolysis produce smaller peptides that have reduced surface viscosity and hence reduced stability to drainage and film rupture. As a result, coalescence of droplets begins to occur. It was noted that all the control experiments with emulsions–SGF mixtures (without the addition of

pepsin) were homogenous and stable even after shaking for a period of 4 hours. The ζ-potential was largely positive (> +60 mV) and the droplet size remained fairly constant (~ 0.35 μm) in absence of pepsin for both the emulsions. Hence, emulsion destabilization in the *in vitro* gastric model for both the emulsion types was assumed to be predominantly due to the action of pepsin.

5.4.3 Protein hydrolysis

5.4.3.1 β-lg–stabilized emulsion–SGF mixture

The rates of hydrolysis of *β*-lg solution or *β*-lg–stabilized emulsion mixed with SGF were monitored using SDS-PAGE (Figure 5.4-6). In *β*-lg emulsion–SGF mixtures, the intensity of the *β*-lg band reduced markedly during incubation, with the simultaneous appearance of three major bands (molecular weight in the range 10–15 kDa), designated as A, B and C (Figure 5.4-6 i). The intensity of band A appeared to increase slowly during the 2 h incubation period, whereas the intensities of bands B and C increased up to 30 min of incubation but decreased thereafter. Similar hydrolysis patterns were observed in the SDS-PAGE gels of the cream phases of the *β*-lg–stabilized emulsions (Figure 5.4-6 ii).

Under the conditions of this study, about 65% of the total *β*-lg was adsorbed at the droplet surface. In order to examine the behaviour of unadsorbed protein during SGF treatment, the original *β*-lg–stabilized emulsion was centrifuged, and the subnatant was removed and mixed with SGF. SDS-PAGE showed that the intensity of the *β*-lg band in the continuous phase diminished gradually with incubation time (Figure 5.4-6 iii). However, the loss of the *β*-lg band was much less than that in the emulsion samples. Several faint bands, including those corresponding to A, B and C, were observed. Native *β*-lg solution, containing 0.36% *β*-lg (the same concentration as that in the serum phase of the emulsion), was mixed with SGF and examined using SDS-PAGE (Figure 5.4-6 iv). A slight decrease in the intensity of the *β*-lg band was observed during the 2 h incubation period.

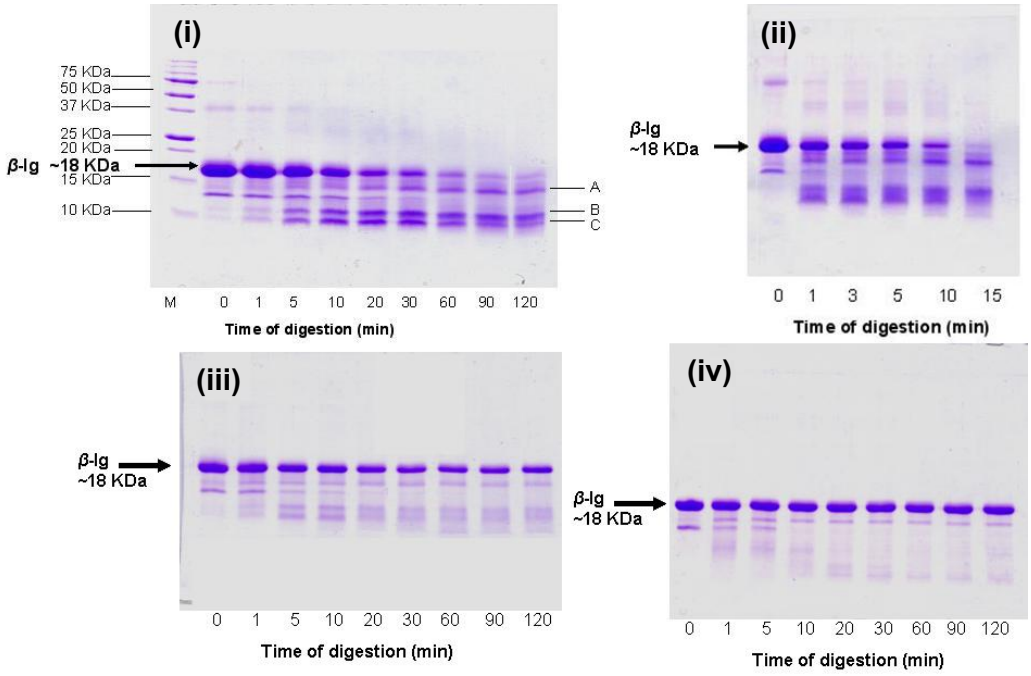

Figure 5.4-6: SDS-PAGE patterns obtained from *β*-lg–stabilized emulsions (i), cream phase of *β*-lg emulsions (ii), continuous phase of *β*-lg emulsions (iii), and native *β*-lg solutions [containing 0.36% *β*-lg (the same as the concentration of *β*-lg in the continuous phase of the emulsion)] (iv), after mixing with SGF, respectively as a function of incubation time.

The rate of hydrolysis of *β*-lg in different systems (estimated by scanning SDS-PAGE gels) is shown in Figure 5.4-7. The proportion of *β*-lg decreased by only about 20% in the native protein solution, compared with about 50% for the subnatant sample and 85% in the emulsion system, after 2 h of incubation. As expected, native *β*-lg solution was largely resistant to pepsin digestion, presumably because its aromatic amino acid side chains were buried inside the folded globular structure, confirming earlier studies *(Reddy et al., 1988; Guo et al., 1995)*. From these results (Figure 5.4-7), it is evident that *β*-lg present in the serum phase (Figure 5.4-6 iii) of an emulsion is more susceptible to pepsin digestion than native *β*-lg in solution (Figure 5.4-6 iv).

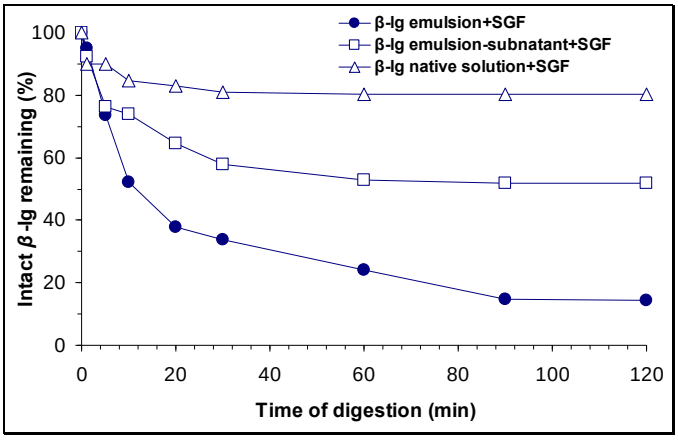

Figure 5.4-7: Rate of hydrolysis of intact *β*-lg in emulsions, the continuous phase of emulsions and native protein solutions on addition of SGF.

This suggests that the conformation of unadsorbed *β*-lg is altered during emulsion formation, possibly as a result of high turbulence during homogenization. This change in conformation could allow greater accessibility of some aromatic amino acid residues to pepsin attack. The susceptibility of non-adsorbed *β*-lg to proteolytic attack has also been reported previously *(Fang & Dalgleish, 1997)*. There is also a possibility that at least a part of continuous phase (primarily consisting of non–adsorbed protein) was also emulsified, with very fine emulsion droplets (*Z*-average = 0.105 μm) which were able to sequentially pass through the 0.45 μm and 0.22 μm filters (Millipore Corp., Bedford, MA, USA) and resulted in increased susceptibility to proteolysis. The presence of these sub-micron–sized emulsion droplets in the non–adsorbed phases have been reported in previous studies involving bovine serum albumin–stabilized emulsion systems *(Castelain & Genot, 1996; Rampon et al., 2003)*.

The marked increase in the hydrolysis of *β*-lg in the emulsion can be explained on the basis of conformational changes caused by the unfolding of the *β*-lg secondary structure at the droplet surface *(Agboola & Dalgleish, 1996)*, improving the accessibility of pepsin-susceptible bonds. It appears that some relatively large fragments of *β*-lg (bands A, B and C) remained inaccessible to pepsin during the early stages of incubation. This could suggest that some portions of adsorbed *β*-lg were not completely unfolded and retained their native structure. The hydrolysis of these relatively large fragments after prolonged

incubation suggests that these fragments were associated with the droplet surface and underwent some reorientation to allow the exposure of further cleavage sites.

5.4.3.2 Lactoferrin–stabilized emulsion–SGF mixture

Lactoferrin has been known to be susceptible to peptic hydrolysis in its native state *(Tomita et al., 1991)*. However, it has been debated that considerable amounts of lactoferrin survive gastric transit and is less susceptible to peptic hydrolysis as compared to casein and transferrin at acidic pH *(Britton & Koldovsky, 1989; Troost et al., 2001)*. An important factor influencing this hydrolysis is the degree of iron saturation of lactoferrin *(Brock et al., 1976; Brines & Brock, 1983)*. It has been reported that 20% iron–saturated lactoferrin is more easily digested than 100% iron–saturated one.

Lactoferrin adsorbed at the droplet surface was almost fully degraded within the first 5 min (Figure 5.4-8 A and B). The proportions of intact lactoferrin in the emulsions remaining after digestion with SGF were negligible due to almost instantaneous hydrolysis of lactoferrin with > 80% within first 1 min. This indicated extensive proteolysis of the lactoferrin layer by pepsin, which generated fast moving shorter peptide fragments that probably diffused out of the 16.0 % resolving gel. The rapid rate of proteolysis of the lactoferrin–stabilized emulsions and absence of larger molecular weight peptides (as seen in case of *β*-lg–stabilized emulsions) might be the reason for higher extent of droplet aggregation and an earlier onset of coalescence as compared to *β*-lg–stabilized emulsions, as observed earlier (Figure 5.4-1 and Figure 5.4-4 B–F). Even, the SDS-PAGE patterns of unadsorbed phase and native lactoferrin during SGF treatment were similar to that of the lactoferrin emulsion (data not shown), *i.e.* the lactoferrin band was depleted almost immediately (before 5 min) after the addition of SGF. This was likely due to the release of bound iron at pH 1.5 in all the lactoferrin systems (native, continuous phase or emulsions), which made the lactoferrin molecules more sensitive to pepsin attack *(Baker et al., 2002; Ye & Singh, 2006a)*.

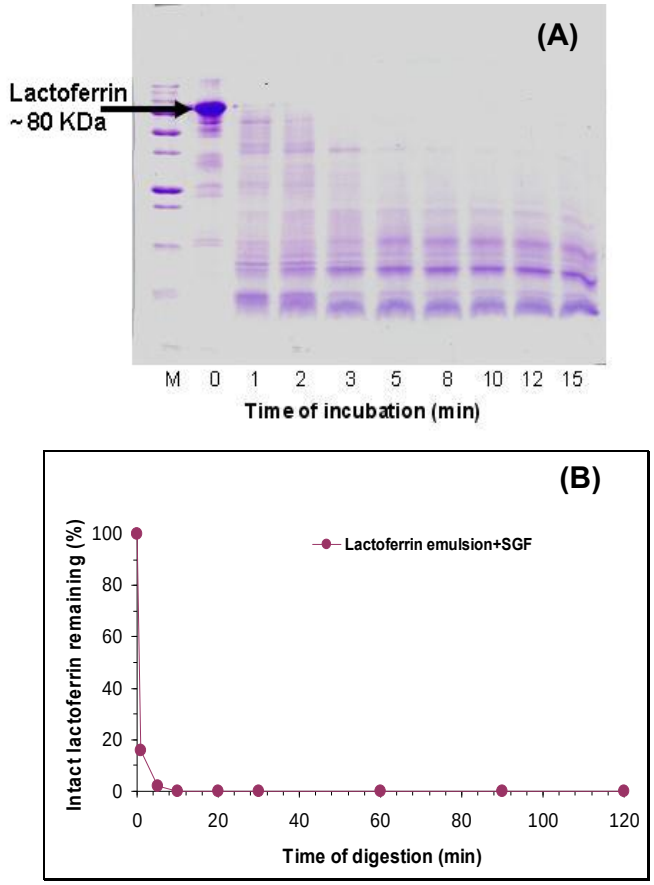

Figure 5.4-8: SDS-PAGE pattern obtained from lactoferrin–stabilized emulsions (A), and rate of hydrolysis of intact lactoferrin in emulsions (B) as a function of time.

It is worth noting here, that lactoferrin– and *β*-lg–stabilized emulsions show different behaviour in presence of SGF, not because of their different initial charges, but due to their different intrinsic nature, molecular conformations and specific accessibility to pepsin.

5.4.4 A model for interaction between pepsin and protein–stabilized emulsion

A schematic diagram is presented to illustrate the physical state of both *β*-lg– and lactoferrin–stabilized emulsions when they are exposed to an *in vitro* gastric condition (Figure 5.4-9). The net charge (-ve or +ve) of the protein used to stabilize the emulsion had no significant impact when exposed to SGF. Due to the acidic pH of the SGF (pH 1.2), the net charges of both the *β*-lg– and

lactoferrin–stabilized emulsions were positive. So initially at pH 7.0 and even after the addition of SGF (pH 1.5), both types of emulsions were stabilized by strong positive charges and steric effects were provided by chains of *β*-lg or lactoferrin protruding into the aqueous phase in corresponding emulsion systems. Hence, the pH did not influence the stability of the emulsions but only provided suitable conditions for the pepsin activity.

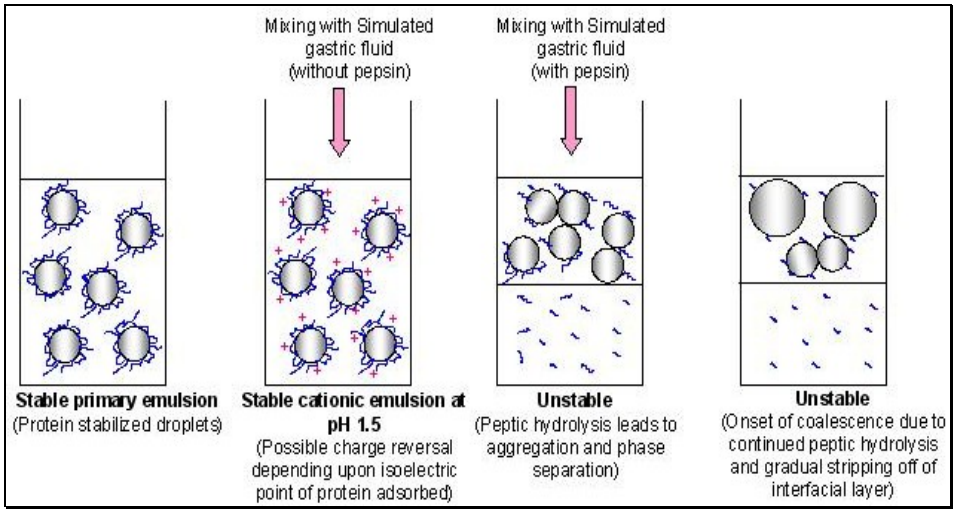

Figure 5.4-9: Schematic diagram of interaction of a protein–stabilized emulsion with SGF. The big shaded circles represent either lactoferrin– or *β*-lg–stabilized emulsion droplets, the blue long coil structures represent the proteins at the interfacial layer and the smaller coil structures represent the peptides formed later.

The emulsions were very stable at the low pH of SGF, but once pepsin is introduced into the system, several physico-chemical changes occur in both the emulsions. The hydrolysis of the interfacial protein layer by pepsin causes a gradual loss of positive charge at the droplet surface and presumably also leads to a reduction in the thickness of the adsorbed layer. The peptides that remain at the interfacial layer are unable to create strong interfacial layers with sufficient electrostatic repulsion and steric barriers. Consequently, the emulsions become susceptible to flocculation, and the presence of high concentrations of salt in the SGF further enhances the process of flocculation. The peptide adsorbed layers on some of the droplets are obviously not effective at preventing coalescence of the droplets.

β-Lg, which is largely resistant to pepsin attack in its native state, is hydrolysed by pepsin when present as the adsorbed layer in emulsions. The change in conformation as a result of unfolding at the emulsion interface exposes the peptic cleavage sites and thus significantly decreases the resistance of *β*-lg to pepsin. Lactoferrin, which is susceptible to proteolysis by pepsin in its native state, is also hydrolysed when present as an interfacial layer coating the oil droplets. This study showed that both *β*-lg– and lactoferrin–stabilized emulsions undergo peptic hydrolysis, leading to flocculation and coalescence of droplets. Such a phenomenon is likely to occur in the stomach *in vivo*. This type of flocculation followed by coalescence might reduce the overall surface area of the emulsions, potentially influencing the accessibility of gastric lipase and finally affecting the rate of lipid digestion *(Armand et al., 1999)*. In addition, the coalesced droplets might interact with the receptors to send signals to the brain, giving a feeling of satiety *(Norton et al., 2007)*.

5.5 Conclusions

This study provided a better understanding of the mechanisms of flocculation in both positively and negatively charged milk protein–stabilized emulsion systems in the presence of SGF containing pepsin at acidic pH. It was observed that both lactoferrin– and *β*-lg–stabilized emulsions underwent flocculation followed by some degree of coalescence on being exposed to simulated gastric environments depending upon protein conformation at the adsorbed layer and incubation time with pepsin. It is recognized that the substrate:enzyme ratio (3:1) used in this model is considerably higher than that in some of the previous substrate–enzyme studies *(Dalgalarrondo et al., 1995; Guo et al., 1995)*. However, it is difficult to select an optimal substrate:pepsin ratio that exactly mimics the secretion found physiologically in humans because a wide variation (up to about 10,000 fold) in gastric and pancreatic secretions has been suggested depending on the individual's health and the type of food intake *(da Silva Gomes et al., 2003; Moreno, 2007)*.

Another interesting finding of this study was that *β*-lg, which is usually resistant to pepsin attack in its native state, became susceptible to proteolysis when present

as the interfacial layer in emulsions. A change in the conformation of the *β*-lg molecules upon adsorption at the oil–water interface exposes the peptic cleavage sites for proteolysis, leading to emulsion instability and coalescence.

It is recognized that the ionic strength and pH varies significantly in real physiological circumstances *(Kalantzi et al., 2006)*. Furthermore, the role of mucin, which is a high molecular weight glycosylated protein (molecular weight about 2.0–4.0 × 10^6 Da) and forms a self-associated networked structure under gastric conditions (low pH and at high mucin concentrations) *(Nordman et al., 2002; Lee et al., 2005; Bansil & Turner, 2006)*, has not been explored. Therefore, the interactions of emulsions in SGF media containing pepsin and mucin under different gastric pH and ionic strength conditions need to be determined to better understand their effects on gastric digestion of protein–stabilized emulsions. Since, the initial charges of the emulsions have been shown to play an insignificant role in determining the interactions with SGF (as both the emulsions acquired net positive charge at gastric pH), the behaviour of only *β*-lg–stabilized emulsions as affected by different pH, ionic strength in presence of mucin and pepsin was investigated in the next chapter.

Chapter Six: Factors Influencing the Interactions of *β*-lactoglobulin–Stabilized Emulsions with Simulated Gastric Fluid [3]

6.1 Abstract

The effects of pH (6.5–1.5), ionic strength (0–150 mM NaCl) and the presence of mucin (0.1 wt%) on the properties of oil-in-water emulsions [20.0 wt% soy oil, stabilized by 1.0 wt% *β*-lactoglobulin (*β*-lg)] under simulated gastric conditions (with/without 0.32 wt% pepsin at 37 °C, with continuous shaking at approximately 95 rev/min for 2 h) were investigated. Changes in *Z*-average diameter, *ζ*-potential and microstructure were determined as a function of incubation time. The emulsions mixed with simulated gastric fluid (SGF) (without added pepsin) were stable over a wide pH range (except at pH 5 close to the isoelectric point of *β*-lg) and at low ionic strengths (≤ 50 mM NaCl). Extensive droplet flocculation with some degree of coalescence was observed in emulsions with 0.32 wt% added pepsin, the flocculation being potentially accelerated in the presence of NaCl. The addition of 0.1 wt% mucin resulted in a greater extent of flocculation, possibly because of binding of mucin to the positively charged *β*-lg–stabilized emulsion droplets. Ionic strength, pH and the presence of mucin had a significant influence on the rate of hydrolysis of *β*-lg by pepsin. The behaviour of the emulsion in SGF was predominantly driven by electrostatic interactions, which varied as a function of digestion time, pH, ionic strength and the presence of pepsin and mucin.

6.2 Introduction

In Chapter 5, it was found that an almost instantaneous change in the electrostatic charge of *β*-lactoglobulin (*β*-lg)–stabilized emulsions droplets (from negative charge to positive charge) occurs in a simulated gastric fluid (SGF) environment.

[3] Part of the contents presented in this chapter has been published previously as a peer-reviewed paper: Sarkar, A., Goh, K. K. T., and Singh, H. (2010), Properties of oil-in-water emulsions stabilized by *β*-lactoglobulin in simulated gastric fluid as influenced by ionic strength and presence of mucin. *Food Hydrocolloids*, *24*(5), 534–541.

β-Lg, which is largely known to be resistant to pepsin attack in its native state because of its folded structure, became accessible to proteolysis by pepsin when present as the adsorbed layer in emulsions. A change in the conformation of the *β*-lg molecules upon adsorption at the oil–water interface exposes the peptic cleavage sites for proteolysis, leading to emulsion instability and some degree of coalescence. However, the emulsion–SGF interaction studies were limited to pH 1.5 and ionic strength of 34 mM NaCl. Generally, the pH and ionic strengths vary significantly during real gastric processing conditions *(Kalantzi et al., 2006)*. Moreover, the presence of high molecular weight glycosylated mucin in the gastric system might influence the behaviour of emulsions and proteolysis patterns by pepsin. Mucin has been shown to play an important role in the flocculation of emulsions in the oral environment because of its negative charge at neutral pH (Chapter 4). However, the influence of mucin at acidic pH and at higher ionic strengths on the stability of emulsions, particularly in the presence of a proteolytic enzyme, has not been explored to date.

Hence, the aim of this chapter was to elucidate the interactions of *β*-lg–stabilized emulsions in SGF media taking into consideration the role of different gastric variables, such as pH and ionic strength in presence of pepsin and mucin. The focus was on the changes in the physico-chemical properties, microstructures and proteolysis patterns (indicated by SDS-PAGE) of the emulsions.

6.3 Materials and Methods

6.3.1 Materials

Pepsin and mucin from porcine gastric mucosa were used (details mentioned in sections 4.3.1 and 5.3.1).

6.3.2 Mixing *β*-lg–stabilized emulsions with SGF

Simulated gastric fluid (SGF) at pH 1.2 (with or without 0.32 wt% pepsin) was prepared according to the procedure described previously in Chapter 5 (Section 5.3.2). In some experiments, 0.1 wt% mucin was added to SGF *(O'Gara et al., 2008)*. Each stock emulsion [20.0 wt% soy oil, stabilized by 1.0 wt% *β*-lg] was

mixed with SGF (protein:pepsin ratio 3:1 w/w) at 37 °C with continuous shaking at ~ 95 rpm for 2 h. The pH of SGF was adjusted using 1 M HCl to have final mixture pH of 1.5–6.5 and ionic strength of SGF was varied from 0–150 mM NaCl. The final mixture contained 10.0 wt% dispersed phase. The emulsion–SGF mixtures were periodically analyzed as a function of digestion time upto 2 h.

6.3.3 Analysis of emulsion–SGF mixtures

Emulsion–SGF mixtures at different pH and ionic strengths, without or with the addition of pepsin and mucin, were characterized using physicochemical and microstructural techniques, and SDS-PAGE analysis, as described previously in Chapter 5 (Section 5.3.4).

6.4 Results and Discussion

6.4.1 Effects of ionic strength on stability of emulsion–SGF mixtures

Upon the ingestion of food, the ionic strength and the osmolality in a gastric environment vary substantially depending on the concentration of solutes (salts, glucose *etc.*) generated from the food intake *(Kalantzi et al., 2006)*. In this section, the influence of ionic strength (0–150 mM NaCl) on emulsions in SGF fluid was studied. Figure 6.4-1 A and Figure 6.4-1 B show the effects of ionic strengths on the droplet size of *β*-lg emulsions treated with SGF without and with the addition of 0.32 wt% pepsin at pH 1.5, respectively. Freshly prepared *β*-lg emulsion at pH 7.0 had an average droplet size of approximately 0.33 μm at pH 7.0. When emulsions were treated with SGF (final mixture pH 1.5) without pepsin (Figure 6.4-1 A), the droplet size remained fairly stable over 2 h of incubation ($p > 0.05$) at the lower range of ionic strength from 0 to 50 mM NaCl but increased moderately at 100 mM NaCl (approximately 0.5 μm) and appreciably at 150 mM NaCl (approximately 10 μm) within the first hour of incubation.

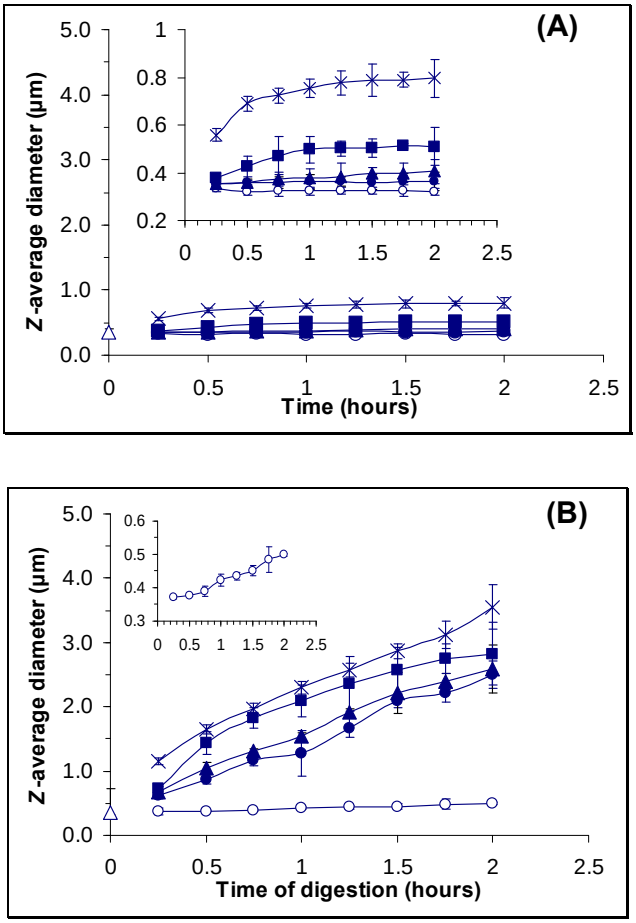

Figure 6.4-1: Change in *Z*-average diameter (µm) of *β*-lg emulsion droplets (△) [20 wt% soy oil, 1.0 wt% *β*-lg] after mixing with SGF, without pepsin (A) or with 0.32 wt% added pepsin (B) at pH 1.5 and ionic strengths of 0 mM (○), 34 mM (●), 50 mM (▲), 100 mM (■) and 150 mM (×), as a function of time. Error bars indicate standard deviations. Inserts correspond to a diminished Y-axis scale. Time 0.0 h represents *β*-lg emulsion mixed with milli-Q water at pH 7.0.

The droplet size within the first 15 min of incubation was not included in the figures because 15 min was regarded as the equilibration time that was required for the droplets to mix with the electrolytes efficiently. The droplet size showed a relatively smaller increase in *Z*-average diameter with an increase in ionic strength after 30 min of incubation than after 2 h of incubation. A marked increase in the *Z*-average diameter was observed for the sample containing 150 mM NaCl in the initial stages of incubation. From the confocal micrographs, the emulsion droplets appeared to be fairly monodispersed at low ionic strength from

0 to 50 mM NaCl (data shown only for 0 mM NaCl, Figure 6.4-2) but showed some droplet aggregation in the presence of 100 mM NaCl.

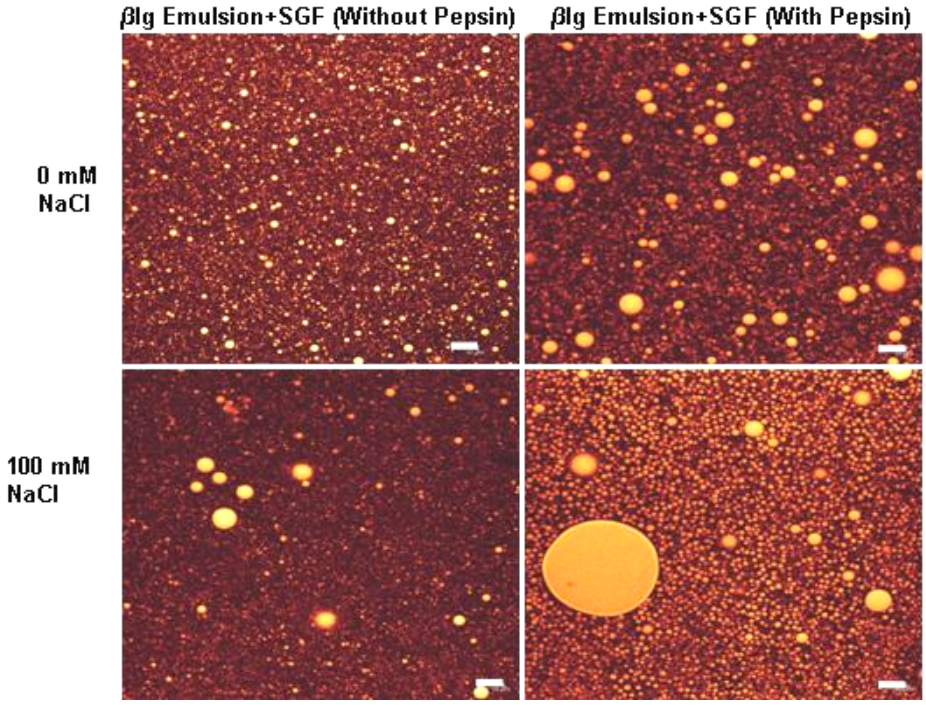

Figure 6.4-2: Confocal micrographs of *β*-lg–stabilized emulsions after mixing with SGF without or with pepsin (pH 1.5; ionic strengths of 0 and 100 mM NaCl) after 2 h of incubation. Scale bar corresponds to 10 µm.

With the addition of 0.32 wt% pepsin to the emulsions (Figure 6.4-1 B), the droplets showed a significant increase in *Z*-average diameter with an increase in incubation time up to 2 h ($p < 0.05$). The magnitude of the increase in the *Z*-average diameter was substantial for samples with added salt. In the absence of salt, the *Z*-average diameter increased less markedly from approximately 0.35 µm to approximately 0.5 µm. The increase in droplet size observed in the confocal micrographs (Figure 6.4-2) was generally in good agreement with the *Z*-average diameter values obtained. The addition of 0.32 wt% pepsin resulted in comparatively larger emulsion droplets, with a prominent increase in the proportion of droplet sizes ranging from about 5 to 10 µm. At higher ionic strength (100 mM NaCl), the large discrete droplets (> 50 µm) that were observed after 2 h of incubation (Figure 6.4-2) were in agreement with the large *Z*-average diameter obtained from the light scattering measurement (Figure 6.4-1

B). The very large droplets were the result of coalescence of smaller droplets, as described previously in Chapter 5.

To determine the effects of ionic strength (0–150 mM NaCl) on the charge of emulsion droplets in the SGF medium, ζ-potential values of β-lg emulsions mixed with SGF (final mixture pH 1.5), in the absence and presence of 0.32 wt% pepsin, were measured (Figure 6.4-3 A and Figure 6.4-3 B respectively). Initially, the β-lg emulsion (pH 7.0) formed a strongly anionic emulsion with a ζ-potential of approximately –60 mV (as described previously in Chapters 4 and 5). With the addition of SGF (without pepsin and pH adjusted to 1.5), there was an instantaneous charge reversal and the ζ-potential of the emulsion acquired a net positive value of approximately +70 mV (Figure 6.4-3 A). There was no significant change in the ζ-potential of the droplets as a function of time. However, increasing the ionic strength resulted in a decrease in ζ-potential (about +30 mV at 150 mM NaCl) over the 2 h of incubation. This reduction in ζ-potential and corresponding increase in *Z*-average diameter at higher ionic strengths ($\geq$ 100 mM NaCl) could be attributed to progressive charge screening by counterions (Na^+ and Cl^-) surrounding the droplets (*via* reducing the Debye screening length) and ion binding to the β-lg interface *(Keowmaneechai & McClements, 2002; Djordjevic et al., 2004; Harnsilawat et al., 2006)*. It should be noted that the emulsion droplets retained a significant net positive surface charge even at the higher ionic strengths. In addition, no clear phase separation was observed possibly because, at extremely low pH values (pH 1.5), electrostatic repulsions between the positively charged emulsion droplets prevented extensive flocculation and coalescence *(Kulmyrzaev & Schubert, 2004)*.

When the emulsion was mixed with SGF containing 0.32 wt% pepsin (Figure 6.4-3 B), all samples showed an almost linear decrease in ζ-potential with an increase in the incubation time up to 2 h, with the lowest ζ-potential being obtained at the highest ionic strength of 150 mM NaCl. The steady loss of the net positive surface charge of the emulsion droplets could be attributed to hydrolysis of adsorbed protein by the action of pepsin, as described in Chapter 5.

In addition, the hydrolysis of adsorbed protein would reduce steric repulsion between the droplets, as the resulting peptides at the interface would be considerably smaller in molecular weight than the original protein (*β*-lg). The loss of the net electrostatic charge and steric repulsion results initially in droplet flocculation. Further changes in the adsorbed peptide layers within the flocculated droplets could lead to the film rupture, leading to coalescence of droplets (Figure 6.4-2) as described in previous chapter (Chapter 5).

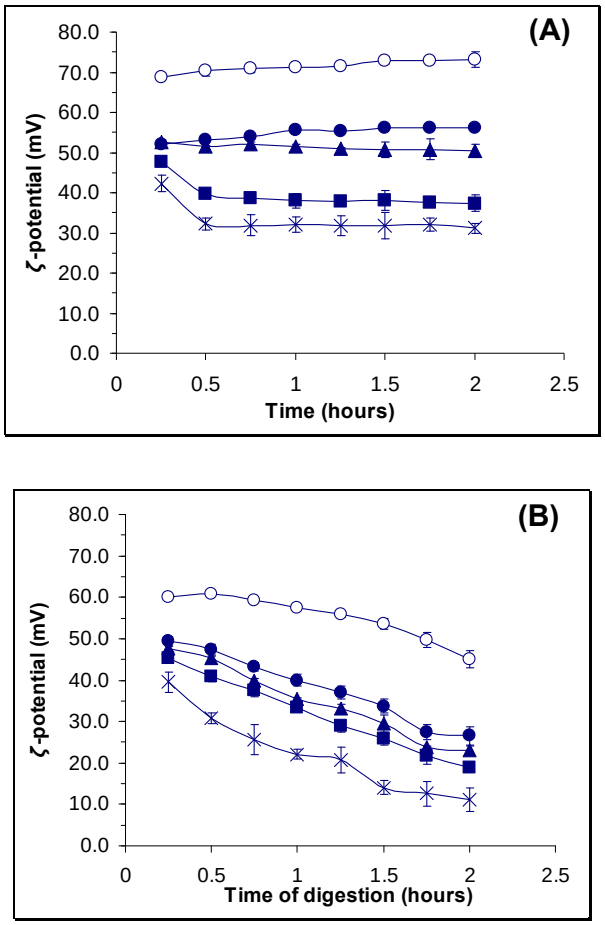

Figure 6.4-3: Change in *ζ*-potential (mV) of *β*-lg emulsion droplets [20 wt% soy oil, 1.0 wt% *β*-lg] after mixing with SGF, without pepsin (A) or with 0.32 wt% added pepsin (B) at pH 1.5 and ionic strengths of 0 mM (○), 34 mM (●), 50 mM (▲), 100 mM (■) and 150 mM (×), as a function of time. Error bars indicate standard deviations.

It should be noted that, after 2 h of incubation, the ζ-potential values of the emulsion–SGF mixtures containing pepsin decreased from approximately +45 mV to approximately +11 mV as the ionic strength increased from 0 to 150 mM

NaCl. For the emulsion–SGF mixture samples without added pepsin, the change in ζ-potential values (from approximately +70 mV to approximately +30 mV) was due to the influence of ionic strength alone. However, in the presence of pepsin, the further decrease in ζ-potential could be attributed to the combined effects of enzymatic action and ionic strength, which are discussed later.

6.4.2 Effects of pH on aggregation of emulsion–SGF mixtures

Generally, when food of neutral pH is consumed and mixed with saliva, it has a pH of 6.5–7.0. However, the pH drops gradually as it mixes with the gastric fluid. In this section, experiments (Figure 6.4-4 to Figure 6.4-6) were carried out to simulate a fed state situation (food entering the gastric system) *(Beysseriat et al., 2006)*, when pH of food–gastric fluid mixture changes because of the buffering capacity of the food contents. This buffering capacity is gradually overcome by the secretion of more HCl into the stomach and the gastric emptying of the food *(Lundin et al., 2008)*.

At pH 6.5, which represents the pH of food entering the stomach, the *Z*-average diameter of emulsion droplets in SGF with or without pepsin was nearly similar even after 2 h of incubation ($p > 0.05$), irrespective of ionic strengths (Figure 6.4-4). This is because pepsin has almost no proteolytic activity near neutral pH conditions *(Mickelsen & Ernstrom, 1972)*. The *β*-lg–stabilized emulsions showed no droplet aggregation and were fairly monodisperse when they were mixed with SGF (with or without pepsin) at pH 6.5 (confocal micrographs not shown as they were similar to that of freshly prepared emulsions at pH 7.0).

At pH 5, the emulsions formed densely aggregated microstructures for both samples with and without pepsin (Figure 6.4-5). This was because the pH of the emulsions approached the isoelectric point of *β*-lg (pI ~ 5.2) *(Harnsilawat et al., 2006; Hong & McClements, 2007)*. The hydrodynamic diameters of emulsion–SGF mixtures were extremely high, resulting in droplet creaming (size data not shown as quality results were not achieved due to extensive droplet flocculation).

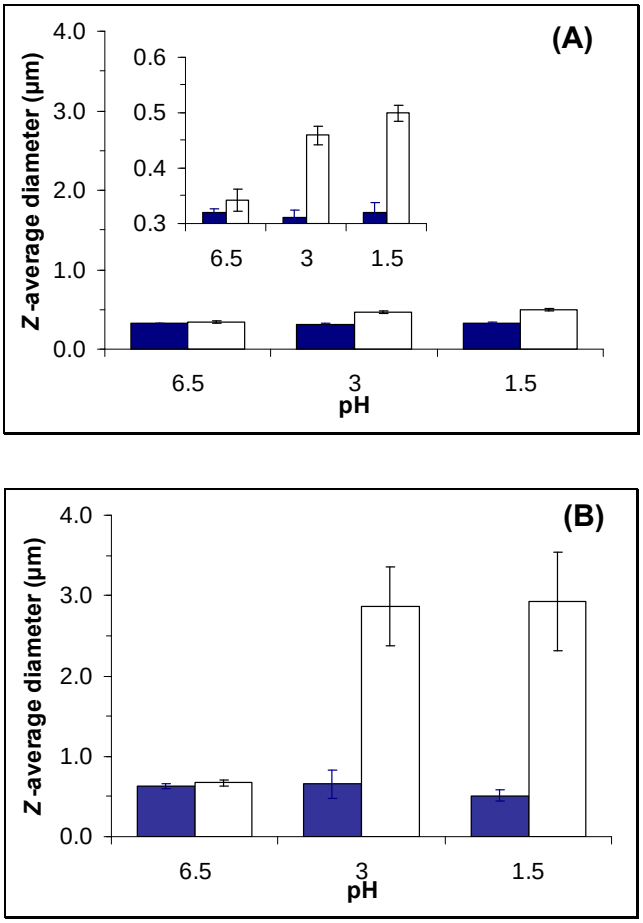

Figure 6.4-4: *Z*-average diameter (µm) of *β*-lg emulsion after mixing with SGF, without pepsin (dark blue) or with 0.32 wt% added pepsin (white) as a function of varying gastric pH at 0 mM NaCl (A) and 100 mM NaCl (B) respectively. Time of incubation in gastric fluid is 2 h. Error bars indicate standard deviations.

The *Z*-average diameters of the emulsion samples mixed with SGF without added pepsin containing no salt (at 0 mM NaCl) remained fairly constant over the pH range studied except the emulsion with pH around the p*I* as discussed above ($p > 0.05$) (Figure 6.4-4 A). Even in presence of salts, the emulsion droplets remained homogeneous with no sign of flocculation at pH 1.5 and 3.0 (Figure 6.4-4 B and Figure 6.4-5). However, at both pH 3 and 1.5, the droplet size increased dramatically when pepsin was introduced, which was also clearly observed in the confocal micrographs showing some larger droplets of ~ 10–15 µm size (Figure 6.4-5). The increase in droplet size due to pepsin in SGF was more prominent when electrolytes were present in the system (100 mM NaCl) (Figure 6.4-4 B).

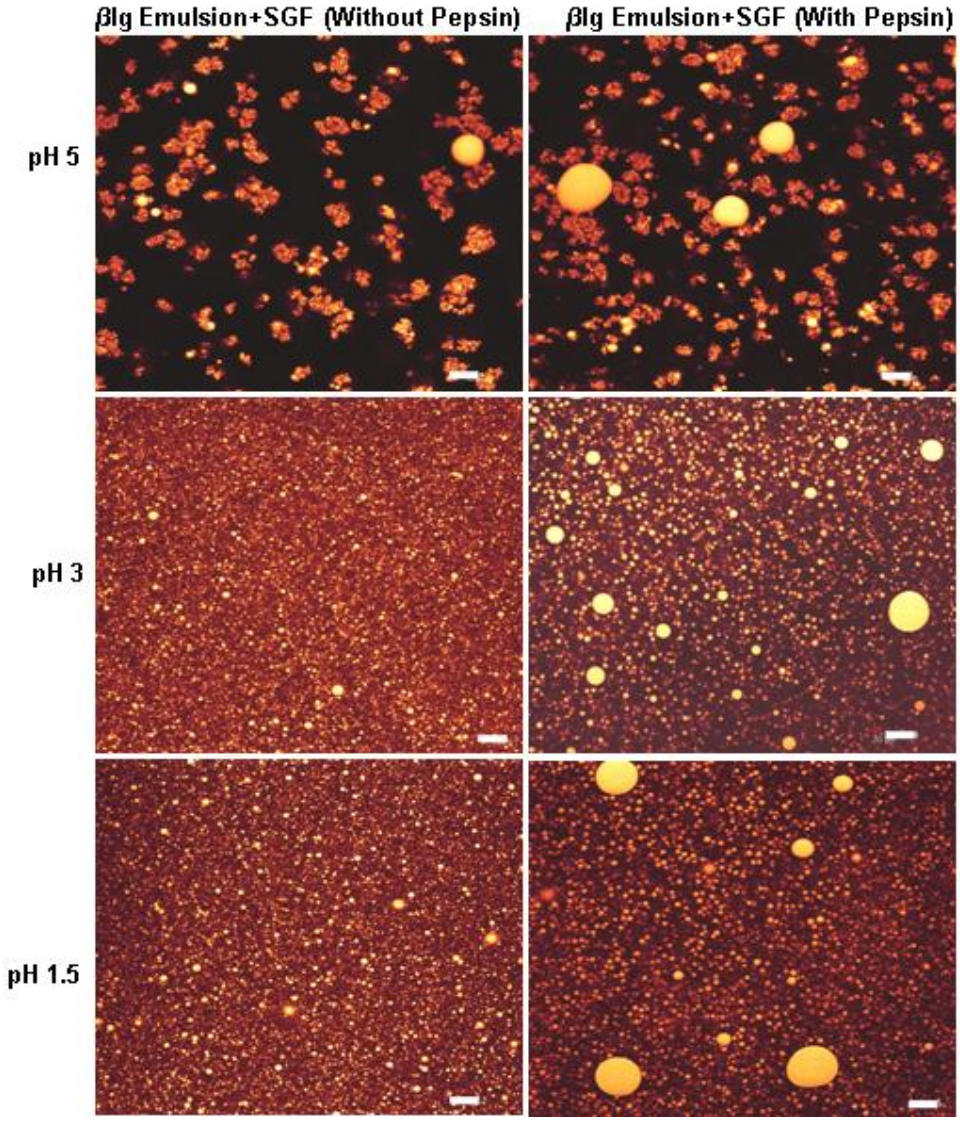

Figure 6.4-5: Confocal micrographs of *β*-lg emulsions after mixing with SGF with or without pepsin (ionic strengths: pH 1.5, 3.0 and 5.0 at 34 mM NaCl, respectively) after 2h of incubation. Scale bar corresponds to 10 µm.

The sign of *ζ*-potential of the *β*-lg-stabilized droplets went from being highly negative (−61.6 mV ± 1.4 mV) to highly positive (+73.1 ± 1.9 mV) as the emulsion−SGF mixture pH was decreased from 6.5 to 1.5 (Figure 6.4-6 A) because the *β*-lg molecules stabilizing the droplets were moving from above to below their p*I* of ~ 5.2 *(Hong & McClements, 2007)*. The magnitude of the *ζ*-potential of the emulsion−SGF mixture droplets decreased significantly at all pH studied when 100 mM NaCl was present in the SGF (Figure 6.4-6 B), which is attributed to the salt screening effects, as described earlier.

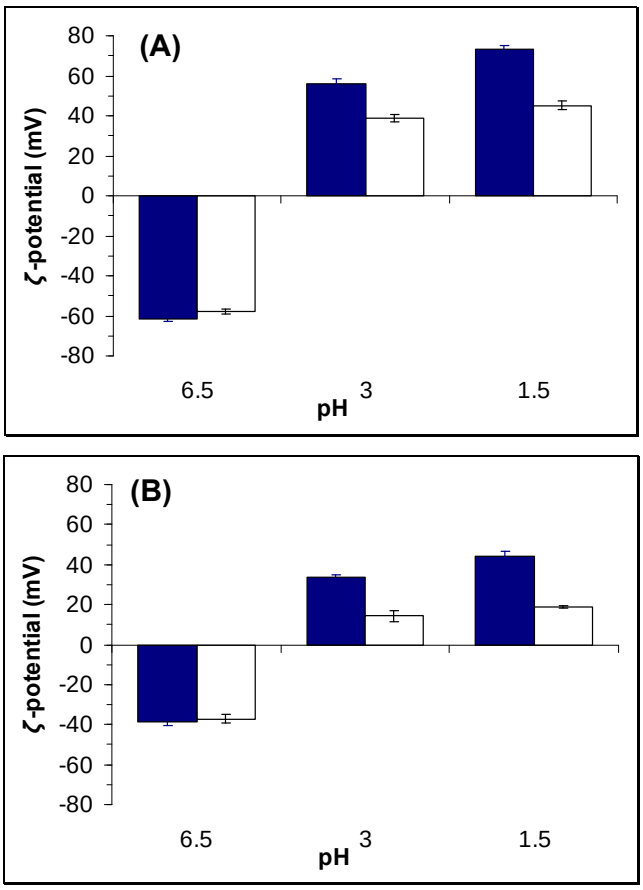

Figure 6.4-6: Change in ζ-potential (mV) of β-lg emulsion droplets after mixing with SGF, without pepsin (dark blue) or with 0.32 wt% added pepsin (white) at 0 mM NaCl (A) and 100 mM NaCl (B), respectively as a function of pH. Time of incubation in SGF is 2 h. Error bars indicate standard deviations.

As expected, the ζ-potential values of the emulsion droplets in the presence of pepsin were appreciably lower than those samples without pepsin ($p < 0.05$) (Figure 6.4-6). This was due to the hydrolysis of protein at the oil interface. The magnitude of ζ-potential of pepsin treated emulsion samples was not significantly different between pH 3.0 and 1.5, respectively, at both ionic strengths of 0 and 100 mM NaCl (Figure 6.4-6). However, at the fasted state pH of 1.5, the ζ-potential was lowered significantly to +18.8 ± 0.7 mV at higher ionic strength (100 mM NaCl) as compared to +45.1 ± 2.0 mV at 0 mM NaCl. This might imply that higher ionic strengths might potentially influence the proteolysis pattern of β-lg emulsion by pepsin.

6.4.3 Pepsin activity as a function of pH and ionic strength

It was apparent from the droplet size, ζ-potential values and confocal micrographs that in the absence of pepsin, the effects of pH and ionic strengths largely influence emulsion stability. However, in the presence of pepsin, the mechanism influencing emulsion stability is not completely understood. To examine whether or not ionic strength and pH might affect the proteolysis rate of *β*-lg emulsions, the degree of *β*-lg degradation in emulsions mixed with SGF containing pepsin at different ionic strengths (0–150 mM NaCl) at pH 1.5 (simulating fasted state) and pH 3.0 (simulating fed state), was determined using quantification of SDS-PAGE gels (Figure 6.4-7 and Figure 6.4-8). The SDS-PAGE gel patterns at all ionic strengths at pH 1.5 (Figure 6.4-7 A) were similar to the patterns shown in Chapter 5 [Figure 5.4-6 (i)]. Quantitative gel analysis based on band intensity suggested that about 25–40% of intact *β*-lg remained after 1 h of incubation in the presence of 0.32 wt% pepsin at pH 1.5 for ionic strengths ranging from 0 to 150 mM NaCl (Figure 6.4-8 A). However, the rate of hydrolysis increased with increasing ionic strength. The proportion of intact *β*-lg decreased by about 25% in the absence of salts, compared with about 50% in the presence of salts (34–150 mM NaCl), after 10 min of incubation. The increased rate of hydrolysis of the interfacial *β*-lg in the presence of NaCl could be attributed to the progressive screening of the electrostatic charges of the interfacial *β*-lg at the droplet surface. Consequently, a decrease in electrostatic repulsion between cationic pepsin and the interfacial *β*-lg at pH 1.5 may promote the binding of pepsin to the cleavage sites of *β*-lg adsorbed at the droplet surface, thus increasing the overall rate of proteolysis.

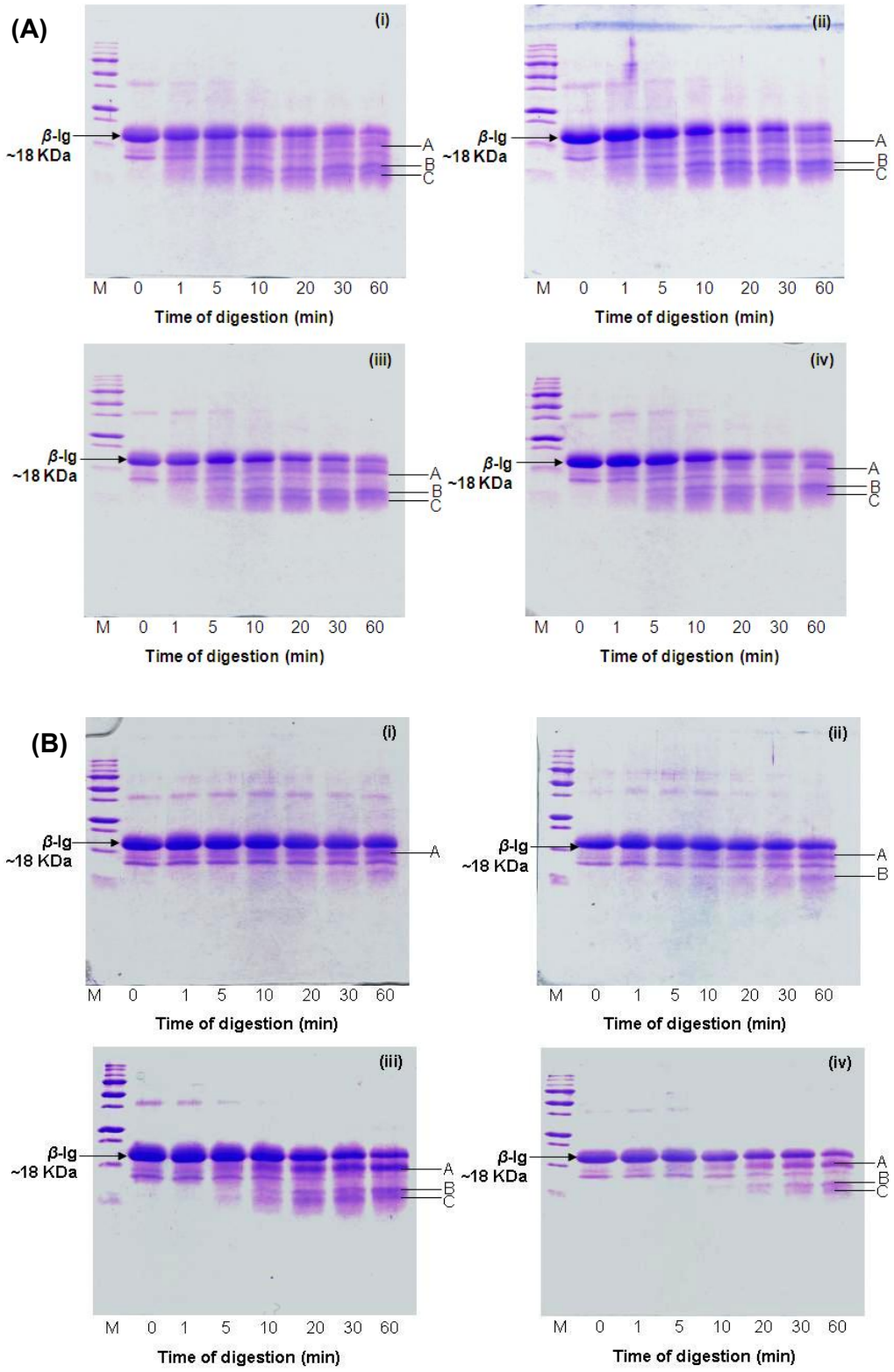

Figure 6.4-7: SDS-PAGE patterns obtained from *β*-lg emulsions after mixing with SGF containing 0.32 wt% pepsin at (i) 0 mM, (ii) 34 mM, (iii) 50 mM, or (iv) 100 mM NaCl, at pH 1.5 (simulating fasted state) (A) and pH 3.0 (simulating fed state) (B), respectively as a function of incubation time.

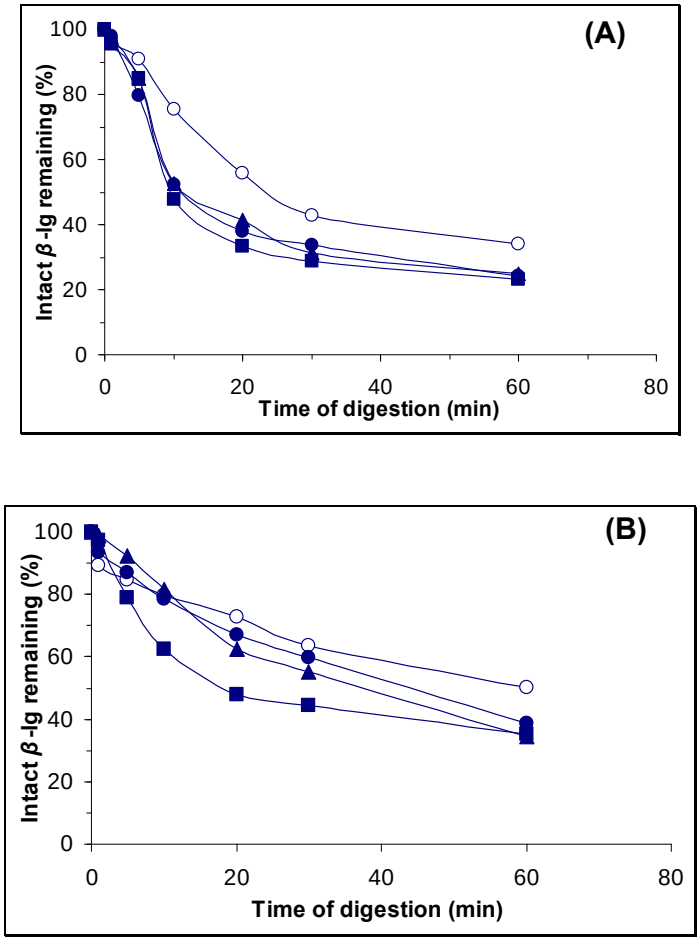

Figure 6.4-8: Rate of hydrolysis of intact *β*-lg in emulsions on the addition of SGF containing 0.32 wt% pepsin at ionic strengths of 0 mM (○), 34 mM (●), 50 mM (▲), and 100 mM NaCl (■) at pH 1.5 (A) and pH 3.0 (B), respectively as a function of time, as estimated by quantification of SDS-PAGE gel patterns mentioned in Figure 6.4-7.

At pH 3.0 (Figure 6.4-7 B), the proteolytic pattern was considerably different from that at pH 1.5. The major resultant proteolytic bands (A, B and C) observed in Figure 6.4-7 A were almost invisible at pH 3.0 (Figure 6.4-7 B). Very faint intensity of band A was seen in Figure 6.4-7 B i with progressive increase in intensities at higher ionic strengths (Figure 6.4-7 B ii–iv) after 1 h incubation. Bands B and C were detectable only at higher ionic strengths (50–100 mM NaCl). The rates of hydrolysis by pepsin were slightly lower at pH 3.0 (Figure 6.4-8 B). It was worth noting that even at pH 3.0, the hydrolysis rate increased with ionic strength.

Almost no hydrolysis was observed at higher pH values of 6.5 (PAGE gel not shown) as compared to that of pH 1.5 due to specificity of pepsin *(Mickelsen & Ernstrom, 1972)*. Even at pH 5.0, the band intensities of *β*-lg did not show significant change possibly because of the aggregation effect near the p*I*. At p*I*, the hydrophobic amino acid residues were possibly 'buried' inside the aggregates, thus reducing the action of pepsin on the adsorbed *β*-lg layer as reported in other studies involving caseinates *(Guo et al., 1995)*. These results clearly suggest that parameters like pH and ionic strength together with buffering capacity of food matrix could play significant roles in gastric digestion of emulsions.

To understand how the degree of interfacial *β*-lg hydrolysis influenced the hydrodynamic size and the electrostatic charge of the emulsion droplets, *Z*-average diameter (Figure 6.4-9 A) and *ζ*-potential (Figure 6.4-9 B) values were plotted as a function of the percentage of hydrolysed *β*-lg (data obtained from the quantitative SDS-PAGE shown in Figure 6.4-8). The *Z*-average diameters were relatively similar when the emulsions contained at least 80–85% intact interfacial *β*-lg (*i.e.* 15–20% hydrolysis in Figure 6.4-9 A). The diameter values increased gradually as the degree of hydrolysis approached 60%. This was then followed by a marked increase in *Z*-average diameter as the degree of *β*-lg hydrolysis increased above 60%, indicating extensive aggregation and instability of the emulsion (*Z*-average diameter approximately 2.3 μm at an ionic strength of 150 mM NaCl). In addition, the *Z*-average diameter values were noticeably higher in the presence of salt (34–150 mM) than in the absence of salt (Figure 6.4-9 A). Therefore, these results indicated that the large–scale aggregation and the extensive emulsion instability were predominantly caused by the hydrolysis of *β*-lg.

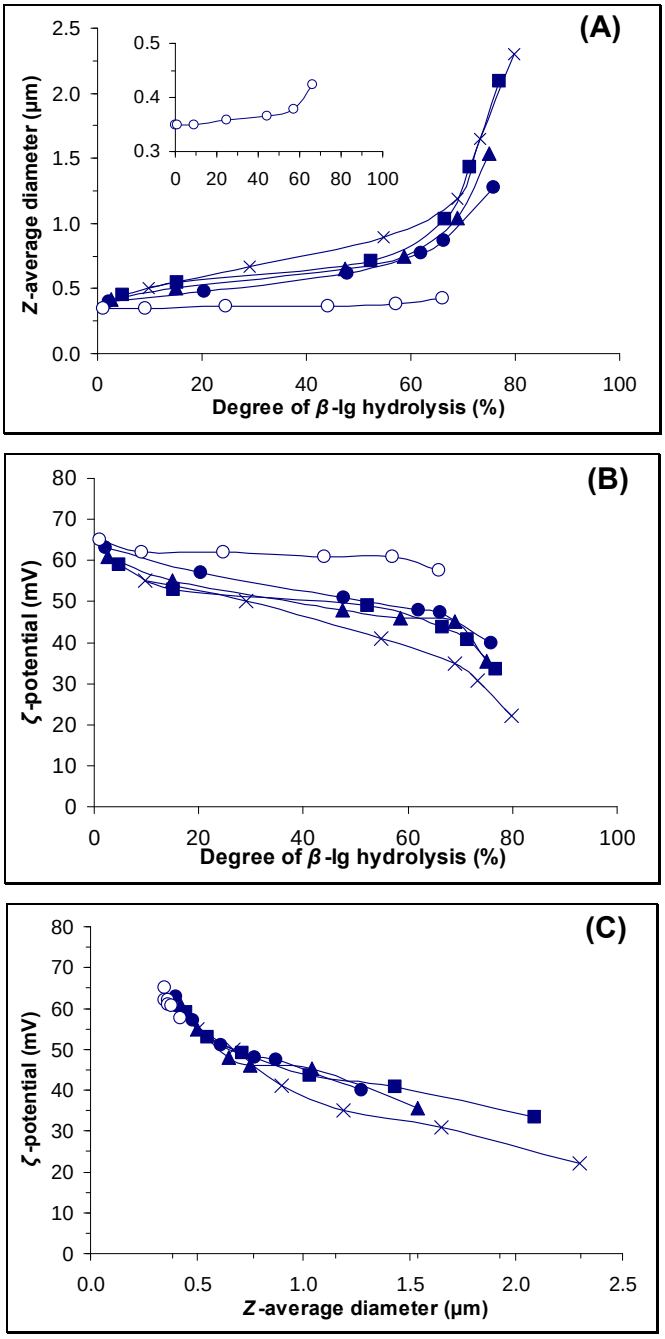

Figure 6.4-9: Change in *Z*-average diameter (µm) (A) and ζ-potential (mV) (B) of *β*-lg emulsions, at pH 1.5 and ionic strengths of 0 mM (○), 34 mM (●), 50 mM (▲), 100 mM NaCl (■) and 150 mM NaCl (×), as a function of degree of *β*-lg hydrolysis. Change in ζ-potential (mV) of *β*-lg emulsions as a function of *Z*-average diameter (µm) at the ionic strengths stated above (C).

The ζ-potential values decreased as a function of the percentage of interfacial *β*-lg hydrolysis. The ζ-potential values decreased further in the presence of salts (Figure 6.4-9 B). Although the reduction in positive charge of the droplets was

largely due to the gradual proteolysis of the interfacial layers by pepsin, the presence of salts above 34 mM NaCl reduced the surface charges further but to a lesser extent and in the following order of ionic strength: 0 mM < 34–100 mM < 150 mM NaCl. The positive ζ-potential values observed in all samples, even at about 80% hydrolysis of *β*-lg, could suggest that the interfacial peptides remained attached to the droplet, providing an overall positive surface charge. Figure 6.4-9 C showed a gradual decrease in ζ-potential as a function of increasing hydrodynamic diameter in the presence of salts (34–150 mM NaCl). This result indicates that electrostatic charge played an important role in the extent of aggregation of *β*-lg emulsion–SGF mixture systems in addition to the predominant proteolytic action of pepsin. Hence, the observations clearly demonstrated that the addition of salt could facilitate gastric digestion by inducing droplet aggregation. Such conditions could occur *in vivo* as a result of the presence of gastric enzyme and salt through food intake.

6.4.4 Interactions of mucin in emulsion–SGF mixtures

To understand another important variable in real gastric luminal digestion, the influence of mucin on the emulsion behaviour in the simulated gastric model was examined. In addition to 0.32 wt% pepsin, when 0.1 wt% mucin was added to the mixture, the emulsion showed extensive droplet flocculation with a densely packed network-like structure at 0 and 100 mM NaCl, as shown in the confocal micrographs (Figure 6.4-10). Similar droplet flocculation (although to a lesser extent) was observed even in the absence of pepsin (micrograph not shown), suggesting a possible interaction between mucin and *β*-lg emulsion droplets.

ζ-Potential measurements to gain insight into the changes in interfacial composition upon mucin addition (Figure 6.4-11) were carried out. As expected, there were significant differences in ζ-potential values without and with the addition of mucin ($p < 0.05$), which suggested some electrostatic binding of negatively charged mucin (the ζ-potential value of a 0.1 wt% mucin dispersion was −3.63 ± 0.34 mV at pH 1.5 and −5.25 ± 0.42 mV at pH 3.0) to the positively charged *β*-lg emulsion droplets.

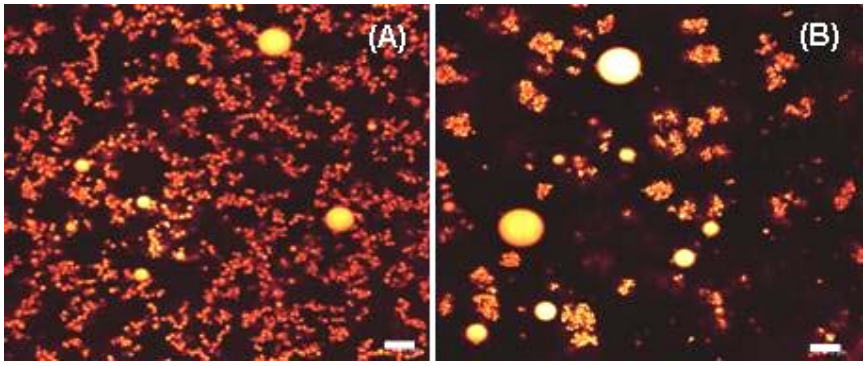

Figure 6.4-10: Confocal micrographs of *β*-lg emulsions after mixing with SGF with 0.32 wt% pepsin and 0.1 wt% mucin at ionic strengths of 0 mM NaCl (A) and 100 mM NaCl (B), at pH 1.5, respectively after 2 h of incubation. Scale bar corresponds to 10 µm.

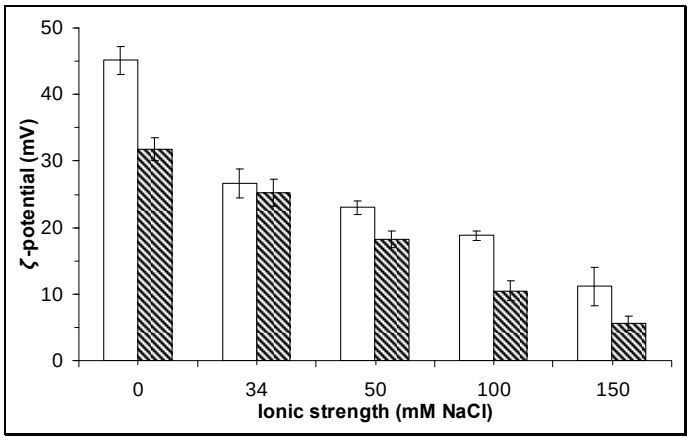

Figure 6.4-11: Change in *ζ*-potential (mV) of *β*-lg emulsion droplets after mixing with SGF containing 0.32 wt% pepsin (white) or both 0.32 wt% pepsin and 0.1 wt% mucin (shaded) at pH 1.5, respectively. Time of incubation in the gastric fluid was 2 h. Error bars indicate standard deviations.

This is in agreement with previous studies showing bridging flocculation between salivary mucins and *β*-lg emulsion droplets at acidic pH *(Silletti et al., 2007b)*. It should be noted that an interaction between the mucin and the unadsorbed *β*-lg in the continuous phase could also occur *via* the general phenomenon of complex coacervation, as seen in aqueous phase biopolymer interaction studies *(Goh et al., 2008)*, thus augmenting the degree of flocculation seen in the confocal micrographs (Figure 6.4-10). To further analyse, whether such interaction with mucin could influence the pattern of proteolysis by pepsin,

β-lg emulsions mixed with SGF (containing 0.32 wt% pepsin or both 0.1 wt% mucin and 0.32 wt% pepsin) were examined using SDS-PAGE and the band intensities were quantified and compared (Figure 6.4-12 A–C). In the presence of mucin, there was almost instantaneous hydrolysis, with the loss of > 40% intact *β*-lg in the first 5 min and with virtually complete digestion after 2 h. Although the kinetics of proteolysis were slightly different, the patterns of digestion of *β*-lg emulsions mixed with SGF (Figure 6.4-12 A and Figure 6.4-12 B) without and with mucin were very similar. There were no new bands in the gel when mucin was added, compared with the gel without added mucin. This indicated that there was possibly some non–specific and dynamic binding between mucin and the *β*-lg emulsion, which might have slightly promoted the access of pepsin to the proteolytic sites of *β*-lg. However, the addition of mucin did not affect the overall pattern of proteolysis by pepsin. It should be noted here that, as mucin is a very high molecular weight glycoprotein, it could not be resolved through the 16.0% gel and hence it was unfortunately a constraint in using SDS-PAGE analysis in this case.

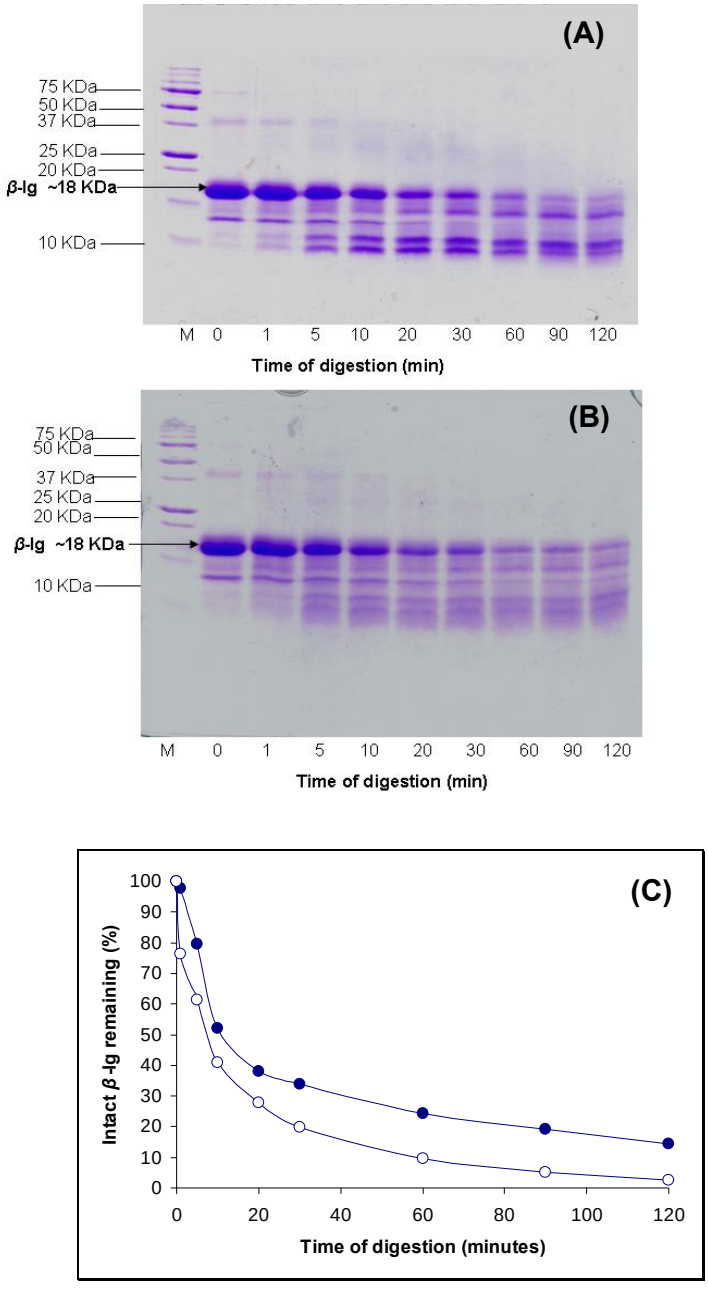

Figure 6.4-12: SDS-PAGE patterns of *β*-lg emulsions after mixing with SGF containing 0.32 wt% pepsin (A) and both 0.32 wt% pepsin and 0.1 wt% mucin (B) at 34 mM NaCl and pH 1.5, as a function of time. Rate of hydrolysis of intact *β*-lg in emulsions in the presence of 0.32 wt% pepsin (●) and both 0.32 wt% pepsin and 0.1 wt% mucin (○) at 34 mM NaCl and pH 1.5 as a function of time (C).

6.4.5 Possible mechanisms of interaction

The mechanism involved in the interaction of *β*-lg–stabilized emulsions in the presence of SGF, pepsin and mucin can be postulated based on the results from particle size analysis, confocal microscopy, SDS-PAGE quantification, and ζ-potential measurement. A schematic representation of the possible interactions is given in Figure 6.4-13. When SGF without pepsin and mucin is added to a *β*-lg emulsion, immediate charge reversal takes place because of the acidic pH (pH of 1.2 for SGF) but the emulsion remains stable at this low pH. However, the presence of salts promotes aggregation of the oil droplets, which can be attributed to the screening of the positive charges of the interfacial *β*-lg molecules by the negatively charged electrolytes, such as chlorides, in the SGF. Low levels of mucin (0.1 wt%) appear to bind strongly to the *β*-lg emulsion droplets, causing droplet flocculation.

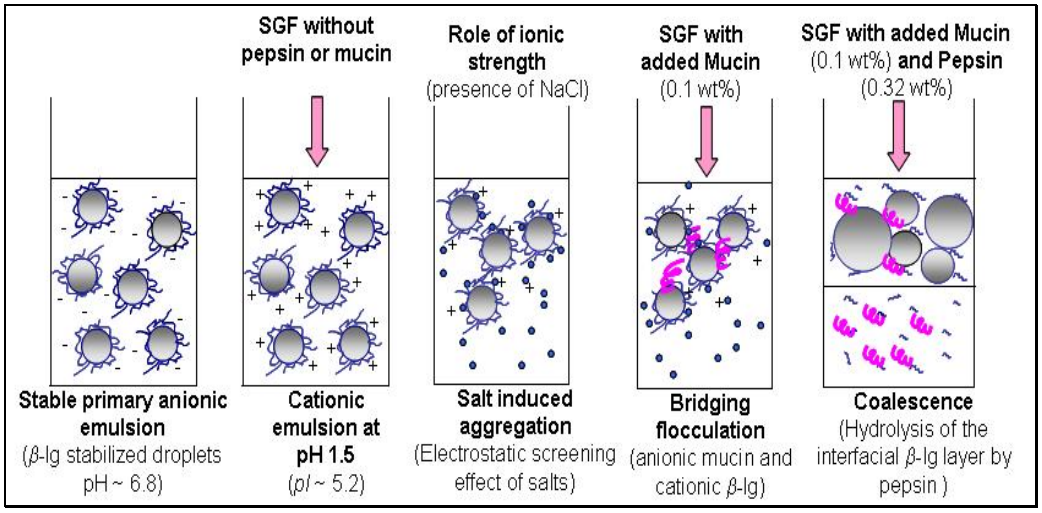

Figure 6.4-13: Schematic diagram illustrating the behaviour of *β*-lg–stabilized emulsions in a simulated gastric environment containing both pepsin and mucin. The big shaded circles represent emulsion droplets, the small blue dots represent salts (NaCl), the long thin blue curved lines represent the interfacial *β*-lg, small blue curved lines represent peptides formed later and the pink thick flexible coil structures represent mucin.

Finally, introducing a significant amount of pepsin (0.32 wt%) into the system causes proteolysis of the interfacial layer, leading to the loss of net positive charge and steric repulsion. As the molecular weights of the adsorbed peptides

are much lower than that of the intact protein, the interfacial layers are rather weak and are prone to rupture, resulting in coalescence of the droplets. Furthermore, this emulsion destabilization is accelerated by the presence of high concentrations of salt and low levels of mucin in the SGF.

6.5 Conclusions

This study unravelled some of the key interactions of *β*-lg–stabilized emulsion systems in the presence of simulated gastric fluid at physiological pH and ionic strengths in presence of pepsin and mucin. It was clearly understood that not only pepsin, but the variable pH and ionic strengths prevailing in the gastric tract may potentially lead to emulsion destabilization. The presence of mucin also promotes the flocculation of the *β*-lg–stabilized emulsion through bridging mechanism. It is well known that, at physiological concentration (> 2.0 wt%) and in an acidic environment, mucin forms a gel *(Lee et al., 2005; Bansil & Turner, 2006)*, which protects the stomach lining; thus, mucin might not be available for binding to the *β*-lg emulsion droplets. However, mucin (approximately 0.02–0.1 wt% concentration) coming from the saliva into the gastric tract could have some potential aggregation effects at low pH, which could subsequently influence the rate of proteolysis and thus the characteristics of the emulsion droplets. Hence, the interactions of *β*-lg emulsion droplets in the complicated *in vitro* gastric model clearly identify the physiological variables, which might influence the physicochemical behaviour of a protein–stabilized emulsion droplets during their gastric transit.

After passing through the gastric tract, food emulsions are exposed to alkaline pH, various electrolytes, enzymes (lipases, proteases, amylases) as well as highly surface active bile salts, *etc.* as they enter the intestine. Bile salts are generally known to displace protein–stabilized interfaces by virtue of their higher surface activities *(Maldonado-Valderrama et al., 2008)*. The interfacial composition of emulsion droplets in the intestine might be highly complicated due to the surface active and enzymatic pancreatic secretions. Hence, a control study involving only the interaction of individual pancreatic variable, such as bile salts, with protein–stabilized emulsions is required to shed light on fundamental principles

underlying the interfacial interactions in the upper intestine, which might dictate the lipid digestion of emulsions by pancreatic lipase. Therefore, the behaviour of two oppositely charged protein–stabilized emulsions (lactoferrin– and *β*-lg–stabilized emulsion) in the presence of simulated intestinal fluid containing intestinal electrolytes and bile salts (without added enzymes) was investigated in the next chapter.

Chapter Seven: Colloidal Interactions of Milk Protein–Stabilized Emulsions with Intestinal Bile Salts [4]

7.1 Abstract

The behaviour of milk protein–stabilized emulsions (1.0 wt% protein) as influenced by the addition of bile salts was studied in simulated intestinal conditions (37 °C; pH 7.5; 39 mM K_2HPO_4, 150 mM NaCl, 30 mM $CaCl_2$; with continuous agitation at ~ 95 rpm for 2 h). Oil-in-water emulsions (20.0 wt% soy oil) stabilized by lactoferrin or *β*-lactoglobulin (*β*-lg) were prepared at pH 6.8 to produce cationic or anionic interfaces, respectively. Varying physiological concentrations of bile salts (0.0–25.0 mg/mL) were added to each emulsion. The changes in droplet size, *ζ*-potential and confocal microstructures were monitored as a function of incubation time. Pre-heat treatment of simulated intestinal buffer containing bile salts was performed to eliminate any residual enzymatic activities.

For *β*-lg–stabilized droplets, *ζ*-potential significantly changed from −63.1 ± 0.5 mV to −37.2 ± 0.3 mV in presence of bile salts due to competitive interfacial displacement of *β*-lg by bile salts as characterized by SDS-PAGE analysis of the continuous phase. On the other hand, lactoferrin–stabilized emulsion droplets showed considerable aggregation in presence of intestinal electrolytes alone at pH 7.5. The *ζ*-potential values of lactoferrin emulsion decreased gradually from +53.5 ± 0.6 mV to −12.2 ± 0.2 mV in presence of bile salts due to certain electrostatic effects (*e.g.* pH shift towards the isoelectric point, binding of anionic bile salts to cationic interfacial lactoferrin layer).

[4] Part of the contents presented in this chapter has been accepted for publication as a peer-reviewed paper: Sarkar, A., Horne, D. S., and Singh, H. (2010), Interactions of milk protein–stabilized oil-in-water emulsions with bile salts in a simulated upper intestinal model. *Food Hydrocolloids*, *24*(1–2), 142–151.

7.2 Introduction

The majority of the lipid digestion (~ 70–90%) in healthy human adults occurs in the small intestine by pancreatic lipases *(Fave et al., 2004; Bauer et al., 2005; Mun et al., 2006; Singh et al., 2009)*. When the partially digested emulsion enters the small intestine from the stomach, it is generally subjected to a wide range of physicochemical conditions, including mixing with various enzymes, such as trypsin, chymotrypsin and lipases, co-enzymes, such as co-lipases, surface active agents, such as bile salts and phospholipids. Moreover, it undergoes a drastic change in pH (from ~ 1.5–3.0 in the stomach to ~ 6.0–7.5 in the intestine) and a variation in ionic strength due to the presence of different electrolytes such as Na^+, Ca^{2+}, HCO_3^- *etc.* in the pancreatic secretions *(McClements et al., 2008; Singh et al., 2009)*. Thus the interfacial composition of the emulsion droplets in the small intestine could be extremely complicated and largely dependent on the concentrations and surface activities of the intestinal components at any given period of time. In order to understand such complex conditions, model systems are beneficial because they allow separate investigation of interactions of emulsions in the context of individual physiological components.

In this chapter, lactoferrin– or *β*-lg–stabilized oil-in-water emulsions were exposed to biochemical conditions using an *in vitro* intestinal model at pH 7.5, 39 mM K_2HPO_4, 150 mM NaCl, 30 mM $CaCl_2$ with or without the addition of bile salts, for up to 2 h. Bile salts are highly surface active mixtures consisting mainly of cholic acid derivatives conjugated to glycine and/or taurine; these can possibly displace the adsorbed materials from the surface of emulsion droplets promoting the accessibility of active site of lipase to the hydrophobic lipid core *(Wickham et al., 1998; Fave et al., 2004; Mun et al., 2006)*. Broadly, the surface activities of interfacial material adsorbed on the emulsion droplets and the thickness of the adsorbed layer influence the displacement mechanism of bile salts but very little attention has been paid to the initial electrostatic charge of interfacial material coated on the emulsion droplets, which might potentially affect the bile salt–induced displacement mechanism.

In this chapter, an extremely controlled case study is envisaged in which protein–stabilized emulsion remains intact before entering the intestine ignoring the important physicochemical changes that might have occurred to the oil phase during oral and gastric processing (as described previously in Chapters 4–6). Also, pancreatic enzymes (lipases, trypsin *etc.*) have been deliberately excluded in the simulated intestinal fluid (SIF) in this study to focus on understanding the kinetics of interfacial exchange between the adsorbed protein layer and intestinal bile salts, and its influence on emulsion stability. Particularly, the aim of this chapter is to unravel the mechanisms of interactions between protein–stabilized oil–water interfaces and small molecular surface active bile salts and some of the electrolytes present in the intestine.

7.3 Materials and Methods

7.3.1 Materials

Dried un-fractionated bovine bile salts (B3883) was purchased from Sigma-Aldrich Chemical Company (St. Louis, MO, USA). The bile acid standards *i.e.* sodium salts of glycocholic acid (GCA), glycodeoxycholic acid (GDCA), taurocholic acid (TCA) and taurodeoxycholic acid (TDCA) were obtained from Sigma-Aldrich Chemical Company (St. Louis, MO, USA). Methanol was HPLC-grade from BDH Merck Ltd., Poole, England. The reagents used for making the SIF and all other chemicals were purchased from BDH Chemicals (BDH Ltd, Poole, England) unless otherwise specified. All the chemicals used were of analytical grade.

7.3.2 Analysis of bile salts using HPLC

The characterization of bile salts was carried out using a high performance liquid chromatography (HPLC) procedure *(Martoni et al., 2007)* using the Agilent Technologies, 1200 Series HPLC system (Agilent Technologies Inc., Palo Alto, CA, USA). The system was composed of a G1311A Agilent quaternary pump, a G1322A Agilent vacuum solvent delivery degasser, a G1329A Agilent auto-sampler and a G1314B Agilent UV-Vis photodiode array detector. The liquid chromatographic system was controlled and the collected data were processed by

the EZ Chrome Elite software (Version 3.3.1, Agilent Technologies Inc., Palo Alto, CA, USA). The analysis of bile salts was performed using a reversed-phase C–18 column: LiChrosorb RP-18, 5 μm, 250 × 4.6 mm from HiChrom (Winlab Pty Ltd., Queensland, Australia). The solvents used were HPLC-grade Methanol (solvent A), and acidified acetate buffer (solvent B) prepared daily using 0.05 M sodium acetate, adjusted to pH 4.3 using orthophosphoric acid, and filtered through a 0.22 μm filter (Millipore Corp., Bedford, MA, USA). An isocratic elution of 70% solvent A and 30% solvent B was used at a flow rate of 1.0 mL per min at ambient temperature. An injection loop was set to 5 μL, and detection occurred at 210 nm within 30 min after the injection of standard bile acids. For bile salt samples, injection loop was set at 10 μL.

Standard solutions of GCA, GDCA, TCA and TDCA were prepared in HPLC-grade methanol and then filtered through a 0.22 μm PVDF (Polyvinylidene Fluoride) filter (Millipore Corp., Bedford, MA, USA). To determine the composition of bile salts (B3883), SIF containing bile salts were extracted using methanol (1:1; v/v). Bile salt–methanol mixtures were vigorously agitated and centrifuged at 1000 *g* for 15 min. The supernatants were then filtered through a 0.22 μm PVDF filter (Millipore Corp., Bedford, MA, USA) and injected into the column, and the peaks were compared with those of the standard bile acids to identify and quantify various bile acids present in the dried un-fractionated commercial bile salt. Quantification was based on area under the curve of a given bile acid of known concentration under these defined experimental conditions.

7.3.3 Simulated intestinal fluid (SIF)

SIF containing 6.8 g of K_2HPO_4 and 190 mL of 0.2 N NaOH diluted to 1 L and pH being maintained at 7.5 *(Pharmacopeia, 1995)* was prepared with slight modification in ionic strength using 150 mM NaCl and 30 mM $CaCl_2$ with or without the addition of bile salts, to simulate the *in vivo* intestinal conditions *(Wickham et al., 1998)*. Bile salt concentrations of 0.0–25.0 mg/mL were selected to ensure realistic physiological situations *(MacGregor et al., 1997; Porter & Charman, 2001; Wright et al., 2008)*. In some of the experiments, the

SIF containing bile salts were pre-heated at ~ 95 °C for 5 minutes (more details in results and discussion, section 7.4.3).

The *in vitro* intestinal model (without any added enzymes) consisted of a conical flask (250 mL) containing SIF with or without bile salts maintained at 37 °C. The flask was continuously agitated at ~ 95 rpm for 2 h in a temperature-controlled water bath (Lab-Line shaker bath, Model LZ33070, Barnstead International, Dubuque, IA, USA). The pH and the temperature were continuously monitored and controlled.

7.3.4 Mixing emulsions with simulated intestinal fluid (SIF)

Experiments were conducted in the simulated upper intestinal model (as previously described in section 7.3.3) by dispersing appropriate quantities of stock emulsion in SIF. The final emulsion–SIF mixture contained 10.0 wt% oil and was incubated at 37 °C for up to 2 h during which small aliquots were periodically removed for physicochemical characterization.

7.3.5 Characterization of emulsion–SIF mixtures

The mean hydrodynamic diameter, ζ-potential and microstructures of the emulsion–SIF mixtures with or without addition of bile salts were determined. To determine the change in the interfacial composition of the emulsions after treatment with SIF for 2 h, the unadsorbed *β*-lg or lactoferrin (present in the continuous phase) was examined by centrifuging the emulsion–SIF mixtures for 40 min at 45,000 *g* and 20 °C (Sorvall RC5C, DuPont Co., Wilmington, DE, USA). The subnatants were carefully removed using a syringe, filtered sequentially through 0.45 and 0.22 μm filters (Millipore Corp., Bedford, MA, USA) and finally examined using SDS-PAGE technique (sample:sample buffer = 150 μL:800 μL, with 10 μL of sample being loaded)

The subnatants of the emulsion–SIF mixtures were also analysed separately for nitrogen content (N) using the Kjeldahl method to quantitatively estimate the amount of protein displaced from the adsorbed phase to the non-adsorbed phase.

The amount of N present in bile salts was also measured and used as blank for bile salts–emulsion interaction studies.

Details of the physicochemical, microstructural characterization, protein content determination and SDS-PAGE techniques have been described in Chapter 3 (Section 3.2.2).

7.4 Results and Discussion

7.4.1 Characterization of bile salts

Figure 7.4-1 and Figure 7.4-2 show the chromatograms of different concentrations of standards bile acids (GCA, GDCA, TCA and TDCA respectively). The different retention times of the individual bile acids allowed adequate resolution of the peaks. The reproducibility of retention times for bile acids was calculated over three consecutive runs. Relative standard deviations of retention times for the bile acids ranged from 0 to 2.5%. The calibration curves had R^2 values ranging from 0.9846 to 0.9938.

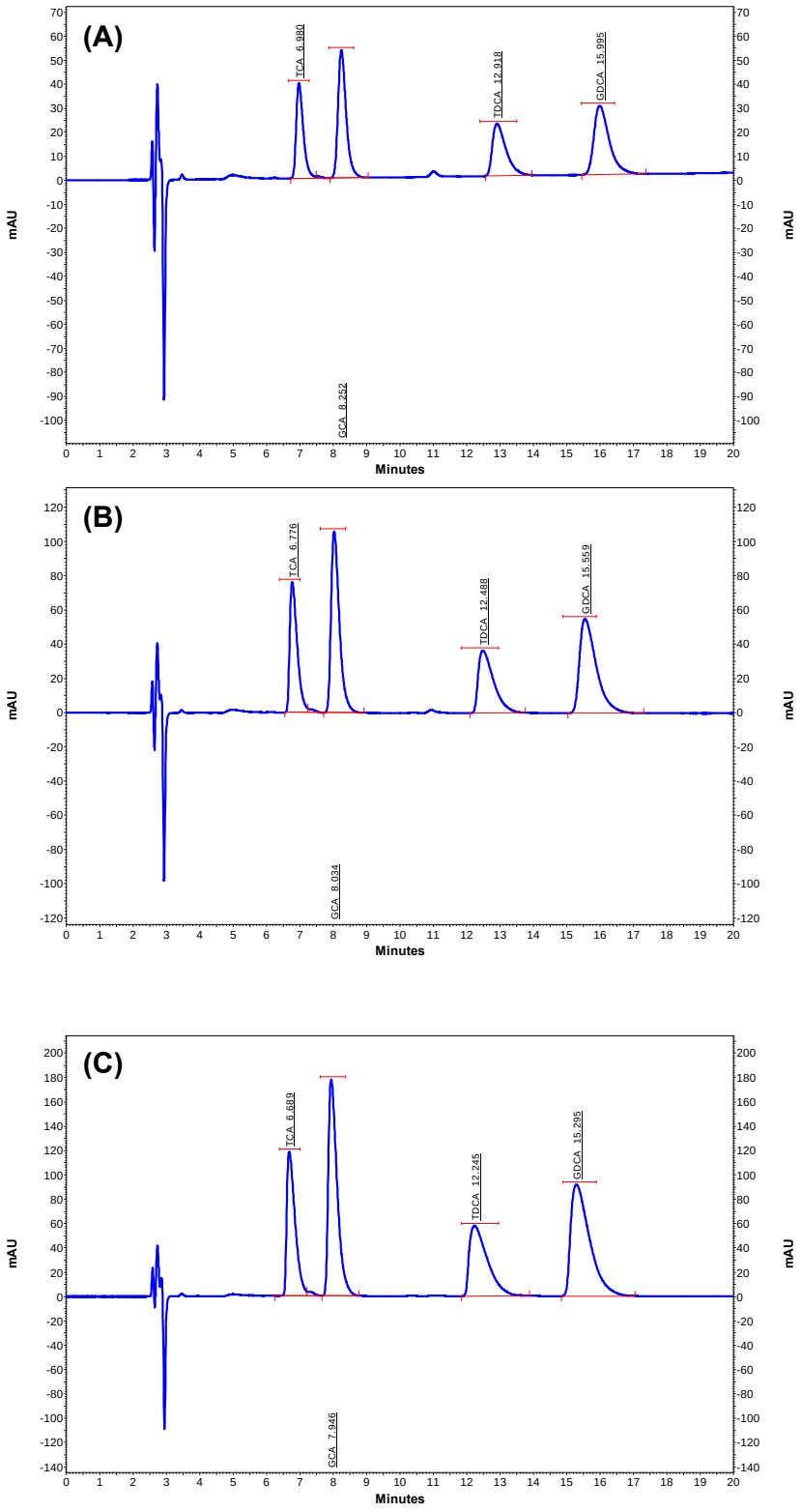

Figure 7.4-1: HPLC chromatograms of bile acid standards of concentrations: 3 mM (A), 6 mM (B) and 10 mM (C) in methanol (5 µL injection), respectively.

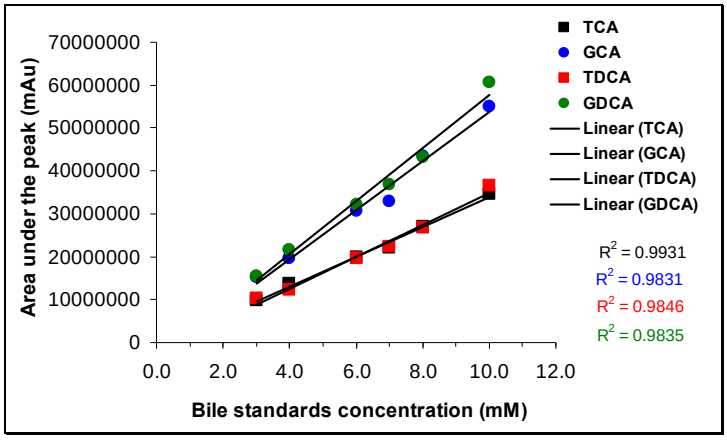

Figure 7.4-2: Calibration curves of bile acid standards.

The bile salt (B3883) from Sigma Aldrich was analysed using methanol extraction. Figure 7.4-3 and Figure 7.4-4 show selected chromatograms of varying concentrations of bile salts and their corresponding calibration curves. The R^2 values ranged from 0.9962 to 0.9973. Injection of bile salt samples showed a slight shift in retention time from those of the standard bile acids. This difference in retention times might be attributed to the difference in matrix between the sample and the standards. Bile salt concentration of 0.5–25.0 mg/mL was used to analyse its composition.

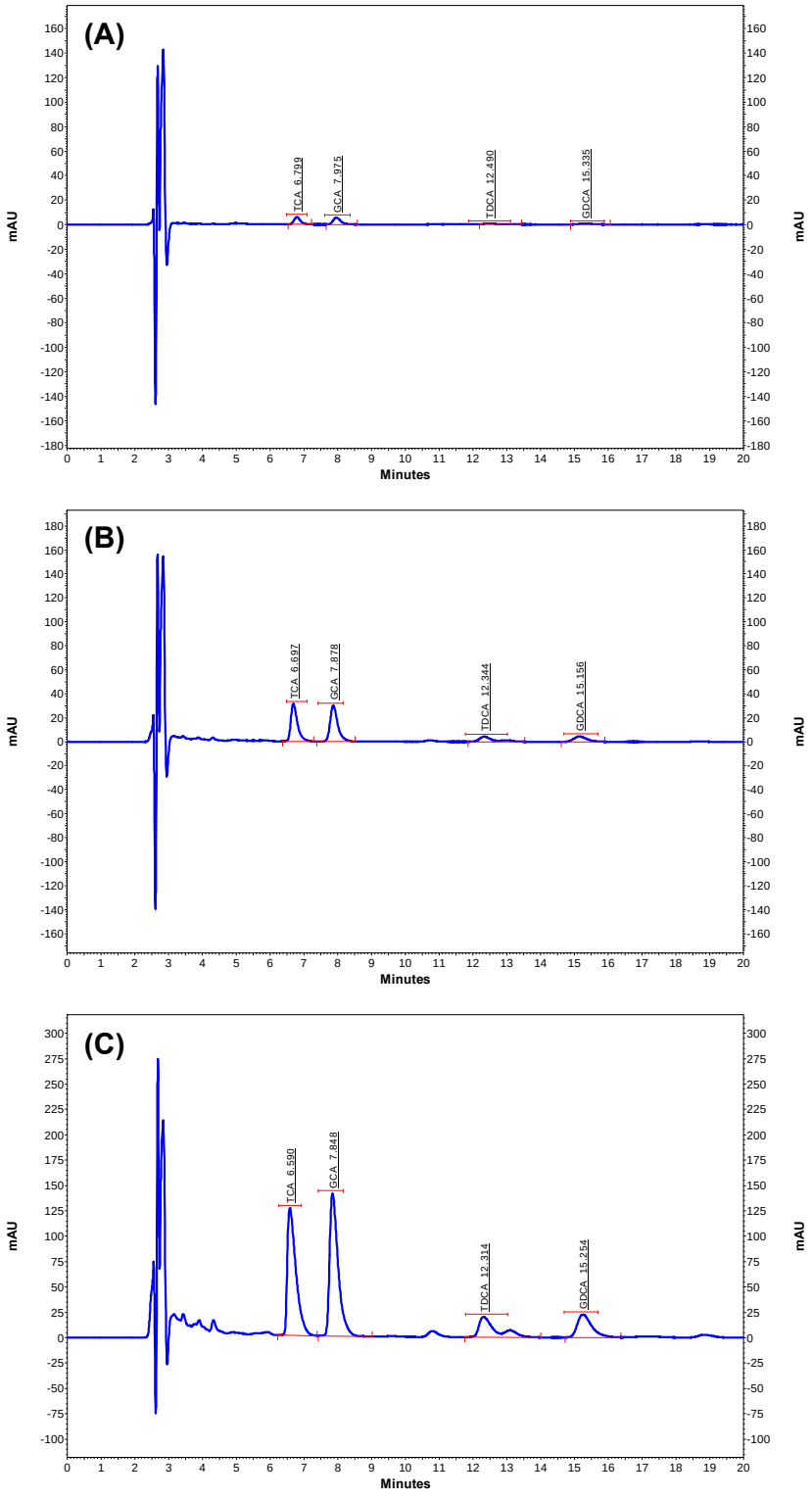

Figure 7.4-3: HPLC chromatograms of bile salt samples of concentrations: 1.0 mg/mL (A), 5.0 mg/mL (B), and 25.0 mg/mL (C) extracted with methanol in the ratio of 1:1 v/v (10 µL injection), respectively.

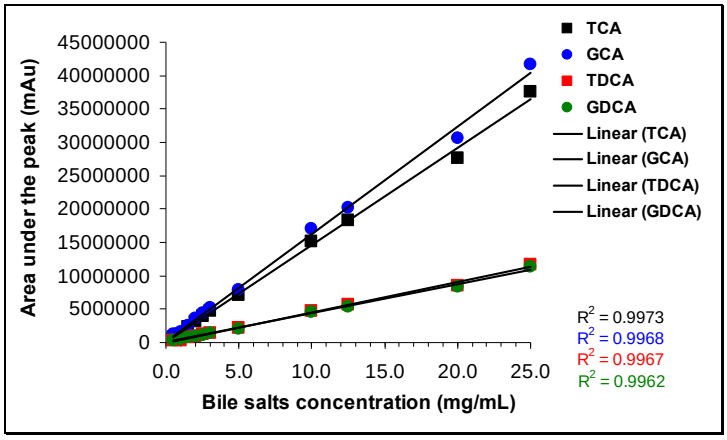

Figure 7.4-4: Calibration curves of bile salt (B3883).

Comparing the calibration curves (Figure 7.4-2 and Figure 7.4-4), the composition of bile salts was calculated (Table 7.4-1).

Table 7.4-1: Chemical composition of commercial bile salts (B3883) supplied by Sigma Aldrich Chemical Co., USA.

Bile Acids	Composition (wt%)
TCA	25.6
GCA	15
TDCA	9.4
GDCA	5

Four components in the bile salts *i.e.* glycocholic acid, glycodeoxycholic acid, taurocholic acid and taurodeoxycholic acid were identified. The total bile acid content was 55.0 wt% of the bile salts.

7.4.2 Effects of intestinal electrolytes on emulsion stability

Initially the characteristics of the emulsions in the presence of only intestinal salts (without the addition of any bile salts) were investigated to clearly identify any underlying role of intestinal pH and ionic strength on emulsion stability. The ζ-potential data of the emulsion–SIF mixture droplets (in absence of bile salts) as affected by intestinal pH and ionic strength are shown in Figure 7.4-5. Generally, after gastric emptying of food, the ionic strength and pH of the duodenum significantly varies depending on the meal contents, presence of

buffering salts and release of digestion products such as fatty acids *(Kalantzi et al., 2006)*. In this study, two different pH systems (pH 7.5 and 6.0) were used to simulate the fasted and fed state condition, respectively, after 2 h of incubation time.

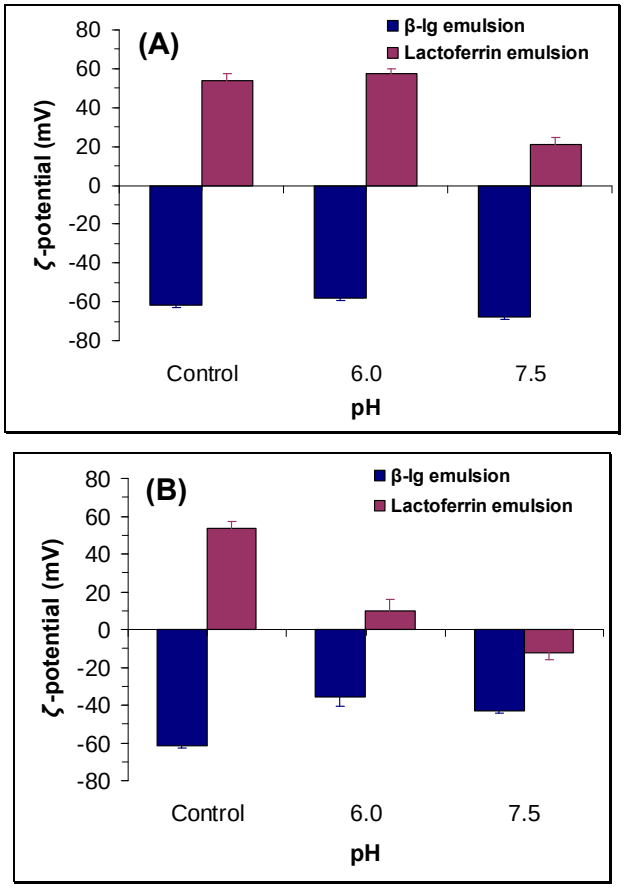

Figure 7.4-5: ζ-potential of emulsions mixed with Milli-Q water (A) or SIF (B) adjusted to pH 6.0 and 7.5, respectively.

Originally, *β*-lg–stabilized emulsion (–61.6 ± 1.2 mV) or lactoferrin–stabilized emulsion (+53.7 ± 3.5 mV) was strongly anionic or cationic at pH 6.8 (control emulsions), respectively. Both emulsions contained an array of finely dispersed droplets (Figure 7.4-6) with Z-average diameter of ~ 0.35 µm and monomodal size distribution (as seen in Chapter 4, section 4.4.2). The *ζ*-potential of *β*-lg–SIF mixture did not change significantly as a function of pH ($p > 0.05$) (Figure 7.4-5 A). However, the *ζ*-potential showed a considerable decrease in the magnitude in presence of intestinal salts ($p < 0.05$) (Figure 7.4-5 B), which can be

predominantly attributed to the screening of the electrostatic charges on the *β*-lg–coated droplets by Ca^{2+}, Na^{+} and K^{+} salts in addition to some ion binding at the droplet surfaces *(Agboola & Dalgleish, 1995; Kulmyrzaev et al., 2000; Güzey et al., 2004)*. Significant salt–mediated aggregation was also visible in the confocal micrographs of *β*-lg-SIF mixture (Figure 7.4-6 A).

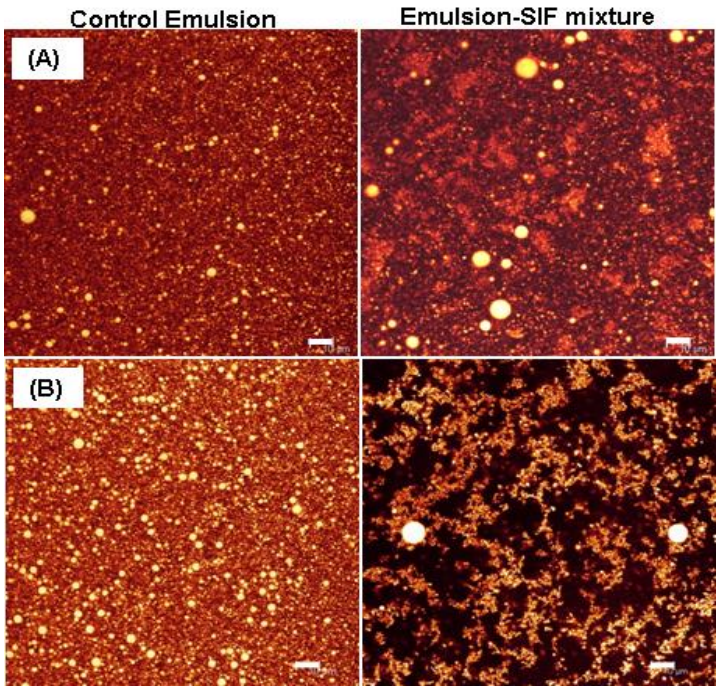

Figure 7.4-6: Confocal micrographs of *β*-lg– (A) or lactoferrin–stabilized emulsions (B) after treatment with SIF (without the addition of bile salts), respectively. Scale bar corresponds to 10 µm.

For the lactoferrin–stabilized emulsions, the *ζ*-potential was significantly reduced from +58.1 ± 1.2 mV at pH 6.0 to +21.1 ± 3.7 mV (Figure 7.4-5 A) at pH 7.5 as the adsorbed lactoferrin species were approaching the protein isoelectric point (p*I* ~ 8.0) *(Ye & Singh, 2006a)*. The magnitude of *ζ*-potential of the lactoferrin–coated droplets was further decreased to –8.5 ± 3.6 mV when 39 mM K_2HPO_4, 150 mM NaCl, 30 mM $CaCl_2$ was present in the continuous phase (Figure 7.4-5 B). This decrease might be attributed to the binding of negatively charged Cl^{-} and PO_4^{3-} ions to the droplet surface.

To understand the mechanism further, SDS-PAGE analysis of the subnatant of lactoferrin–stabilized emulsions treated with different intestinal salts showed that the concentration of lactoferrin in the continuous phase decreased in presence of salts, which indicated no displacement, but rather further adsorption of the lactoferrin molecules from the continuous phase to the interface (Figure 7.4-7 A and Figure 7.4-7 B). Extensive aggregation of droplets to form a network structure was observed in the confocal micrographs (Figure 7.4-6 B) along with significant increase in Z-average diameter (~ 0.65 μm) (data point shown: zero time in Figure 7.4-10) clearly demonstrating the combined effects of a pH shift towards the isoelectric point and salt–induced aggregation in lactoferrin emulsions on treatment with SIF.

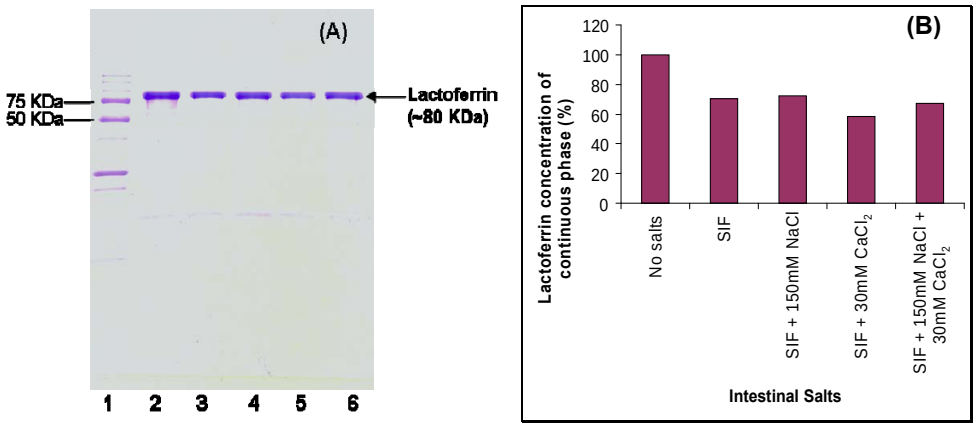

Figure 7.4-7: SDS-PAGE patterns of the continuous phase of lactoferrin–stabilized emulsions after mixing with different intestinal salts at pH 7.5 (A). Molecular weight marker, Lane 1: subnatants of lactoferrin emulsions without SIF (control), Lane 2: subnatants of lactoferrin emulsions mixed with SIF (containing only 39 mM K_2HPO_4), Lane 3: with added 150 mM NaCl in SIF, Lane 4: with added 30 mM $CaCl_2$ in SIF, Lane 5: with added 150 mM NaCl and 30 mM $CaCl_2$ in SIF, Lane 6 respectively. Lactoferrin (%) of the continuous phase quantified by gel scanning (B).

7.4.3 Effects of bile salts on emulsion characteristics

The hypothesis is that initial charge on the emulsion droplets would influence their interaction with the bile salts, assuming the mechanism to be *via* electrostatic interactions.

Generally, the intestinal bile acid concentrations in the fasted and fed states varies from 4–6 and 10–20 mM, respectively *(Porter & Charman, 2001; Rich et al., 2003)*. Since commercial bile salts (B3883) used in this study, constitute nearly 55 wt% of the weight of the bile acids (as previously described in section 7.4.1), and assuming an average bile acid molecular weight of 500 g/mol *(Nielsen et al., 2001)*, the concentrations of bile salt examined in this study (*i.e.*, 0.0, 1.0, 2.0, 3.0, 5.0, 10.0, 25.0 mg/mL) correspond to bile acid concentrations of approximately 0.0, 1.8, 2.7, 4.5, 9.1 and 22.7 mmol/L. Therefore, all experiments include a range of bile salt concentrations with potential physiological relevance.

SDS-PAGE patterns of the subnatants (non–adsorbed phase) of the emulsions after treatment with different concentrations of bile salts in the intestinal buffer are shown in Figure 7.4-8. In the case of *β*-lg–stabilized emulsions, the bands appeared to become more intense whereas in case of lactoferrin–stabilized emulsions the bands gradually became fainter as a function of increasing bile salts concentration. This behaviour could be interpreted as indicating that there was some displacement of protein from the droplet interface by bile salts in the case of *β*-lg emulsion resulting in an increase in the concentration of *β*-lg in the continuous phase (Figure 7.4-8 A).

In contrast, in the case of lactoferrin emulsions, there appeared to be a re-adsorption of lactoferrin molecules from the continuous phase to the interface (Figure 7.4-8 B). The presence of the low molecular weight bands in the SDS-PAGE of both the emulsions, particularly at high concentrations of bile salts (5.0–25.0 mg/mL) clearly indicated some hydrolysis of the protein.

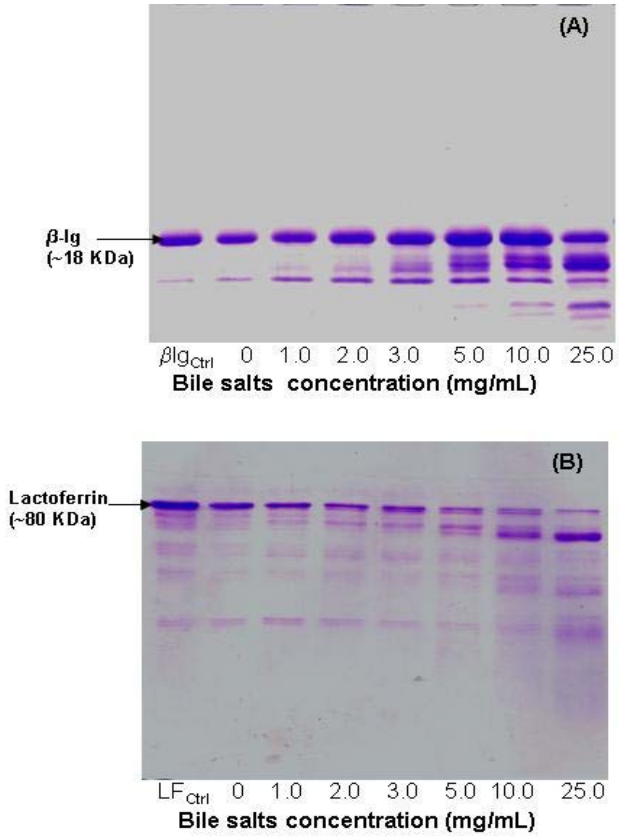

Figure 7.4-8: SDS-PAGE patterns of the continuous phase of *β*-lg– (A) and lactoferrin–stabilized emulsions (B) after mixing with SIF containing different concentrations of bile salts, respectively. Subnatants of lactoferrin or *β*-lg emulsions respectively without SIF (control in each case), Lane 1 and subnatant of emulsions treated with the SIF buffer (no bile salts added), Lane 2.

It was interesting to note that for both the emulsions, the ζ-potential values decreased as a function of bile salts (Figure 7.4-9). For the *β*-lg–stabilized droplets (Figure 7.4-9), the ζ-potential became more negative from −30.7 ± 1.5 mV to −46.2 ± 1.2 mV as a function of bile salts concentration ($p < 0.05$). Under the same conditions, the ζ-potential values of lactoferrin emulsions also diminished from −7.5 ± 1.1 mV to −20.4 ± 1.6 mV showing some electrostatic interactions, as hypothesized.

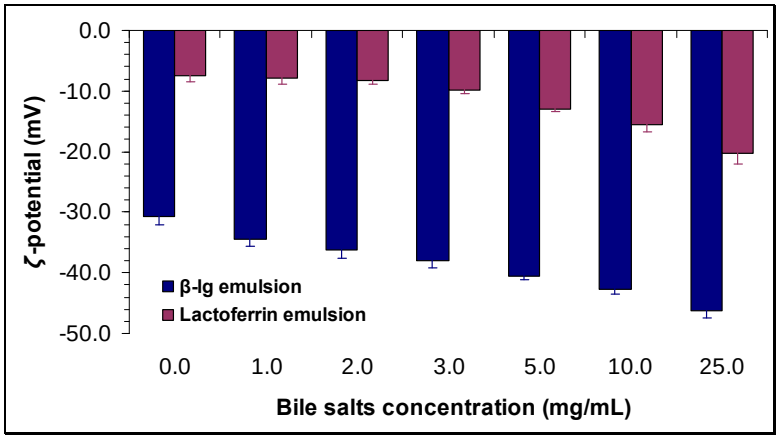

Figure 7.4-9: The change in ζ-potential (mV) of emulsions on addition of SIF as a function of bile salt concentration after 2 h (B). Standard deviations are indicated by error bars.

However, the SDS-PAGE results (Figure 7.4-8) strongly suggests that the ζ-potential results (Figure 7.4-9) might have been influenced by the presence of contaminating trypsin or other proteolytic enzymes, such as chymotrypsin, α-carboxy peptidases present in the un-fractionated commercial bile salts (B3883, Sigma Aldrich Chemical Co., USA) preparation. These enzymes caused the breakdown of non–adsorbed and most probably the interfacial layer of protein coating the emulsion droplets. Furthermore, the bile salts might also contain residual lipase activities which could have resulted in generation of lipolytic digestion products, such as surface active monoglycerides and fatty acids, at the interface displacing the adsorbed protein *(Singh et al., 2009)*, thus confounding the ζ-potential results.

7.4.4 Pre-heat treatment of SIF containing bile salts

Accordingly, to eliminate all the residual pancreatic enzyme activities as seen in the previous section, the SIF containing bile salts was pre-heated at ~ 95 °C for 5 min and then cooled to room temperature prior to addition to the emulsions.

The influence of pre-heated SIF containing bile salts was investigated for both emulsions by monitoring the Z-average diameter (Figure 7.4-10). For the β-lg–stabilized emulsion, both the addition of SIF containing 5 mg/mL of bile salts

for 2 h and treatment with different levels of bile salts (0–25.0 mg/mL) had no significant effect on the droplet size ($p > 0.05$). In contrast, lactoferrin–stabilized emulsions showed a gradual reduction in hydrodynamic diameter (~ 0.65 μm to 0.33 μm) over time under the same conditions (5 mg/mL bile salts), which suggested some interaction of lactoferrin–coated droplets with the bile salts (Figure 7.4-10 A). Above 5.0 mg/mL of bile salts concentration, the droplet diameter curve had declined to a constant low level with no further decrease (Figure 7.4-10 B).

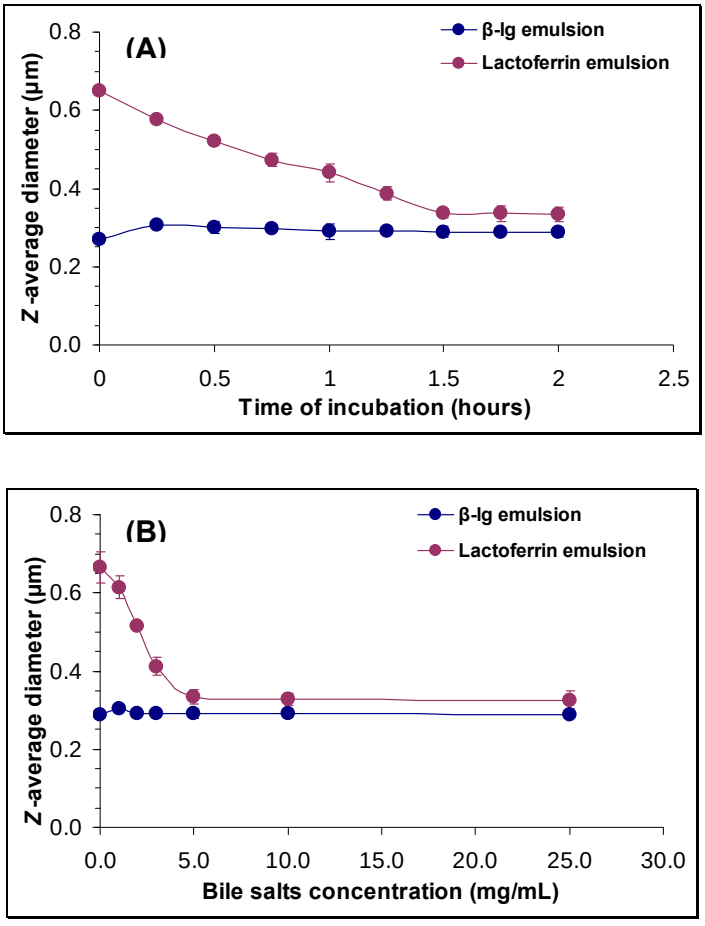

Figure 7.4-10: The change in *Z*-average diameter of emulsions on addition of pre-heated SIF containing 5 mg/mL of bile salts as a function of time (A) and as a function of bile salt concentration after treatment for 2 h (B). Standard deviations are indicated by error bars.

The droplet size distributions of lactoferrin emulsions after mixing with SIF are shown in Figure 7.4-11. The reduction in proportion of larger droplets (above 10

μm and between 1 and 5 μm) in the presence of bile salts was also evidenced by the microstructural changes of the lactoferrin emulsion–SIF mixtures from an aggregated to a uniformly dispersed system with the addition of bile salts (insert in Figure 7.4-11). It appears that the salt–induced aggregation in lactoferrin emulsion was minimized and reversed (closer to similar size to those found in original lactoferrin emulsion) in the presence of bile salts, possibly because of gradual electrostatic binding of small amounts of bile salts to the emulsion droplets. Furthermore, the decrease in apparent size with addition of increased amount of bile salts might be as a consequence of the break-up of the salt–induced aggregates.

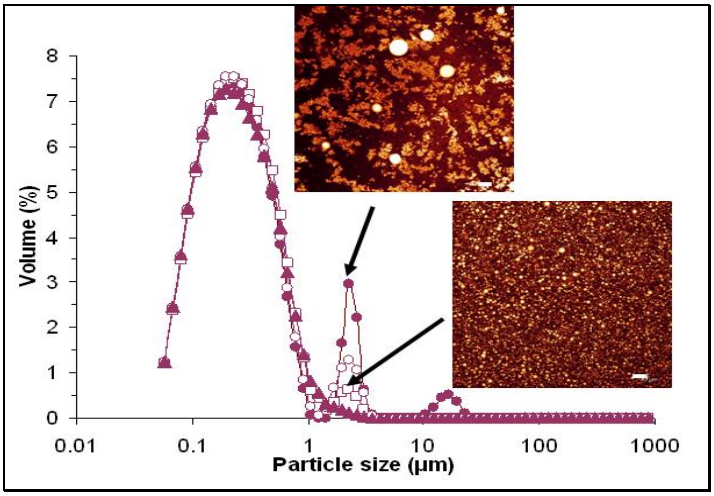

Figure 7.4-11: Droplet size distribution and corresponding confocal micrograph of lactoferrin–stabilized emulsions (▲) on mixing with SIF containing no bile salts (●), 5 mg/mL bile salts (○) or 25 mg/mL bile salts (□) at pH 7.5 after 2 h of incubation. Scale bar corresponds to 10 μm. In case of bile salts addition, pre-heated SIF has been used.

To gain further insights, ζ-potential measurements of the emulsion droplets were carried out after treatment with pre-heated SIF containing bile salts. For the lactoferrin–stabilized emulsions mixed with bile salts, the magnitude of ζ-potential decreased slightly from –8.5 ± 3.6 mV to –10.6 ± 0.5 mV at added bile salt concentration of 5.0 mg/mL as a function of time (Figure 7.4-12 A). On increasing the bile salt concentration to 25.0 mg/mL, the ζ-potential became slightly more negative (–12.2 ± 0.2 mV) although the change was not significant

(Figure 7.4-12 B). The ζ-potential of the lactoferrin–coated droplets never reached the ζ-potential of a droplet completely saturated with bile salts (–51.3 ± 2.5 mV), which clearly indicates that lactoferrin was neither fully displaced nor had a full secondary coverage by bile salts.

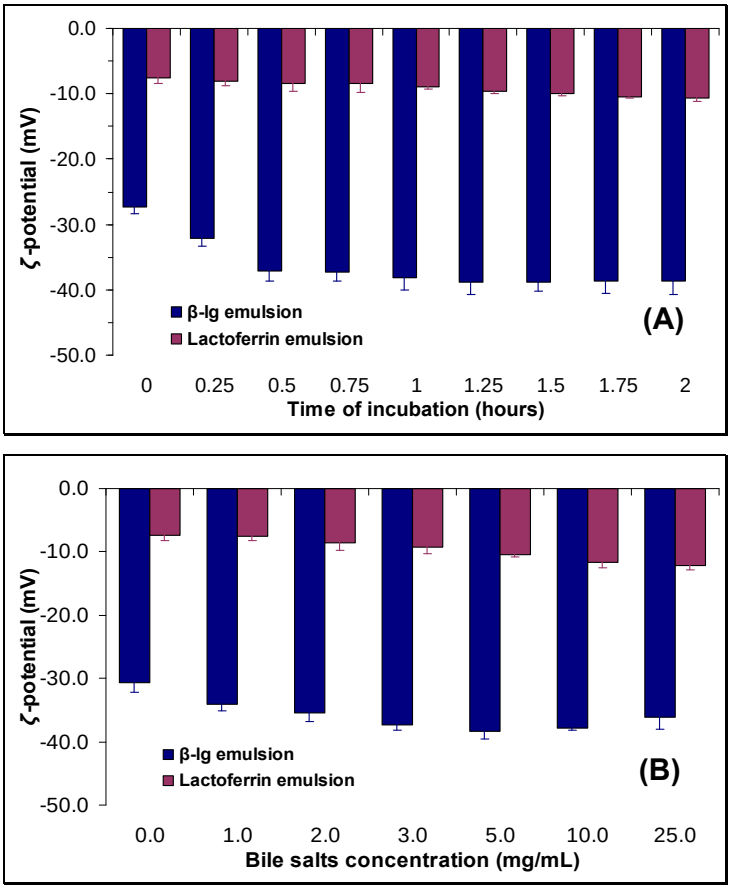

Figure 7.4-12: The change in ζ-potential (mV) of emulsions on addition of pre-heated SIF containing 5 mg/mL of bile salts as a function of time (A) and as a function of bile salt concentration after treatment for 2 h (B). Standard deviations are indicated by error bars.

In case of *β*-lg–stabilized emulsions, the ζ-potential became more negative in presence of bile salt (both as a function of time and concentration) (Figure 7.4-12) at pH 7.5, which could imply some coverage of bile salts to *β*-lg–coated emulsion droplets or possible displacement of *β*-lg interfacial layer thereby increasing the negative ζ-potential. The binding of bile salts seemed to be less plausible as anionic bile salts would not be expected to adsorb onto the anionic *β*-lg-droplet surface unless some other attractive forces existed.

It was worth noting here that the change in ζ-potential on addition of pre-heated SIF ($\Delta\zeta$ = ~ −4.7 mV for lactoferrin– and ~ −5.5 mV for β-lg–stabilized emulsions) was significantly less than that of unheated SIF ($\Delta\zeta$ = ~ −12.9 mV for lactoferrin and ~ −15.3 mV for β-lg emulsions) at the highest bile salts concentration (25.0 mg/mL). This is consistent with the previous suggestion of the presence of contaminating lipase activities in the unheated bile salts (Figure 7.4-8 and Figure 7.4-12).

To unravel the mechanism of interactions between the emulsion droplets and bile salts, displacement studies were carried out. The non–adsorbed phases, *i.e.* the emulsion–SIF subnatants (after treatment of the emulsions with different levels of pre-heated bile salts for 2 h in intestinal buffer), obtained by centrifugation were filtered and characterized using SDS-PAGE (Figure 7.4-13).

The band intensities were estimated using GelQuant software and the protein content in the continuous phase was quantified using Kjeldahl estimation (Figure 7.4-14). Under the conditions of these experiments, ~ 50% of the total proteins were initially adsorbed at the droplet surface. On treatment with SIF buffer (no bile salts), there was a reduction in band intensities of subnatants for both the emulsions. The protein peak content in the continuous phase decreased to ~ 70–90 % of the initial value (data shown: 0 mg/mL bile salts in Figure 7.4-13 and Figure 7.4-14) for both the emulsions indicating salt–induced destabilization as hypothesized previously, due to which more protein molecules were possibly migrating from the continuous phase to the interface to stabilize the emulsion against aggregation. This was also confirmed by the total protein content of the subnatant, which showed that about 0.12–0.15 wt% of protein in both the emulsions was present in the aqueous phase after treatment with the SIF buffer (Figure 7.4-14 B).

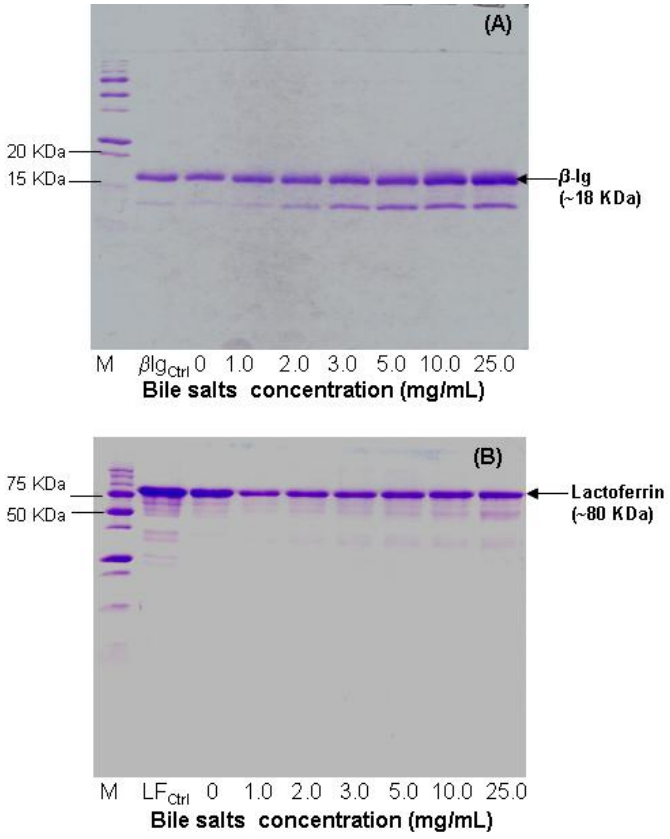

Figure 7.4-13: SDS-PAGE patterns of the continuous phase of *β*-lg– (A) and lactoferrin–stabilized emulsions (B) after mixing with pre-heated SIF containing different concentrations of bile salts, respectively.

On subsequent addition of different quantities of bile salts at pH 7.5, SDS-PAGE analysis of the continuous phases of the emulsion–SIF mixtures showed that the changes in the intensities of the lactoferrin and *β*-lg bands were almost diametrically opposite to each other (Figure 7.4-13 and Figure 7.4-14). In case of *β*-lg–stabilized emulsion–bile salts mixtures, the subnatants showed a dramatic increase in intensities of the *β*-lg band (Figure 7.4-13 A and Figure 7.4-14) as a function of bile salts concentration. The proportion of *β*-lg in the non–adsorbed phase increased by more than 1.5 fold at added bile salts concentration of 5.0 mg/mL and more than 2.5 fold at added bile salts concentration of 25.0 mg/mL after 2 h incubation.

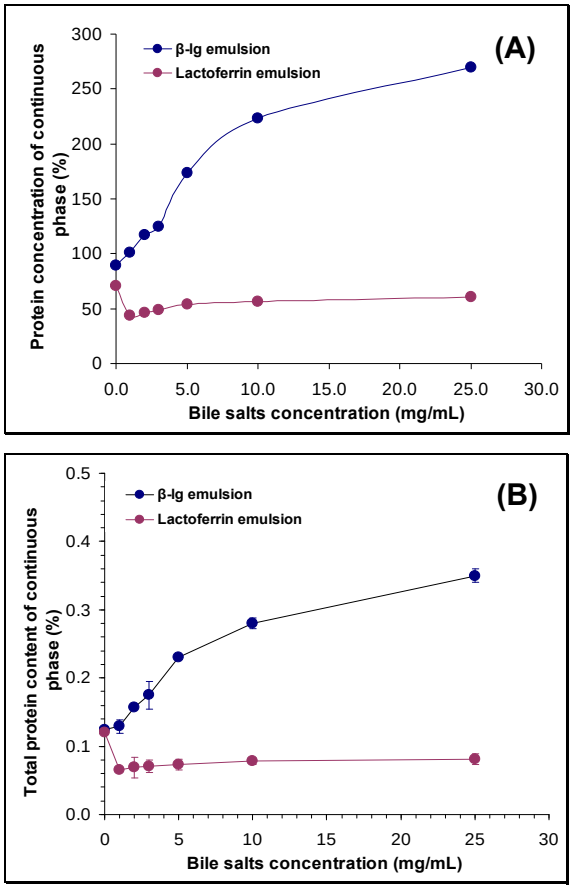

Figure 7.4-14: Changes in protein concentration of the continuous phase of emulsions as a function of bile salts concentration in pre-heated SIF based on relative measurements from scanning of SDS-PAGE gels of Figure 7.4-13 and normalized to zero bile salts concentration (A) and absolute measurements of protein content by the Kjeldahl method (B).

This clearly suggests that bile salts being highly surface active were gradually becoming adsorbed to the emulsion droplet surface with more *β*-lg being pushed off to the continuous phase from the interface confirming the bile salt–induced displacement mechanism, in agreement with previous studies *(Maldonado-Valderrama et al., 2008)*.

In contrast, the effects of addition of bile salts on lactoferrin emulsion appeared to be more complicated than purely a displacement by bile salts (Figure 7.4-13 B and Figure 7.4-14). SDS-PAGE gels showed marked decrease in the intensities of subnatant lactoferrin bands at low levels of bile salts addition (0–1.0 mg/mL) resulting in decline of aqueous phase lactoferrin content to ~ 0.06 wt%. However,

on addition of higher concentrations of bile salts lactoferrin band showed a very slight increase in intensity (Figure 7.4-14 A). This initial decrease in band intensity in the subnatant with bile salts addition up to 1.0 mg/mL indicates that the emulsion system is unstable in the buffer (39 mM K_2HPO_4, 150 mM NaCl, 30 mM $CaCl_2$, pH 7.5) containing low levels of bile salts thus requiring more lactoferrin molecules to migrate from the continuous phase to the interface. This is consistent with the bimodal size distributions and the appearance of the emulsions under confocal microscopy (Figure 7.4-11). Furthermore, this would imply electrostatic binding of small amounts of anionic bile salts to the lactoferrin interfacial layer, which is subsequently inducing more cationic lactoferrin molecules to shift from the continuous phase to the emulsion interface. This is in agreement with the increase of negative ζ-potential of the lactoferrin–coated surface on addition of bile salts (Figure 7.4-11).

At added bile salts concentrations of ≥ 2.0 mg/mL, the band intensities of the lactoferrin subnatants seemed to increase slightly with rise in non–adsorbed lactoferrin content to ~ 0.09 wt%, which could be due to onset of displacement by the bile salts. In general, the displacement was substantially less when compared to that seen in case of β-lg–coated droplets with the same levels of bile salts being added (Figure 7.4-13 and Figure 7.4-14). Clearly, interaction of the protein–stabilized interface with bile salts was largely dependent on the initial protein type, charge of the protein and added bile salt concentrations.

Although it is recognised that bile in the human intestine would never be heated in physiological conditions under any circumstances, this pre-heat treatment process was carried out to better understand the individual influence of bile on emulsion characteristics without the confounding presence of any contaminating enzymes. The bile salts obtained from Sigma Aldrich (B3883) is not a sterile product. It is a crude mixture extracted from the ox gall (bladder), collected, concentrated and vacuum dried. Hence, if the heat treatment is not severe enough during final processing of bile salts at supplier's end as seen in this batch of bile salts sample, there might be the presence of pancreatic proteolytic enzymes and other bacterial enzymes inducing hydrolysis particularly in case of

protein–stabilized emulsions. Thus, the heat treatment of SIF containing bile salts provides a precautionary step to eliminate the presence of any contaminating enzymes due to faulty heat treatment or batch variation at the manufacturer's point of processing.

7.5 Conclusions

This study provided valuable insights into the mechanism of interactions of protein–stabilized emulsions with intestinal electrolytes and surface active bile salts (of physiological concentrations) with a focus on the initial charge of the emulsions. It has stressed the importance of investigating the role of each component and if necessary eliminating confounding effects of unwanted and intrusive agents, such as proteolytic enzymes, by heat treatment. The interactions of interfacial displacement and/or binding between bile salts and protein–stabilized emulsions were successfully studied using SDS-PAGE analysis of the non–adsorbed phase.

The behaviour of protein–stabilized emulsions in presence of SIF was largely driven by electrostatic interactions. Initially, the role of intestinal pH and electrolytes was unravelled, which particularly showed that lactoferrin–stabilized emulsions underwent aggregation on addition of SIF containing only salts (no bile salts added). This aggregation of lactoferrin emulsion was attributed to the charge screening effects by intestinal electrolytes. In addition, the instability was also due to proximity of the pH to the isoelectric point of lactoferrin. On addition of bile salts, release of peptides was observed, which could only have arisen as a result of proteolysis due to the presence of contaminating enzymes in the bile salts. Therefore, SIF containing bile salts was heated to eliminate any residual enzymes. On addition of heat treated bile salts, aggregated lactoferrin emulsions (in presence of SIF without bile salts) showed re-stabilization due to electrostatic binding by negatively charged bile salts. On increasing bile salt concentration, surface active bile salts appeared to displace lactoferrin molecules from the interface. Emulsions stabilized by β-lg showed straightforward displacement of protein from the interface as a function of bile salts. Hence, the surface activities

and the initial charge of the protein–water interface largely influence the bile salt displacement reactions.

However, it is recognized that the complexities of lipolytic and proteolytic enzymes in the real duodenal situation have not been taken into account. Hence, the next chapter aims at understanding the behaviour of protein–stabilized emulsions in a more realistic platform using physiological concentrations of pancreatic enzymes with or without the addition of bile salts.

Chapter Eight: Behaviour of Emulsions in a Simulated Upper Intestinal Model [5]

8.1 Abstract

The behaviour of cationic lactoferrin–stabilized and anionic β-lactoglobulin (β-lg)–stabilized oil-in-water emulsions [20.0 wt% soy oil, 1.0 wt% protein] in the presence of simulated intestinal fluid (SIF) containing physiological concentrations of pancreatin (0.0–10.0 mg/mL) and/or bile salts (0.0–25.0 mg/mL) at 37 °C, pH 7.5 and ionic strength (39 mM K_2HPO_4, 150 mM NaCl and 30 mM $CaCl_2$) was investigated. Both emulsions showed a significant degree of coalescence and fatty acid release on mixing with SIF. Appreciably negative ζ-potential values (≥ -50 mV) for both types of emulsion droplets at the highest pancreatin/bile salts concentration could be attributed to the displacement of and/or binding to the interfacial proteins by bile salts, together with interfacial proteolysis by pancreatin, which enhanced the potential for lipase to act on the hydrophobic lipid core, thus generating free fatty acids and possibly mono- and/or diglycerides at the droplet surface.

8.2 Introduction

Generally, emulsified lipid droplets undergo a series of physical and biochemical processes on consumption and digestion. During these processes, the droplets are exposed to different gastrointestinal pHs, inorganic salts (Na^+, K^+, Ca^{2+}, Cl^-, HCO_3^-), organic compounds (urea, glucose), various enzymes (salivary amylases, pepsin, trypsin, chymotrypsin, lipases), co-enzymes, biopolymers (mucins), proteins (proline-rich proteins, immunoglobulins, bovine serum albumin), surface active agents (bile salts, phospholipids) and peristalsis–mediated mechanical shear. These treatments result in flocculation, phase separation, salt–induced aggregation, droplet disruption, coalescence,

[5] Part of the contents presented in this chapter has been accepted for publication as a peer-reviewed paper: Sarkar, A., Horne, D. S., and Singh, H. (*In Press*), Pancreatin–induced coalescence of oil-in-water emulsions in an *in vitro* duodenal model. *International Dairy Journal*, doi:10.1016/j.idairyj.2009.12.007.

interfacial layer hydrolysis, competitive adsorption, micelle formation and absorption of lipid micelles *(Beysseriat et al., 2006; Mun et al., 2007; Silletti et al., 2007b; Hur et al., 2009)*.

The majority of lipid digestion occurs in the upper part of the intestine by the pancreatic lipases *(Fave et al., 2004; Bauer et al., 2005; Mun et al., 2006)*. The presence of various lipolytic as well as proteolytic enzymes at different concentrations, inorganic salts, surface active bile acids and the neutral–alkaline pH (~ 6.0–7.5) of the upper intestinal fluid *(Maldonado-Valderrama et al., 2008; McClements et al., 2008; Singh et al., 2009)* together with the remnants of oral and gastric digestion make the overall intestinal processing highly complex and difficult to unravel.

In the previous chapter (Chapter 7), a controlled study was conducted to understand the interactions of protein–stabilized droplets with intestinal electrolytes and bile salts. It was found that lactoferrin– and *β*-lg–stabilized oil–water interfaces behave differently in simulated intestinal fluid (SIF) containing only bile salts based on their initial charges and surface activities. There were considerable difference in the kinetics of interfacial exchange between the adsorbed protein layer and the bile salts between the two types of emulsions.

In this study, the aim is to gain further insights into the effects of the addition of simulated intestinal fluid (SIF) to protein–stabilized emulsions at pH 7.5, containing various concentrations of pancreatin and bile salts of physiological relevance. Pancreatin contains a mixture of enzymes secreted from the exocrine cells of pancreas, *i.e.* intestinal lipase, protease and amylase, which makes the overall digestion mechanism of the emulsified lipids even more complicated. Hence, the individual role of pure lipase in generating the lipid digestion products, such as fatty acids and monoglycerides, thus affecting the interfacial displacement reactions of the adsorbed protein layer has also been considered. Particular focus is on understanding the role of initial charge of the emulsion droplets [cationic lactoferrin and anionic *β*-lactoglobulin (*β*-lg) as the interfacial

layer at neutral pH, respectively] in determining the behaviours of the droplets in the *in vitro* duodenal model.

8.3 Materials and Methods

8.3.1 Materials

Porcine pancreatin (P1750; 4×USP), bile salts (B3883; as used in Chapter 7), porcine lipase (Type II, L3126; ≥ 100-400 units/mg protein) and purest commercial lipase (PCL) from porcine pancreas (Type VI-S, L0382; ≥ 20,000 units/mg protein) were obtained from Sigma Aldrich Chemical Company. The reagents used for making the simulated intestinal fluid (SIF) and all other chemicals were purchased from BDH Chemicals (BDH Ltd, Poole, England) unless otherwise specified. All the chemicals used were of analytical grade.

8.3.2 Simulated upper intestinal model

Simulated intestinal fluid (SIF) at pH 7.5 *(Pharmacopeia, 1995)* with slight modification (39 mM K_2HPO_4, 150 mM NaCl and 30 mM $CaCl_2$) was prepared as mentioned in Chapter 7 with the addition of pancreatin and bile salts. Bile salt concentrations of 0.0–25.0 mg/mL at both lower (0.4 mg/mL) and higher (2.4 mg/mL) concentrations of pancreatin were selected to ensure realistic physiological situations of the fasted state and the fed state, respectively *(MacGregor et al., 1997; Porter & Charman, 2001; Wright et al., 2008)*. Correspondingly, in another set of studies, SIF was prepared using different pancreatin concentrations (0.0–10.0 mg/mL) at bile salt concentrations of 5.0 and 20.0 mg/mL, respectively. In some of the experiments, emulsions were mixed with SIF containing only commercially available lipase (L3126) or PCL to understand the effect of lipase on emulsion digestion separately. In case of PCL experiments, SIF containing 0.0–1.0 mg/mL concentrations of PCL was used.

The *in vitro* duodenal or simulated upper intestinal model consisted of a conical flask (250 mL) containing SIF with added pancreatin and/or bile salts or lipase maintained at 37 °C, with continuous agitation at ~ 95 rpm for 2 h in a temperature-controlled water bath (Lab-Line shaker bath, Model LZ33070,

Barnstead International, Dubuque, IA, USA). The pH and the temperature were continuously monitored and controlled.

8.3.3 Mixing emulsions with simulated intestinal fluid (SIF)

Digestion experiments in the *in vitro* duodenal model (as described in Section 8.3.2) were conducted by mixing stock emulsion with SIF so that the final emulsion–SIF mixture contained 10.0 % wt% soy oil. The mixed system was incubated at 37 °C for up to 2 h, during which time aliquots were characterized periodically.

8.3.4 Free fatty acid release

The amount of free fatty acid released from the emulsion after treatment with SIF was determined using a titration method *(Mun et al., 2006; Mun et al., 2007)*. In brief, the emulsion–SIF mixtures containing pancreatin/bile salts were titrated with 0.01 M NaOH to detect the phenolphthalein end point. A standard curve was plotted, using the same titration method to measure the free fatty acids released from emulsions containing known concentrations of oleic acid. The free fatty acid release was then expressed as μmoles of oleic acid per mL of emulsion by using the standard curve. The amount of fatty acids released without the addition of pancreatin was used as the blank.

8.4 Results and Discussion

8.4.1 Influence of various concentrations of bile salts (at a fixed concentration of pancreatin) on droplet aggregation

Changes in d_{43} values (Figure 8.4-1) and size distribution of the emulsion droplets (Figure 8.4-2 and Figure 8.4-3) as influenced by the bile salts concentration at both low (Figure 8.4-1–3 A, 0.4 mg/mL) and high (Figure 8.4-1–3 B, 2.4 mg/mL) concentrations of pancreatin after 2 h of incubation in the SIF buffer [pH 7.5 and ionic strength (39 mM K_2HPO_4, 150 mM NaCl and 30

mM $CaCl_2$)] have been studied. Both lactoferrin–stabilized emulsions and *β*-lg–stabilized emulsions (*i.e.* before mixing with SIF) showed monomodal distributions (Figure 8.4-2 and Figure 8.4-3) with d_{43} value of ~ 0.40 µm (as reported in previous chapters about freshly prepared emulsions) and uniform distribution of fat globule sizes with no signs of flocculation (Figure 8.4-4 A).

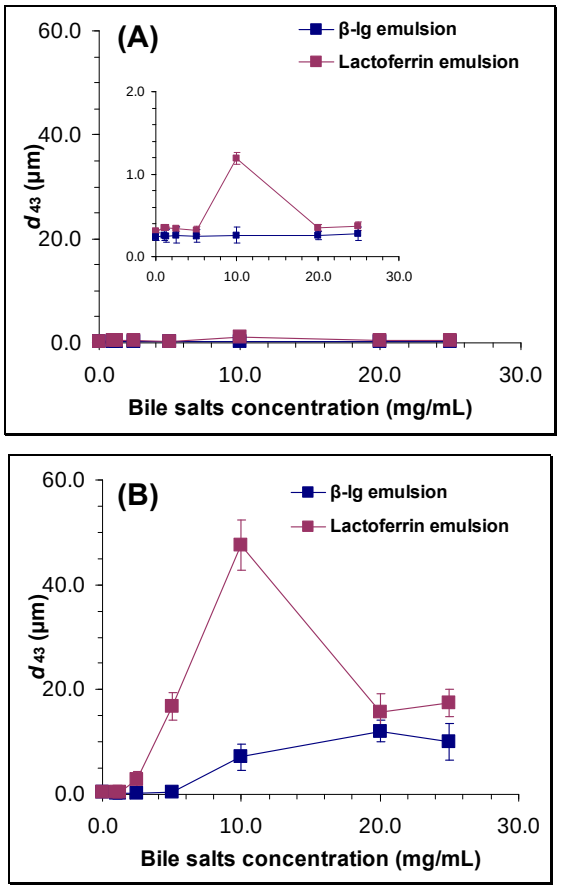

Figure 8.4-1: Changes in d_{43} values (µm) of emulsions on the addition of SIF containing various concentrations of bile salts at 0.4 mg/mL (A) and 2.4 mg/mL (B) of added pancreatin, respectively after 2 h of incubation. Error bars represent standard deviations.

As shown in Figure 8.4-1–Figure 8.4-3, the bile salts concentration appeared to have a significant influence on the d_{43} values of the emulsions, particularly at the higher concentration of pancreatin used in this study ($p < 0.05$).

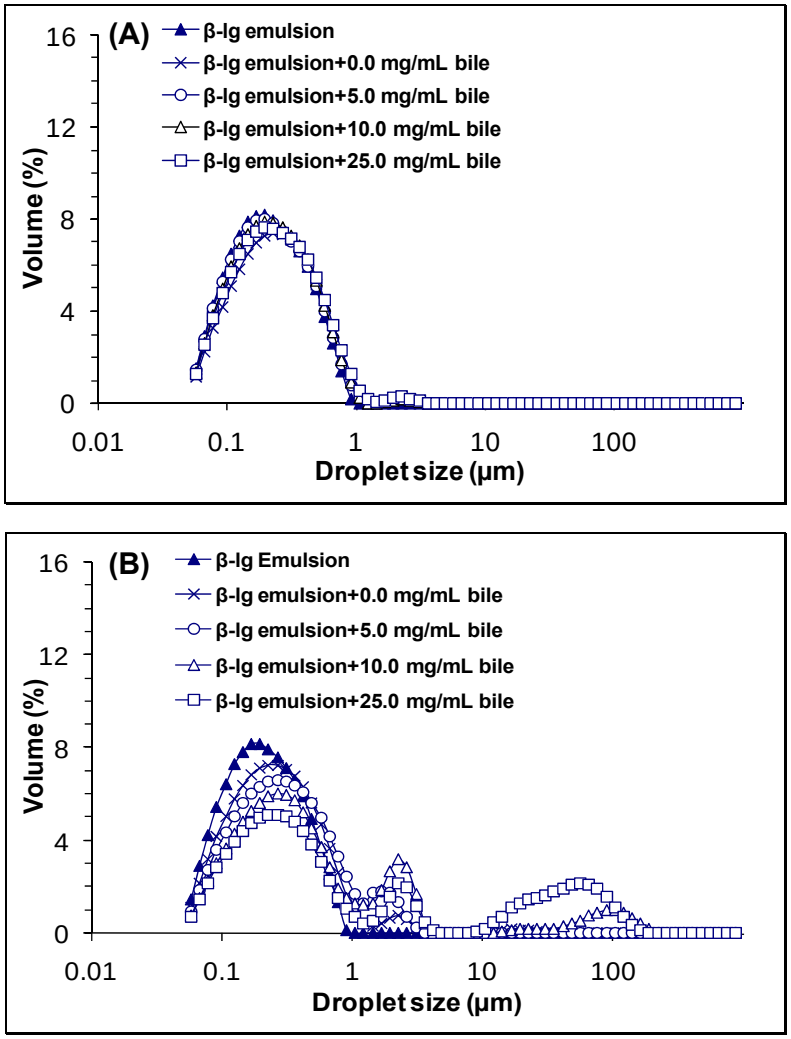

Figure 8.4-2: Droplet size distribution of *β*-lg–stabilized emulsions on the addition of SIF containing various concentrations of bile salts at 0.4 mg/mL (A) and 2.4 mg/mL (B) of added pancreatin, respectively after 2 h of incubation. Each data point is the average of measurements on duplicate samples.

In the absence of bile salts, the d_{43} values did not show a significant change for either emulsion (~ 0.35–0.50 μm at both 0.4 and 2.4 mg/mL of pancreatin). The size distribution remained monomodal with almost all of the droplets being smaller than 1 μm (Figure 8.4-2). This may have been because the pancreatin could not gain entry into the hydrophobic lipid core unless highly surface active bile salts were present. Bile salts tend to preferentially adsorb at the oil–water interface, displacing the protein or binding to the protein–coated droplets

(previously discussed in Chapter 7), thereby allowing lipase to act on the lipid soluble substrates *(Gargouri et al., 1983; Ivanova et al., 1990; Mun et al., 2007)*.

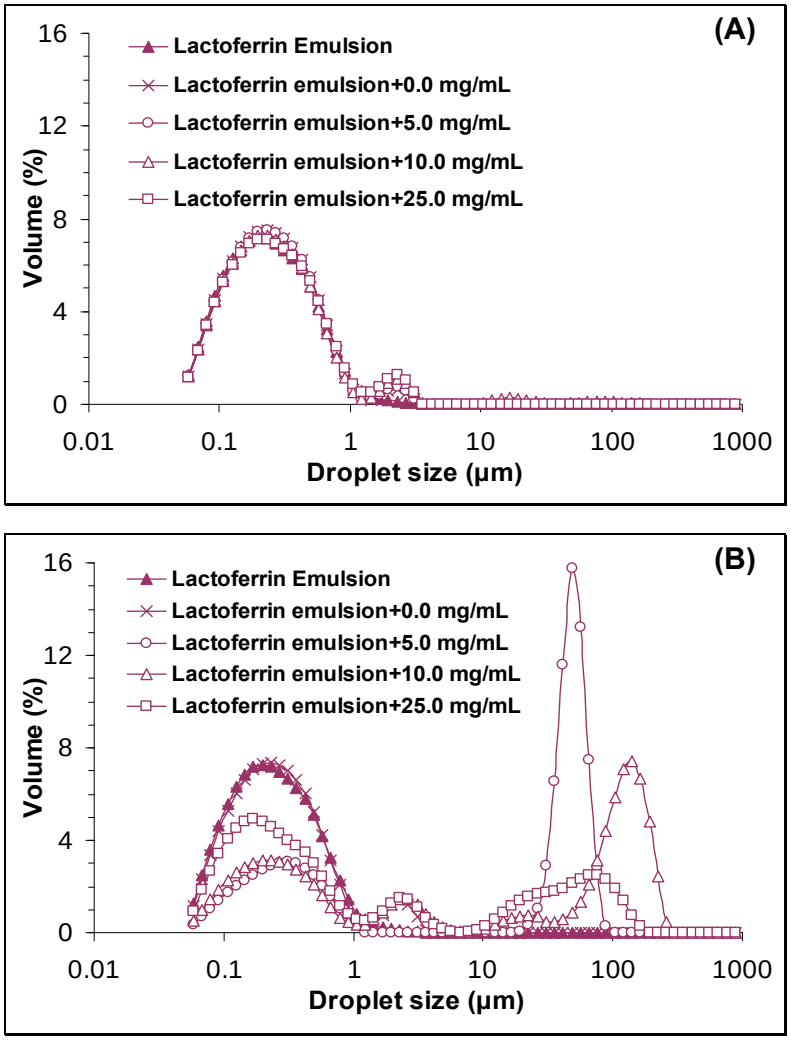

Figure 8.4-3: Droplet size distribution of lactoferrin–stabilized emulsions on the addition of SIF containing various concentrations of bile salts at 0.4 mg/mL (A) and 2.4 mg/mL (B) of added pancreatin, respectively after 2 h of incubation. Each data point is the average of measurements on duplicate samples.

The d_{43} values did not change significantly ($p > 0.05$) for the β-lg–stabilized emulsions with increasing concentration of bile salts at 0.4 mg/mL of pancreatin (Figure 8.4-1 A and Figure 8.4-2 A). Interestingly, at 2.4 mg/mL of pancreatin, the β-lg–stabilized emulsions showed a dramatic increase in d_{43} at above 5.0 mg/mL of added bile salts (d_{43} ~ 10.08 ± 3.5 μm at 25.0 mg/mL of bile salts),

resulting in multimodal distributions containing a considerable proportion of the droplets in the size range of 10–100 μm (Figure 8.4-1 B and Figure 8.4-2 B). When these *β*-lg–stabilized emulsion–bile salts mixture samples were dispersed in 2.0% SDS buffer, the proportions of larger–sized droplets were reduced but the size distribution still remained multimodal, which indicated droplet coalescence.

Further examination of the *β*-lg–stabilized emulsions by confocal laser scanning microscopy (Figure 8.4-4) confirmed that in the presence of 0.0 mg/mL of bile salts (at 2.4 mg/mL of pancreatin), the droplets were rather evenly distributed (Figure 8.4-4 B).

In the presence of bile salts, coalescence between emulsion droplets seemed to occur, resulting in oiling-off and breakdown of the *β*-lg–stabilized emulsion system. This was possibly due to the lipolytic activities of pancreatin, being favoured by the bile salts displacing the interfacial *β*-lg as mentioned in Chapter 7 (Figure 8.4-4 C–E). These results were in agreement with the droplet size distributions (Figure 8.4-2).

In the case of lactoferrin–stabilized emulsions, the d_{43} values changed moderately with increasing concentration of bile salts at 0.4 mg/mL of pancreatin with an exception of a sharp increase to ~ 1.2 ± 0.3 μm at 10 mg/mL of added bile salts (Figure 8.4-1 A and Figure 8.4-3 A). In contrast to the behaviour of the *β*-lg–stabilized emulsions, the lactoferrin–stabilized emulsions showed a slight tendency towards a bimodal distribution even at low concentrations of pancreatin. On the addition of various concentrations of bile salts at 2.4 mg/mL of pancreatin, pronounced increases in d_{43} values were observed, appreciably higher than those seen for the *β*-lg–stabilized emulsions (Figure 8.4-1B and Figure 8.4-3 B).

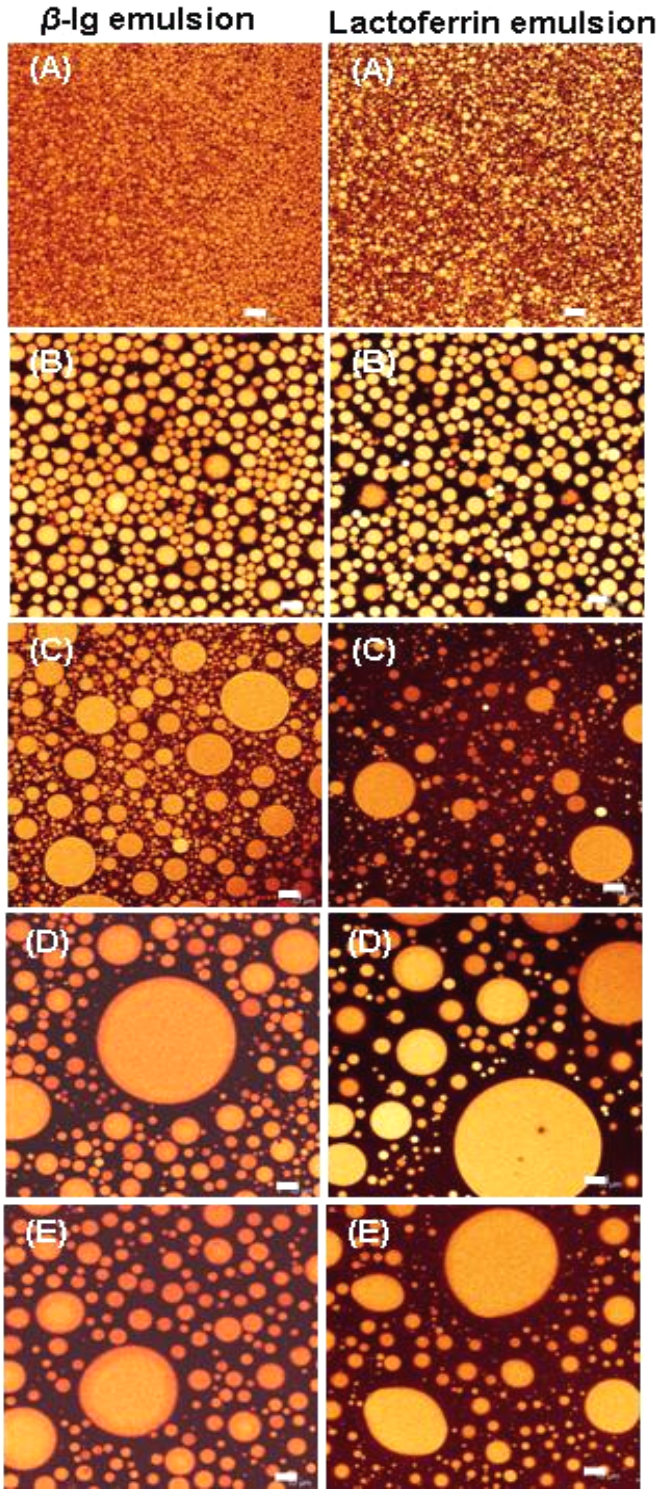

Figure 8.4-4: Confocal micrographs of freshly prepared milk protein–stabilized emulsions (A) on mixing with SIF containing 0.0 (B), 5.0 (C), 10.0 (D) and 25.0 (E) mg/mL of bile salts at 2.4 mg/mL of added pancreatin, respectively after 2 h of incubation. Scale bar corresponds to 10 µm.

The size distribution of the lactoferrin–stabilized emulsion–SIF mixture droplets became multimodal, with a third peak appearing in the range 10–500 μm and a corresponding reduction in the area of the first peak; this was also observed in the confocal micrographs (Figure 8.4-4). The comparatively greater extent of coalescence observed in the lactoferrin–stabilized emulsions compared to *β*-lg–stabilized emulsions may be attributed to the binding of anionic bile salts to mutually oppositely charged (positive) lactoferrin molecules adsorbed at the droplet surface (as previously discussed in Chapter 7). This might have increased the accessibility of pancreatin to the fat substrate, thus accelerating the lipid digestion process.

It is worth noting that, in the absence of bile salts and the presence of pancreatin (both low and high concentrations), although the system was rather monodisperse as described earlier, the droplets observed by confocal microscopy in both emulsions seemed to be more spherical and totally different in appearance from the original emulsion (emulsion without any SIF treatment) (Figure 8.4-4). Moreover, there was also an increased negative *ζ*-potential value [(–18.1 ± 1.1 mV for lactoferrin–stabilized emulsions and –32.3 ± 0.6 mV for *β*-lg–stabilized emulsions) at 0.4 mg/mL of pancreatin (Figure 8.4-5 A) and (–34.5 ± 1.1 mV for lactoferrin–stabilized emulsions and –49.9 ± 4.6 mV for *β*-lg–stabilized emulsions) at 2.4 mg/mL of pancreatin (Figure 8.4-5 B)], indicating interaction of the protein–stabilized interface with pancreatin even in the absence of bile salts. This possibly results in generation of fatty acids as digestion products of the emulsified lipids by pancreatic lipase, which could displace the protein from the interface. The effects of the proteolytic activity of pancreatin on the emulsion droplets are discussed later (Sections 8.4.4 and 8.4.5).

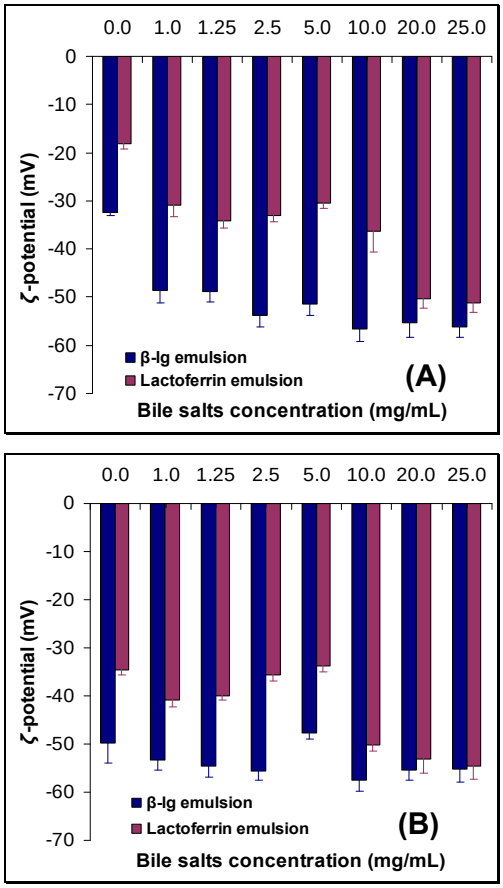

Figure 8.4-5: The change in ζ-potential (mV) of emulsions on the addition of SIF containing various concentrations of bile salts at 0.4 mg/mL (A) and 2.4 mg/mL (B) of added pancreatin, respectively after 2 h of incubation. Error bars represents standard deviations.

8.4.2 Influence of various concentrations of pancreatin (at a fixed concentration of bile salts) on droplet aggregation

As observed in Figure 8.4-1–Figure 8.4-4, the pancreatin concentration had a significant influence on the droplet size distribution and the microstructure of the emulsions. A greater extent of emulsion destabilization was observed at 2.4 mg/mL of pancreatin (Figure 8.4-1 B–3 B) than at 0.4 mg/mL of pancreatin (Figure 8.4-1 A–3 A). The effects of different concentrations of pancreatin on the changes in the d_{43} values, size distribution and confocal micrographs of the emulsion droplets at the lower and higher concentrations of bile salts (5.0 and 20.0 mg/mL, respectively) that are usually available in the upper part of the intestine *(Wright et al., 2008)* are shown in Figure 8.4-6–Figure 8.4-9.

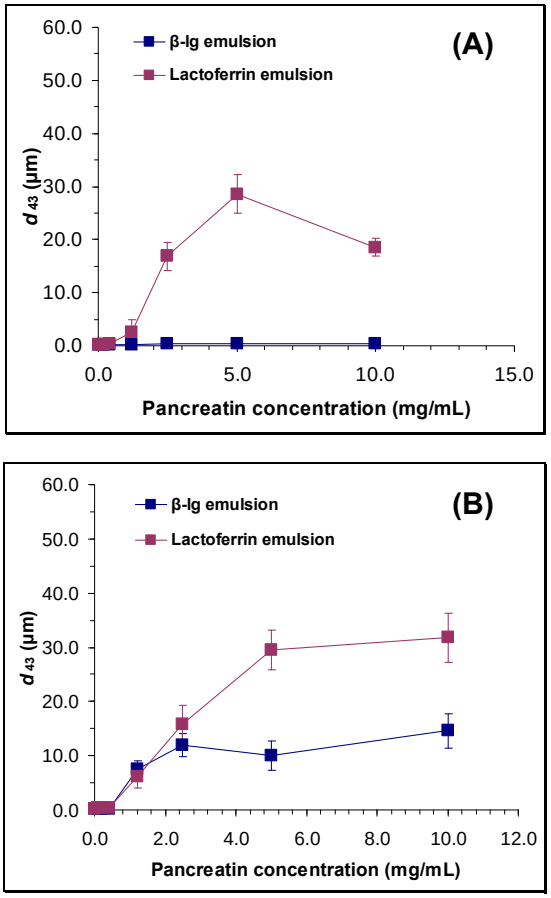

Figure 8.4-6: Changes in d_{43} values (μm) of emulsions on the addition of SIF containing various concentrations of pancreatin at 5.0 mg/mL (A) and 20.0 mg/mL (B) of added bile salts, respectively after 2 h of incubation. Error bars represent standard deviations.

It was interesting to note that in the absence of pancreatin (0 mg/mL), the d_{43} values did not change in the presence of bile salts (both 5.0 and 20.0 mg/mL) and that both emulsions showed nearly monomodal distributions. It appears that binding and/or exchange of the interface by bile salts took place without destabilizing the emulsions (as previously described in Chapter 7). For the *β*-lg–stabilized emulsions, the d_{43} values changed slightly as a function of pancreatin concentration at 5.0 mg/mL of bile salts (Figure 8.4-6 A and Figure 8.4-7 A), with the size distributions showing a small second peak containing particles in the range 1–10 μm. However, when the *β*-lg–stabilized emulsions were treated with pancreatin at 20.0 mg/mL of bile salts, the d_{43} values increased significantly (d_{43} ~ 14.6 ± 3.2 μm at 10.0 mg/mL of pancreatin) and multimodal size distributions were observed (Figure 8.4-6 B and Figure 8.4-7 B).

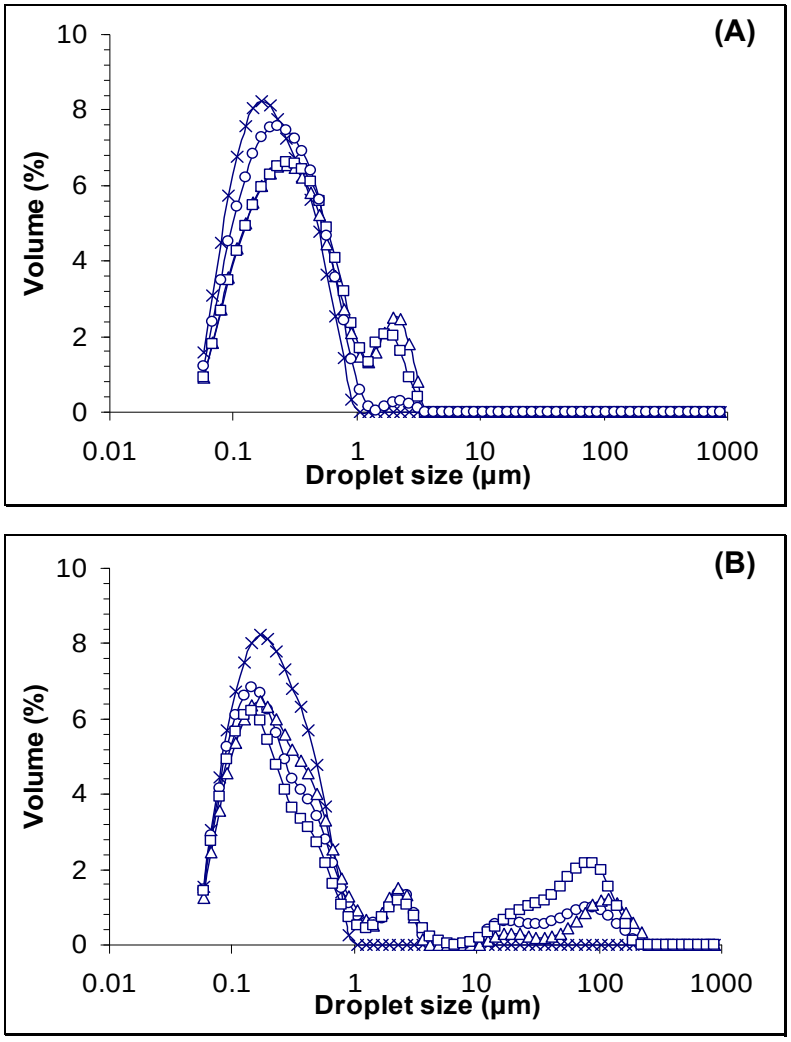

Figure 8.4-7: Droplet size distribution of *β*-lg–stabilized emulsions on the addition of SIF containing 0.0 (×), 1.2 (○), 5.0 (Δ) and 10.0 (□) mg/mL of pancreatin at 5.0 mg/mL (A) and 20.0 mg/mL (B) of added bile salts, respectively after 2 h of incubation. Each data point is the average of measurements on duplicate samples.

The multimodal distributions in the destabilized *β*-lg–stabilized emulsions could also be observed as coalescence of the oil droplets by confocal microscopy (Figure 8.4-9 B–D).

In contrast, the lactoferrin–stabilized emulsions showed a marked increase in d_{43} values and multimodal distributions even in the presence of 5.0 mg/mL of bile salts (Figure 8.4-6 A and Figure 8.4-8 A) over the range of pancreatin concentrations. At 5.0 mg/mL of pancreatin and 5.0 mg/mL of bile salts, the d_{43}

values of the lactoferrin–stabilized emulsions increased dramatically to ~ 28.6 ± 3.6 μm and then gradually declined.

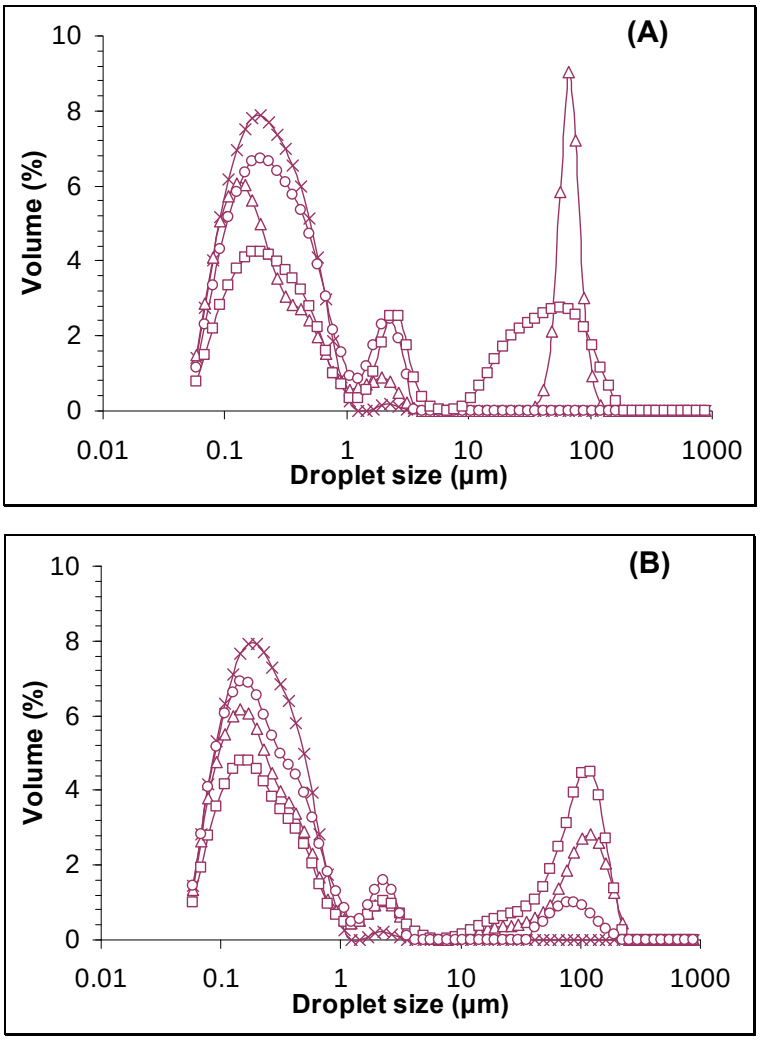

Figure 8.4-8: Droplet size distribution of lactoferrin–stabilized emulsions on the addition of SIF containing 0.0 (×), 1.2 (○), 5.0 (Δ) and 10.0 (□) mg/mL of pancreatin at 5.0 mg/mL (A) and 20.0 mg/mL (B) of added bile salts, respectively, after 2 h of incubation. Each data point is the average of measurements on duplicate samples.

The incidence of multimodality became more severe when the bile salts concentration was increased to 20.0 mg/mL (Figure 8.4-6 B and Figure 8.4-8 B) and large coalesced droplets were observed (Figure 8.4-9 B–D).

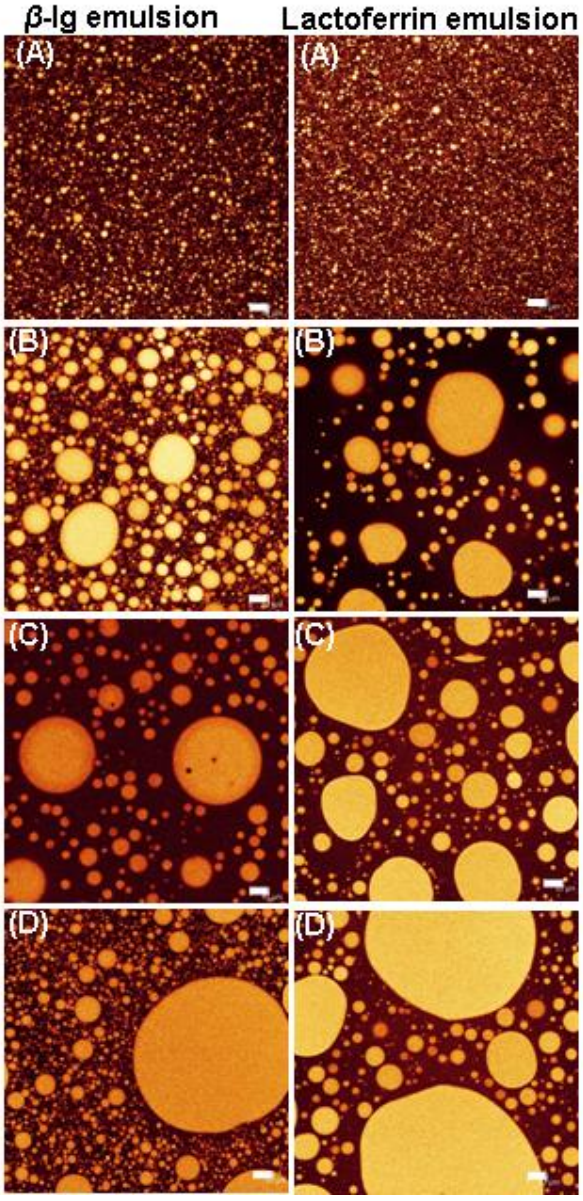

Figure 8.4-9: Confocal micrographs of freshly prepared lactoferrin– and *β*-lg–stabilized emulsions on mixing with SIF containing 0.0 (A), 1.2 (B), 5.0 (C) and 10.0 (D) mg/mL of pancreatin at 20.0 mg/mL of added bile salts, respectively after 2 h of incubation. Scale bar corresponds to 10 µm.

8.4.3 Rate of coalescence and fatty acid release

Generally, protein–stabilized emulsions are stable to coalescence as the protein molecules adsorb at the droplet surfaces forming a dense viscoelastic interfacial layer *(Dickinson & Stainsby, 1988)*. The addition of SIF containing comparatively more surface active bile salts possibly resulted in gradual

displacement of interfacial *β*-lg *(Maldonado-Valderrama et al., 2008)*. In case of the cationic lactoferrin layer, binding of anionic bile salts occurred as described previously in Chapter 7. Both situations allowed the lipase fractions of the pancreatin to hydrolyse the lipid core, causing coalescence as seen in the confocal micrographs (Figure 8.4-4 B–D and Figure 8.4-9 B–D).

Generally, coalescence of emulsion droplets can be mathematically expressed by the following equation as previously described in Chapter 2 *(Walstra, 1987)*:

$$\frac{N_t}{N_0} = e^{-K_c t} \qquad \textbf{(8.4-1)}$$

where, N_t is the number concentration of emulsion droplets after mixing with SIF at incubation time t, N_0 is the initial number concentration of freshly homogenized emulsion droplets (time zero) and K_c is the coalescence rate constant in the digestion time t *(Darling, 1987)*. This apparent rate of coalescence (K_c) was estimated by plotting ln (N_t/N_0) *versus* time t. When the volume of the emulsion droplets remains constant with no oiling-off or phase separation, the relative number proportion (N_t/N_0) of the emulsion droplets can be correlated to the number-volume mean diameter (d_{30}) *(Das & Chattoraj, 1982)* by the following expression:

$$\frac{4}{3}\pi\left(\frac{d_{30}}{2}\right)^3 N = \text{constant} \qquad \textbf{(8.4-2)}$$

The number-volume mean droplet diameter, d_{30} ($=[\sum n_i d_i^3/\sum n_i]^{1/3}$), was calculated from the Mastersizer volume distribution data. To obtain the n_i values in the d_{30} calculation, transformation of the Mastersizer volume distribution V_i to the number distribution N_i was mathematically accomplished using the following expression derived from mineral processing theories *(Hogg, 2003)*:

$$N_i = \frac{100V_i / d_i^3}{\sum V_i / d_i^3} \qquad \textbf{(8.4-3)}$$

The number proportion of droplets was then obtained from the following derived equation:

$$\frac{N_t}{N_0} = \left[\frac{(d_{30})_{t=0}}{(d_{30})_{t=t}} \right]^3 \qquad \textbf{(8.4-4)}$$

Kinetic plots of ln (N_t/N_0) versus incubation time t (for an intestinal digestion duration of 2 h) of emulsion–SIF mixtures containing different concentrations of pancreatin at the highest concentration of bile salts (20.0 mg mL^{-1}) or different concentrations of bile salts at the highest concentration of pancreatin (2.4 mg mL^{-1}) gave linear trend lines ($R^2 > 0.95$), with the slope being the apparent rate of coalescence (K_c).

As shown in Figure 8.4-10 A, the apparent rate of coalescence (K_c) was plotted as a function of the added bile salts concentration in the emulsions. For both emulsions, the magnitude of K_c increased with increasing concentration of added bile salts up to 10 mg/mL and then decreased. This increase in the rate of coalescence indicated that the role of the bile salts was to provide access to the possible point of contact between the pancreatin and the emulsified lipid core, in agreement with previous studies *(Gargouri et al., 1983; Mun et al., 2007)*. However, the addition of bile salts at above 10 mg/mL displaced the *β*-lg almost completely and saturated the lactoferrin interfacial layer by electrostatic binding (as shown in Chapter 7), and thereby possibly inhibited further lipase action as there was no co-lipase in the system *(Gargouri et al., 1983)*. In the case of an increasing concentration of pancreatin at a fixed concentration of bile salts (20 mg/mL), the magnitude of K_c increased with increasing concentration of added pancreatin and then became fairly constant, with minimal increase for both emulsions (Figure 8.4-10 B). This may have been because the rate of release of free fatty acids with the addition of higher concentrations of pancreatin was fast

enough to hinder further lipolysis and thus reduce the K_c value. It is worth mentioning here that, apart from the possible lipolytic action of the pancreatin causing coalescence, the proteolysis of the adsorbed protein layer (due to the trypsin–chymotrypsin fractions present in pancreatin) at the droplet surface in both emulsions would possibly have resulted in reduced surface viscosity compared with intact protein interfaces. This could have led to reduced stability to film rupture and coalescence, as seen in earlier hydrolysed whey-protein–stabilized emulsion studies *(Ye et al., 2004)*.

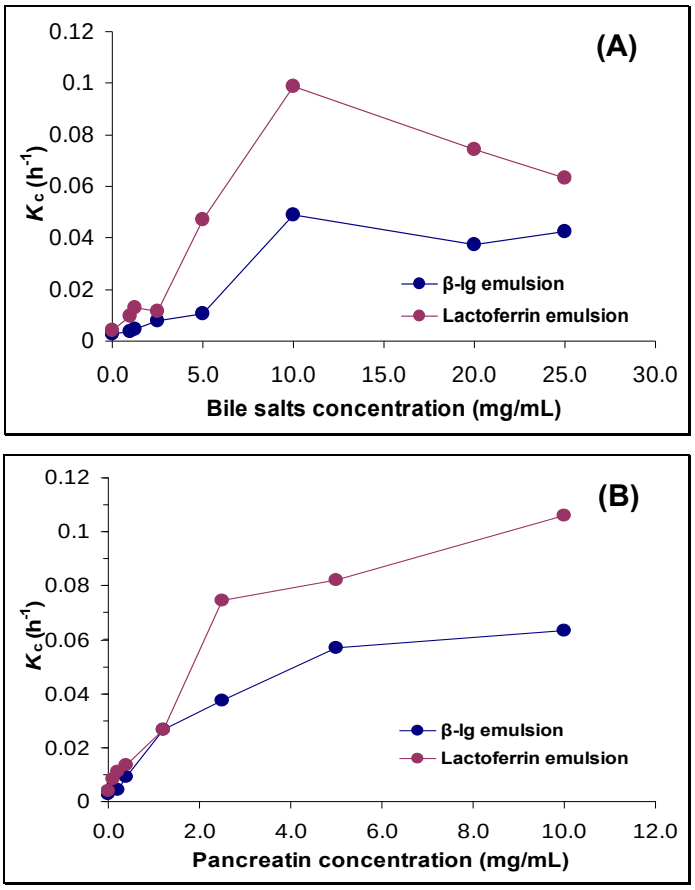

Figure 8.4-10: Apparent coalescence rate constant (K_c) of milk protein–stabilized emulsions on the addition of SIF containing various concentrations of bile salts at a fixed concentration of 2.4 mg/mL of added pancreatin (A) and various concentration of pancreatin at a fixed concentration of 20.0 mg/mL of added bile salts (B).

When the two types of emulsion were compared, the rate constant was greater for the lactoferrin–stabilized emulsion than for the β-lg–stabilized emulsion at the

same concentration of added pancreatin or added bile salts, which clearly showed the greater sensitivity of lactoferrin–stabilized emulsions to coalescence under the simulated duodenal conditions.

To gain further knowledge about the coalescence observed in both the lactoferrin–stabilized emulsions and the *β*-lg–stabilized emulsions as influenced by pancreatin/bile salts mixtures, the release of free fatty acids from the emulsified lipids due to pancreatic lipase activity was monitored (Figure 8.4-11). Clearly, lactoferrin–stabilized emulsion was slightly more susceptible than *β*-lg–stabilized emulsion to pancreatic lipase attack, with the former releasing 291 ± 15 μmol/mL and the latter releasing 203 ± 10 μmol/mL of free fatty acids from the emulsified lipids at 10.0 mg/mL of pancreatin added (bile salts concentration 5.0 mg/mL). The release of free fatty acids for both emulsions was greater in the presence of the higher concentration of bile salts, showing the significance of bile salts in promoting lipid hydrolysis (Figure 8.4-11).

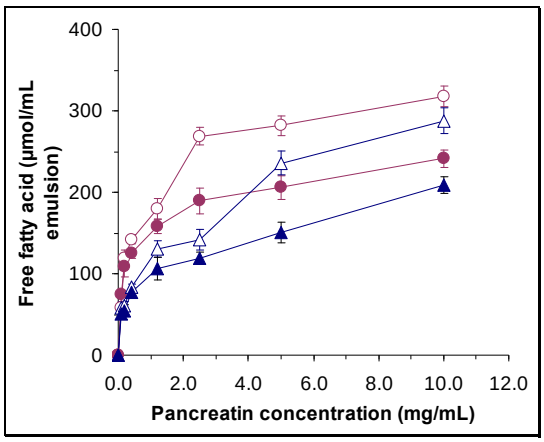

Figure 8.4-11: The amount of free fatty acid (μmol) released from each mL of lactoferrin– (red) and *β*-lg– (blue) stabilized emulsions on the addition of SIF containing various concentrations of pancreatin at 5.0 mg/mL (Δ and ▲) and 20.0 mg/mL (○ and ●) of added bile salts, respectively after 2 h of incubation.

8.4.4 Influence of various concentrations of pancreatin (at a fixed concentration of bile salts) on interfacial composition

ζ-Potential measurements were carried out to investigate the influence of pancreatin addition on the droplet charge of protein–stabilized interfaces. When different concentrations of pancreatin were added to the emulsions at the lower concentration (Figure 8.4-12 A, 5.0 mg /mL) and the higher concentration (Figure 8.4-12 B, 20.0 mg /mL) of bile salts, respectively, there was a substantial increase in the negative ζ-potential on both emulsion droplets. At 5.0 mg/mL of bile salts, the negative ζ-potential of both the lactoferrin–stabilized emulsion and the *β*-lg–stabilized emulsion gradually increased as a function of the pancreatin concentration.

In the presence of 20.0 mg/mL of bile salts, there was a further increase in negative surface charge for the lactoferrin–stabilized emulsion and the *β*-lg–stabilized emulsion as a function of the pancreatin concentration. This suggests that pancreatin was adsorbed to the protein–stabilized interface, generating fatty acids, which imparted a net negative charge at the droplet surface, in agreement with previous assumptions of lipase–catalysed reactions *(Mun et al., 2007)*. Moreover, in the presence 20.0 mg/mL of bile salts (Figure 8.4-12 B), the change in ζ-potential values was even greater, which may have been due to the binding of the bile salts, thus enhancing the accessibility of pancreatin to the lipid core, resulting in generation of increased quantities of surface active lipolytic products.

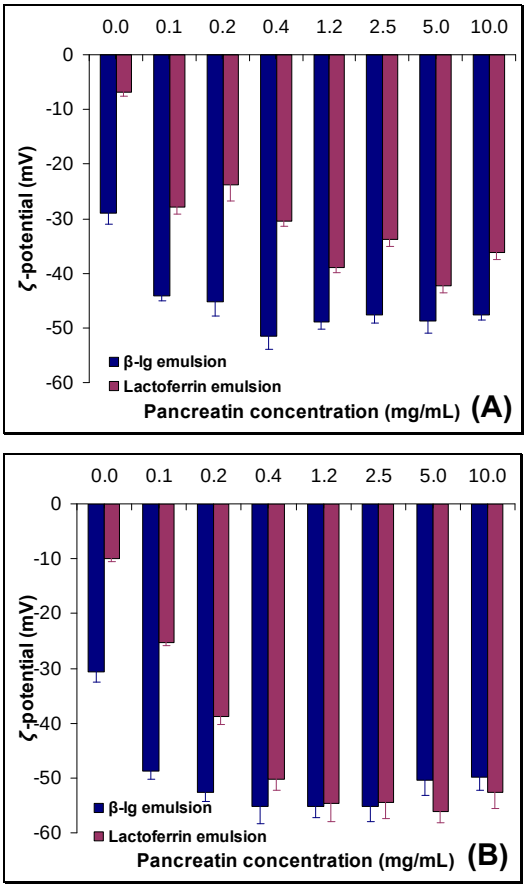

Figure 8.4-12: The change in ζ-potential (mV) of emulsions on the addition of SIF containing various concentrations of pancreatin at 5.0 mg/mL (A) and 20.0 mg/mL (B) of added bile salts, respectively after 2 h of incubation.

To further investigate the interfacial interactions between the emulsion droplets and SIF, SDS-PAGE of the continuous phase was carried out after mixing the emulsions with different concentrations of pancreatin at the higher concentration of bile salts (20.0 mg/mL) assuming optimum bile salts/pancreatin action. Figure 8.4-13 A and Figure 8.4-13 B, respectively show the hydrolysis patterns of the *β*-lg–stabilized emulsion and the lactoferrin–stabilized emulsion mixed with SIF and Figure 8.4-13 C shows the control pancreatin bands. No band of *β*-lg protein was visible even at the lowest concentration of pancreatin (0.1 mg/mL) added, which clearly indicates that *β*-lg was digested by the proteolytic fraction of the pancreatin.

In the case of both non–adsorbed *β*-lg and lactoferrin, obtained by centrifuging emulsion–SIF mixtures, the intact parent proteins bands were not detected and

were assumed to be digested by the pancreatic trypsin, respectively (Figure 8.4-13 A and B). The bile salts also showed some residual proteolytic activity and thus, even in the absence of pancreatin and the presence of 20.0 mg/mL of bile salts, the lactoferrin bands were digested (as described previously in Chapter 7).

The SDS-PAGE gel of the lactoferrin emulsion subnatant (Figure 8.4-13 B) interestingly showed the generation of a potential high molecular weight lactoferrin peptide band (~ 50 kDa), which gradually underwent an increase in intensity at up to 1.2 mg/mL of added pancreatin followed by a decrease in intensity thereafter.

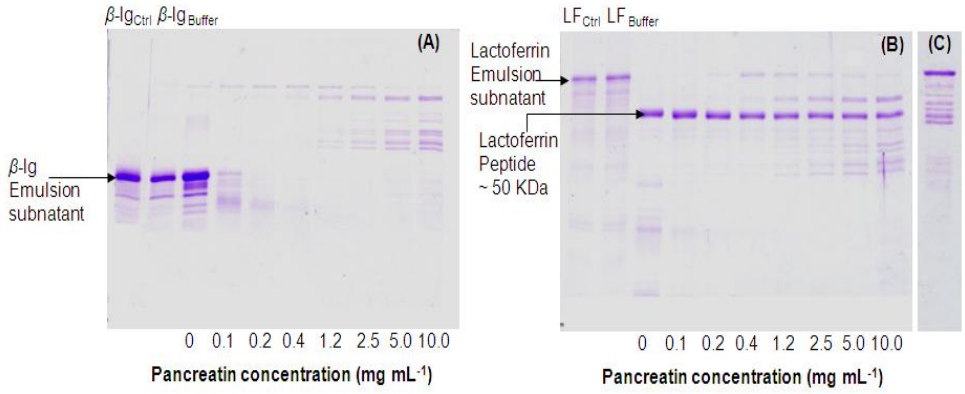

Figure 8.4-13: SDS-PAGE patterns of the continuous phase of *β*-lg– (A) and lactoferrin–stabilized emulsions (B) after mixing with SIF containing different concentrations of pancreatin at 20 mg/mL of added bile salts, respectively after 2 h of incubation. Pancreatin enzyme fractions (1.0 wt%) (C). In figures A and B: β-lg$_{Ctrl}$ or LF$_{Ctrl}$ indicates control samples (subnatants of *β*-lg– or lactoferrin–stabilized emulsions without any treatments respectively) and β-lg$_{Buffer}$ or LF$_{Buffer}$ indicates subnatants of *β*-lg– or lactoferrin–stabilized emulsions after treatment with the SIF buffer (without any bile salts or pancreatin respectively). 0 mg/ml pancreatin indicates the subnatants of emulsions treated with 20.0 mg/ml of bile salts, respectively (no pancreatin added).

This increase in intensity of the lactoferrin peptide band in the non–adsorbed phase may have been due to the generation of diglycerides and/or monoglycerides at the interface, thus pushing the interfacial lactoferrin into the continuous phase, where it subsequently underwent digestion by the proteolytic

fraction of pancreatin. However, at higher concentrations of pancreatin, the lactoferrin peptide band (~ 50 kDa) gradually became fainter, possibly because of further digestion of this high molecular weight fraction to smaller lactoferrin peptide fragments, which probably diffused out of the 16.0% resolving gel.

8.4.5 Interfacial displacement in presence of pure lipase

To understand more precisely, whether or not the lipid digestion products *i.e.* fatty acids, monoglycerides have any influence on displacing the adsorbed protein layers, a study with pure lipase (without any confounding proteolytic activity) was highly recommended. Hence, digestion experiments were carried out by adding SIF containing only 1.6 mg/mL of commercially available lipase (L3126) (with no added bile salts) to the emulsions. This porcine lipase has been previously used in the *in vitro* systems to simulate lipid digestion *(Mun et al., 2007)*. However, it was observed that this commercial pancreatic lipase L3126 (as supplied by Sigma–Aldrich) did contain significant proteolytic activity and that even its addition to *β*-lg solution caused breakdown of native protein as shown in Figure 8.4-14. Thus, using this commercial lipase (L3126), the results of *Mun et al (2007)* might have been influenced by the possible presence of contaminating trypsin and other proteolytic residues in the enzyme preparation.

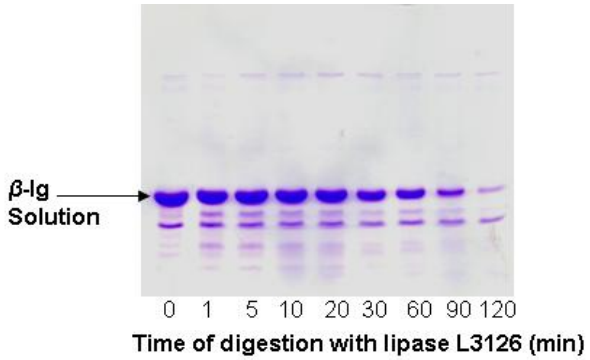

Figure 8.4-14: SDS–PAGE patterns obtained from 1.0% *β*-lg solution mixed with commercial lipase (L3126, obtained from Sigma-Aldrich Company) (1.6 mg/mL) at pH 7.0 as a function of incubation time.

Hence, the purest form of lipase (PCL), available from Sigma (L0382), was used. Figure 8.4-15 A and Figure 8.4-15 B shows the SDS-PAGE patterns of lipid

digestion of *β*-lg– and lactoferrin–stabilized emulsions, respectively on addition of SIF containing only 0–1.0 mg/mL of PCL (with no added bile salts). Interestingly, even this most purified form of commercial lipase PCL contained residual proteolytic activities that can be clearly evidenced from the fainter peptide fractions shown in the gel in case of the continuous phases of both *β*-lg– and lactoferrin–stabilized emulsions. The presence of contaminating proteolytic fractions even in purest form of commercial lipases has also been reported previously *(Birner-Grünberger et al., 2004)*.

However, quantification of SDS-PAGE gels in Figure 8.4-15 and scanning of individual protein as well as all bands (protein and peptides taken together) in case of both the emulsions (Figure 8.4-16 A and Figure 8.4-16 B) provided some important insights.

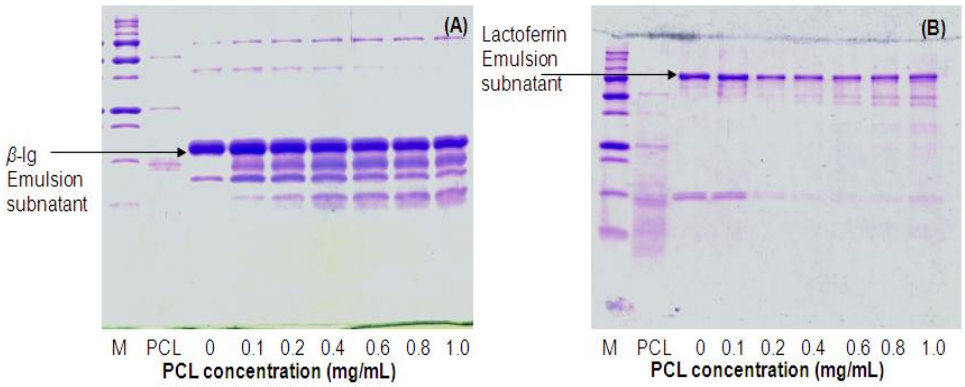

Figure 8.4-15: SDS-PAGE patterns of the subnatants of *β*-lg– (A) and lactoferrin–stabilized emulsions (B) after mixing with different concentrations of purest commercial lipase L0382 (PCL) in presence of SIF buffer for 2 h. M: Molecular weight standard, PCL: Purest commercial lipase of concentration 1 mg/ml. 0 mg/ml PCL indicates subnatants of emulsions treated with SIF buffer (no bile salts added).

In case of *β*-lg–stabilized emulsions (Figure 8.4-16 A), scanning all the bands together (intact *β*-lg and peptides) showed that the intensity of total protein in the subnatant increased with increasing concentration of lipase, which indicates interfacial displacement by the lipid digestion products. Band intensity appeared to increase upto 0.4 mg/mL of lipase, and then decreased. It is possible that the displacement still continued with increased levels of added lipase. However,

further proteolysis (due to more concentration of trypsin or other proteolytic fractions at higher concentration of lipase) might have resulted in generation of smaller peptides, which escaped the 16% resolving gel. The intensity of intact *β*-lg band increased first and then started decreasing, possibly due to considerable proteolysis. Thus, there definitely seemed to be displacement of the intact proteins by lipid digestion products in case of *β*-lg–stabilized emulsions even at the lowest lipase level, though there were also peptides present in significant amounts.

The quantification of the intact lactoferrin and peptides in the gel (Figure 8.4-16 B) showed that the band intensity increased slightly, and then decreased followed by a further increase.

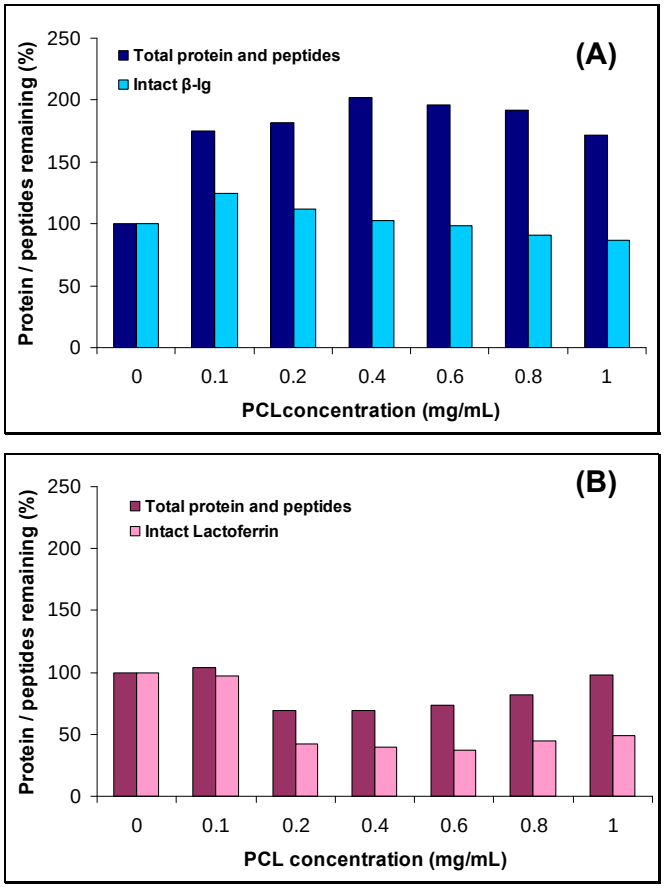

Figure 8.4-16: Intact proteins or peptides remaining in the continuous phase *β*-lg– (A) and lactoferrin–stabilized emulsions (B) on addition of SIF containing PCL), quantified by scanning of gels shown in Figure 8.4-15.

It is possible that the displacement of lactoferrin from the interface had started on addition of 0.4 mg/mL of purest lipase, but not captured by gel quantification due to proteolysis resulting in smaller peptides. Even in case of intact lactoferrin band, the intensity decreased possibly due to hydrolysis by the proteolytic residues in the PCL. Moreover, it might be possible that the lactoferrin–stabilized emulsion system was highly unstable in SIF containing PCL (generating fatty acids due to lipolysis), allowing more lactoferrin to move from the continuous phase to the interface to provide some re-stabilization. Overall, the rate and extent of displacement of protein from the interface by lipase digestion products was clearly higher in β-lg–stabilized emulsion than in lactoferrin–stabilized emulsion.

8.5 Conclusions

This simulated duodenal model study provided valuable insights into the mechanism of interactions of food emulsions with complex pancreatic secretions. Lactoferrin– and β-lg–stabilized emulsions underwent significant degree of coalescence on addition of physiological concentrations of pancreatin and bile salts. This emulsion destabilization in SIF was largely attributed to the lipolysis of the lipid hydrophobic core by the lipase fractions of the pancreatin as well as the proteolysis of the adsorbed protein layer by the trypsin or other proteolytic fractions present in pancreatin.

The rate of coalescence (K_c) was higher in case of lactoferrin–stabilized emulsions as compared to β-lg–stabilized justified in terms of higher levels of fatty acids released during digestion in case of the former. However, regardless of the initial charge of emulsifier present at the oil–water interface, both the emulsions acquired significant negative charge presumably because of the ability of the original emulsifiers to be partially or fully digested by enzymes and/or displaced by bile salts and lipid digestion products *i.e.* fatty acids and monoglycerides, as confirmed by ζ-potential values of the emulsion droplets and SDS-PAGE analysis of the non–adsorbed phases.

In order to unravel the overall mechanism of physicochemical and structural changes that may occur to emulsified lipids during digestion (in entire gastrointestinal tract taking into account the pre-processing in the mouth), the droplet behaviour of *β*-lg– and lactoferrin–stabilized emulsions on sequential addition of simulated oral, gastric and intestinal fluids have been studied in the next chapter.

Chapter Nine: Interactions of Milk Protein–Stabilized Oil-in-Water Emulsions in an Entire Simulated Oral–to–Gastrointestinal Model

9.1 Abstract

The aim of this study was to understand the influence of initial charge of the milk protein–stabilized oil-in-water emulsions on the physicochemical and microstructural modifications that they undergo, as they pass through a model physiological system. Oil-in-water type emulsions (20.0 wt% soy oil) stabilized by 1.0 wt% lactoferrin or *β*-lactoglobulin (*β*-lg) were prepared using a two–stage valve homogenizer at pH 6.8 to produce cationic or anionic interfaces respectively. The behaviour of the emulsions as influenced by sequential treatment with artificial saliva (AS), simulated gastric fluid (SGF) and simulated intestinal fluid (SIF) (modelling in terms of pH, electrolytes, surfactants and enzymes) was investigated using light scattering, confocal laser scanning microscopy, free fatty acid release and electrophoretic mobility measurements. Broadly, both the protein–stabilized emulsions underwent charge reversals, extensive droplet flocculation and some degree of coalescence followed by disruption of droplets as they passed through the *in vitro* digestion model. Except in the simulated oral environment, the initial charge of the interface had relatively insignificant influence on droplet behaviour during the simulated digestion.

9.2 Introduction

Emulsified lipids undergo significant changes in their physicochemical and microstructural organisation on ingestion *(McClements et al., 2008; Singh et al., 2009)*. In the mouth, emulsions interact differently with saliva depending upon their initial electrostatic charge. Positively charged emulsions (lactoferrin–stabilized emulsions) generally undergo bridging flocculation (due to interactions with the negatively charged mucin) and salt–induced aggregation due to the presence of electrolytes in the saliva. By contrast, anionic emulsions (*β*-lg–stabilized emulsions) show depletion interactions due to unadsorbed

mucins as described in Chapter 4. However, when the emulsions reach the stomach, the initial droplet charge of the emulsions appears to play little role in the gastric digestion as most of the protein–stabilized emulsion droplets acquire a net positive charge as indicated in Chapters 5 and 6. This is because the isoelectric point of majority of food proteins are well above the acidic pH of the gastric juice (~ pH 1.2). Hence, irrespective of their initial charges, they are hydrolysed by pepsin based on their conformation and accessibility to enzyme. On reaching the upper part of the intestine, not only the initial charge, but also the surface activities of the protein stabilizing the emulsion droplets might influence the interactions with bile salts, lipases and proteases together with the alkaline pH and intestinal electrolytes as pointed out in Chapters 7 and 8. Studies described in previous chapters attempted to understand the interaction of protein–stabilized emulsions at a particular site (mouth, stomach or duodenum) to gain fundamental insights about the influence of individual physiological variables. However, significant physicochemical changes that might have occurred during pre-processing in the mouth, followed by sequential gastric digestion have not been explored, when studying the lipid digestion in the intestines.

Recently, *in vitro* studies have been attempted in unravelling the behaviour of food emulsions in simulated mouth–intestinal model systems *(Beysseriat et al., 2006; Hur et al., 2009)* or gastro–duodenal behaviour *(Macierzanka et al., 2009)*. However, the role of initial charge of the emulsions on droplet interactions during the entire physiological regime has received very little attention. In this study, the aim is to build upon the knowledge gained in the previous chapters and further explore the interactions of cationic (lactoferrin) and anionic [*β*-lactoglobulin (*β*-lg)] protein–stabilized oil–water interfaces with simulated oral–to–gastrointestinal fluids added in order of their sequence during real digestion.

9.3 Materials and Methods

9.3.1 Materials

Reagents used in this study (other than mentioned in Chapters 3–8) were of analytical grade obtained from either BDH Chemicals (BDH Ltd, Poole, England) or Sigma-Aldrich Chemical Company (St. Louis, MO, USA) unless otherwise specified. Milli-Q water (water purified by treatment with a Milli-Q apparatus, Millipore Corp., Bedford, MA, USA) was the solvent in all the experiments.

9.3.2 *In vitro* physiological model

The *in vitro* physiological model used in this study was a modified method in terms of composition and constituents of artificial media *(Versantvoort et al., 2005; Hur et al., 2009)*. Basically, it consisted of a conical flask (250 mL) containing the simulated fluids (mimicking conditions in mouth, stomach and small intestine) maintained at 37 °C with continuous shaking at 95 rpm in a temperature-controlled water bath (Lab-Line shaker bath, Model LZ33070, Barnstead International, Dubuque, IA, USA). The artificial saliva, simulated gastric and intestinal fluid were prepared according to the composition shown in Table 9.3-1. The pH and the temperature were continuously monitored. The *in vitro* physiological model is used as described below:

a) *Before ingestion:* Emulsion samples (20 wt% soy oil stabilized by 1 wt% lactoferrin or β-lg) at neutral pH before any treatment.

b) *Artificial oral conditions:* 10 mL of emulsion samples were mixed with 10 mL of artificial saliva (AS) containing 0.02 wt% porcine mucin for 5 min (Chapter 4).

c) *Simulated gastric conditions:* Nearly 20 mL of simulated gastric fluid (SGF) *(Pharmacopeia, 2000)* containing 0.32 wt% pepsin was added (mixture pH ~ 1.5) and the mixture was agitated for 2 h (Chapter 5).

d) *Simulated small intestinal conditions:* About 5 mL of 0.5 M HCO_3^- solution was added to change the pH of the gastric digested emulsion samples to ~ 6.5. Nearly 20 mL of simulated intestinal fluid (SIF) at pH 7.5 *(Pharmacopeia, 1995)* with slight modification (39 mM K_2HPO_4, 150 mM NaCl and 30 mM $CaCl_2$) containing 0.5 wt% bile salts and 1.0 wt% pancreatin was subsequently added (mixture pH ~ 7.2) and the mixture was agitated for 2 h (Chapter 8).

The soy oil concentration was 20 wt% initially, diluted to 10.0 wt% in the oral, to 5.0 wt% in the gastric, to 1.8 wt% in the duodenal step.

Table 9.3-1: Chemical composition of various simulated fluids used in the *in vitro* physiological model.

	Artificial Saliva	**SGF**	**HCO_3^-**	**SIF**
Components	0.1594 wt% NaCl	0.32 wt% Pepsin	0.5 M $NaHCO_3$	0.68 wt% K_2HPO_4
	0.0328 wt% NH_4NO_3	0.7 ml Conc. HCl		150 mM NaCl
	0.0636 wt% KH_2PO_4	0.2 wt% NaCl		30 mM $CaCl_2$
	0.0202 wt% KCl			1.0 wt% Pancreatin
	0.0308 wt% $C_6H_5K_3O_7$			0.5 wt% Bile salts
	0.002 wt% Uric acid-sodium salt			19 ml 0.2 N NaOH
	0.0146 wt% Lactic acid-sodium salt			
Antimicrobial agent	0.02 wt% NaN_3	0.02 wt% NaN_3	0.02 wt% NaN_3	0.02 wt% NaN_3
pH	~ 6.8	~ 1.2	~ 6.5	~ 7.5

9.4 Results and Discussion

9.4.1 Change in pH of emulsion droplets

The pH changes of the emulsion samples as they pass through each step of the *in vitro* physiological model are shown in Figure 9.4-1. Initially both the emulsions had a neutral pH (~ 7.0) simulating the condition before ingestion of food. In the oral environment, pH values largely remained the same. However, when the

emulsions entered the gastric system, the pH significantly declined to ~ 1.5 due to the highly acidic stomach conditions. In the simulated duodenal conditions, the pH again increased to ~ 7.2. No significant differences were found in the pH of two emulsions indicating similar buffering capacities of *β*-lg and lactoferrin, respectively.

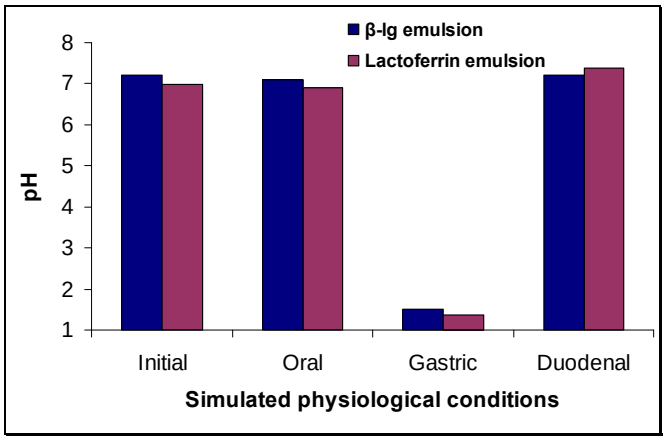

Figure 9.4-1: Change in pH of lactoferrin– and *β*-lg–stabilized emulsions as they pass through the *in vitro* physiological model.

However, in real conditions, the pH of food systems could vary a lot when consumed. The pH is affected by initial acid contents, residence time in the physiological regime, meal quantity and buffering capacities (*e.g.* ~ 1.7 to 6.0 in the stomach conditions) of foods *(Gardner et al., 2002; Kalantzi et al., 2006; Jantratid et al., 2008)*.

9.4.2 Droplet size and microstructure

Figure 9.4-2 illustrates the mean hydrodynamic diameter (μm) of the emulsion–simulated physiological mixtures, determined using dynamic light scattering. Initially, both *β*-lg and lactoferrin formed homogenous emulsions with a *Z*-average diameter of ~ 0.35 μm at pH 7.0. The droplet size distributions of the emulsions studied using static light scattering (MasterSizer 2000 Hydro) showed that both the *β*-lg– and lactoferrin–stabilized emulsions were uniformly dispersed with all the droplets being under 5 μm in size (Figure 9.4-3 A and Figure 9.4-3 B) before passing through the *in vitro* model. Confocal laser scanning

microscopy showed that the fresh emulsions made with *β*-lg or lactoferrin (Figure 9.4-4 A and Figure 9.4-5 A) before any treatment had fine and rather monodisperse droplets confirming light scattering results (Figure 9.4-2 and Figure 9.4-3).

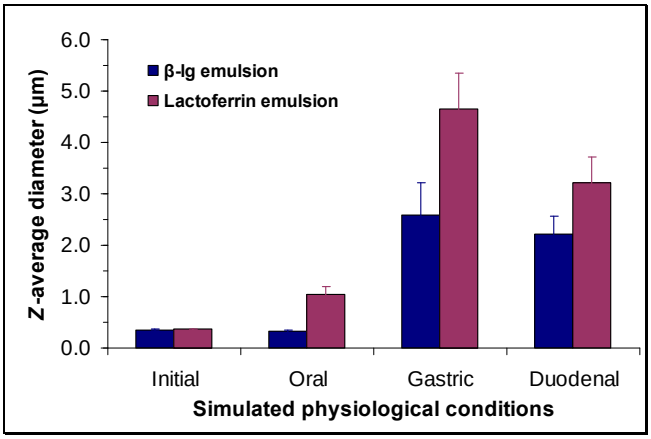

Figure 9.4-2: Change in hydrodynamic diameters of lactoferrin– and *β*-lg–stabilized emulsions as they pass through the *in vitro* physiological model. Error bars represent standard deviations.

On mixing with AS, the *β*-lg emulsion droplets did not change in size ($p > 0.05$) and the size distribution curve almost overlapped with that of the original emulsion (Figure 9.4-2 and Figure 9.4-3A). The *β*-lg–stabilized emulsions showed no droplet aggregation and showed similar microstructures (to that of the initial emulsions) when they were mixed with AS (Figure 9.4-4 B).

In contrast to *β*-lg–stabilized emulsions, lactoferrin emulsions showed an instantaneous increase in hydrodynamic diameter to ~ 1.2 µm (Figure 9.4-2) with a significant population of larger droplets (5-10 µm) and a bimodal size distribution under the same conditions (Figure 9.4-3 B). Pronounced droplet aggregation was observed in the lactoferrin–stabilized emulsions in the presence of AS (Figure 9.4-4 B). When the lactoferrin emulsion–saliva mixtures were mixed gently with 2.0% SDS to break up the aggregates, the bimodal distributions reverted to nearly monomodal, similar to that of the untreated emulsion with *Z*-average diameter of ~ 0.4 µm indicating that the larger size droplets was due to flocculation rather than coalescence.

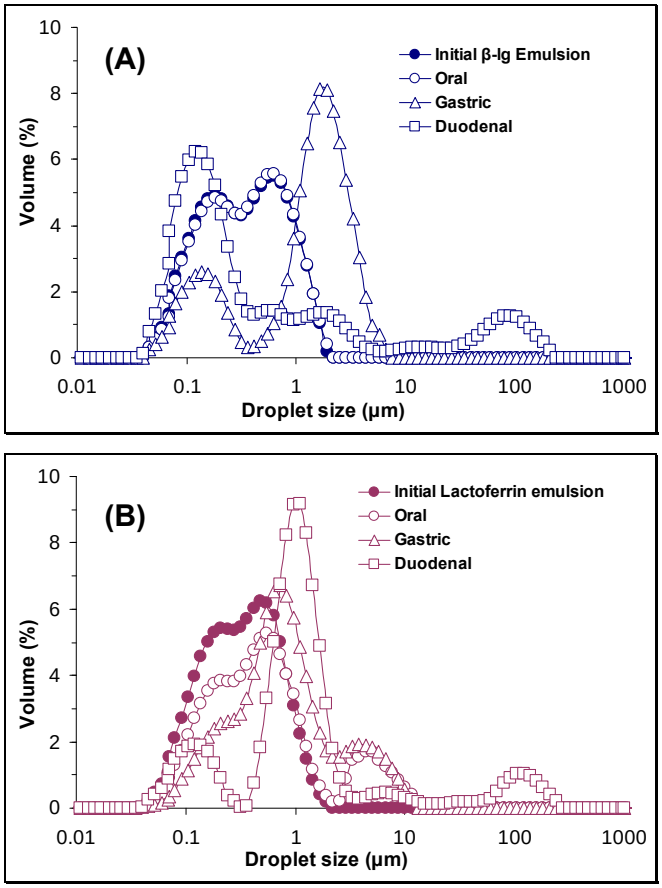

Figure 9.4-3: Droplet size distribution of and *β*-lg– (A) and lactoferrin– (B) stabilized emulsions as they pass through the *in vitro* physiological model. Each data points is the average of measurements on triplicate samples.

This flocculation of lactoferrin emulsion droplets in simulated oral environment can be attributed to the combination of salivary salt–induced aggregation and mucin–mediated bridging of the positively charged emulsion droplets, in agreement with the results discussed in Chapter 4. On mixing the emulsion–saliva mixtures with SGF for 2 h, there was significant increase in droplet diameter for both the emulsions ($p < 0.05$) (Figure 9.4-2). For the *β*-lg–stabilized droplets, the *Z*-average diameter gradually increased from ~ 0.35 μm to ~ 2.5 μm in the *in vitro* mouth–stomach conditions. For the lactoferrin–stabilized droplets, the *Z*-average diameter progressively increased from ~ 1.2 μm to ~ 4.6 μm under the same conditions. Bimodal distributions, with a second peak in the region 5–10 μm and a corresponding decrease in the area of the first peak, were observed (Figure 9.4-3 A and B). When these samples

(showing bimodal peaks) were dispersed in 2.0% SDS buffer, the population of larger droplets was minimized, although the size distribution remained bimodal. This indicated that, in addition to droplet flocculation, some coalescence of the emulsion droplets in these systems had occurred, which was clearly evidenced by the appearance of some distinct large droplets (> 10 μm) in confocal micrographs of both emulsions (Figure 9.4-4 C and Figure 9.4-5 C).

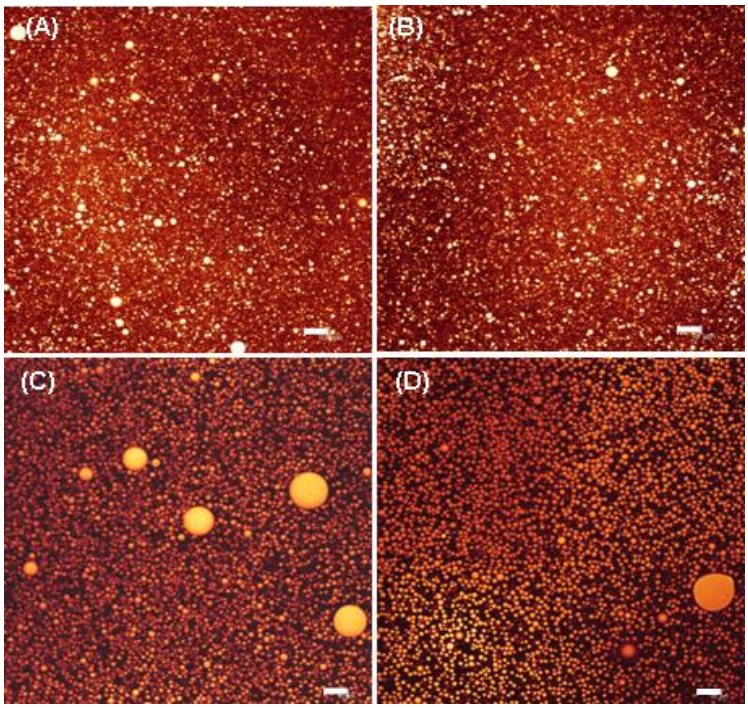

Figure 9.4-4: Confocal micrographs of *β*-lg–stabilized emulsions as they pass though the *in vitro* physiological model: initially before digestion (A), after oral treatment for 5 min (B), after gastric digestion for 2 h (C), and after duodenal digestion for 2 h (D).

This significant change in the droplet characteristics and microstructures of both the protein–stabilized emulsions in the simulated gastric system can be attributed to the pH change and pepsin–induced hydrolysis of the interfacial protein (*β*-lg or lactoferrin) layer as seen in Chapter 5. On passing the emulsion–digested samples through the last step of the *in vitro* model, *i.e.* mixing with the SIF in the artificial duodenal system interestingly decreased the mean droplet diameter (Figure 9.4-2). However, the size distribution data showed a trimodal curve for both the emulsions with a third peak appearing in the range 10–150 μm. When these

samples (showing trimodal peaks) were dispersed in the SDS, size distribution remained multimodal with a slight reduction in population of ~ 10–100 μm sized droplets, which suggested the presence of some coalesced emulsion droplets.

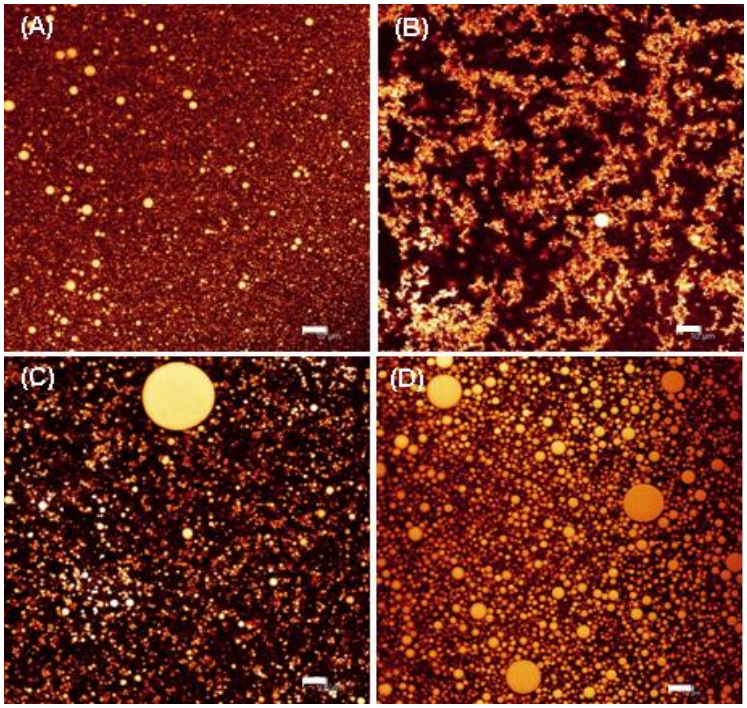

Figure 9.4-5: Confocal micrographs of lactoferrin–stabilized emulsions as they pass though the *in vitro* physiological model: initially before digestion (A), after oral treatment for 5 min (B), after gastric digestion for 2 h (C), and after duodenal digestion for 2 h (D).

The *Z*-average diameter did not correlate to the coalescence or aggregation seen in the Mastersizer volumetric distribution data. In the Zetasizer, the bigger coalesced droplets might have oiled off to the top of the experimental cell and thus escaped detection by the laser resulting in lower calculated hydrodynamic diameter *(Mun et al., 2007)*. The high shear forces applied on the aggregated emulsion during MasterSizer measurements might have increased or decreased the degree of flocculation and coalescence *(Agboola & Dalgleish, 1996; Schokker & Dalgleish, 1998)*. Hence, confocal microscopy images have been studied to gain further insights.

It was worth noting that in presence of SIF, the extent of coalescence appeared to be slightly less as compared to that in the gastric step (Figure 9.4-4 C–D and Figure 9.4-5 C–D). Furthermore, the system also showed some finely dispersed droplets of 0.5–2.0 μm in size in both emulsions after treatment with SIF; these droplets seemed to be more spherical and very different in appearance from those in the initial emulsion (Figure 9.4-4 D and Figure 9.4-5 D). Coalescence for both kinds of emulsion droplets at the duodenal step together with appearance of these smaller droplets (< 5 μm) could be attributed to the displacement of and/ or binding to the interfacial proteins by bile salts together with the interfacial proteolysis by the trypsin fractions of the pancreatin, as previously discussed in Chapter 7 and 8. This displacement might have further promoted the accessibility of lipase to act on the hydrophobic lipid core generating lipid digestion products (mono- and/or diglycerides, fatty acids *etc.*) at the droplet surface, thus showing some spherical droplets largely stabilized by the lipid digestion products.

9.4.3 ζ-Potential

The dependence of ζ-potential of emulsion droplets on the conditions in the *in vitro* physiological model is shown in Figure 9.4-6. Freshly prepared *β*-lg– and lactoferrin–stabilized emulsions at pH 7.0 had a ζ-potential of ~ –55 mV and ~ + 52 mV, respectively. The ζ-potential values showed that the intensity of electrostatic repulsion between the emulsion droplets was significantly influenced by initial emulsifier type in the oral environment. Addition of AS drastically reduced the ζ-potential (~ + 7 mV) in case of lactoferrin–stabilized emulsion in agreement with the pronounced aggregation described in the previous sections. There were no significant changes in the ζ-potential of *β*-lg–stabilized emulsion droplets in the oral environment ($p > 0.05$). This is in agreement with no significant change in observed droplet size and can be attributed to the repulsive forces between anionic *β*-lg–stabilized emulsion droplets and the negatively charged mucin in the saliva (Chapter 4).

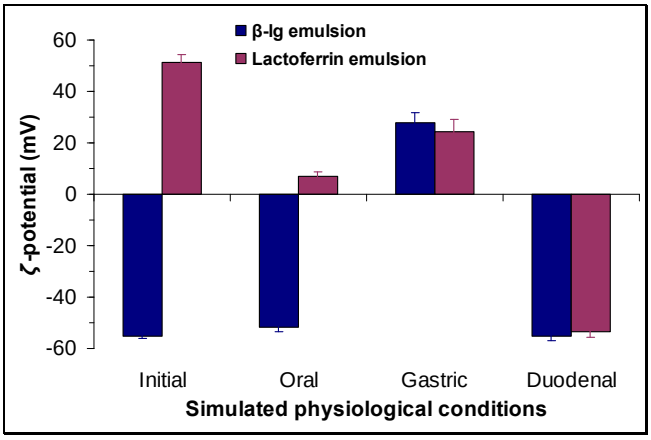

Figure 9.4-6: Changes in hydrodynamic diameters of lactoferrin– and β-lg–stabilized emulsions as they pass through the *in vitro* physiological model. Error bars represent standard deviations.

Addition of SGF to the emulsions resulted in charge reversal for *β*-lg–stabilized emulsion and significantly affected the *ζ*-potential values of both the emulsions from the oral environment. In the gastric system, both the emulsion droplets had significant amount of positive charge after 2 h of incubation in SGF although peptic hydrolysis had taken place. This indicates that the presence of some amphiphilic interfacial peptides provided some protection to the droplets against complete coalescence.

The most prominent change in *ζ*-potential occurred when the emulsion droplets moved to the *in vitro* duodenal model resulting in highly negative droplet charge for both the emulsions. The *ζ*-potential values in the presence of SIF were fairly similar for both types of emulsion droplets ($p > 0.05$), irrespective of the initial droplet charge as the initial interfacial layers were possibly digested by the proteolytic fractions of the pancreatin and displaced by bile salts and/or lipid digestion products.

9.4.4 Free fatty acids

The impact of initial protein type on the extent of lipolysis by measuring the release of free fatty acids was determined as a function of incubation time in the SIF after the gastric digestion step (Figure 9.4-7). The amount of free fatty acids

released per unit volume of emulsion was similar in case of both the emulsions ($p > 0.05$). Interestingly in the previous chapter (Chapter 8), it was found that free fatty acid release as a function of pancreatin concentration was significantly higher in case of lactoferrin emulsion as compared to that in β-lg emulsion in presence of simulated intestinal fluid alone.

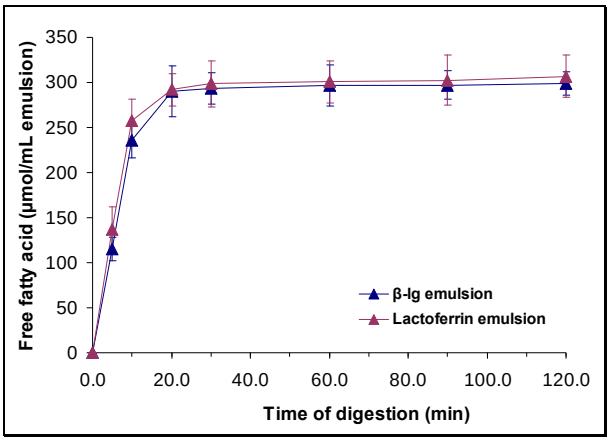

Figure 9.4-7: The amount of free fatty acid (µmol) released from each mL of emulsions on the addition of SIF containing 1.0 wt% of pancreatin at 0.5 wt% of added bile salts as a function of time.

This discrepancy in amount of free fatty acid released between intestinal study (simulating conditions at intestine individually) and sequential digestion study (simulating conditions at mouth, stomach and intestine sequentially) might be attributed to the interference from one or more of the components in the compositionally complex simulated digestion media used in this sequential digestion process.

9.4.5 Overall mechanism

Figure 9.4-8 illustrates the possible changes in protein–stabilized emulsions after they are taken inside the mouth and subsequently as they traverse through the gastrointestinal tract using a simulated physiological model.

Protein–stabilized emulsion on ingestion, is mixed with saliva, undergoes a change in pH, ionic strength, temperature, becomes exposed to enzymes (amylases) and biopolymers (mucin, other proteins), and also experiences a

complex salivary flow and friction with the oral surfaces. The interactions of the emulsions with the saliva largely depend on the initial charge of the emulsions as saliva largely contains negatively charged electrolytes and anionic mucin. Broadly, neutral and negatively charged emulsions undergo reversible depletion flocculation whereas cationic emulsions show irreversible associative electrostatic interactions with mucin and salivary salts when mixed with saliva.

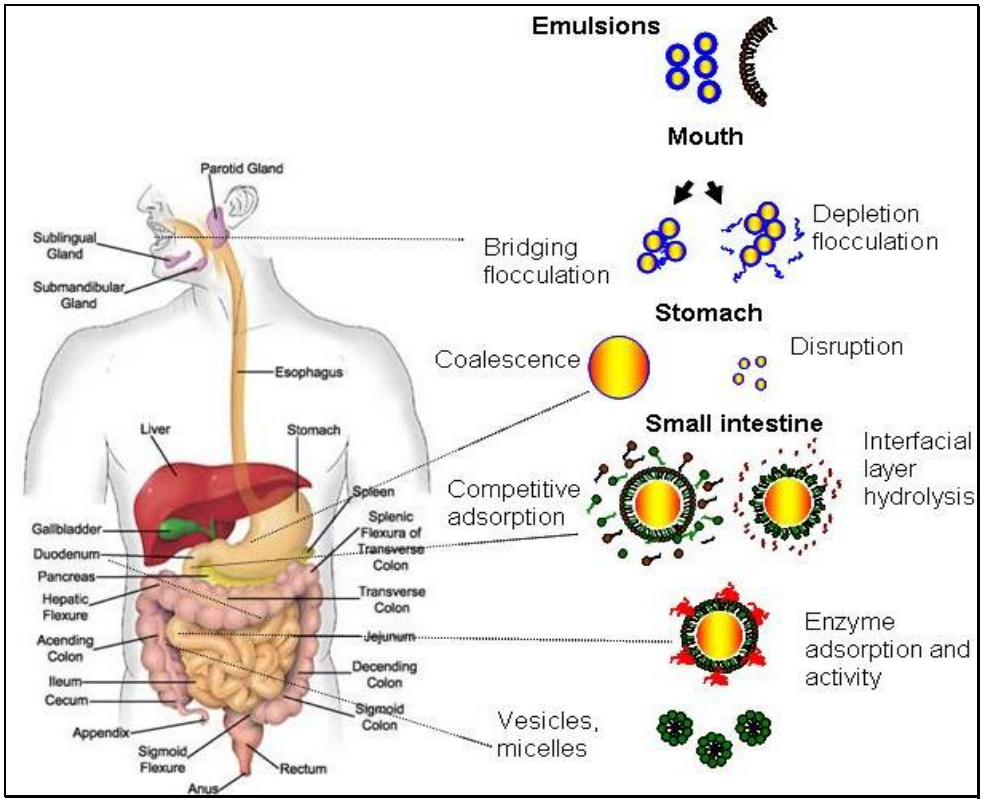

Figure 9.4-8: Schematic illustration of the possible changes in emulsions as they pass through the simulated physiological model [adapted from *(Singh et al., 2009)*].

In the stomach, the emulsion–saliva mixtures undergo a drastic shift in pH due to the highly acidic gastric environment (pH 1–3) and also exposed to proteolytic enzyme (pepsin). Since the pH is well below the isoelectric point of most of the milk proteins, most of the emulsions acquire a net positive charge under gastric conditions. Hence, rather than the initial charge of the emulsifier, it is the nature of the protein coated on the droplet surface and its susceptibility to pepsin that drives the emulsion destabilization process. Although globular proteins, such as

β-lg, are highly resistant to pepsin digestion in its native state, the unfolding of the protein structure during emulsion formation renders the proteolytic sites susceptible to pepsin attack. Due to proteolysis of the interfacial protein layer, the peptides generated are not strong enough to provide emulsion stability, thus resulting in film drainage and coalescence.

On entering the intestine, the gastric digested emulsion droplets are mixed with lipases, proteases, surface active bile salts, and bicarbonates. The pH in the small intestine moves close to neutral due to the mixing of the alkaline intestinal fluid with the gastric digested emulsions. The surfactants already present in the intestinal fluid together with the surface active fatty acids, monoglycerides generated as lipid digestion products of the inner soy oil core by lipase alter the interfacial composition by competitively displacing the proteins from the droplet surface. Due to the presence of trypsin and other proteolytic enzymes in the intestinal fluid, hydrolysis of the protein interfacial layer also occurs. The various lipid digestion products are then incorporated within bile/phospholipids micelles and vesicles that are transported to the enterocyte cells, where they are absorbed.

Hence, the initial charge of the protein layers play an insignificant role, when considering the overall complexities of lipid digestion phenomenon possibly because they are partially or completely displaced by bile salts and lipid digestion products and/or digested by the proteolytic enzymes.

9.5 Conclusions

This study enhanced the understanding of physicochemical and structural changes that may occur to protein–stabilized emulsion droplets on their passage through the oral–gastrointestinal tract. Lipid droplets initially coated by lactoferrin (cationic) and *β*-lg (anionic) were treated sequentially with simulated oral, gastric and intestinal fluids in an *in vitro* physiological model. The *in vitro* physiological model used in this study was fairly complex involving simulation of some important chemical constituents, pH and ionic strengths found in mouth, stomach and small intestine, respectively.

This study identified that milk protein–stabilized interfaces, irrespective of their high initial electrostatic charges, provided little protection to the droplets against pepsin and pancreatin–induced destabilization and thus cannot help individually in controlling the lipid digestion. Nevertheless, anionic or cationic milk proteins interfacial layers might provide different sensorial attributes based on their difference in aggregation effects in the mouth environment.

Interestingly, the mechanism of destabilization and re-stabilization in the intestinal fluid following the pre-processing in the oral and gastric fluid could not be interpreted reliably due to interference from one or more of the metabolites in the chemically complex simulated physiological media used in the present study. This model definitely provides insights about the interfacial behaviour of emulsions in simulated physiological conditions, which will further help to understand the complexities in designing of food matrices for controlled lipid delivery applications.

Chapter Ten: Overall Conclusions and Recommendations for Future Work

The lipids derived from plant and animal sources perform important functions in human diet, providing a concentrated source of energy, essential nutrients (*e.g.* essential fatty acids, carriers of pre-formed fat-soluble vitamins A, D, E and K), bioactive compounds and also influencing the texture, aroma and taste profile of foods. Less beneficial is their role as being carriers of toxic fat components and their contribution to trans fatty acids, saturated fats and/or cholesterol that can have serious negative impact on human health. Lipids are generally incorporated in food matrix in the form of emulsions. The bioavailability of lipid nutrients is dependent on the chemical structure and physicochemical properties of the food emulsions. Moreover the release of nutrients also depends on the way the emulsified lipid behaves and breaks down during different stages of digestion *i.e.* the physical, biochemical, and physiological interactions of the food emulsion with the physiological components post consumption. Due to the appreciable increase in obesity, atherosclerosis and other food–linked diseases, there has been a growing interest to design food microstructures, such as emulsions, that can help to regulate calorie intake, provide increased satiety responses, control lipid digestion and/or deliver bioactive molecules without sacrificing sensory perception. Hence, knowledge concerning the behaviour of food emulsions during gastrointestinal transit is a subject of paramount importance for developing specific strategies to modulate lipid digestion, and thus influence the bioavailability of lipid nutrients. In this dissertation, the physiological behaviour of food structures (using model protein–stabilized oil-in-water emulsions) has been investigated using *in vitro* oral and gastrointestinal conditions (simulating the major biochemical conditions and constituents).

The first objective (Chapter 4) of this thesis was to develop stable food structures *i.e.* milk protein–stabilized soy oil-in-water emulsions using lactoferrin or *β*-lactoglobulin as the interfacial layer to allow the formation of cationic and anionic droplets at neutral pH, respectively, and to investigate their interactions

with high molecular weight mucin and electrolytes present in artificial saliva. Secondly, the aim (Chapter 5) was to determine the microstructural and physicochemical changes in the emulsions in terms of droplet flocculation and/or coalescence in simulated gastric conditions in the presence of pepsin. Questions have been raised about the variations in pH and ionic strengths in stomach, to which the emulsion droplets might be exposed to during their gastric transit. Hence, a study was undertaken to evaluate the effects of different gastric pH, ionic strengths and presence of mucin on the degree of emulsion destabilization in the simulated gastric system (Chapter 6). Thirdly, a set of studies (Chapters 7 and 8) were carried out to understand the mechanism of droplet interactions in simulated upper intestinal system, to unravel the role of bile salts and products of lipid hydrolysis (such as fatty acids, mono-and/or diglycerides) in exchanging or displacing the original protein material from the droplet surface. The final objective (Chapter 9) was to explore the behaviour of the negatively and positively charged emulsions on sequential mixing with simulated oral and gastrointestinal fluids (conditions at which a food matrix is exposed to during its passage through the gastrointestinal tract) using a combination of physicochemical and microstructural characterization techniques.

The first objective of understanding the interactions of protein–stabilized emulsion systems stabilized by positively (lactoferrin) and negatively charged (*β*-lg) milk proteins at pH 6.8 with the artificial saliva containing mucin and salts was achieved. The study described the important roles of both the electrolytes and the highly glycosylated mucins present in saliva in influencing emulsion stability. A range of mucin concentrations was used in the artificial saliva composition to deal with wide variability and rheological implications of human saliva *in vivo*. The interactions of the emulsions upon mixing with saliva were determined by the initial surface charge on the emulsion droplet, interactions of mucins with the droplet surface and the presence of salts using different characterization techniques. Using the size of emulsion droplets, the amount of protein bound and the radius of gyration of the mucin molecule, the main driving force for flocculation was demonstrated. The mechanism of emulsion flocculation in presence of saliva was largely driven by electrostatic interactions in protein–stabilized emulsions.

This study particularly showed that negatively charged protein–stabilized emulsions *i.e.* β-lg emulsions did not interact with saliva due to strong repulsive forces between anionic mucin and anionic β-lg interfacial layer at neutral pH, but underwent depletion flocculation on addition of higher concentrations of mucin (≥ 1.0 wt%). In contrast, positively charged lactoferrin–stabilized emulsions showed salt–induced aggregation on addition of saliva containing only salts (even without the addition of mucin), which was never reported before. Additionally, lactoferrin–stabilized emulsions showed typical biopolymer–biopolymer kind of colloidal interactions *i.e.* bridging–to–stable–to–depletion type of flocculation behaviour on addition of low–to–sufficient–to–high concentrations of negatively charged mucin, respectively. These kinds of emulsion–saliva electrostatic interactions might occur upon consumption of emulsion in real situations and could result in different sensorial and textural perception *in vivo*.

Food emulsions, after residing for a relatively shorter period (few seconds to few minutes) in the mouth, are generally subjected to harsh physical and biochemical processing conditions, broadly acidic pH, ionic strength, proteolytic enzyme (pepsin), biopolymer (mucin), peristaltic shear, *etc.* as they enter the gastric tract. Hence, the physicochemical changes, structure, stability and interfacial characteristics of emulsions during the passage of milk protein–stabilized emulsions through *in vitro* gastric model was unravelled using simulated gastric fluid (SGF) containing pepsin at acidic pH. It was observed that both lactoferrin– and β-lg–stabilized emulsions underwent flocculation followed by some degree of coalescence on exposure to simulated gastric conditions, depending upon protein conformation at the adsorbed layer and incubation time with pepsin.

Another interesting finding of this study was that β-lg, which is usually resistant to pepsin attack in its native state, became susceptible to proteolysis when present as the interfacial layer in emulsions. A change in the conformation of the β-lg molecules upon adsorption at the oil–water interface exposed the peptic cleavage sites for proteolysis, leading to emulsion instability and coalescence.

However, it was recognized that the ionic strength and pH varies significantly in real physiological circumstances. Furthermore, the role of mucin, which forms a gelled structure under gastric conditions (low pH and at high mucin concentrations) was not explored. Hence, the interaction of emulsions in SGF containing pepsin and mucin under different gastric pH and ionic strength conditions was investigated. Since, the initial charges of the emulsions have been shown to play an insignificant role in determining the interactions with SGF (as both the emulsions acquired net positive charge at gastric pH); the behaviour of *β*-lg–stabilized emulsions as affected by variable gastric parameters was investigated. This study indicated that not only pepsin but also the variable pH and ionic strengths prevailing in the gastric tract might potentially result in emulsion destabilization. The presence of mucin also promotes the flocculation of the *β*-lg–stabilized emulsion through bridging mechanism. Hence, the interactions of *β*-lg emulsion droplets in the complicated *in vitro* gastric model clearly identify the physiological variables, which might potentially influence the physicochemical behaviour of a protein–stabilized emulsion droplets during their gastric transit.

After passing through the gastric tract, food emulsions are exposed to alkaline pH, various electrolytes, enzymes (lipases, proteases, amylases) as well as highly surface active bile salts as they enter the intestine. Bile salts are generally known to displace protein–stabilized interfaces by virtue of their higher surface activities. The interfacial composition of emulsion droplets in intestine might be highly complicated due to the surface active and enzymatic pancreatic secretions. Hence, the fourth aim of carrying out a control study involving only the interaction of individual pancreatic variable such as bile salts with protein–stabilized emulsions to understand the fundamental principles underlying the interfacial interactions in the upper intestine was successfully achieved.

Behaviour of two oppositely charged protein–stabilized emulsions (lactoferrin– and *β*-lg–stabilized emulsion) in the presence of simulated intestinal fluid containing intestinal electrolytes and bile salts (without added enzymes) was investigated. This study provided valuable insights into the mechanism of

interactions of protein–stabilized emulsions with pancreatic electrolytes and surface active bile salts (of physiological concentrations) with a focus on the initial charge of the emulsions. It emphasized the importance of investigating the role of each component and if necessary removing the confounding effects of proteolytic enzymes by heat treatment. The interactions of interfacial displacement and/or binding between bile salts and protein–stabilized emulsions were successfully studied using SDS-PAGE analysis of the non–adsorbed phase.

The behaviour of protein–stabilized emulsions in presence of SIF was largely driven by electrostatic interactions. Initially, the role of intestinal pH and electrolytes were explored, which particularly showed that lactoferrin–stabilized emulsions underwent aggregation on addition of SIF containing only salts (no bile salts added). This aggregation of lactoferrin emulsion was attributed to the shift of pH near to p*I* of lactoferrin in presence of SIF as well as charge screening effects by intestinal electrolytes. On addition of bile salts, release of peptides was observed, which could have arisen only as a result of proteolysis due to the presence of contaminating enzymes in the bile salts. Therefore, SIF containing bile salts was heated to eliminate any residual enzymes. On addition of heat–treated bile salts, aggregated lactoferrin emulsions (in presence of SIF without bile salts) showed stabilization due to electrostatic binding by negatively charged bile salts. On increasing bile salt concentration, surface active bile salts appeared to displace lactoferrin molecules from the surface as shown by a gradual increase in subnatant lactoferrin concentration. In case of emulsions stabilized by β-lg, displacement of protein was observed even at the lowest concentration of bile salts. Hence, the surface activities and the initial charge of the protein–water interface largely influence the bile salt displacement reactions.

The complexities of lipolytic and proteolytic enzymes in the real duodenal situation required the inclusion of intestinal enzymes. Hence, the behaviour of protein–stabilized emulsions in a more realistic platform using physiological concentrations of pancreatic enzymes with or without the addition of bile salts was investigated. This simulated duodenal model study provided valuable insights into the mechanism of interactions of food emulsions with complex pancreatic secretions. Lactoferrin– and β-lg–stabilized emulsions underwent

significant degree of coalescence on addition of physiological concentrations of pancreatin and bile salts. This emulsion destabilization in SIF was largely attributed to the lipolysis of the lipid hydrophobic core by the lipase fractions of the pancreatin as well as the proteolysis of the adsorbed protein layer by the trypsin or other proteolytic fractions present in pancreatin in case of both of the emulsions.

The rate of coalescence (K_c) was higher in case of lactoferrin–stabilized emulsions as compared to β-lg–stabilized, which was justified in terms of higher levels of fatty acids released during digestion in case of the former as compared to the latter, respectively. However, regardless of the initial charge of emulsifier present at the oil–water interface, both the emulsions acquired significant negative charge presumably because of the ability of the original emulsifiers to be partially or fully digested by enzymes and/or displaced by bile salts and lipid digestion products *i.e.* fatty acids and monoglycerides, as confirmed by ζ-potential values of the emulsion droplets and SDS-PAGE analysis of the non–adsorbed phases.

In order to unravel the overall mechanism of physicochemical and structural changes that may occur to emulsified lipids during digestion (in entire gastrointestinal tract taking into account the pre-processing in the mouth), the final objective of understanding the droplet behaviour of β-lg– and lactoferrin–stabilized emulsions on sequential addition of simulated oral, gastric and intestinal fluids has been successfully achieved. Lipid droplets initially coated by lactoferrin (cationic) and β-lg (anionic) were treated sequentially with simulated oral, gastric and intestinal fluids in an *in vitro* physiological model. The *in vitro* physiological model used in this study was fairly complex involving simulation of some important chemical constituents, pH, and ionic strengths found in mouth, stomach, and small intestine, respectively. This study identified that milk protein–stabilized interfaces irrespective of their high initial electrostatic charges, provided little protection to the droplets against pepsin and pancreatin–induced destabilization and thus cannot help individually in controlling the lipid digestion. Nevertheless, anionic or cationic milk proteins

interfacial layers might provide different sensorial attributes based on their difference in aggregation effects in the mouth environment.

The mechanisms of destabilization and re-stabilization in the intestinal fluid following the pre-processing in the oral and gastric fluid could not be interpreted reliably due to interference from one or more of the metabolites in the chemically complex simulated physiological media used in the present study. However, the *in vitro* model definitely provided unique insights about the destabilization behaviour of milk protein–stabilized emulsion droplets in simulated physiological conditions, which will help to understand the complexities of physiological factors influencing the designing of food matrices for controlled delivery applications.

In conclusion, the findings presented in this thesis provided novel insights about the physicochemical and structural changes that may occur to positively and negatively charged protein–stabilized oil-in-water emulsions within the physiological regime using *in vitro* digestion model, which might have important consequences when designing functional foods with improved health and wellness attributes.

Future Directions

To bridge the important gaps that arose during this PhD research, future investigations have been recommended as follows:

- The artificial saliva composition used was a good representative model for human saliva (widely used in pharmacological studies) and the electrostatic interactions of emulsions in the saliva were successfully demonstrated. The investigation of oral interactions in presence of other salivary peptides, enzymes (amylases) and proteins would provide valuable information. For example, use of proline–rich proteins, lysozyme and other positive charged fractions present in saliva may result in bridging flocculation of even negatively charged emulsion droplets at the neutral pH of the mouth environment.

- The impact of physicochemical interactions between the protein–stabilized emulsions and artificial saliva on emulsion destabilization has been studied. However, their effects on mouthfeel should also be investigated using sensory analysis, since aggregation pattern seen in positively charged lactoferrin emulsions may influence fat perception. Recent studies by *Vingerhoeds et al. (2009)* showed that positively charged lysozyme–stabilized emulsions which underwent irreversible flocculation with saliva were perceived to be dry and astringent in the mouth. This astringent perception was related to the loss of lubricating effect of saliva, most likely due to the precipitation of salivary proteins by lysozyme molecules.

- The high shear processing of liquid emulsions in the mouth and frictional effects due to the oral surfaces and intense salivary flow on emulsion stability need to be thoroughly investigated, as the mechanical forces might result in further coalescence or droplet break up, thus modifying the flavour release and perceived sensorial attributes.

- The role of pH, ionic strength, pepsin and mucin was successfully investigated in the gastric digestion of emulsions. Human gastric fluid does contains acid stable gastric lipase. Generally gastric lipases accounts for 10–30% of overall lipid digestion of ingested triacylglycerols in human adults *(Carriere et al., 1993; Armand et al., 1994; Pafumi et al., 2002; Armand, 2007)*. These acid stable lipases could act on emulsions, resulting in generation of surface active fatty acids and monoglycerides from hydrophobic lipid core. Some of these compounds could competitively displace the initial emulsifier materials from the emulsion interface either fully or partially *(Armand et al., 1994; Pafumi et al., 2002)*. It is possible that the gastric lipase digestion products would displace intact or hydrolysed protein from the interface in case of protein–stabilized emulsions. This could lead to a change in droplet size and impact the overall stability of the emulsion. However, there are no reported studies on how protein–stabilized emulsions are affected by the

action of gastric lipase. This is largely due to the unavailability of commercial gastric lipases. Systematic studies on the behaviour of protein–stabilized emulsions on addition of gastric lipase in simulated gastric conditions need to be carried out, involving proper lab-scale purification methods of gastric lipases obtained from human subjects.

- The peristaltic shear, when the emulsions enter the stomach, needs to be thoroughly replicated in the *in vitro* digestion models to understand the shear–induced changes of emulsion droplets in gastric tract.

- The properties of emulsion systems containing bile salts have been studied. However, whether the bile–displacement interactions differ from those containing simple surfactants, such as Tween 20, sodium dodecyl sulphate or not (based on different structure of bile salts than other surface active agents), needs to be determined. This would help to make systematic progress at the fundamental level and result in coherence in relation to the existing body of knowledge in the field of emulsion science.

- In the intestinal study, there was no colipase used in the simulated system, the role of which needs to be explored in the digestion of emulsified lipid substrates by lipase.

- Even the purest commercially available lipase shows some proteolytic activity but it is not certain whether or not the enzymatic activities would be prevented or reduced by introducing trypsin–chymotrypsin inhibitor and other proteolytic inhibitors. It would be worthwhile looking at this in a more detailed manner by checking the fatty acid release or droplet flocculation upon addition of some proteolytic inhibitors to the commercial lipases. Another study may be attempted to enhance the purity of the lipase by using chromatography purification techniques.

- The results presented in this thesis provided a detailed investigation of the most of the important physiological components. However, results may not be easy to interpret in terms of what happens *in vivo* as physiological components do not act individually but together in a rather complex manner. Hence, *in vitro* findings need to be validated with *in vivo* systems using pig or rat models. For example, feeding emulsions to pigs followed by collecting samples at various stages of the gastrointestinal tract (such as duodenum, jejunum and ileum) and analyzing the samples can provide understanding of how *in vitro* studies correlate to *in vivo* trials.

- In addition to *in vivo* with animals, clinical trials with human subjects needs to be carried out in order to better understand the complex physicochemical processes occurring during lipid digestion. Recently non–invasive techniques such as magnetic resonance imaging (MRI) revealed the intra-gastric behaviour of emulsions in relation to understanding their effects of satiety in human *(Marciani et al., 2006; Marciani et al., 2007; Marciani et al., 2009)*. These methods might be used to provide useful information on the intra-lumen distribution of lipid droplets and gastric emptying.

- Since, food systems are more complex than model oil-in-water emulsions systems investigated in this study, it would be interesting to study the physiological interactions in multi-component systems. Interactions of emulsified lipids containing mixed biopolymer systems (proteins, carbohydrates) in presence of simulated physiological fluid are worth investigating. The latter would provide better understanding about the macromolecular interactions within the nutrients together with their influence on controlling lipid digestion. For example, the presence of polysaccharides might significantly saturate the protein–stabilized lipid droplets, thereby preventing the enzymes to come in contact with the lipid hydrophobic core, and thus influence the overall lipid digestion.

Manipulation of food structures together with mapping their physical, chemical and biological fate during physiological lipid digestion (using *in vitro*, *in vivo* and clinical trials) will help to fabricate future foods rationally with designed functional behaviour in the body, such as controlled release of lipid bioactives. Such foods might have the potential benefits to fight against obesity, cardiovascular diseases and other food–linked health issues and/or provide improved satiety responses.

Bibliography

Agboola, S. O., & Dalgleish, D. G. (1995). Calcium–induced destabilization of oil-in-water emulsions stabilized by caseinate or by *β*-lactoglobulin. *Journal of Food Science*, *60*(2), 399–404.

Agboola, S. O., & Dalgleish, D. G. (1996). Enzymatic hydrolysis of milk proteins used for emulsion formation. 1. Kinetics of protein breakdown and storage stability of the emulsions. *Journal of Agricultural and Food Chemistry*, *44*(11), 3631–3636.

Agboola, S. O., Singh, H., Munro, P. A., Dalgleish, D. G., & Singh, A. M. (1998a). Destabilization of oil-in-water emulsions formed using highly hydrolyzed whey proteins. *Journal of Agricultural and Food Chemistry*, *46*(1), 84–90.

Agboola, S. O., Singh, H., Munro, P. A., Dalgleish, D. G., & Singh, A. M. (1998b). Stability of emulsions formed using whey protein hydrolysate: effects of lecithin addition and retorting. *Journal of Agricultural and Food Chemistry*, *46*(5), 1814–1819.

Allen, M. S., Bradford, B. J., & Harvatine, K. J. (2005). The cow as a model to study food intake regulation. *Annual Reviews of Nutrition*, *25*(1), 523–547.

Amado, F. M. L., Vitorino, R. M. P., Domingues, P. M. D. N., Lobo, M. J. C., & Duarte, J. A. R. (2005). Analysis of the human saliva proteome. *Expert Review of Proteomics*, *2*(4), 521–539.

Anal, A. K., Bhopatkar, D., Tokura, S., Tamura, H., & Stevens, W. F. (2003). Chitosan–alginate multilayer beads for gastric passage and controlled intestinal release of protein. *Drug development and industrial pharmacy*, *29*(6), 713–724.

AnnMarie, K., Ben, J. B., Christopher, J. H. P., & William, N. C. (2004). Drug solubilization behavior during *in vitro* digestion of simple triglyceride lipid solution formulations. *Pharmaceutical Research*, *21*(2), 245–253.

Aps, J. K. M., & Martens, L. C. (2005). Review: the physiology of saliva and transfer of drugs into saliva. *Forensic Science International*, *150*(2-3), 119–131.

Armand, M. (2007). Lipases and lipolysis in the human digestive tract: where do we stand? *Current Opinion in Clinical Nutrition and Metabolic Care*, *10*(2), 156–164.

Armand, M., Borel, P., Dubois, C., Senft, M., Peyrot, J., Salducci, J., Lafont, H., & Lairon, D. (1994). Characterization of emulsions and lipolysis of dietary lipids in the human stomach. *American Journal of Physiology-Gastrointestinal and Liver Physiology*, *266*(3), G372–G381.

Armand, M., Borel, P., Pasquier, B., Dubois, C., Senft, M., Andre, M., Peyrot, J., Salducci, J., & Lairon, D. (1996a). Physicochemical characteristics of emulsions during fat digestion in human stomach and duodenum. *American Journal of Physiology-Gastrointestinal and Liver Physiology*, *271*(1), G172–G183.

Armand, M., Borel, P., Ythier, P., Dutot, G., Melin, C., Senft, M., Lafont, H., & Lairon, D. (1992). Effects of droplet size, triacylglycerol composition, and calcium on the hydrolysis of complex emulsions by pancreatic lipase: an *in vitro* study. *The Journal of Nutritional Biochemistry*, *3*(7), 333–341.

Armand, M., Hamosh, M., Mehta, N. R., Angelus, A. A., Philpott, J. R., Henderson, T. R., Dwyer, N. K., Lairon, D., & Hamosh, P. (1996b). Effect of human milk or formula on gastric function and fat digestion in the premature infant. *Pediatric Research*, *40*(3), 429–437.

Armand, M., Pasquier, B., André, M., Borel, P., Senft, M., Peyrot, J., Salducci, J., Portugal, H., Jaussan, V., & Lairon, D. (1999). Digestion and absorption of 2 fat emulsions with different droplet sizes in the human digestive tract. *The American Journal of Clinical Nutrition*, *70*(6), 1096–1106.

Avula, C. P. R., & Fernandes, G. (1999). Modulation of antioxidant enzymes and apoptosis in mice by dietary lipids and treadmill exercise. *Journal of Clinical Immunology*, *19*, 35–44.

Baker, E. N., & Baker, H. M. (2005). Molecular structure, binding properties and dynamics of lactoferrin. *Cellular and Molecular Life Sciences*, *62*(22), 2531–2539.

Baker, E. N., Baker, H. M., & Kidd, R. D. (2002). Lactoferrin and transferrin: functional variations on a common structural framework. *Biochemistry and Cell Biology*, *80*(1), 27–34.

Bansil, R., & Turner, B. S. (2006). Mucin structure, aggregation, physiological functions and biomedical applications. *Current Opinion in Colloid & Interface Science*, *11*(2-3), 164–170.

Bardow, A., Moe, D., Nyvad, B., & Nauntofte, B. (2000). The buffer capacity and buffer systems of human whole saliva measured without loss of CO_2. *Archives of Oral Biology*, *45*(1), 1–12.

Bauer, E., Jakob, S., & Mosenthin, R. (2005). Principles of physiology of lipid digestion. *Asian-Australasian Journal of Animal Sciences*, *18*(2), 282–295.

Baumy, J. J., & Brulé, G. (1988). Binding of bivalent cations to α-lactalbumin and β-lactoglobulin: effect of pH and ionic strength. *Lait*, *68*(4), 33–48.

Benichou, A., Aserin, A., & Garti, N. (2002). Protein–polysaccharide interactions for stabilization of food emulsions. *Journal of Dispersion Science and Technology*, *23*(1–3), 93–123.

Bernkop-Schnürch, A., Schwarz, V., & Steininger, S. (1999). Polymers with thiol groups: a new generation of mucoadhesive polymers? *Pharmaceutical Research*, *16*(6), 876–881.

Beysseriat, M., Decker, E. A., & McClements, D. J. (2006). Preliminary study of the influence of dietary fibre on the properties of oil-in-water emulsions passing through an *in vitro* human digestion model. *Food Hydrocolloids*, *20*(6), 800–809.

Birner-Grünberger, R., Scholze, H., Faber, K., & Hermetter, A. (2004). Identification of various lipolytic enzymes in crude porcine pancreatic lipase preparations using covalent fluorescent inhibitors. *Biotechnology and bioengineering*, *85*(2), 147–154.

Bläckberg, L., Hernell, O., Bengtsson, G., & Olivecrona, T. (1979). Colipase enhances hydrolysis of dietary triglycerides in the absence of bile salts. *The Journal of Clinical Investigation*, *64*(5), 1303–1308.

Blackman, D. S. (1994). Limited hydrolysis of proteins. *Logic of Biochemical Sequencing* (pp. 11–26). Boca Raton, Florida, USA: CRC Press.

Blanquet, S., Zeijdner, E., Beyssac, E., Meunier, J.-P., Denis, S., Havenaar, R., & Alric, M. (2004). A dynamic artificial gastrointestinal system for studying the behaviour of orally administered drug dosage forms under various physiological conditions. *Pharmaceutical Research*, *21*(4), 585–591.

Blijdenstein, T. B. J., van Vliet, T., van der Linden, E., & van Aken, G. A. (2003). Suppression of depletion flocculation in oil-in-water emulsions: a kinetic effect of *β*-lactoglobulin. *Food Hydrocolloids*, *17*(5), 661–669.

Blijdenstein, T. B. J., Winden, A. J. M. v., Vliet, T. v., Linden, E. v. d., & van Aken, G. A. (2004a). Serum separation and structure of depletion- and bridging-flocculated emulsions: a comparison. *Colloids and Surfaces A: Physicochemical and Engineering Aspects*, *245*(1–3), 41–48.

Blijdenstein, T. B. J., Zoet, F. D., van Vliet, T., van der Linden, E., & van Aken, G. A. (2004b). Dextran–induced depletion flocculation in oil-in-water emulsions in the presence of sucrose. *Food Hydrocolloids*, *18*(5), 857–863.

Bonnaire, L., Sandra, S., Helgason, T., Decker, E. A., Weiss, J., & McClements, D. J. (2008). Influence of lipid physical state on the *in vitro* digestibility of emulsified lipids. *Journal of Agricultural and Food Chemistry*, *56*(10), 3791–3797.

Borel, P., Armand, M., Pasquier, B., Senft, M., Dutot, G., Melin, C., Lafont, H., & Lairon, D. (1994). Digestion and absorption of tube-feeding emulsions with different droplet sizes and compositions in the rat. *Journal of Parenteral and Enteral Nutrition*, *18*(6), 534–543.

Boulby, Moore, Gowland, & Spiller (1999). Fat delays emptying but increases forward and backward antral flow as assessed by flow-sensitive magnetic resonance imaging. *Neurogastroenterology and Motility*, *11*(1), 27–36.

Brew, K., & Grobler, J. A. (1992). α-Lactalbumin. In: P. F. Fox, *Advanced Dairy Chemistry - I: Proteins* (pp. 191–229). New York, USA: Elsevier Applied Science.

Brines, R. D., & Brock, J. H. (1983). The effect of trypsin and chymotrypsin on the *in vitro* antimicrobial and iron–binding properties of lactoferrin in human milk and bovine colostrums: unusual resistance of human apolactoferrin to proteolytic digestion. *Biochimica et Biophysica Acta*, *759*(3), 229–235.

Britton, J. R., & Koldovsky, O. (1989). Gastric luminal digestion of lactoferrin and transferrin by preterm infants. *Early Human Development*, *19*(2), 127–135.

Brock, J. H., Arzabe, F., Lampreave, F., & Pineiro, A. (1976). The effect of trypsin on bovine transferrin and lactoferrin. *Biochimica et biophysica acta*, *446*(1), 214-225.

Brooksbank, D. V., Leaver, J., & Horne, D. S. (1993). Adsorption of milk-proteins to phosphatidyl-glycerol and phosphatidyl choline liposomes. *Journal of Colloid and Interface Science*, *161*(1), 38–42.

Caessens, P. W. J. R., Daamen, W. F., Gruppen, H., Visser, S., & Voragen, A. G. J. (1999). β-Lactoglobulin hydrolysis. 2. Peptide identification, SH/SS exchange, and functional properties of hydrolysate fractions formed by the action of plasmin. *Journal of Agricultural and Food Chemistry*, *47*(8), 2980–2990.

Calvo, P., Remuñán-López, C., Vila-Jato, J. L., & Alonso, M. J. (1997). Development of positively charged colloidal drug carriers: chitosan–coated polyester nanocapsules and submicron–emulsions. *Colloid & Polymer Science*, *275*(1), 46–53.

Cao, X., Bansil, R., Bhaskar, K. R., Turner, B. S., LaMont, J. T., Niu, N., & Afdhal, N. H. (1999). pH-Dependent conformational change of gastric mucin leads to sol–gel transition. *Biophysical Journal*, *76*(3), 1250–1258.

Carey, M. C., Small, D. M., & Bliss, C. M. (1983). Lipid digestion and absorption. *Annual Review of Physiology*, *45*, 651–677.

Carreau, P. J., De Kee, D. C. R., & Chhabra, R. P. (1997). *Rheology of polymeric Systems, Principles and Applications*. Cincinnati, OH, USA: Hanser/Gardner Publications.

Carrière, F., Barrowman, J. A., Verger, R., & Laugier, R. (1993). Secretion and contribution to lipolysis of gastric and pancreatic lipases during a test meal in humans. *Gastroenterology*, *105*(3), 876–888.

Carrière, F., Grandval, P., Gregory, P. C., Renou, C., Henniges, F., Sander-Struckmeier, S., & Laugier, R. (2005). Does the pancreas really produce much more lipase than required for fat digestion? *Journal of the Pancreas*, *6*(3), 206–215.

Cassin, G., Heinrich, E., & Spikes, H. A. (2001). The influence of surface roughness on the lubrication properties of adsorbing and non–adsorbing biopolymers. *Tribology Letters*, *11*(2), 95–102.

Castelain, C., & Genot, C. (1996). Partition of adsorbed and non–adsorbed bovine serum albumin in dodecane-in-water emulsions calculated from front-face intrinsic fluorescence measurements. *Journal of Agricultural and Food Chemistry*, *44*(7), 1635–1640.

Chanamai, R., & McClements, D. J. (2001). Depletion flocculation of beverage emulsions by gum arabic and modified starch. *Journal of Food Science*, *66*(3), 457–463.

Chen, J. (2009). Food oral processing: a review. *Food Hydrocolloids*, *23*(1), 1–25.

Chevalier, F., Chobert, J. M., Dalgalarrondo, M., Choiset , Y., & Haertlé, T. (2002). Maillard glycation of β-lactoglobulin induces conformation changes. *Nahrung/Food*, *48*(2), 58–63.

Chiappin, S., Antonelli, G., Gatti, R., & De Palo, E. F. (2007). Saliva specimen: a new laboratory tool for diagnostic and basic investigation. *Clinica Chimica Acta*, *383*(1–2), 30–40.

Chobert, J. M., Bertrand-Harb, C., & Nicolas, M. G. (1988). Solubility and emulsifying properties of caseins and whey proteins modified enzymically by trypsin. *Journal of Agricultural and Food Chemistry*, *36*(5), 883–892.

Chung, C., Sanguansri, L., & Augustin, M. (2008). Effects of modification of encapsulant materials on the susceptibility of fish oil microcapsules to lipolysis. *Food Biophysics*, *3*(2), 140–145.

Crandall, W. V., & Lowe, M. E. (2001). Colipase residues glu64 and arg65 are essential for normal lipase–mediated fat digestion in the presence of bile salt micelles. *The Journal of Biological Chemistry*, *276*(16), 12505–12512.

da Silva Gomes, R. A., Batista, R. P., de Almeida, A. C., da Fonseca, D. N., Juliano, L., & Hial, V. (2003). A fluorimetric method for the determination of pepsin activity. *Analytical Biochemistry, 316*(1), 11–14.

Dalgalarrondo, M., Dufour, E., Chobert, J.-M., Bertrand-Harb, C., & Haertlé, T. (1995). Proteolysis of *β*-lactoglobulin and *β*-casein by pepsin in ethanolic media. *International Dairy Journal*, *5*(1), 1–14.

Dalgleish, D. G. (1993). The sizes and conformations of the proteins in adsorbed layers of individual caseins on latices and in oil-in-water interfaces. *Colloids and Surfaces B-Biointerfaces*, *1*(1), 1–8.

Dalgleish, D. G. (1995). Structures and properties of adsorbed layers in emulsions containing milk proteins. In: E. Dickinson, & D. Lorient, *Food Macromolecules and Colloids* (pp. 23–34). Cambridge, UK: Royal Society of Chemistry.

Dalgleish, D. G. (1996a). Conformations and structures of milk proteins adsorbed to oil-water interfaces. *Food Research International*, *29*(5–6), 541–547.

Dalgleish, D. G. (1996b). Food emulsions. In: J. Sjoblom, *Emulsions and Emulsion Stability* (pp. 287–325). New York, USA: Marcel Dekker.

Dalgleish, D. G. (1997). Adsorption of protein and the stability of emulsions. *Trends in Food Science & Technology*, *8*(1), 1–6.

Dalgleish, D. G. (2004). Food Emulsions: their structures and properties. In: S. E. Friberg, K. Larsson, & J. Sjöhlom, *Food Emulsions* (pp. 1–44). New York, USA: Marcel Dekker.

Dalgleish, D. G. (2006). Food emulsions-their structures and structure-forming properties. *Food Hydrocolloids*, *20*(4), 415–422.

Dalgleish, D. G., Goff, H. D., & Luan, B. (2002). Exchange reactions between whey proteins and caseins in heated soya oil-in-water emulsion systems–behaviour of individual proteins. *Food Hydrocolloids*, *16*(4), 295–302.

Dalgleish, D. G., Senaratne, V., & Francois, S. (1997). Interactions between *α*-lactalbumin and *β*-lactoglobulin in the early stages of heat denaturation. *Journal of Agricultural and Food Chemistry*, *45*(9), 3459–3464.

Damodaran, S. (1997). Food proteins: an overview. In: S. Damodaran, & A. Paraf, *Food Proteins and Their Applications* (pp. 1–24). New York, USA: Marcel Dekker.

Damodaran, S., & Anand, K. (1997). Sulfhydryl–disulfide interchange–induced interparticle protein polymerization in whey protein–stabilized emulsions and its

relation to emulsion stability. *Journal of Agricultural and Food Chemistry, 45*(10), 3813–3820.

Darling, D. F. (1987). Kinetic aspects of food emulsion behaviour. In: J. M. V. Blanshard, & P. Lillford, *Food structure and Behaviour* (pp. 107–145). London, UK: Academic Press.

Das, K. P., & Chattoraj, D. K. (1982). Kinetics of coalescence of polar oil/water emulsion stabilized by ionic detergents and proteins. *Colloids and Surfaces, 5*(1), 75–78.

de Roos, K. B. (2003). Effect of texture and microstructure on flavour retention and release. *International Dairy Journal, 13*(8), 593–605.

de Wijk, R. A., & Prinz, J. F. (2005). The role of friction in perceived oral texture. *Food Quality and Preference, 16*(2), 121–129.

de Wijk, R. A., Prinz, J. F., Engelen, L., & Weenen, H. (2004). The role of α-amylase in the perception of oral texture and flavour in custards. *Physiology & Behavior, 83*(1), 81–91.

de Wijk, R. A., van Gemert, L. J., Terpstra, M. E. J., & Wilkinson, C. L. (2003). Texture of semi-solids; sensory and instrumental measurements on vanilla custard desserts. *Food Quality and Preference, 14*(4), 305–317.

de Zwart, L. L., Haenen, H. E. M. G., Versantvoort, C. H. M., Wolterink, G., van Engelen, J. G. M., & Sips, A. J. A. M. (2004). Role of biokinetics in risk assessment of drugs and chemicals in children. *Regulatory Toxicology and Pharmacology, 39*(3), 282–309.

Demetriades, K., Coupland, J. N., & McClements, D. J. (1997). Physicochemical properties of whey protein–stabilized emulsions as affected by heating and ionic strength. *Journal of Food Science, 62*(3), 462–467.

Demetriades, K., & McClements, D. J. (1998). Influence of pH and heating on physicochemical properties of whey protein–stabilized emulsions containing a non–ionic surfactant. *Journal of Agricultural and Food Chemistry, 46*(10), 3936–3942.

Dickinson, E. (1989). Surface and emulsifying properties of caseins. *Journal of Dairy Research, 56*(3), 471-477.

Dickinson, E. (1992). *Introduction to Food Colloids*. Oxford, UK: Oxford University Press.

Dickinson, E. (1994). Protein–stabilized emulsions. *Journal of Food Engineering, 22*(1–4), 59–74.

Dickinson, E. (1997a). Aggregation processes, particle interactions, and colloidal structure In: E. Dickinson, & B. Bergenstahl, *Food Colloids: Proteins, Lipids and Polysaccharides* (pp. 107–126). Cambridge, UK: Royal Society of Chemistry.

Dickinson, E. (1997b). Properties of emulsions stabilized with milk proteins: overview of some recent developments. *Journal of Dairy Science*, *80*(10), 2607–2619.

Dickinson, E. (1998). Stability and rheological implications of electrostatic milk protein–polysaccharide interactions. *Trends in Food Science & Technology*, *9*(10), 347–354.

Dickinson, E. (1999). Caseins in emulsions: interfacial properties and interactions. *International Dairy Journal*, *9*(3–6), 305–312.

Dickinson, E. (2001). Milk protein interfacial layers and the relationship to emulsion stability and rheology. *Colloids and Surfaces B: Biointerfaces*, *20*(3), 197–210.

Dickinson, E. (2003). Hydrocolloids at interfaces and the influence on the properties of dispersed systems. *Food Hydrocolloids*, *17*(1), 25–39.

Dickinson, E. (2006). Structure formation in casein–based gels, foams, and emulsions. *Colloids and Surfaces A-Physicochemical and Engineering Aspects*, *288*(1–3), 3–11.

Dickinson, E. (2008). Interfacial structure and stability of food emulsions as affected by protein-polysaccharide interactions. *Soft Matter*, *4*(5), 932–942.

Dickinson, E., & Eriksson, L. (1991). Particle flocculation by adsorbing polymers. *Advances in Colloid Interface Science*, *34*(1), 1–29.

Dickinson, E., & Euston, S. R. (1991). Stability of food emulsions containing both protein and polysaccharide. In: E. Dickinson, *Food Polymers, Gels and Colloids* (pp. 132–146). Cambridge, UK: Royal Society of Chemistry.

Dickinson, E., Flint, F. O., & Hunt, J. A. (1989a). Bridging flocculation in binary protein stabilized emulsions. *Food Hydrocolloids*, *3*(5), 389–397.

Dickinson, E., & Galazka, V. B. (1991). Emulsion stabilization by ionic and covalent complexes of β-lactoglobulin with polysaccharides. *Food Hydrocolloids*, *5*(3), 281–296.

Dickinson, E., & Golding, M. (1997). Depletion flocculation of emulsions containing unadsorbed sodium caseinate. *Food Hydrocolloids*, *11*(1), 13–18.

Dickinson, E., & Golding, M. (1998). Influence of calcium ions on creaming and rheology of emulsions containing sodium caseinate. *Colloids and Surfaces A: Physicochemical and Engineering Aspects*, *144*(1–3), 167–177.

Dickinson, E., Golding, M., & Povey, M. J. W. (1997). Creaming and flocculation of oil-in-water emulsions containing sodium caseinate. *Journal of Colloid and Interface Science*, *185*(2), 515–529.

Dickinson, E., & Matsumura, Y. (1991). Time-dependent polymerization of β-lactoglobulin through disulfide bonds at the oil-water interface in emulsions. *International Journal of Biological Macromolecules*, *13*(1), 26–30.

Dickinson, E., Mauffret, A., Rolfe, S. E., & Woskett, C. M. (1989b). Adsorption at interfaces in dairy systems. *Journal of the Society of Dairy Technology*, *42*(1), 18–22.

Dickinson, E., & Pawlowsky, K. (1997). Effect of ι-carrageenan on flocculation, creaming, and rheology of a protein–stabilized emulsion. *Journal of Agricultural and Food Chemistry*, *45*(10), 3799–3806.

Dickinson, E., & Pawlowsky, K. (1998). Influence of κ–carrageenan on the properties of a protein–stabilized emulsion. *Food Hydrocolloids*, *12*(4), 417–423.

Dickinson, E., Radford, S. J., & Golding, M. (2003). Stability and rheology of emulsions containing sodium caseinate: combined effects of ionic calcium and non–ionic surfactant. *Food Hydrocolloids*, *17*(2), 211–220.

Dickinson, E., Rolfe, S. E., & Dalgleish, D. G. (1988). Competitive adsorption of α_{s1}-casein and β-casein in oil-in-water emulsions. *Food Hydrocolloids*, *2*(5), 397-405.

Dickinson, E., Semenova, M. G., & Antipova, A. S. (1998). Salt stability of casein emulsions. *Food Hydrocolloids*, *12*(2), 227–235.

Dickinson, E., & Stainsby, G. (1982). *Colloids in Foods*. London, UK: Applied Science.

Dickinson, E., & Stainsby, G. (1988). Emulsion stability. In: E. Dickinson, & G. Stainsby, *Advances in Food Emulsions and Foams* (pp. 1–173). London, UK: Elsevier Applied Science.

Dickinson, E., Whyman, R. H., & Dalgleish, D. G. (1987). Colloidal properties of model oil-in-water emulsions stabilized separately by α_{s1}-casein; β-casein and κ-casein. In: E. Dickinson, *Food Emulsions and Foams* (pp. 40–51). London. UK: Royal Society of Chemistry.

Djordjevic, D., Kim, H. J., McClements, D. J., & Decker, E. A. (2004). Physical stability of whey protein–stabilized oil-in-water emulsions at pH 3: potential ω-3 fatty acid delivery systems (Part A). *Journal of Food Science, 69*(5), C351–C355.

Dodds, M. W. J., Johnson, D. A., & Yeh, C.-K. (2005). Health benefits of saliva: a review. *Journal of Dentistry*, *33*(3), 223–233.

Dongowski, G. (1997). Effect of pH on the *in vitro* interactions between bile acids and pectin. *Zeitschrift für Lebensmitteluntersuchung und -Forschung A, 205*(3), 185–192.

Doyen, K., Carey, M., Linforth, R. S. T., Marin, M., & Taylor, A. J. (2001). Volatile release from an emulsion: headspace and in–mouth studies. *Journal of Agricultural and Food Chemistry*, *49*(2), 804–810.

Dresselhuis, D. M., de Hoog, E. H. A., Cohen Stuart, M. A., & van Aken, G. A. (2007). Tribology as a tool to study emulsion behaviour in the mouth. In: E. Dickinson, & M. E. Leser, *Food Colloids: Self Assembly and Material Science* (pp. 451–461). Cambridge, UK: Royal Society of Chemistry.

Dresselhuis, D. M., de Hoog, E. H. A., Cohen Stuart, M. A., & van Aken, G. A. (2008). Application of oral tissue in tribological measurements in an emulsion perception context. *Food Hydrocolloids*, *22*(2), 323–335.

Ebihara, K., & Schneeman, B. O. (1989). Interaction of bile acids, phospholipids, cholesterol and triglyceride with dietary fibres in the small intestine of rats. *The Journal of Nutrition*, *119*(8), 1100–1106.

Ekmekcioglu, C. (2002). A physiological approach for preparing and conducting intestinal bioavailability studies using experimental systems. *Food Chemistry*, *76*(2), 225–230.

Engelen, L., de Wijk, R. A., Prinz, J. F., van der Bilt, A., & Bosman, F. (2003). The relation between saliva flow after different stimulations and the perception of flavor and texture attributes in custard desserts. *Physiology & Behavior, 78*(1), 165–169.

Engstrom, B. E., Ohrvall, M., Sundbom, M., Lind, L., & Karlsson, F. A. (2006). Meal suppression of circulating ghrelin is normalized in obese individuals following gastric bypass surgery. *International Journal of Obesity*, *31*(3), 476–480.

Ennis, M. P., & Mulvihill, D. M. (2000). Milk proteins. In: G. O. Phillips, & P. A. Williams, *Handbook of Hydrocolloids* (pp. 189–217). Cambridge, UK: Woodhead Publishing Limited.

Erlanson-Albertsson, C. (1992). Pancreatic colipase. Structural and physiological aspects. *Biochimica et Biophysica Acta (BBA)–Lipids and Lipid Metabolism*, *1125*(1), 1–7.

Euston, S. E., Singh, H., Munro, P. A., & Dalgleish, D. G. (1996). Oil-in-water emulsions stabilized by sodium caseinate or whey protein isolate as influenced by glycerol monostearate. *Journal of Food Science*, *61*(5), 916–920.

Faas, H., Steingoetter, A., Feinle, C., Rades, T., Lengsfeld, H., Boesiger, P., Fried, M., & Schwizer, W. (2002). Effects of meal consistency and ingested fluid volume on the intragastric distribution of a drug model in humans: a magnetic resonance imaging study. *Alimentary Pharmacology and Therapeutics*, *16*(2), 217–224.

Fäldt, P., Bergenståhl, B., & Claesson, P. M. (1993). Stabilization by chitosan of soybean oil emulsions coated with phospholipid and glycocholic acid. *Colloids and Surfaces A: Physicochemical and Engineering Aspects*, *71*(2), 187–195.

Fang, Y., & Dalgleish, D. G. (1997). Conformation of *β*-lactoglobulin studied by FTIR: effect of pH, temperature, and adsorption to the oil-water interface. *Journal of Colloid and Interface Science*, *196*(2), 292–298.

Fang, Y., Tung, M. A., Britt, I. J., Yada, S., & Dalgleish, D. G. (2002). Tensile and barrier properties of edible films made from whey proteins. *Journal of Food Science*, *67*(1), 188–193.

Fave, G., Coste, T. C., & Armand, M. (2004). Physicochemical properties of lipids: new strategies to manage fatty acid bioavailability. *Cellular and Molecular Biology*, *50*(7), 815–831.

Feinle, C., Kunz, P., Boesiger, P., Fried, M., & Schwizer, W. (1999). Scintigraphic validation of a magnetic resonance imaging method to study gastric emptying of a solid meal in humans. *Gut*, *44*(1), 106–111.

Fellows, C. M., & Doherty, W. O. S. (2006). Insights into bridging flocculation. *Macromolecular Symposia*, *231*(1), 1–10.

Florence, A. T., & Whitehill, D. (1981). Some features of breakdown in water-in-oil-in-water multiple emulsions. *Journal of Colloid and Interface Science*, *79*(1), 243–256.

Florence, A. T., & Whitehill, D. (1982). The formulation and stability of multiple emulsions. *International Journal of Pharmaceutics*, *11*(4), 277–308.

Foegeding, E. A., Davis, J. P., Doucet, D., & McGuffey, M. K. (2002). Advances in modifying and understanding whey protein functionality. *Trends in Food Science & Technology*, *13*(5), 151-159.

Friberg, S. E., Larsson, K., & Sjöhlom, J. (2004). *Food Emulsions*. New York, USA: Marcel Dekker.

Gal, J.-Y., Fovet, Y., & Adib-Yadzi, M. (2001). About a synthetic saliva for *in vitro* studies. *Talanta, 53*(6), 1103–1115.

Gallaher, D. D. (1992). Animal models in human nutrition research. *Nutrition in Clinical Practice, 7*(1), 37–39.

Gardner, J. D., Ciociola, A. A., & Robinson, M. (2002). Measurement of meal–stimulated gastric acid secretion by *in vivo* gastric auto-titration. *Journal of Applied Physiology, 92*(2), 427–434.

Gargouri, Y., Julien, R., Bois, A. G., Verger, R., & Sarda, L. (1983). Studies on the detergent inhibition of pancreatic lipase activity. *Journal of Lipid Research, 24*, 1336–1342.

Garti, N. (1997). Progress in stabilization and transport phenomena of double emulsions in food applications. *Lebensmittel-Wissenschaft und-Technologie, 30*(3), 222–235.

Gauthier, S. F., Vachon, C., & Savoie, L. (1986). Enzymatic conditions of an *in vitro* method to study protein digestion. *Journal of Food Science, 51*(4), 960–964.

Glantz, P.-O. (1997). Interfacial phenomena in the oral cavity. *Colloids and Surfaces A: Physicochemical and Engineering Aspects, 123–124*, 657–670.

Goh, K. K. T., Sarkar, A., & Singh, H. (2008). Milk protein–polysaccharide interactions. In: A. Thompson, M. Boland, & H. Singh, *Milk Proteins* (pp. 347–376). San Diego, CA, USA: Academic Press.

Golding, M., & Wooster, T. J. (2010). The influence of emulsion structure and stability on lipid digestion. *Current Opinion in Colloid & Interface Science 15*(1–2), 90–101.

Graham, D. E., & Phillips, M. C. (1979). Proteins at liquid interfaces. II. Adsorption isotherms. *Journal of Colloid and Interface Science, 70*(3), 415–426.

Gu, Y.-S., Decker, E. A., & McClements, D. J. (2007). Formation of colloidosomes by adsorption of small charged oil droplets onto the surface of large oppositely charged oil droplets. *Food Hydrocolloids, 21*(4), 516–526.

Gu, Y. S., Decker, E. A., & McClements, D. J. (2005). Influence of pH and carrageenan type on properties of β-lactoglobulin–stabilized oil-in-water emulsions. *Food Hydrocolloids, 19*(1), 83–91.

Guo, M. R., Fox, P. F., Flynn, A., & Kindstedt, P. S. (1995). Susceptibility of *β*-lactoglobulin and sodium caseinate to proteolysis by pepsin and trypsin. *Journal of Dairy Science, 78*(11), 2336–2344.

Güzey, D., Kim, H. J., & McClements, D. J. (2004). Factors influencing the production of o/w emulsions stabilized by *β*-lactoglobulin–pectin membranes. *Food Hydrocolloids*, *18*(6), 967–975.

Güzey, D., & McClements, D. J. (2006). Influence of environmental stresses on o/w emulsions stabilized by *β*-lactoglobulin–pectin and *β*-lactoglobulin–pectin–chitosan membranes produced by the electrostatic layer-by-layer deposition technique. *Food Biophysics*, *1*(1), 30-40.

Han, L. K., Kimura, Y., & Okuda, H. (1999). Reduction in fat storage during chitin–chitosan treatment in mice fed a high-fat diet. *International Journal of Obesity*, *23*(2), 174–179.

Haque, Z. U., & Mozaffar, Z. (1992). Casein hydrolysate. II. Functional properties of peptides. *Food Hydrocolloids*, *5*(6), 559–571.

Harding, S. E., Deacon, M. P., Fiebrig, I., & Davis, S. S. (1999). Biopolymer mucoadhesives. *Biotechnology and Genetic Engineering Reviews*, *16*(1), 41–86.

Harnsilawat, T., Pongsawatmanit, R., & McClements, D. J. (2006). Influence of pH and ionic strength on formation and stability of emulsions containing oil droplets coated by *β*–lactoglobulin–alginate interfaces. *Biomacromolecules*, *7*(6), 2052–2058.

Hogg, R. (2003). Particle characterization. In: M. C. Fuerstenau, & K. N. Han, *Principles of mineral processing* (pp. 9–60). Denver, CO, USA: Society for Mining, Metallurgy & Exploration Publishers.

Holt, C., & Sawyer, L. (1988). Primary and predicted secondary structures of the caseins in relation to their biological functions *Protein Engineering*, *2*(4), 251–259.

Honey, N. K., Sakaguchi, A. Y., Quinto, C., MacDonald, R. J., Bell, G. I., Craik, C., Rutter, W. J., & Naylor, S. L. (1984). Chromosomal assignments of human genes for serine proteases trypsin, chymotrypsin B, and elastase. *Somatic Cell and Molecular Genetics*, *10*(4), 369–376.

Hong, Y.-H., & McClements, D. (2007). Modulation of pH sensitivity of surface charge and aggregation stability of protein–coated lipid droplets by chitosan addition. *Food Biophysics*, *2*(1), 46–55.

Horne, D. S. (1998). Casein Interactions: Casting light on the black boxes, the structure in dairy products. *International Dairy Journal*, *8*(3), 171–177.

Horne, D. S., & Leaver, J. (1995). Milk proteins on surfaces. *Food Hydrocolloids*, *9*(2), 91–95.

Hu, S., Loo, J. A., & Wong, D. T. (2007). Human saliva proteome analysis. *Annals of the New York Academy of Sciences*, *1098*(1), 323–329

Humphrey, S. P., & Williamson, R. T. (2001). A review of saliva: normal composition, flow, and function. *The Journal of Prosthetic Dentistry*, *85*(2), 162–169.

Hunt, J. A., & Dalgleish, D. G. (1994). Adsorption behaviour of whey protein isolate and caseinate in soya oil-in-water emulsions. *Food Hydrocolloids*, *8*(2), 175–187.

Hunt, J. A., & Dalgleish, D. G. (1995). Heat stability of oil-in-water emulsions containing milk proteins: effect of ionic strength and pH. *Journal of Food Science*, *60*(5), 1120–1123.

Hunt, J. A., & Dalgleish, D. G. (1996). The effect of the presence of KCl on the adsorption behaviour of whey protein and caseinate in oil-in-water emulsions. *Food Hydrocolloids*, *10*(2), 159–165.

Hunter, R. J. (1986). *Foundations of Colloid Science–I*. Oxford, UK: Oxford University Press.

Hunter, R. J. (1989). *Foundations of Colloid Science–II*. Oxford, UK: Oxford University Press.

Hur, S. J., Decker, E. A., & McClements, D. J. (2009). Influence of initial emulsifier type on microstructural changes occurring in emulsified lipids during *in vitro* digestion. *Food Chemistry*, *114*(1), 253–262.

Ivanova, M. G., Panaiotov, I., Bois, A., Gargouri, Y., & Verger, R. (1990). Inhibition of pancreatic lipase by ovalbumin and β-lactoglobulin A at the air/water interface. *Journal of Colloid and Interface Science*, *136*(2), 363–374.

Jantratid, E., Janssen, N., Reppas, C., & Dressman, J. (2008). Dissolution media simulating conditions in the proximal human gastrointestinal tract: an update. *Pharmaceutical Research*, *25*(7), 1663–1676.

Kalantzi, L., Goumas, K., Kalioras, V., Abrahamsson, B., Dressman, J., & Reppas, C. (2006). Characterization of the human upper gastrointestinal contents under conditions simulating bioavailability/ bioequivalence studies. *Pharmaceutical Research*, *23*(1), 165–176.

Kaminogawa, S., Shimizu, M., Ametai, A., Lee, S., & Yamauchi, K. (1987). Proteolysis in structural analysis of α_{s1}-casein adsorbed onto oil surfaces of emulsions and improvement of the emulsifying properties of protein. *Journal of the American Oil Chemists' Society*, *64*(12), 1688–1691.

Kananen, A., Savolainen, J., Mäkinen, J., Perttilä, U., Myllykoski, L., & Pihlanto-Leppälä, A. (2000). Influence of chemical modification of whey protein conformation on hydrolysis with pepsin and trypsin. *International Dairy Journal*, *10*(10), 691–697.

Keowmaneechai, E., & McClements, D. J. (2002). Effect of $CaCl_2$ and KCl on physiochemical properties of model nutritional beverages based on whey protein stabilized oil-in-water emulsions. *Journal of Food Science*, *67*(2), 665–671.

Kern, F., Jr., Birkner, H. J., & Ostrower, V. S. (1978). Binding of bile acids by dietary fiber. *The American Journal of Clinical Nutrition*, *31*(10), 175S–179S.

Kilcast, D., & Clegg, S. (2002). Sensory perception of creaminess and its relationship with food structure. *Food Quality and Preference*, *13*(7–8), 609–623.

Kim, H. J., Decker, E. A., & McClements, D. J. (2006). Preparation of multiple emulsions based on thermodynamic incompatibility of heat–denatured whey protein and pectin solutions. *Food Hydrocolloids*, *20*(5), 586–595.

Kinsella, J. E. (1984). Milk proteins: physical and functional properties. *Critical Reviews in Food Science and Nutrition*, *21*(3), 197–262.

Kinsella, J. E., & Whitehead, D. M. (1989). Proteins in whey: chemical and physical and functional properties. *Advances in Food and Nutrition Research*, *33*, 343–438.

Koppel, D. E. (1972). Analysis of macromolecular polydispersity in intensity correlation spectroscopy: the method of cumulants. *The Journal of Chemical Physics*, *57*(11), 4814-4820.

Korhonen, H., Pihlanto-Leppala, A., Rantamaki, P., & Tupasela, T. (1998). Impact of processing on bioactive proteins and peptides. *Trends in Food Science & Technology*, *9*(8–9), 307–319.

Kulmyrzaev, A., Chanamai, R., & McClements, D. J. (2000). Influence of pH and $CaCl_2$ on the stability of dilute whey protein stabilized emulsions. *Food Research International*, *33*(1), 15–20.

Kulmyrzaev, A. A., & Schubert, H. (2004). Influence of KCl on the physicochemical properties of whey protein–stabilized emulsions. *Food Hydrocolloids*, *18*(1), 13–19.

Kunz, P., Crelier, G. R., Schwizer, W., Borovicka, J., Kreiss, C., Fried, M., & Boesiger, P. (1998). Gastric emptying and motility: assessment with MR imaging: preliminary observations. *Radiology*, *207*(1), 33–40.

Laemmli, U. K. (1970). Cleavage of structural proteins during the assembly of the head of bacteriophage T4. *Nature*, *227*(5259), 680–685.

Lairon, D., Lafont, H., Vigne, J. L., Nalbone, G., Leonardi, J., & Hauton, J. C. (1985). Effects of dietary fibres and cholestyramine on the activity of pancreatic lipase *in vitro*. *The American Journal of Clinical Nutrition*, *42*(4), 629–638.

Lairon, D., Play, B., & Jourdheuil-Rahmani, D. (2007). Digestible and indigestible carbohydrates: interactions with postprandial lipid metabolism. *The Journal of Nutritional Biochemistry*, *18*(4), 217–227.

Layer, P., & Keller, J. (2005). Gastric lipase and pancreatic exocrine insufficiency. *Clinical Gastroenterology and Hepatology*, *3*(1), 25–27.

Leaver, J., & Dalgleish, D. G. (1990). The topography of bovine *β*-casein at an oil/water interface as determined from the kinetics of trypsin-catalysed hydrolysis. *Biochimica et Biophysica Acta (BBA)–Protein Structure and Molecular Enzymology*, *1041*(3), 217–222.

Lee, S., Heuberger, M., Rousset, P., & Spencer, N. D. (2004). A tribological model for chocolate in the mouth: general implications for slurry–lubricated hard/soft sliding counterfaces. *Tribology Letters*, *16*(3), 239–249.

Lee, S., Muller, M., Rezwan, K., & Spencer, N. D. (2005). Porcine gastric mucin (PGM) at the water/poly(dimethylsiloxane) (PDMS) interface: influence of pH and ionic strength on its conformation, adsorption, and aqueous lubrication properties. *Langmuir*, *21*(18), 8344–8353.

Lefèvre, T., & Subirade, M. (2003). Formation of intermolecular *β*-sheet structures: a phenomenon relevant to protein film structure at oil–water interfaces of emulsions. *Journal of Colloid and Interface Science*, *263*(1), 59–67.

Lehninger, A. L., Nelson, D. L., & Cox, M. M. (1993). Amino acid oxidation and the production of urea. *Principles of Biochemistry* (pp. 506–541). Irving Place, New York, USA: Worth Publishers.

Leitner, V. M., Walker, G. F., & Bernkop-Schnürch, A. (2003). Thiolated polymers: evidence for the formation of disulphide bonds with mucus glycoproteins. *European Journal of Pharmaceutics and Biopharmaceutics*, *56*(2), 207–214.

Leung, V. W. H., & Darvell, B. W. (1997). Artificial salivas for *in vitro* studies of dental materials. *Journal of Dentistry*, *25*(6), 475–484.

Leung, V. W. H., & Darvell, B. W. (1991). Calcium phosphate system in saliva–like media. *Journal of the Chemical Society, Faraday Transactions*, *87*(11), 1759–1764.

Lindahl, A., Ungell, A.-L., Knutson, L., & Lennernäs, H. (1997). Characterization of fluids from the stomach and proximal jejunum in men and women. *Pharmaceutical Research*, *14*(4), 497–502.

Lorient, D., Closs, B., & Courthaudon, J. L. (1989). Surface properties of the bovine casein components: Relationships between structure and foaming properties. *Journal of Dairy Research*, *56*, 495–502.

Lowe, M. E. (2002). The triglyceride lipases of the pancreas. *The Journal of Lipid Research*, *43*(12), 2007–2016.

Lucey, J. A., Srinivasan, M., Singh, H., & Munro, P. A. (2000). Characterization of commercial and experimental sodium caseinates by multiangle laser light scattering and size-exclusion chromatography. *Journal of Agricultural and Food Chemistry*, *48*(5), 1610–1616.

Lundin, L., Golding, M., & Wooster, T. J. (2008). Understanding food structure and function in developing food for appetite control. *Nutrition and Dietetics*, *65*(s3), S79–S85.

Ma, W., Tang, C., & Lai, L. (2005). Specificity of trypsin and chymotrypsin: loop–motion–controlled dynamic correlation as a determinant. *Biophysical Journal*, *89*(2), 1183–1193.

MacGregor, K. J., Embleton, J. K., Lacy, J. E., Perry, E. A., Solomon, L. J., Seager, H., & Pouton, C. W. (1997). Influence of lipolysis on drug absorption from the gastro-intestinal tract. *Advanced Drug Delivery Reviews*, *25*(1), 33–46.

Macierzanka, A., Sancho, A. I., Mills, E. N. C., Rigby, N. M., & Mackie, A. R. (2009). Emulsification alters simulated gastrointestinal proteolysis of β-casein and β-lactoglobulin. *Soft Matter*, *5*(3), 538–550.

Malagelada, J. R., & Azpiroz, F. (1989). Determinants of gastric emptying and transit in small intestine. In: S. G. Schultz, J. D. Wood, & B. B. Rauner, *Handbook of Physiology. Section VI: The Gastrointestinal System, Vol. 1* (pp. 909–937). Bethesda, Maryland, USA: American Physiological Society.

Maldonado-Valderrama, J., Woodward, N. C., Gunning, A. P., Ridout, M. J., Husband, F. A., Mackie, A. R., Morris, V. J., & Wilde, P. J. (2008). Interfacial

characterization of β-lactoglobulin networks: displacement by bile salts. *Langmuir*, *24*(13), 6759–6767.

Malone, M. E., Appelqvist, I. A. M., & Norton, I. T. (2003a). Oral behaviour of food hydrocolloids and emulsions. Part 1. Lubrication and deposition considerations. *Food Hydrocolloids*, *17*(6), 763–773.

Malone, M. E., Appelqvist, I. A. M., & Norton, I. T. (2003b). Oral behaviour of food hydrocolloids and emulsions. Part 2. Taste and aroma release. *Food Hydrocolloids*, *17*(6), 775–784.

Marciani, L., Faulks, R., Wickham, M. S. J., Bush, D., Pick, B., Wright, J., Cox, E. F., Fillery-Travis, A., Gowland, P. A., & Spiller, R. C. (2009). Effect of intragastric acid stability of fat emulsions on gastric emptying, plasma lipid profile and postprandial satiety. *British Journal of Nutrition*, *101*(6), 919–928

Marciani, L., Wickham, M., Singh, G., Bush, D., Pick, B., Cox, E., Fillery-Travis, A., Faulks, R., Marsden, C., Gowland, P. A., & Spiller, R. C. (2007). Enhancement of intragastric acid stability of a fat emulsion meal delays gastric emptying and increases cholecystokinin release and gallbladder contraction. *American Journal of Physiology-Gastrointestinal and Liver Physiology*, *292*(6), G1607–G1613.

Marciani, L., Wickham, M. S. J., Bush, D., Faulks, R., Wright, J., Fillery-Travis, A., Spiller, R. C., & Gowland, P. A. (2006). Magnetic resonance imaging of the behaviour of oil-in-water emulsions in the gastric lumen of man. *British Journal of Nutrition*, *95*(6), 331–339.

Martoni, C., Bhathena, J., Jones, M. L., Urbanska, A. M., Chen, H., & Prakash, S. (2007). Investigation of microencapsulated BSH active Lactobacillus in the simulated human GI tract. *Journal of Biomedicine and Biotechnology*, *2007*(13684), 1–9.

McClements, D. J. (2000). Comments on viscosity enhancement and depletion flocculation by polysaccharides. *Food Hydrocolloids*, *14*(2), 173–177.

McClements, D. J. (2004). Protein-stabilized emulsions. *Current Opinion in Colloid & Interface Science*, *9*(5), 305–313.

McClements, D. J. (2005). *Food Emulsions: Principles, practices and techniques*. Boca Raton, Florida, USA: CRC Press.

McClements, D. J., & Decker, E. A. (2000). Lipid oxidation in oil-in-water emulsions: impact of molecular environment on chemical reactions in heterogeneous food systems. *Journal of Food Science*, *65*(8), 1270–1282.

McClements, D. J., Decker, E. A., & Park, Y. (2009). Controlling lipid bioavailability through physicochemical and structural approaches. *Critical Reviews in Food Science and Nutrition*, *49*(1), 48–67.

McClements, D. J., Decker, E. A., Park, Y., & Weiss, J. (2008). Designing food structure to control stability, digestion, release and absorption of lipophilic food components. *Food Biophysics*, *3*(2), 219–228.

McClements, D. J., Decker, E. A., & Weiss, J. (2007). Emulsion-based delivery systems for lipophilic bioactive components. *Journal of Food Science*, *72*(8), R109–R124.

Mcclements, D. J., Monahan, F. J., & Kinsella, J. E. (1993). Disulfide bond formation affects stability of whey protein isolate emulsions. *Journal of Food Science*, *58*(5), 1036–1039.

McKenzie, H. A. (1971). *β*-Lactoglobulins. In: H. A. McKenzie, *Milk Proteins*, *Vol. 2* (pp. 257). New York, USA: Academic.

McKenzie, H. A., & Sawyer, W. H. (1967). Effect of pH on *β*-lactoglobulins. *Nature*, *214*(5093), 1101–1104.

Metcalf, K. L., & Vickers, Z. M. (2002). Taste intensities of oil-in-water emulsions with varying fat content. *Journal of Sensory Studies*, *17*(5), 379–390.

Michalski, M. C., Briard, V., Desage, M., & Geloen, A. (2005). The dispersion state of milk fat influences triglyceride metabolism in the rat: a $^{13}CO_2$ breath test study. *European Journal of Nutrition*, *44*(7), 436-444.

Mickelsen, R., & Ernstrom, C. A. (1972). Effect of pH on the stability of rennin-porcine pepsin blends. *Journal of Dairy Science*, *55*(3), 294–297.

Miettinen, S.-M., Tuorila, H., Piironen, V., Vehkalahti, K., & Hyvonen, L. (2002). Effect of emulsion characteristics on the release of aroma as detected by sensory evaluation, static headspace gas chromatography, and electronic nose. *Journal of Agricultural and Food Chemistry*, *50*(15), 4232–4239.

Miled, N., Riviere, M., Cavalier, J. F., Buono, G., Berti, L., & Verger, R. (2005). Discrimination between closed and open forms of lipases using electrophoretic techniques. *Analytical Biochemistry*, *338*(2), 171–178.

Miller, E. R., & Ullrey, D. E. (1987). The pig as a model for human nutrition. *Annual Review of Nutrition*, *7*(1), 361–382.

Minekus, M., & Havenaar, R. (1996). *In vitro* model of an *in vivo* digestive tract. United States Patent; No. 5525305, dated 11.06.96.

Minekus, M., & Havenaar, R. (1998). Reactor system. European Patent; No. 0642382, dated 11.02.98.

Minekus, M., Marteau, P., Havenaar, R., & Huis in't Veld, J. H. J. (1995). A multi−compartmental dynamic computer−controlled model simulating the stomach and the small intestine. *Alternatives to Laboratory Animals*, *23*, 197−209.

Minekus, M., Smeets-Peeters, M., Bernalier, A., Marol-Bonnin, S., Havenaar, R., Marteau, P., Alric, M., Fonty, G., & Huis in't Veld, J. H. J. (1999). A computer−controlled system to simulate conditions of the large intestine with peristaltic mixing, water absorption and absorption of fermentation products. *Applied Microbiology and Biotechnology*, *53*(1), 108−114.

Modler, H. W. (1985). Functional properties of non−fat dairy ingredients: a review. Modification of products containing casein. *Journal of Dairy Science*, *68*(9), 2195−2205.

Monahan, F. J., McClements, D. J., & Kinsella, J. E. (1995). Polymerization of whey proteins in whey protein−stabilized emulsions *Journal of Agricultural and Food Chemistry*, *41*(11), 1826−1829

Moreau, H., Bernadac, A., Gargouri, Y., Benkouka, F., Laugier, R., & Verger, R. (1989). Immunocytolocalization of human gastric lipase in chief cells of the fundic mucosa. *Histochemistry and Cell Biology, 91*(5), 419−423.

Moreau, H., Laugier, R., Gargouri, Y., Ferrato, F., & Verger, R. (1988). Human preduodenal lipase is entirely of gastric fundic origin. *Gastroenterology*, *95*(5), 1221−1226.

Moreno, F. J. (2007). Gastrointestinal digestion of food allergens: Effect on their allergenicity. *Biomedecine & Pharmacotherapy*, *61*(1), 50-60.

Morr, C. V. (1982). Functional properties of milk proteins and their use as food ingredients. In: P. F. Fox, *Developments in Dairy Chemistry−I* (pp. 375−399). London, UK: Elsevier Applied Science.

Morr, C. V., & Ha, E. Y. W. (1993). Whey protein concentrates and isolates: Processing and functional properties. *Critical Reviews in Food Science and Nutrition*, *33*(6), 431−476.

Mu, H., & Hoy, C. E. (2004). The digestion of dietary triacylglycerols. *Progress in Lipid Research*, *43*(2), 105−133.

Mukherjee, M. (2003). Human digestive and metabolic lipases: a brief review. *Journal of Molecular Catalysis B: Enzymatic*, *22*(5-6), 369–376.

Mukuddem-Petersen, J., Oosthuizen, W., & Jerling, J. C. (2005). A Systematic Review of the Effects of Nuts on Blood Lipid Profiles in Humans. *The Journal of Nutrition*, *135*(9), 2082–2089.

Muller, R. H., & Keck, C. M. (2004). Challenges and solutions for the delivery of biotech drugs - a review of drug nanocrystal technology and lipid nanoparticles. *Journal of Biotechnology*, *113*(1-3), 151–170.

Müller, R. H., Mäder, K., & Gohla, S. (2000). Solid lipid nanoparticles (SLN) for controlled drug delivery: a review of the state of the art. *European Journal of Pharmaceutics and Biopharmaceutics*, *50*(1), 161–177.

Mulvihill, D. M. (1989). Caseins and caseinates: Manufacture. In: P. F. Fox, *Developments in Dairy Chemistry–IV* (pp. 97–130). London, UK: Elsevier Applied Science.

Mulvihill, D. M., & Ennis, M. P. (2003). Functional milk proteins: production and utilization. In: P. F. Fox, & P. L. H. McSweeney, *Advanced Dairy Chemistry: Proteins*, *Vol. 1* (pp. 1175–1228). New York, USA: Kluwer Academic/Plenum Publishers.

Mulvihill, D. M., & Fox, P. F. (1989). Physicochemical and functional properties of milk proteins. In: P. F. Fox, *Developments in Dairy Chemistry–IV* (pp. 131–172). London, UK: Elsevier Applied Science.

Mun, S., Decker, E. A., & McClements, D. J. (2007). Influence of emulsifier type on *in vitro* digestibility of lipid droplets by pancreatic lipase. *Food Research International*, *40*(6), 770–781.

Mun, S., Decker, E. A., Park, Y., Weiss, J., & McClements, D. J. (2006). Influence of interfacial composition on *in vitro* digestibility of emulsified lipids: potential mechanism for chitosan's ability to inhibit fat digestion. *Food Biophysics*, *1*(1), 21–29.

Murray, B. S., & Stainsby, G. (1987). Properties of adsorbed layers in emulsions containing a mixture of caseinate and gelatin. In: E. Dickinson, *Food Emulsions and Foams* (pp. 86–99). London. UK: Royal Society of Chemistry.

Navarro, V., Macarulla, M., Fernández-Quintela, A., Rodríguez, V., Simón, E., & Portillo, M. (2007). Effects of *trans*–10, *cis*–12 conjugated linoleic acid on cholesterol metabolism in hypercholesterolaemic hamsters. *European Journal of Nutrition*, *46*(4), 213–219.

Neyraud, E., Prinz, J., & Dransfield, E. (2003). NaCl and sugar release, salivation and taste during mastication of salted chewing gum. *Physiology & Behavior*, *79*(4–5), 731–737.

Nielsen, P. B., Müllertz, A., Norling, T., & Kristensen, H. G. (2001). The effect of α-tocopherol on the *in vitro* solubilisation of lipophilic drugs. *International Journal of Pharmaceutics*, *222*(2), 217–224.

Nordman, H., Davies, J. R., Lindell, G., de Bolos, C., Real, F., & Carlsted, I. (2002). Gastric MUC5AC and MUC6 are large oligomeric mucins that differ in size, glycosylation and tissue distribution. *Biochemical Journal*, *364*(1), 191–200.

Norton, I., Moore, S., & Fryer, P. (2007). Understanding food structuring and breakdown: engineering approaches to obesity. *Obesity Reviews*, *8*(s1), 83–88.

Norton, I. T., Frith, W. J., & Ablett, S. (2006). Fluid gels, mixed fluid gels and satiety. *Food Hydrocolloids*, *20*(2–3), 229–239.

O'Connor, C. J., Sun, D., Smith, B. G., & Melton, L. D. (2003). Effect of soluble dietary fibers on lipase-catalyzed hydrolysis of tributyrin. *Journal of Food Science*, *68*(2), 1093–1099.

Offner, G. D., Nunes, D. P., Keates, A. C., Afdhal, N. H., & Troxler, R. F. (1998). The amino-terminal sequence of MUC5B contains conserved multifunctional D domains: Implications for tissue-specific mucin functions. *Biochemical and Biophysical Research Communications*, *251*(1), 350–355.

O'Gara, E. A., Maslin, D. J., Nevill, A. M., & Hill, D. J. (2008). The effect of simulated gastric environments on the anti-*Helicobacter* activity of garlic oil. *Journal of Applied Microbiology*, *104*(5), 1324–1331.

Ogawa, S., Decker, E. A., & McClements, D. J. (2003). Production and characterization of o/w emulsions containing cationic droplets stabilized by lecithin–chitosan membranes. *Journal of Agricultural and Food Chemistry*, *51*(9), 2806–2812.

Olbrich, C., Kayser, O., & Müller, R. H. (2002). Lipase degradation of Dynasan 114 and 116 solid lipid nanoparticles (SLN): effect of surfactants, storage time and crystallinity. *International Journal of Pharmaceutics*, *237*(1–2), 119–128.

Oliveira, K. M. G., Valente-Mesquita, V. L., Botelho, M. M., Sawyer, L., Ferreira, S. T., & Polikarpov, I. (2001). Crystal structures of bovine β-lactoglobulin in the orthorhombic space group C2221. Structural differences between genetic variants A and B and features of the tanford transition. *European Journal of Biochemistry*, *268*(2), 477–483.

Olsen, J. V., Ong, S.-E., & Mann, M. (2004). Trypsin cleaves exclusively *C*-terminal to arginine and lysine residues. *Molecular and Cellular Proteomics*, *3*(6), 608-614.

Pafumi, Y., Lairon, D., de la Porte, P. L., Juhel, C., Storch, J., Hamosh, M., & Armand, M. (2002). Mechanisms of inhibition of triacylglycerol hydrolysis by human gastric lipase. *The Journal of Biological Chemistry*, *277*(31), 28070–28079.

Pal, A., Brasseur, J. G., & Abrahamsson, B. (2007). A stomach road or "magenstrasse" for gastric emptying. *Journal of Biomechanics*, *40*(6), 1202–1210.

Panyam, D., & Kilara, A. (1996). Enhancing the functionality of food proteins by enzymatic modification. *Trends in Food Science & Technology*, *7*(4), 120–125.

Papiz, M. Z., Sawyer, L., Eliopoulos, E. E., North, A. C. T., Findley, J. B. C., Sivapradadarao, R., Jones, T. A., Newcomer, M. E., & Kraulis, P. J. (1986). The structure of *β*-lactoglobulin and its similarity to plasma retinol–binding protein *Nature*, *324*(6095), 383–385.

Park, G. Y., Mun, S., Park, Y., Rhee, S., Decker, E. A., Weiss, J., McClements, D. J., & Park, Y. (2007). Influence of encapsulation of emulsified lipids with chitosan on their *in vivo* digestibility. *Food Chemistry*, *104*(2), 761–767.

Pasquier, B., Armand, M., Guillon, F., Castelain, C., Borel, P., Barry, J.-L., Pleroni, G., & Lairon, D. (1996). Viscous soluble dietary fibers alter emulsification and lipolysis of triacylglycerols in duodenal medium *in vitro*. *The Journal of Nutritional Biochemistry*, *7*(5), 293–302.

Patton, J. S., Albertsson, P. A., Erlanson, C., & Borgström, B. (1978). Binding of porcine pancreatic lipase and colipase in the absence of substrate studies by two-phase partition and affinity chromatography. *The Journal of Biological Chemistry*, *253*(12), 4195–4202.

Patton, J. S., & Carey, M. C. (1981). Inhibition of human pancreatic lipase-colipase activity by mixed bile salt-phospholipid micelles. *American Journal of Physiology-Gastrointestinal and Liver Physiology*, *241*(4), G328–336.

Peniche, C., Fernández, M., Gallardo, A., López-Bravo, A., & Román, J. S. (2003). Drug delivery systems based on porous chitosan/polyacrylic acid microspheres. *Macromolecular Bioscience*, *3*(10), 540–545.

Pharmacopeia, U. S. (2000). Simulated gastric fluid. *United States Pharmacopeial Convention*, vol. 24 (pp. 2235). Rockville, Maryland, USA: The National Formulary 9 (U.S. Pharmacopeia Board of Trustees).

Pharmacopeia, U. S. (1995). Simulated intestinal fluid. *United States Pharmacopeial Convention*, vol. 23 (pp. 2053). Rockville, Maryland, USA: The National Formulary 9 (U.S. Pharmacopeia Board of Trustees).

Picot, A., & Lacroix, C. (2004). Encapsulation of *bifidobacteria* in whey protein-based microcapsules and survival in simulated gastrointestinal conditions and in yoghurt. *International Dairy Journal*, *14*(6), 505–515.

Pond, W. G., & Houpt, K. A. (1978). *The Biology of The Pig*. Ithaca, New York, USA: Cornell University Press.

Porter, C. J. H., & Charman, W. N. (2001). *In vitro* assessment of oral lipid based formulations. *Advanced Drug Delivery Reviews*, *50*(s1), S127–S147.

Qi, K., Seo, T., Jiang, Z., Carpentier, Y. A., & Deckelbaum, R. J. (2006). Triglycerides in fish oil affect the blood clearance of lipid emulsions containing long– and medium–chain triglycerides in mice. *The Journal of Nutrition*, *136*(11), 2766–2772.

Rampon, V., Riaublanc, A., Anton, M., Genot, C., & McClements, D. J. (2003). Evidence that homogenization of BSA–stabilized hexadecane-in-water emulsions induces structure modification of the non–adsorbed protein. *Journal of Agricultural and Food Chemistry*, *51*(20), 5900–5905.

Rayment, S. A., Liu, B., Offner, G. D., Oppenheim, F. G., & Troxler, R. F. (2000). Immunoquantification of human salivary mucins MG1 and MG2 in stimulated whole saliva: factors influencing mucin levels. *Journal of Dental Research*, *79*(10), 1765–1772.

Reddy, M., Kella, N. K. D., & Kinsella, J. E. (1988). Structural and conformational basis of the resistance of β-lactoglobulin to peptic and chymotryptic digestion. *Journal of Agricultural and Food Chemistry*, *36*(4), 737–741.

Reid, I. R. (2004). Effects of calcium supplementation on circulating lipids: potential pharmacoeconomic implications. *Drugs and Aging*, *21*(1), 7–17.

Reiffers-Magnani, C. K., Cuq, J. L., & Watzke, H. J. (2000). Depletion flocculation and thermodynamic incompatibility in whey protein–stabilised o/w emulsions. *Food Hydrocolloids*, *14*(6), 521–530.

Ribeiro, H. S., Ax, K., & Schubert, H. (2003). Stability of lycopene emulsions in food systems. *Journal of Food Science*, *68*(9), 2730–2734.

Rich, G., Faulks, R., Wickham, M., & Fillery-Travis, A. (2003). Solubilization of carotenoids from carrot juice and spinach in lipid phases: II. Modelling the duodenal environment. *Lipids*, *38*(9), 947–956.

Robson, E. W., & Dalgleish, D. G. (1987). Interfacial composition of sodium caseinate emulsions. *Journal of Food Science*, *52*(6), 1694–1698.

Sanchez, C., Pouliot, M., Gauthier, S. F., & Paquin, P. (1997). Thermal aggregation of whey protein isolate containing microparticulated or hydrolyzed whey proteins. *Journal of Agricultural and Food Chemistry*, *45*(7), 2384–2392.

Saupe, A., Wissing, S. A., Lenk, A., Schmidt, C., & Müller, R. H. (2005). Solid lipid nanoparticles (SLN) and nanostructured lipid carriers (NLC): structural investigations on two different carrier systems. *Bio-Medical Materials and Engineering*, *15*(5), 393–402.

Sawyer, L., Papiz, M. Z., North, A. C. T., & Eliopoulos, E. E. (1985). Structure and function of bovine *β*-lactoglobulin. *Biochemical Society Transactions*, *13*(1), 265–266.

Schipper, R. G., Silletti, E., & Vingerhoeds, M. H. (2007). Saliva as research material: Biochemical, physicochemical and practical aspects. *Archives of Oral Biology*, *52*(12), 1114–1135.

Schmidt, D. G., & Poll, J. K. (1991). Enzymatic hydrolysis of whey proteins. Hydrolysis of *α*-lactalbumin and *β*-lactoglobulin in buffer solutions by proteolytic enzymes. *Netherlands Milk and Dairy Journal*, *45*(4), 225–240.

Schmidt, D. G., & van Markwijk, B. W. (1993). Enzymatic hydrolysis of whey proteins. Influence of heat treatment of *α*-lactalbumin and *β*-lactoglobulin on their proteolysis by pepsin and papain. *Netherlands Milk and Dairy Journal*, *47*(1), 15–22.

Schmitt, C., Sanchez, C., Desobry-Banon, S., & Hardy, J. (1998). Structure and technofunctional properties of protein–polysaccharide complexes: a review. *Critical Reviews in Food Science and Nutrition*, *38*(8), 689–753.

Schokker, E. P., & Dalgleish, D. G. (1998). The shear–induced destabilization of oil-in-water emulsions using caseinate as emulsifier. *Colloids and Surfaces A: Physicochemical and Engineering Aspects*, *145*(1–3), 61–69.

Schulze, K. (2006). Imaging and modelling of digestion in the stomach and the duodenum. *Neurogastroenterology and Motility*, *18*(3), 172-183.

Schwizer, W., Fox, M., & Steingotter, A. (2003). Non–invasive investigation of gastrointestinal functions with magnetic resonance imaging: towards an "ideal" investigation of gastrointestinal function. *Gut*, *52*(iv), 34–39.

Shellis, R. P. (1978). A synthetic saliva for cultural studies of dental plaque. *Archives of oral biology*, *23*(6), 485–489.

Shimizu, M., Ametani, A., Kaminogawa, S., & Yamauchi, K. (1986). The topography of α_{s1}-casein adsorbed to an oil/water interface: an analytical approach using proteolysis. *Biochimica et Biophysica Acta (BBA)–Protein Structure and Molecular Enzymology*, *869*(3), 259–264.

Silletti, E., Vingerhoeds, M. H., Norde, W., & van Aken, G. A. (2007a). Complex formation in mixtures of lysozyme–stabilized emulsions and human saliva. *Journal of Colloid and Interface Science*, *313*(2), 485–493.

Silletti, E., Vingerhoeds, M. H., Norde, W., & van Aken, G. A. (2007b). The role of electrostatics in saliva–induced emulsion flocculation. *Food Hydrocolloids*, *21*(4), 596–606.

Silvestre, M. P. C., Decker, E. A., & McClements, D. J. (1999). Influence of copper on the stability of whey protein–stabilized emulsions. *Food Hydrocolloids*, *13*(5), 419–424.

Singh, A. M., & Dalgleish, D. G. (1998). The emulsifying properties of hydrolyzates of whey proteins. *Journal of Dairy Science*, *81*(4), 918–924.

Singh, H. (2005). Milk protein functionality in food colloids. In: E. Dickinson, *Food Colloids: Interactions, Microstructure and Processing* (pp. 179–193). Cambridge, UK: The Royal Society of Chemistry.

Singh, H., Tamehana, M., Hemar, Y., & Munro, P. A. (2003). Interfacial compositions, microstructure and stability of oil-in-water emulsions formed with mixtures of milk proteins and κ-carrageenan: 2. Whey protein isolate (WPI). *Food Hydrocolloids*, *17*(4), 549–561.

Singh, H., Ye, A., & Horne, D. (2009). Structuring food emulsions in the gastrointestinal tract to modify lipid digestion. *Progress in Lipid Research*, *48*(2), 92–100.

Souto, E. B., Wissing, S. A., Barbosa, C. M., & Müller, R. H. (2004). Development of a controlled release formulation based on SLN and NLC for topical clotrimazole delivery. *International Journal of Pharmaceutics*, *278*(1), 71–77.

Srinivasan, M., Singh, H., & Munro, P. A. (1996). Sodium caseinate-stabilized emulsions: factors affecting coverage and composition of surface proteins. *Journal of Agricultural and Food Chemistry*, *44*(12), 3807–3811.

Srinivasan, M., Singh, H., & Munro, P. A. (1999). Adsorption behaviour of sodium and calcium caseinates in oil-in-water emulsions. *International Dairy Journal*, *9*(3–6), 337–341.

Srinivasan, M., Singh, H., & Munro, P. A. (2000). The effect of sodium chloride on the formation and stability of sodium caseinate emulsions. *Food Hydrocolloids*, *14*(5), 497–507.

Stellaard, F. (2005). Use of dual isotope tracers in biomedical research. *Isotopes in Environmental and Health Studies*, *41*(3), 275–286.

Surh, J., Decker, E. A., & McClements, D. J. (2006). Influence of pH and pectin type on properties and stability of sodium-caseinate stabilized oil-in-water emulsions. *Food Hydrocolloids*, *20*(5), 607–618.

Swaisgood, H. E. (1982). Chemistry of milk protein. In: P. F. Fox, *Developments in Dairy Chemistry–I* (pp. 1–59). London, UK: Elsevier Applied Science.

Swaisgood, H. E. (1992). Chemistry of the caseins. In: P. F. Fox, *Advanced Dairy Chemistry–I* (pp. 63–110). Barking, UK: Elsevier Applied Science.

Sweeney, P. J., & Walker, J. M. (1993). Proteolytic enzymes for peptide production. In: M. M. Burrell, *Enzymes of Molecular Biology*, *Vol. 16* (pp. 277–303). Totowa, New Jersey, USA: Humana Press.

Szarka, L. A., & Camilleri, M. (2009). Gastric Emptying. *Clinical Gastroenterology and Hepatology*, *7*(8), 823–827.

Tang, J. (1963). Specificity of pepsin and its dependence on a possible 'hydrophobic binding site'. *Nature*, *199*(4898), 1094–1095.

Thomsson, K. A., Prakobphol, A., Leffler, H., Reddy, M. S., Levine, M. J., Fisher, S. J., & Hansson, G. C. (2002). The salivary mucin MG1 (MUC5B) carries a repertoire of unique oligosaccharides that is large and diverse. *Glycobiology*, *12*(1), 1–14.

Thongngam, M., & McClements, D. J. (2005). Isothermal titration calorimetry study of the interactions between chitosan and a bile salt (sodium taurocholate). *Food Hydrocolloids*, *19*(5), 813–819.

Tolstoguzov, V. B. (1991). Functional properties of food proteins and role of protein–polysaccharide interaction. *Food Hydrocolloids*, *4*(6), 429–468.

Tomita, M., Bellamy, W., Takase, M., Yamauchi, K., Wakabayashi, H., & Kawase, K. (1991). Potent antibacterial peptides generated by pepsin digestion of bovine lactoferrin. *Journal of Dairy Science*, *74*(12), 4137–4142.

Ton, M. N., Chang, C., Carpentier, Y. A., & Deckelbaum, R. J. (2005). *In vivo* and *in vitro* properties of an intravenous lipid emulsion containing only medium chain and fish oil triglycerides. *Clinical Nutrition*, *24*(4), 492–501.

Troost, F. J., Steijns, J., Saris, W. H. M., & Brummer, R.-J. M. (2001). Gastric digestion of bovine lactoferrin *in vivo* in adults. *The Journal of Nutrition*, *131*(8), 2101–2104.

Tso, P. (2000). Overview of digestion and absorption. In: K. D. Crissinger, & M. H. Stipanuk, *Biochemical and Physiological Aspects of Human Nutrition* (pp. 75–90). Philadelphia, Pennsylvania, USA: W.B. Saunders Company.

Tuinier, R., Dhont, J. K. G., & de Kruif, C. G. (2000). Depletion–induced phase separation of aggregated whey protein colloids by an exocellular polysaccharide. *Langmuir*, *16*(4), 1497-1507.

Tuinier, R., ten Grotenhuis, E., Holt, C., Timmins, P. A., & de Kruif, C. G. (1999). Depletion interaction of casein micelles and an exocellular polysaccharide. *Physical Review E*, *60*(1), 848–856.

Turgeon, S. L., Gauthier, S. F., Molle, D., & Leonil, J. (1992). Interfacial properties of tryptic peptides of β-lactoglobulin. *Journal of Agricultural and Food Chemistry*, *40*(4), 669–675.

Üner, M., Wissing, S. A., Yener, G., & Müller, R. H. (2004). Influence of surfactants on the physical stability of solid lipid nanoparticle (SLN) formulations *Pharmazie*, *59*(4), 331–332.

Vajda, T., & Szabó, T. (1976). Specificity of trypsin and alpha-chymotrypsin towards neutral substrates. *Acta Biochimica et Biophysica: Academiae Scientiarum Hungaricae*, *11*(4), 287–294.

van Aken, G. A. (2004). Coalescence mechanisms in protein-stabilized emulsions. In: S. E. Friberg, K. Larsson, & J. Sjöblom, *Food emulsions* (pp. 299–325). New York, USA: Marcel Dekker.

van Aken, G. A. (2007). Relating food microstructure to sensory quality. In: D. J. McClements, *Understanding and Controlling the Microstructure of Complex Foods* (pp. 449–482). Cambridge, UK: Woodhead Publishing Limited.

van Aken, G. A., Blijdenstein, T. B. J., & Hotrum, N. E. (2003). Colloidal destabilisation mechanisms in protein-stabilised emulsions. *Current Opinion in Colloid & Interface Science*, *8*(4–5), 371-379.

van Aken, G. A., Vingerhoeds, M. H., & De Hoog, E. H. A. (2005). Colloidal behaviour of food emulsions under oral conditions. In: E. Dickinson, *Food Colloids: Interactions, Microstructure and Processing* (pp. 356–366). Cambridge, UK: Royal Society of Chemistry.

van der Ven, C., Gruppen, H., de Bont, D. B. A., & Voragen, A. G. J. (2001). Emulsion properties of casein and whey protein hydrolysates and the relation with other hydrolysate characteristics. *Journal of Agricultural and Food Chemistry*, *49*(10), 5005–5012.

van der Werf, M. J., & Venema, K. (2000). Bifidobacteria: genetic modification and the study of their role in the colon. *Journal of Agricultural and Food Chemistry*, *49*(1), 378–383.

van Klinken, B. J. W., Einerhand, A. W. C., Büller, H. A., & Dekker, J. (1998). Strategic biochemical analysis of mucins. *Analytical Biochemistry*, *265*(1), 103–116.

van Ruth, S. M., King, C., & Giannouli, P. (2002). Influence of lipid fraction, emulsifier fraction, and mean particle diameter of oil-in-water emulsions on the release of 20 aroma compounds. *Journal of Agricultural and Food Chemistry*, *50*(8), 2365–2371.

van Ruth, S. M., & Roozen, J. P. (2000a). Aroma compounds of oxidised sunflower oil and its oil-in-water emulsion: volatility and release under mouth conditions. *European Food Research and Technology*, *210*(4), 258–262.

van Ruth, S. M., & Roozen, J. P. (2000b). Influence of mastication and saliva on aroma release in a model mouth system. *Food Chemistry*, *71*(3), 339–345.

Vaskonen, T. (2003). Dietary minerals and modification of cardiovascular risk factors. *The Journal of Nutritional Biochemistry*, *14*(9), 492–506.

Versantvoort, C. H. M., Oomen, A. G., Van de Kamp, E., Rompelberg, C. J. M., & Sips, A. J. A. M. (2005). Applicability of an *in vitro* digestion model in assessing the bioaccessibility of mycotoxins from food. *Food and Chemical Toxicology*, *43*(1), 31–40.

Vingerhoeds, M. H., Blijdenstein, T. B. J., Zoet, F. D., & van Aken, G. A. (2005). Emulsion flocculation induced by saliva and mucin. *Food Hydrocolloids*, *19*(5), 915–922.

Vingerhoeds, M. H., Silletti, E., de Groot, J., Schipper, R. G., & van Aken, G. A. (2009). Relating the effect of saliva-induced emulsion flocculation on rheological properties and retention on the tongue surface with sensory perception. *Food Hydrocolloids*, *23*(3), 773–785.

Wahlgren, M. C., Arnebrant, T., & Paulsson, M. A. (1993). The adsorption from solutions of β-lactoglobulin mixed with lactoferrin or lysozyme onto silica and methylated silica surfaces. *Journal of Colloid and Interface Science*, *158*(1), 46–53.

Waigh, T. A., Papagiannopoulos, A., Voice, A., Bansil, R., Unwin, A. P., Dewhurst, C. D., Turner, B., & Afdhal, N. (2002). Entanglement coupling in porcine stomach mucin. *Langmuir*, *18*(19), 7188–7195.

Walstra, P. (1987). Physical principles of emulsion science. In: J. M. V. Blanshard, & P. Lillford, *Food Structure and Behaviour* (pp. 87–106). London, UK: Academic Press.

Weintraub, M., Ragetli, H. W. J., & Schroeder, B. (1971). The protein composition of nuclear crystals in leaf cells. *American Journal of Botany*, *58*(2), 182–190.

Weisbrodt, N. W. (2001a). Gastric emptying. In: L. R. Johnson, *Gastrointestinal Physiology* (pp. 37–46). Mosby, St. Louis, MO: USA.

Weisbrodt, N. W. (2001b). Swallowing. In: L. R. Johnson, *Gastrointestinal Physiology* (pp. 27–35). Mosby, St. Louis, MO: USA.

West, C. E., Hardcastle, Joanna L., & Compton, Richard G. (2002). Sono-electroanalytical determination of lead in saliva. *Electroanalysis*, *14*(21), 1470-1478.

Wickham, M., Faulks, R., & Mills, C. (2009). *In vitro* digestion methods for assessing the effect of food structure on allergen breakdown. *Molecular Nutrition & Food Research*, *53*(8), 952–958.

Wickham, M., Garrood, M., Leney, J., Wilson, P. D. G., & Fillery-Travis, A. (1998). Modification of a phospholipid stabilized emulsion interface by bile salt: effect on pancreatic lipase activity. *The Journal of Lipid Research*, *39*(3), 623–632.

Wissing, S. A., Kayser, O., & Müller, R. H. (2004). Solid lipid nanoparticles for parenteral drug delivery. *Advanced Drug Delivery Reviews*, *56*(9), 1257–1272.

Wissing, S. A., & Müller, R. H. (2002). The influence of the crystallinity of lipid nanoparticles on their occlusive properties. *International Journal of Pharmaceutics*, *242*(1-2), 377–379.

Wong, D. W. S., Camirand, W. M., & Pavlath, A. E. (1996). Structures and functionalities of milk proteins. *Critical Reviews in Food Science and Nutrition*, *36*(8), 807–844.

Wright, A. J., Pietrangelo, C., & MacNaughton, A. (2008). Influence of simulated upper intestinal parameters on the efficiency of beta carotene micellarisation using an *in vitro* model of digestion. *Food Chemistry*, *107*(3), 1253–1260.

Wu, A. M., Csako, G., & Herp, A. (1994). Structure, biosynthesis, and function of salivary mucins. *Molecular and Cellular Biochemistry*, *137*(1), 39–55.

Ye, A., & Singh, H. (2000). Influence of calcium chloride addition on the properties of emulsions stabilized by whey protein concentrate. *Food Hydrocolloids*, *14*(4), 337-346.

Ye, A., Hemar, Y., & Singh, H. (2004). Influence of polysaccharides on the rate of coalescence in oil-in-water emulsions formed with highly hydrolyzed whey proteins. *Journal of Agricultural and Food Chemistry*, *52*(17), 5491–5498.

Ye, A., & Singh, H. (2006a). Adsorption behaviour of lactoferrin in oil-in-water emulsions as influenced by interactions with *β*-lactoglobulin. *Journal of Colloid and Interface Science*, *295*(1), 249–254.

Ye, A., & Singh, H. (2007). Formation of multilayers at the interface of oil-in-water emulsion *via* interactions between lactoferrin and *β*-lactoglobulin. *Food Biophysics*, *2*(4), 125–132.

Ye, A., & Singh, H. (2006b). Heat stability of oil-in-water emulsions formed with intact or hydrolysed whey proteins: influence of polysaccharides. *Food Hydrocolloids*, *20*(2–3), 269–276.

Yeom, K. H., Trierum, G. V., Lee, K. W., & Beynen, A. C. (2003). Influence of feeding a milk replacer deficient in *α*-linolenic acid on fatty acid composition of various tissues in goat kids. *Small Ruminant Research*, *48*(2), 141–148.

Zalewska, A., Zwierz, K., Zólkowski, K., & Gindzienski, A. (2000). Structure and biosynthesis of human salivary mucins. *Acta Biochimica Polonica*, *47*(4), 1067–1079.

Ziegler, G. R., & Foegeding, E. A. (1990). The gelation of proteins. *Advances in Food and Nutrition Research 34*, 203–298.